

UCLA

UCLA Electronic Theses and Dissertations

Title

From Chlamydomonas reinhardtii to Caenorhabditis elegans: Investigations into the environmental regulation of eukaryotic Cu-handling mechanisms

Permalink

<https://escholarship.org/uc/item/7jn341xs>

Author

Shafer, Catherine Michelle

Publication Date

2022

Peer reviewed|Thesis/dissertation

UNIVERSITY OF CALIFORNIA

Los Angeles

From *Chlamydomonas reinhardtii* to *Caenorhabditis elegans*:

Investigations into the environmental regulation of eukaryotic Cu-handling mechanisms

A dissertation submitted in partial satisfaction

of the requirements for the degree Doctor of Philosophy

in Molecular Toxicology

by

Catherine Michelle Shafer

2022

ABSTRACT OF THE THESIS

From *Chlamydomonas reinhardtii* to *Caenorhabditis elegans*:

Investigations into the environmental regulation of eukaryotic Cu-handling mechanisms

by

Catherine Michelle Shafer

Doctor of Philosophy in Molecular Toxicology

University of California, Los Angeles, 2022

Professor Megan M. McEvoy, Chair

Abstract

This dissertation investigated the environmental factors that contribute to eukaryotic Cu homeostasis. Using a single-celled eukaryote, *Chlamydomonas reinhardtii*, this work expanded upon the knowledge of Cu uptake transporters (CTRs). The noncanonical CTR3 was found to be periplasmic and, despite validating mutant strains for the protein, was not identified to play any role in the accumulation of Cu in conditions that increased expression of CTR3 with CTR1 and CTR2. However, another soluble

factor, glutathione (GSH), was found to contribute to Cu accumulation driven by canonical CTRs during Zn deficiency. However, despite this potential for increased accumulation through CTRs, GSH also consistently protected *Chlamydomonas* from nonessential Ag toxicity. The two canonical CTRs, CTR1 and CTR2, were further distinguished by their varying affinity for Cu during Cu deficient and Zn deficient conditions. Therefore, it was concluded that CTR1 and CTR2 are not redundant because they could not substitute for one another's function.

In subsequent investigations, the use of *Caenorhabditis elegans* allowed for the study of bacterial Cu-resistance responses within a host-microbe system. These investigations identified increasing bacterial Cu-efflux as an environmental factor contributing to the sensitization of host *C. elegans* to Cu exposures by changing the spatial localization of metal stress within the adult nematode in a tissue specific manner instead of reducing the overall body burden of the metal exposure. Consequently, *C. elegans* raised on bacterial lawns with reduced bacterial Cu-efflux capacity, achieved by targeted deletions in the *cusRS* two component system in *Escherichia coli*, exhibited 1) increased survival, 2) reduced matricidal hatching, 3) improved growth, and 3) a shifted nuclear metal responsive gene (*numr-1*) reporter to the posterior of the pharynx where Cu accumulated by bacteria is released by the pharyngeal grinder in response to high environmental Cu stress. These investigations present health implications for the increasing Cu resistance observed in bacterial populations due to increased industry and metal deposition and for the compounding challenges facing transition metal homeostasis in these increasingly manmade environments.

The dissertation of Catherine Michelle Shafer is approved.

Patrick Allard

Elissa A. Hallem

Shaily Mahendra

Oliver Hankinson

Megan M. McEvoy, Committee Chair

University of California, Los Angeles

2022

DEDICATION:

First, I would like to acknowledge and thank Professor Megan McEvoy. Without her support and mentorship these last years, the work presented in this dissertation would not have been possible. I admire her for her patience and dedication to the pursuit and application of science for the good of everyone. From being a committee member for my qualifying exams to accepting me into her lab as a student entering their third year at UCLA, she welcomed me into her lab, guided me through the ins and outs of scientific research and facilitated collaborations necessary for a broad, interdisciplinary project.

One such collaborator, Professor Patrick Allard, is another person for whom this research would have been impossible without. The serendipity of his lab moving next door to Dr. McEvoy's just as I was joining her lab facilitated the development of the research presented in the second half of this dissertation. His guidance from when I first met him to talk about the possibility of applying to be a student in the Molecular Toxicology IDP to years later when he helped me write my first publication has been invaluable. I'd also like to thank my committee members Professors Elissa Hallem, Shaily Mahendra, and Oliver Hankinson for their advice and guidance through these years. And lastly, I would like to thank Professor Sabeeha Merchant. Her valuable mentorship provided the support for the first part of the work presented here and gave me the foundational knowledge that I continue to use in all my scientific pursuits to this day.

The members of the McEvoy, Allard and Merchant labs have been equally invaluable in the development of this project. In particular, I would like to express my gratitude for Dr. Andy Hausrath, Dr. Lisa Truong, Abby Blin, Rio Barrere-Cain, Dr.

Daniella Strenkert, Dr. Stefan Schmollinger, and Dr. Collen Hui. Their support, both inside and outside the lab, will be dearly remembered.

Outside of the world of science, I have a wonderful support system that has helped me through each step of this journey. My parents, Joanie and Bill, and brothers, Carl and Troy, have been with me through every step of the way supporting my decisions and patiently listening to me talk about my research and lab stories even when they had no idea what was going on. I will cherish the memory of their yearly visits to Los Angeles exploring the sights and sounds of Hollywood, the Miracle Mile and getting stuck in traffic on Wilshire.

Finally, I want to thank my husband, Brent. I truly cannot thank him enough for his love, support and unwavering belief in my ability to do anything I set my mind to even when I don't believe it myself. I'm so excited to see what the future brings next for us and our daughter, Phoebe, who has only just begun her journey in this world.

TABLE OF CONTENTS

LIST OF FIGURES.....	xiii
LIST OF TABLES.....	xviii
ACKNOWLEDGEMENTS.....	xix
BIOGRAPHICAL SKETCH.....	xxi
CHAPTER 1: INTRODUCTION.....	1
1.1 Essential transition metal homeostasis.....	1
1.2 Biological roles of copper.....	2
1.3 Mechanisms of copper toxicity.....	4
1.4 Sources of environmental copper.....	7
1.5 Model of prokaryotic copper homeostasis: <i>E. coli</i>	8
1.6 Copper homeostasis in Eukaryotic systems.....	10
1.7 Copper homeostasis in <i>Caenorhabditis elegans</i> host-microbe system.....	12
1.8 Figures.....	14
1.9 References.....	22
CHAPTER 2: THE ROLE OF CTR UPREGULATION AND CYTOSOLIC GLUTATHIONE DURING CRR1-DRIVEN CU UPTAKE AND TOLERANCE IN <i>CHLAMYDOMONAS REINHARDTII</i>	
2.1 Abstract.....	33

2.2 Introduction.....34

2.2.1 *Chlamydomonas reinhardtii*.....34

2.2.2 Condition for Cu uptake by *Chlamydomonas reinhardtii*.....34

2.2.3 Copper complexation and distribution through the cytosol.....35

2.2.4 Copper export out of the cytosol.....36

2.2.5 Copper storage in the acidocalcisome.....37

2.3 Materials & Methods.....39

2.3.1 Strains and culture conditions.....39

2.3.2 Growth rate determination.....39

2.3.3 Immunoblot analysis.....39

2.3.4 Determination of metal concentrations.....40

2.3.5 Establishment of Zn deficiency.....41

2.4 Results.....42

2.4.1 CTR3 is secreted to the periplasm during Cu deficiency.....42

2.4.2 *ctr3.1* does not produce CTR3 nor disrupt other CRR1-dependent activity.....42

2.4.3 CTR3 is not required for Cu-uptake during Cu-deficiency unlike CTR2.....43

2.4.4 CTR2 mediates Cu hyperaccumulation in transition to Zn deficiency.....44

2.4.5 GSH drives CTR2-mediated Cu accumulation in transition to Zn deficiency....45

2.4.6 Loss of GSH sensitizes Chlamydomonas to non-essential metal toxicity.....	45
2.5 Paper in preparation.....	47
2.6 Discussion.....	75
2.6.1 Consequences of Cu accumulation in cellular environments.....	75
2.6.2 CRR1: master Cu quota determinant to avoid deficiency and toxicity.....	75
2.6.3 CTR3 and GSH: coordinating periplasmic and cytosolic free metal pools.....	77
2.7 Conclusions.....	79
2.8 Figures.....	81
2.9 References.....	120
 CHAPTER 3: STRENGTH OF CU-EFFLUX RESPONSE IN <i>E. COLI</i> COORDINATES METAL RESISTANCE IN <i>C. ELEGANS</i> AND CONTRIBUTES TO THE SEVERITY OF ENVIRONMENT TOXICITY	
3.1 Abstract.....	133
3.2 Introduction.....	134
3.3 Materials & Methods.....	137
3.3.1 <i>C. elegans</i> genetics and strains.....	137
3.3.2 <i>E. coli</i> genetics and strains.....	137
3.3.3 Bacterial culture conditions.....	138
3.3.4 Bacterial growth rate and plate density.....	138

3.3.5 Exposure conditions.....	138
3.3.6 Length determination.....	139
3.3.7 Body-burden measurements.....	139
3.3.8 Lethality.....	140
3.3.9 Cumulative population risk of matricidal hatching.....	141
3.3.10 Brood-size measurement.....	142
3.3.11 Imaging.....	142
3.3.12 Statistical Analysis.....	143
3.4 Results.....	144
3.4.1 A simplified exposure paradigm to test the impact of bacterial Cu-efflux capacity on host Cu sensitivity.....	144
3.4.2 Role for Bacterial Cu-efflux capacity in host toxicity endpoints.....	146
3.4.3 Temporal dependence of MH on bacterial Cu-efflux capacity.....	147
3.4.4 Early Cu toxicity does not coincide with Cu-body burden in <i>C. elegans</i>	148
3.4.5 Spatial activation of <i>numr-1</i> is dependent on bacterial Cu-efflux capacity.....	150
3.4.6 <i>numr-1</i> mediates toxicity responses to bacterially-accumulated Cu.....	153
3.5 Discussion.....	155
3.5.1 Disconnecting does-dependent toxicity in the host.....	156
3.5.2 Pharyngeal signal for protective Cu-stress response.....	157

3.6 Conclusion.....	159
3.7 Figures.....	160
3.8 References.....	170

**CHAPTER 4: BACTERIALLY-DEPENDENT TRANSCRIPTIONAL REGULATION IN
CAENORHABDITIS ELEGANS EXPOSED TO CHRONIC ENVIRONMENTAL CU
EXCESS**

4.1 Abstract.....	178
4.2 Introduction.....	179
4.3 Materials & methods.....	183
4.3.1 <i>C. elegans</i> samples preparation.....	183
4.3.2 Total RNA isolation.....	183
4.3.3 RNA sequencing and analysis.....	183
4.3.4 Generational H ₂ O ₂ stress resistance determination.....	184
4.3.5 Dopamine-dependent slowing in response to food signal.....	184
4.4 Results.....	185
4.4.1 In <i>C. elegans</i> , Cu conditions predict transcriptomic landscape more than bacterial Cu-efflux conditions.....	185
4.4.2 Known Cu-responsive genes identified as DEGs.....	185

4.4.3 Bacterially-dependent Cu resistance independent of increased <i>numr-1</i> gene expression.....	187
4.4.4 Bacterially-dependent DEGs during Cu-stress do not strongly predict neuronal or generational Cu resistance.....	188
4.5 Discussion.....	190
4.5.1 RNAseq analysis limited by experimental design.....	190
4.5.2 Tissue and spatial specificity of bacterially-dependent Cu-stress response in nematodes.....	192
4.6 Conclusions.....	194
4.7 Figures.....	195
4.8 References.....	209
CHAPTER 5: CONCLUSIONS AND FUTURE DIRECTIONS.....	212
5.1 References.....	220

LIST OF FIGURES

Figure 1.1 Transition metals required for survival in all organisms.....	14
Figure 1.2 Dose-dependent response to non-essential metals.....	15
Figure 1.3 Change in bioavailability of transition metals in relation to atmospheric O ₂ .	16
Figure 1.4 Dose-response curve associated with essential transition metals.....	17
Figure 1.5 Inhibition of GSH1.....	18
Figure 1.6 Association between increased anthropogenic Cu deposition and diversification of Cu-resistance in enteric bacteria.....	19
Figure 1.7 CusRS and cusCFBA function.....	20
Figure 1.8 Single-celled organisms homeostatic response to environmental Cu.....	21
Figure 2.1 Requirement for CRR1 in deficiency and excess metal conditions.....	81
Figure 2.2 CTR3 is a secreted protein.....	82
Figure 2.3 Chlamydomonas strains.....	83
Figure 2.4 Validation of <i>ctr3-1</i>	84
Figure 2.5 <i>ctr3-1</i> does not impair Cu-deficiency response.....	85
Figure 2.6 CTR1 and CTR2 are functional Cu importers with varying affinity.....	86
Figure 2.7 Experimental paradigm for capturing transition of Zn-replete to Zn-deficient conditions for wild-type cc4533 Chlamydomonas.....	87
Figure 2.8 Zinc Deficiency established after transfer to Zn-deficient media.....	88

Figure 2.9 Cu hyperaccumulation established after transfer to Zn-deficient media.....	89
Figure 2.10 Growth rate of Chlamydomonas after transfer to Zn-deficient media.....	90
Figure 2.11 <i>ctr2-1</i> doesn't impair establishment of Zn deficiency.....	91
Figure 2.12 <i>ctr2-1</i> impairs establishment of Cu hyperaccumulation in response to Zn deficiency.....	92
Figure 2.13 Experimental design for capturing the role of GSH in transition to Zn deficiency.....	93
Figure 2.14 GSH contributes to establishment of Cu hyperaccumulation during Zn deficiency.....	94
Figure 2.15 Ag toxicity via CTR uptake is minimized by GSH.....	95
Figure 2.16 Growth rate of gamma-glutamyl synthetase mutants.....	96
Figure 2.17 Ag-induced growth impairment in gamma-glutamyl synthetase mutants...	97
Figure 2.18 Cu uptake is impaired in <i>crr1</i> , consistent with Cu- and <i>crr1</i> dependent expression of <i>CTR1</i> , <i>CTR2</i> and <i>CTR3</i>	98
Figure 2.19 Protein similarity network of CTR type proteins.....	99
Figure 2.20 CTR3 is a secreted protein.....	100
Figure 2.21 Molecular analysis of <i>ctr1</i> amiRNA lines, CPf1/CRISPR mediated <i>ctr1</i> mutants and <i>ctr2/ctr3</i> insertional mutants.....	101
Figure 2.22 CTR1 and CTR2 are both implicated in copper import, while Cu conditional growth defect of <i>ctr1</i> CPf1/CRISPR mutants mimics <i>crr1</i> phenotype.....	104

Figure 2.23 CTR1 and CTR2 are both functional copper importers <i>in vivo</i> , but CTR1 specifically mediates high affinity copper import.....	106
Figure 2.24 Zn-deficiency increases uptake but does not inhibit export.....	107
Figure 2.25 Copper accumulation is impaired in zinc deficient <i>ctr1</i> and <i>ctr2</i> mutants.....	108
Figure 2.26 Copper accumulated in zinc deficient <i>crr1</i> is stored in acidocalcisomes, but cannot be mobilized after zinc add back.....	109
Figure 2.27 CTR2 is exporting copper out of the acidocalcisomes.....	111
Figure 2.28 Model of Cu homeostatic network in <i>Chlamydomonas reinhardtii</i>	119
Figure 3.1 CusRS regulates Cu-efflux capacity in an <i>E. coli</i> model system.....	160
Figure 3.2 Host sensitivity to chronic Cu excess is dependent on bacterial Cu-efflux capacity.....	161
Figure 3.3 Association between bacterially-dependent Cu-sensitivity and <i>C. elegans</i> Cu-body burden.....	162
Figure 3.4 Bacterial Cu-efflux capacity effects Cu-dependent pharyngeal <i>numr-1</i> activation.....	163
Figure 3.5 <i>numr-1</i> involvement in bacterially-dependent Cu resistance.....	164
Figure 3.6 Bacterial Cu-efflux capacity acts spatially on host response to environmental metal-stress.....	165
Figure 4.1 Principal component analysis for normalized read counts of biological replicates.....	195

Figure 4.2 DEGs dependent on copper concentration in 100% bacterial Cu-efflux conditions.....	196
Figure 4.3 DEGs dependent on copper concentration in 50% bacterial Cu-efflux conditions.....	198
Figure 4.4 DEGs dependent on bacterial Cu-efflux conditions in the absence of excess copper.....	200
Figure 4.5 DEGs dependent on bacterial Cu-efflux conditions in the presence of excess copper.....	202
Figure 4.6 Basal slowing response to food after Cu exposure on 100% <i>WT</i> Bacterial Cu efflux.....	204
Figure 4.7 Basal slowing response to food after Cu exposure on 50% <i>WT</i> Bacterial Cu efflux ($\Delta cusS$).....	205
Figure 4.8 Basal slowing response to food after Cu exposure on 25% <i>WT</i> Bacterial Cu efflux ($\Delta cusR$).....	206
Figure 4.9 100% <i>WT</i> Bacterial Cu-efflux capacity does not generationally increase oxidative stress resistance in F1 nematodes.....	207
Figure 4.10 50% <i>WT</i> Bacterial Cu-efflux capacity does not generationally increase oxidative stress resistance in F1 nematodes.....	208
Supplemental Figure 2.S1 ssODN mediated CRISPR/CPF1 gene editing introducing two in- frame stop codons in exon 1 of <i>CTR1</i>	112
Supplemental Figure 2.S2 Cytochrome c_6 accumulation indicates internal copper deficiency in <i>ctr2</i>	113
Supplemental Figure 2.S3 Co-regulation between <i>CTR1</i> and <i>CTR2</i> expression.....	114

Supplemental Figure 2.S4. Zinc deficient growth defect is not exacerbated in <i>ctr</i> mutants.....	115
Supplemental Figure 2.S5 Copper accumulated in zinc deficient <i>crr1</i> is stored in distinct foci, but copper cannot be mobilized after zinc add back.....	116
Supplemental Figure 2.S6 Copper accumulated in zinc deficient <i>ctr1</i> mutants.....	117
Supplemental Figure 2.S7 Copper accumulated in zinc deficient <i>ctr2</i> and <i>ctr3</i>	118
Supporting Figure 3.S1. Bacterial growth and density in response to Cu-stress.....	166
Supporting Figure 3.S2 Reproductive impact of Cu-stress exposure in <i>C. elegans</i> ..	167
Supporting Figure 3.S3 Validation of wash steps prior to GFAAS Cu-content analysis.....	168
Supporting Figure 3.S4 Pharyngeal <i>numr-1</i> activation without addition of excess Cu.....	169

LIST OF TABLES

Table 4.1 Enrichment analyses dependent on copper concentration in 100% <i>WT</i> bacterial Cu-efflux conditions.....	197
Table 4.2 Enrichment analyses dependent on copper concentration in 50% <i>WT</i> bacterial Cu-efflux conditions.....	199
Table 4.3 Enrichment analyses dependent on bacterial Cu-efflux conditions in the absence of excess copper.....	201
Table 4.4 Enrichment analysis dependent on bacterial Cu-efflux conditions in the presence of excess copper.....	203

ACKNOWLEDGEMENTS:

Within chapter 2, experiments conducted by Dr. Daniella Strenkert include ami-RNA and KO development in *Chlamydomonas reinhardtii*, the CTR3 western blot looking for secretion during Cu deficiency, and the Cu-addback assays. The remaining experiments presented separately from the paper in preparation (Section 2.5) were performed by Catherine Shafer between 2016-2018. The work presented in the paper in preparation is the result of a collaborative effort: Daniella Strenkert designed and performed experiments, analyzed data, prepared figures and designed the overall project, Stefan Schmollinger designed and performed experiments, analyzed data, and prepared figures, Srinand Paruthiyil performed experiments, analyzed data and prepared figures, Bonnie C. Brown performed experiments, Kristen Holbrook designed, performed and analyzed experiments, Sydnee Green performed experiments, Hosea Nelson designed CS3 synthesis and secured funding, Crysten E. Blaby-Haas prepared figures and Sabeeha Merchant designed project and secured funding. Within the paper in preparation section, Catherine Shafer's specific contribution includes conducting the western blots shown in Figure 4H (ctr3 blot on ctr3 mutants and control lines) and Supplemental Figure 2 (plastocyanin and cox2b in ctr3 mutants and control lines).

Within Chapter 3, Ashley Tseng contributed to imaging pharyngeal expression of numr-1p::GFP and maintaining nematode strains. Catherine Shafer designed and performed experiments, analyzed data, prepared figures, assisted writing the manuscript and designed the overall project. Patrick Allard designed experiments and assisted writing the manuscript. Megan McEvoy designed experiments, assisted writing the manuscript and secured funding.

For data presented within chapter 4, the generational oxidative stress assay, basal slowing response assay, RNA collection and isolation was performed by Catherine Shafer. RNA analysis was performed by Mark I. Duhon II who is a part of UCLA's Technology Center for Genomics & Bioinformatics (TCGB).

BIOGRAPHICAL SKETCH:

EDUCATION:

University Of Colorado at Boulder (*August 2011- May 2014*)

- Bachelor of the Arts with double major in Neuroscience, and MCDB (Molecular, Cellular, and Developmental Biology) with pre-med designation (GPA: 3.514)

PUBLICATIONS:

Paper Publications:

- **Shafer, C. M.**, Tseng A., Allard P., McEvoy M. M. (2021) *Strength of Cu-efflux response in E. coli coordinates metal resistance in C. elegans and contributes to the severity of environmental toxicity.* Journal of Biological Chemistry 297(3), 101060.

Papers in preparation:

- *Copper assimilation in Chlamydomonas revisited: CTR2 as the major copper importer in Chlamydomonas.* Daniela Strenkert, **Catherine M. Shafer**, Stefan Schmollinger, Bonnie Chu Brown, Patrice Salome and Sabeeha S. Merchant.

Poster Presentations:

- **Shafer C. M.** Allard P., McEvoy M. M. (2019, November) *Active bacterial copper-efflux response contributes to environmental metal toxicity in Caenorhabditis elegans.* Southern California Society of Toxicology Meeting.
 - Award: 2019 SCCSOT 3rd place presentation award
- **Shafer C. M.** Allard P., McEvoy M. M. (2019, July) *An Increased Dietary to Environmental copper ratio reduces toxicity endpoints in Caenorhabditis elegans.* *C. elegans* 22nd International Meeting.

- **Shafer C. M.** Allard P., McEvoy M. M. (2019, March) *An Increased Dietary to Environmental copper ratio reduces toxicity endpoints in Caenorhabditis elegans.* Society of Toxicology Annual Meeting.
- Strenkert D., **Shafer C. M.**, Brown B. C., Schmollinger S.R., Castruita M., Merchant, S. S. (2018, June) *Mechanisms of copper hyper-accumulation in Chlamydomonas reinhardtii.* PSU 2018 Bioinorganic Workshop.
- Strenkert D., Brown B. C., **Shafer C. M.**, Schmollinger S.R., Castruita M., Merchant, S. S. (2018, March). *Mechanisms of heavy metal assimilation and detoxification in Chlamydomonas reinhardtii.* Society of Toxicology Annual Meeting.

EMPLOYMENT:

- **Project Assistant** (September 2015 - May 2016) full-time at The Keck School of Medicine at the University of Southern California with the MADRES project
- **Professional Research Assistant** (July 2013 – June 2015) full-time for University of Colorado, Boulder at the CU CHANGE lab
- **Teaching Assistant** (Winter 2021) 50% appointment for SOCGEN 105B Problems of Identity at Biology/Society Interface
- **Teaching Assistant and Program for Excellence in Education and Research in the Sciences (PEERS) Facilitator** (Fall 2021) 50% appointment for LS7A Introduction to Biology
- **Teaching Assistant** (Fall 2019) 50% appointment for LS107A Advanced Genetics

CHAPTER 1: INTRODUCTION

1.1 Essential transition metal homeostasis

Essential transition metals, particularly first row transition metals, are required by organisms from all three domains of life to perform enzymatic reactions that would otherwise be impossible (Fig. 1.1)(1). Today, nearly 50% of all enzymatic proteins are recognized as metalloproteins for this reason (2). Unlike other nutrients that can be synthesized by an organism (often through the function of metalloenzymes), essential transition metals must be acquired from the external environment (3-6). Without a sufficient environmental supply, deficiency of an essential transition metal impairs cellular functions unless coordinated homeostatic accommodations can be made (7). Homeostatic responses to deficiency include sparing mechanisms to reduce the amount required by the cell to survive by mobilizing cellular stores, increasing the efficiency of uptake (8,9), and utilizing alternative pathways that don't require the metal (10,11).

However, homeostatic accommodations can be detrimental if deficiency does not resolve promptly. For instance, depletion of cellular copper stores like those found in the Cu-rich plastocyanin of a single-celled algae, *Chlamydomonas reinhardtii*, during Cu deficiency reduces the capacity of the cell to respond to Cu-deficiency in the future (3). Similarly, increases in high-affinity uptake transporters in response to deficiency carry their own challenges. For instance, iron (Fe) deficiency is a common cause of increased cadmium (Cd) (12), a nonessential transition metal that is toxic to biological functions because many of the same processes that promote increased uptake of Fe²⁺ during deficiency also serve to increase the accumulation of metals with similar properties (8). Consistent with a unique vulnerability to similar toxicants resulting from deficiency, early

studies attributed essential transition metal supplementation in the diet with reductions in observed Cd toxicity (13).

Where any amount of nonessential Cd or Ag can exert detrimental effects on an organism (Fig. 1.2), essential transition metals with similar properties can also be a detriment when the environmental concentration far exceeds an organism's homeostatic quota (14,15). When presented with these circumstances, organisms initiate defensive mechanisms to promote resistance and reduce the influx of the metal (16-18). Specific responses to metal excess complement those initiated by deficiency; for instance, export rather than import of the metal is promoted (17,19) and substitution of vulnerable pathways until detoxification can take place (20). Despite the challenge of balancing deficiency and excess in changing environmental conditions, the universal need for transition metals across all the three domains of life today suggests that the utility for essential transition metals far outweighed these risks (21). While the above examples demonstrate the overlapping nature of homeostatic systems for essential transition metals (Fe, Zn, Ca, Cu, Mn, Mg etc.) this thesis focuses on the role of one essential transition metal, copper.

1.2 Biological Roles of Copper

Biological organisms were first introduced to an abundance of copper in the environment when a rapid increase in atmospheric oxygen, termed the Great Oxidation Event (GOE) some 2.5-2.3 billion years ago, shifted the Cu(I):Cu(II) ratio in favor of the much more bioavailable Cu(II) (Fig.1.3) (1,22). The concurrent increase in the bioavailability of copper and oxygen gave rise to the integration of this redox-active metal within biological systems as they took full advantage of the newfound oxygen chemistry,

mediated by copper's unique reduction potential (23), available to them. The integration of copper into biological systems is observed in the numerous cuproenzymes present in organisms today and containing a variety of mononuclear, dinuclear and trinuclear O₂-reactive copper centers that are essential to the utilization of oxygen within the cell (1,24).

Cuproenzymes exemplify this utility in a number of essential biochemical pathways today that include the homeostasis of other essential transition metals (25,26), norepinephrine biosynthesis (27-29), energy production and oxidative-stress detoxification (25). Energetically, cuproenzymes like plastocyanin and cytochrome c oxidase perform essential functions within the electron transport chain (ETC) of mitochondria and chloroplasts respectively (24,30). Plastocyanin in the electron transport chain of photosynthetic eukaryotes, utilizes copper to transfer electrons between photosystems in the chloroplast (30). Plastocyanin's role in the electron transport chain is so indispensable that copper deficiency in *C. reinhardtii* promotes the degradation of the copper-containing enzyme in favor of a heme-containing replacement, cytochrome C6, that can temporarily substitute its function without the use of copper (31). Similarly, as the last enzyme in the ETC, cytochrome c oxidase functions in catalyzing the reduction of oxygen to water by using the copper centers of CuA and CuB as electron acceptors (32) in mitochondria, bacteria and archaea alike to produce adenosine triphosphate (ATP) at the end of the ETC and maintain the energy requirements of the cell.

Beyond energy requirements, homeostatic regulation of other essential metals and the synthesis of crucial compounds involved in human neurotransmission are dictated by cuproenzymes. Human cytochrome C oxidase, which requires iron in addition to copper (32), is functionally impacted by another essential cuproenzyme found in plasma,

ceruloplasmin, because of its role in mediating iron metabolism (25). Ceruloplasmin's trinuclear copper cluster, carrying 95% of all circulating copper, acts as an oxidoreductase to catalyze and movement of ferrous iron between blood plasma and cells. Just a 1% decrease in plasma ceruloplasmin levels is sufficient to induce hypoferremia (25). In the nervous system, norepinephrine synthesis is also dictated by cuproenzymes; the monooxygenase, dopamine Beta hydroxylase, uses its coupled binuclear copper site to catalyze the conversion of dopamine to norepinephrine in the catecholamine biosynthesis pathway (27).

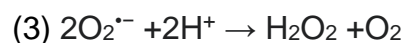
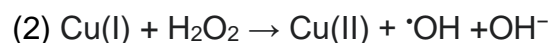
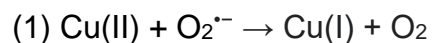
Copper also plays a critical role in preventing the accumulation of oxidative damage via copper zinc superoxide dismutase (CuZnSOD) in all living organisms. Within the mitochondria, the superoxide radicals produced as a byproduct of complex III is scavenged by a CuZnSOD (SOD1) to prevent its buildup by catalyzing its efficient reduction (33,34). Without SOD1, the buildup of superoxide radicals can damage proteins and lipids through uncontrolled oxidation (34) and impair the energetic output of the mitochondria (35,36). On the flipside, uropathogenic *E. coli* also utilize CuZnSODs in their periplasm to protect against macrophage killing by superoxide and contribute to their pathogenicity in a host (37).

1.3 Mechanisms of Copper toxicity

While every organism alive today requires some level of copper to survive, if this essential transition metal exceeds the upper limits of the goldilocks zone maintained by homeostatic mechanisms, toxicity results (Fig.1.4). When this happens, the same properties that make cuprous and cupric copper so valuable in biological systems can just as easily do harm in the absence of tight cellular regulation. For instance, every

macromolecule in the cell bears the burden of 1) reactive oxygen species produced by redox cycling, 2) the disruption of thiol group activity and 3) the mismetallation of other metalloenzymes initiated by excess borderline/soft-acid copper cations (38). While many xenobiotics produce reactive oxygen species and burden the antioxidant thiol pool of glutathione in the cytosol, copper's properties as an essential transition metal with exceptional thermodynamic affinity constants ($Mn^{2+} < Fe^{2+} < Co^{2+} < Ni^{2+} < Cu^{2+} > Zn^{2+}$) are a uniquely hazardous combination for all organisms (31). Where these antimicrobial properties of copper are weaponized in hospital environments and even by human macrophages fighting off pathogens (39), toxicity can arise in humans as well in the form of acute neurotoxicity, hepatotoxicity and nephrotoxicity.

As described in the chemical reactions below, reduction-oxidation (redox) reactions involving copper produce several species of highly reactive chemicals, including singlet oxygen hydroxyl radical, hydroxide ion, peroxide ion and hydrogen peroxide (40).



The formation of reactive oxygen species by the interaction of copper with oxygen can quickly cascade out of control in cellular environment. The catalysis of lipid peroxidation via reactive oxygen species produces a number of lipid hydroperoxides and subsequent aldehydes that can cause more detrimental effects. For instance, malondialdehyde (MDA) is highly mutagenic while 4-hydroxynonenal (4-HNE) is considered both cytotoxic and genotoxic (34). Adriamycin, a drug that was proposed to act as a mutagen through redox cycling, sees a synergistic effect when copper is introduced with it; in the Ames salmonella

test, a 700% increase in mutagenicity is reported in these conditions (41). Similarly, copper synergizes with hydroquinone to increase the formation of double strand DNA breaks mediated by singlet oxygen (42). In the case of DNA oxidation mediated by copper, the addition of glutathione, an abundant tripeptide with a cysteine residue, significantly reduced the damage inflicted by stabilizing the Cu(I) oxidation state to put a stop to the runaway redox cycling that continually produces these reactive oxygen species. All of these uncontrolled reactions can be largely prevented through homeostatic systems that function to severely limit any free $\text{Cu}^+/\text{Cu}^{2+}$ in the cell (43).

While glutathione's antioxidant thiol group is designed to be sacrificial in the face of reactive oxygen species and metal toxicity to prevent damage to important cellular components, as demonstrated by experiments demonstrating increased metal toxicity after inhibiting the synthesis of the abundant cytosolic thiol (Fig. 1.5) (44), the affinity of copper for thiol groups can still impair cellular function if the concentration of metal exceeds that of the available antioxidants. For instance, the binding of copper to the acyl-accepting N-terminal cysteine residue of lipoprotein precursors prevents their maturation by making the cysteine residue unavailable to enzymes necessary for sequential acylation of the polypeptide chain, removal of the signal peptide and translocation to the membrane (20). Similarly, the maturation of peptidoglycan, required for the formation of the cell envelope in enterobacteria, is impaired if copper binds to the active-site cysteines on the transpeptidases responsible for the attachment to membrane lipoproteins (45). Aside from binding to available sulfhydryl groups, copper can also catalyze the formation of inappropriate disulfide bonds within a variety of polypeptides which results in misfolded proteins that are unable to function. While other transition metals can disrupt sulfhydryl

homeostasis, Cu^{2+} has the highest affinity for soft bases like the thiols found in cysteine (20).

The high stability of complexes formed with copper means that other essential metals that function in metalloenzymes risk being replaced by copper (46). With their innumerable and finely tuned functions, mismetallation by copper can disrupt valuable cellular process; one particularly relevant process is disrupted by Cu mismetallation of iron sulfur clusters, with functions. Iron-sulfur clusters are particularly sensitive to this form of damage which is why an upregulation of iron-sulfur cluster synthesis pathways are consistently observed when copper toxicity is present (47).

1.4 Sources of environmental Copper

The concentration of bioavailable copper in an environment determines the regulatory method used to balance this nutrient source with the needs of an organism. While the GOE shift, increasing the bioavailability of copper initiated a series of dramatic evolutionary changes still observed today like the Cu-homeostatic systems and utilization of copper in oxygen chemistry, more recent shifts in the availability of copper in the environment have challenged these homeostatic systems once again. As early as 7000 years ago anthropogenic copper depositions in riverbeds used for early copper smelting operations resulted in greater and greater concentrations of bioavailable copper in the affected areas (48). Today, a further globalized economy has continued the trend of increasing anthropogenic copper production and deposition in the environment. In 2000 alone, it is estimated that industry released nearly 1.4 billion pounds of copper into the environment according to the ATSDR. Mining operations, modern plumbing, fertilizer production, agricultural pesticide application and food supplementation are just some

modern sources of environmental copper. For instance, copper has been used for decades as a feed additive to promote weight gain. It's been sprayed over the surface of vineyards, citrus and tomatoes as an organic pesticide (49). It's used on surfaces in hospitals and within plumbing to reduce bacterial growth (50). Together, these common applications continue to increase the level of copper available in the environment. This increase in copper deposition and availability increases the need for organisms to develop stronger Cu-resistance, a need that drives the increased diversification rate observed in enteric bacteria for systems like the copper homeostasis and silver resistance island (CHASRI) (Fig 1.6)(51).

1.5 Model of prokaryotic copper homeostasis: *E. coli*

Escherichia coli (*E. coli*) is an abundant gram-negative bacterium that can be found in most environments today; colonizing soils, food products, and mammalian digestive tracts. While many strains are known to cause illness in humans, the majority present no danger to human health. Despite this knowledge, medical centers and hospitals alike often utilize the known broad-spectrum biocidal properties of copper to sterilize high-traffic surfaces of all potentially pathogenic bacteria like *E. coli* (50). Evolution found a similar solution to combat potentially pathogenic bacterial colonization by microbes like *E. coli*; macrophages will kill these bacterial invaders with excess levels of Cu by concentrating the metal in specialized organelles that contain the bacterial targets (39,52). These environments reflect the need for the robust Cu-homeostatic systems in *E. coli* that are highly conserved through prokaryotic species.

E. coli, because of this necessity and functionality, has been studied for its ability to handle and respond to Cu-stress. While Cu-uptake mechanisms in the bacteria remain

elusive, potentially involving either a ZIP-family transporter with a broad-substrate spectrum (53) or the simple diffusion of the metal across a membrane over time (54), efflux programs in the bacteria have successfully been described in detail and include the Cue, Pco and Cus systems. The Cue (Cu efflux) system, is responsive to periplasmic Cu via a MerR-like transcriptional activator, CueR. Activation of cueR by Cu(I) controls the expression of an inner membrane P-type ATPase CopA that actively transports Cu(I) to the periplasmic regions from the cytosol, a cytosolic cuprochaperone CopZ, and a periplasmic multicopper oxidase CueO which converts Cu(I) to Cu(II) which is less toxic to the cell (54). While this system does not change the overall cellular concentration of Cu, it reduces the metal's toxicity by shifting its localization to the periplasm (away from DNA in the cytosol) and by modifying its oxidation state.

The Pco (plasmid-born copper resistance system) gene cluster confers resistance to extreme concentrations of copper by recognizing periplasmic Cu(I) through a two component, pcoSR. The recognition of Cu(I) by pcoS, drives increased expression of pcoABCDRE gene cluster via the activation of pcoR in the cytosol. While similar to the Cue system in that overall cellular concentrations of copper are not altered by pco, the presence of this gene cluster in *E. coli* confers nearly 3x resistance to Cu ions than *E. coli* without the plasmid borne Cu resistance system (51,54).

In contrast to the Cue and Pco gene cluster, Cus (Cu sensing Cu efflux system) is responsible for detoxifying copper by reducing the overall copper concentration within *E. coli*. Like the pco gene cluster, the Cus regulon senses excess copper in the periplasm via a two-component system, CusSR. When cusR is temporarily phosphorylated by a cusS that has recognized periplasmic Cu(I)(55,56), the activated cusR promotes the

expression of *cusCFBA*, an antiporter pump specific to Cu(I) and Ag(I) that is a part of the resistance nodulation cell division family (57,58)(RND) (Fig. 1.7). The function of this pump is to detoxify excess copper by actively removing Cu(I) from the periplasmic space and into the extracellular matrix (57).

When homeostatic responses dependent on the direct sensing of copper in either the cytosol or periplasm are insufficient at preventing toxicity, repair systems responsive to Cu-induced cellular damage respond in kind. For instance, lipid oxidation by the uncontrolled redox cycling present during copper excess is addressed by the bacteria's envelope stress response via a two-component system, CpxAR. The activation of CpxR drives the expression of enzymes that acylate lipoproteins and halt further lipoprotein synthesis(20). Similar pathways recognize and remedy indirect copper stress; including correcting disulfide bond formation in maturing proteins, preventing mismetallation of proteins by switching dominant expression to alternative proteins less sensitive to mismetallation, and combating oxidative stress in the periplasm and cytosol (20).

1.6 Copper homeostasis in Eukaryotic systems

Like *E. coli*, singled-celled eukaryotes must prevent copper toxicity by balancing uptake, intracellular distribution and export out of the cell to maintain a strict copper quota. *Chlamydomonas reinhardtii*, a single-celled eukaryotic algae provides insight into the conserved functions of cellular metal homeostasis in eukaryotes. Unlike *E. coli*, balancing copper needs and toxicity demands coordination between export and uptake from multiple copper-pools within the extracellular environment, cytosol, and organelles (Fig. 1.8).

The movement of copper between these labile copper pools is largely dependent on a transcriptional activator, copper response regulator 1 (CRR1) which recognizes sequence GTAC inside copper response elements (CuREs) (10,59). Passive copper uptake transporter (CTR) genes contain CuREs that are responsive to CRR1 (60), allowing for the transport of copper down a concentration gradient which is created by several copper chaperones present in the cytosol. While these uptake systems become upregulated during periods of copper deficiency(60), CRR1-driven upregulation is also present during periods where cells are particularly sensitive to copper toxicity, as is the case with zinc deficiency when mismetallation of a limited number of Zn-containing metalloproteins by Cu can further exacerbate damage caused by zinc deficiency (61). Both conditions, by upregulating the expression of CTRs, increase the intracellular concentration of the metal relative to the extracellular environment. However, the reason for this crosstalk in eukaryotic cells is hypothesized to result from their ability of CRR1 to sequester copper effectively in lysosome-like organelles, like acidocalcisomes, to mobilize it when needed or appropriate (62).

When excess environmental copper is present, eukaryotic cells accumulate damage as increasing intracellular copper levels overwhelm these homeostatic controls. In *Chlamydomonas*, kinetic experiments determined that a decreasing capacity for Cu-efflux from the cell is responsible for the increased intracellular metal burden during these periods (63). Upregulation of sulfur assimilatory pathways and glutathione synthesis respond to the resulting increases in reactive oxygen species concentrations caused by this outsized metal-burden in the cytosol (63).

Mechanisms of copper homeostasis and the eukaryotic response to copper toxicity observed in *Chlamydomonas* are mirrored in multicellular eukaryotes. For instance, increases in the intracellular Cu-burden and increased toxicity derive from disrupted efflux in Cu-accumulating conditions (64,65) like Wilson's disease (66). CTR expression is increased when environmental Cu conditions become deficient to increase high-affinity Cu uptake in humans (67) and nematodes (4) alike. In multicellular organisms where copper is normally obtained through the diet, the expression of these CTRs and Cu-handling systems is particularly concentrated in the digestive tract where copper availability is determined not only by dietary intake but also by the microbial species that colonize the digestive tract (5).

1.7 Copper homeostasis in *Caenorhabditis elegans* host-microbe system

C. elegans are a soil dwelling bacterivore nematode who are raised on single-culture *E. coli* and present conserved copper homeostatic responses that have recently been described; a number of CTR homologs, like CHCA1, were described along the *C. elegans* digestive tract and is responsive to metal concentrations (4). Similarly, the *C. elegans* homolog for the p-type ATPase and active Cu-transporter, ATP7A (the protein who's misregulation is responsible for Wilson's disease in humans) demonstrates the same intestinal localization and enterocyte sequestration of excess copper to lysosome related granules during periods of Cu excess (64). In mutants for the *C. elegans* CUA-1, the ATP7A homolog, increased Cu-sensitivity and accumulation is observed during periods of excess (64).

The localization of these Cu homeostatic factors to the gut where bacterial colonization and activity takes place suggests a role for bacterial activity in mediating Cu

homeostasis (68). In particular, the activation of Cu-detoxification systems in *E. coli* during periods of Cu-excess, like the *cusRS*-mediated activation of increased Cu-efflux (55,57), would overlap with the *C. elegans* Cu-homeostatic response in these conditions (4,64,69,70). However, while the metabolic activity of the live bacteria nematodes feed on has been acknowledged (71,72), limited research has been conducted on their contribution to metal exposures beyond their capacity for passive sorption of free ions (65). Recent advances in *C. elegans* research describing the impact of bacterial activity on xenobiotic stressors in the host nematode (73,74) reflect the need for further research into these host-microbe interactions.

1.8 Figures

hydrogen 1 H 1.0079																	helium 2 He 4.0026												
lithium 3 Li 6.941	beryllium 4 Be 9.0122	<div style="display: flex; align-items: center; justify-content: center;"> <div style="border: 1px solid black; background-color: yellow; padding: 2px 5px; margin-right: 5px;">x # o</div> = essential transition metals </div>														boron 5 B 10.811	carbon 6 C 12.011	nitrogen 7 N 14.007	oxygen 8 O 15.999	fluorine 9 F 18.998	neon 10 Ne 20.180								
sodium 11 Na 22.990	magnesium 12 Mg 24.305	scandium 21 Sc	titanium 22 Ti 47.867	vanadium 23 V 50.942	chromium 24 Cr 51.996	manganese 25 Mn 54.938	iron 26 Fe 55.845	cobalt 27 Co 58.933	nickel 28 Ni 58.693	copper 29 Cu 63.546	zinc 30 Zn 65.38	aluminum 13 Al 26.982	silicon 14 Si 28.086	phosphorus 15 P 30.974	sulfur 16 S 32.065	chlorine 17 Cl 35.453	argon 18 Ar 39.948												
potassium 19 K 39.098	calcium 20 Ca 40.078	yttrium 39 Y 88.906	zirconium 40 Zr 91.224	niobium 41 Nb 92.906	molybdenum 42 Mo 95.96	technetium 43 Tc [98]	ruthenium 44 Ru 101.07	rhodium 45 Rh 102.91	palladium 46 Pd 106.42	silver 47 Ag 107.87	cadmium 48 Cd 112.41	indium 49 In 114.82	tin 50 Sn 118.71	antimony 51 Sb 121.76	tellurium 52 Te 127.60	iodine 53 I 126.90	krypton 36 Kr 83.798												
caesium 55 Cs 132.91	barium 56 Ba 137.33	hafnium 72 Hf 178.49	tantalum 73 Ta 180.95	tungsten 74 W 183.84	rhenium 75 Re 186.21	osmium 76 Os 190.23	iridium 77 Ir 192.22	platinum 78 Pt 195.08	gold 79 Au 196.97	mercury 80 Hg 200.59	thallium 81 Tl 204.38	lead 82 Pb 207.2	bismuth 83 Bi 208.98	polonium 84 Po [209]	astatine 85 At [210]	radon 86 Rn [222]	francium 87 Fr [223]	radium 88 Ra [226]	rutherfordium 104 Rf [261]	dubnium 105 Db [262]	seaborgium 106 Sg [266]	bohrium 107 Bh [264]	hassium 108 Hs [277]	meitnerium 109 Mt [268]	darmstadtium 110 Ds [271]	roentgenium 111 Rg [272]			
lanthanum 57 La 138.91	cerium 58 Ce 140.12	praseodymium 59 Pr 140.91	neodymium 60 Nd 144.24	promethium 61 Pm [145]	samarium 62 Sm 150.36	europtium 63 Eu 151.96	gadolinium 64 Gd 157.25	terbium 65 Tb 158.93	dysprosium 66 Dy 162.50	holmium 67 Ho 164.93	erbium 68 Er 167.26	thulium 69 Tm 168.93	ytterbium 70 Yb 173.05	lutetium 71 Lu 174.97	actinium 89 Ac [227]	thorium 90 Th 232.04	protactinium 91 Pa 231.04	uranium 92 U 238.03	neptunium 93 Np [237]	plutonium 94 Pu [244]	americium 95 Am [243]	curium 96 Cm [247]	berkelium 97 Bk [247]	californium 98 Cf [251]	einsteinium 99 Es [252]	fermium 100 Fm [257]	mendelevium 101 Md [258]	nobelium 102 No [259]	lawrencium 103 Lr [262]

Fig. 1.1 Transition metals required for survival in all organisms. Highlighted elements represent essential transition metals that must be acquired from the environment or diet of organisms to varying degrees. Transition metals that are not highlighted are considered nonessential but the properties they share with essential transition metals increase their potential for cellular toxicity and homeostatic misregulation of essential transition metals.

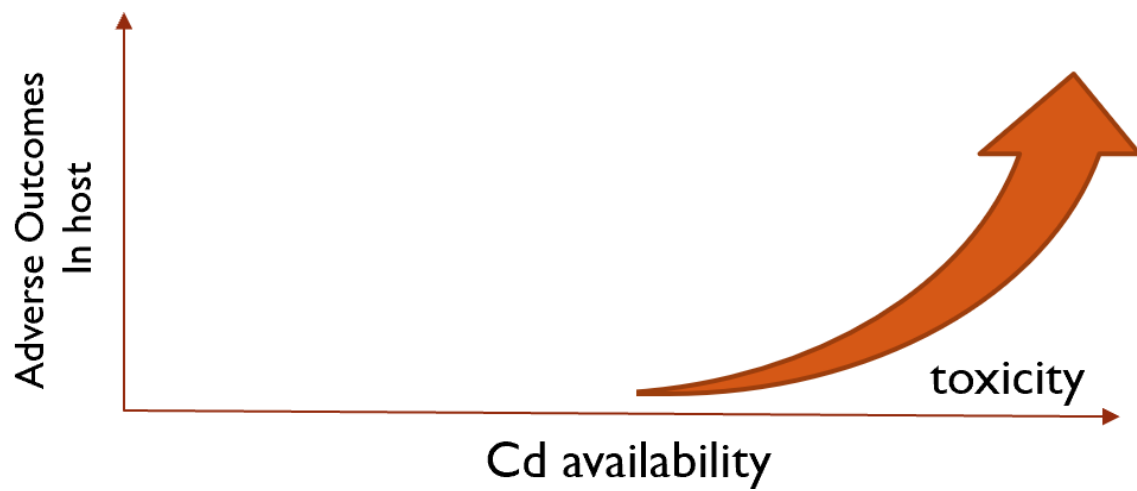


Fig. 1.2 Dose-dependent response to nonessential metals. Relationship with adverse outcomes and increasing concentrations of Cd. As a nonessential metal, there is no adverse outcomes associated with a lack of exposure.

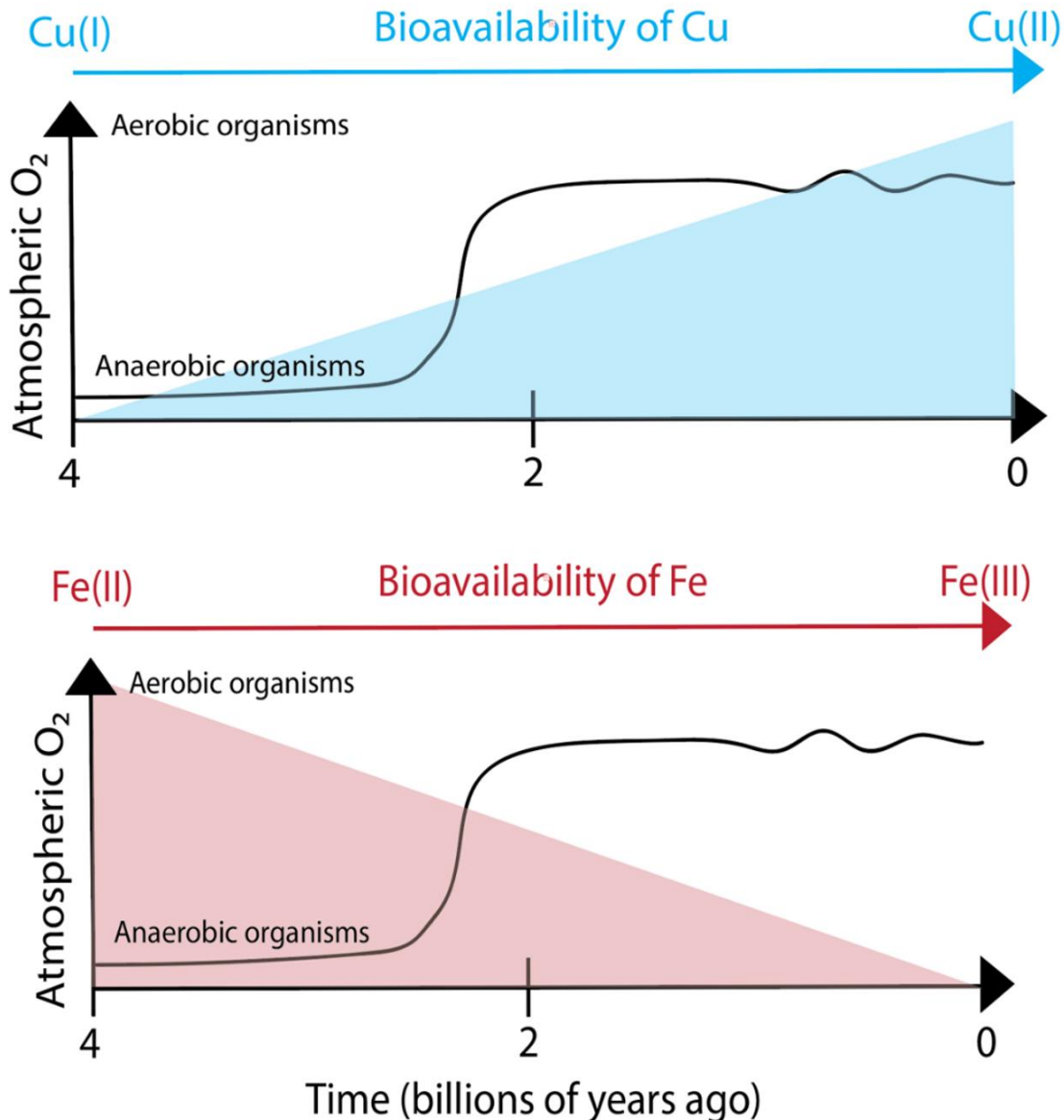


Figure 1.3 Change in the bioavailability of transition metals in relation to atmospheric O₂. Following the sudden increase in atmospheric oxygen, Cu in the form of Cu(II) increased the bioavailability of Cu while more Fe(III) relative to Fe(II) reduced the bioavailability of Fe. For this reason, the evolution of aerobic organisms favors increased usage of Cu-containing proteins when compared to anaerobic organisms who largely evolved prior to GOE.

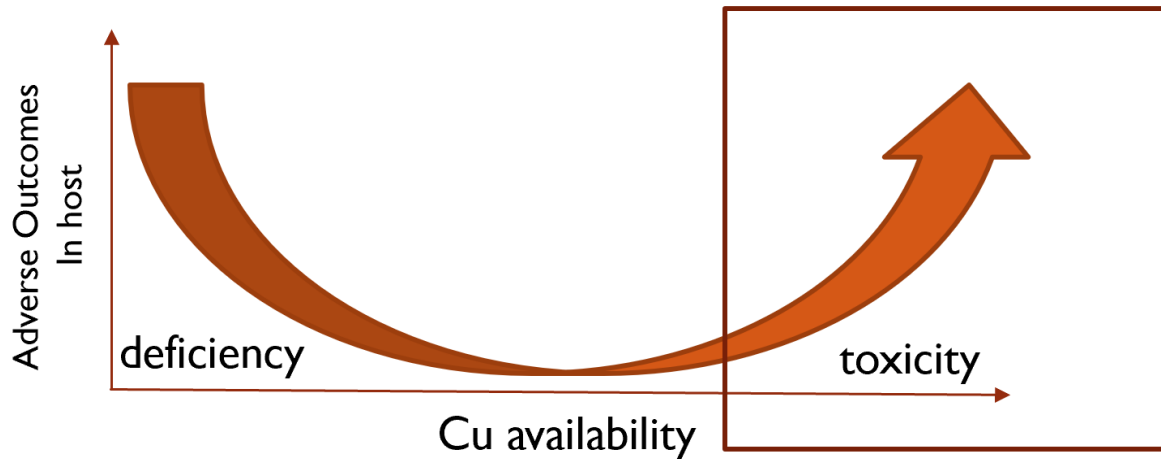


Figure 1.4 Dose-response curve associated with essential transition metals.

Change in Cu availability and relationship to adverse outcomes. As an essential transition metal, both limited and excess concentrations of Cu result in adverse outcomes. Therefore, homeostatic systems are required to prevent both deficiency and toxicity despite changing environmental concentrations.

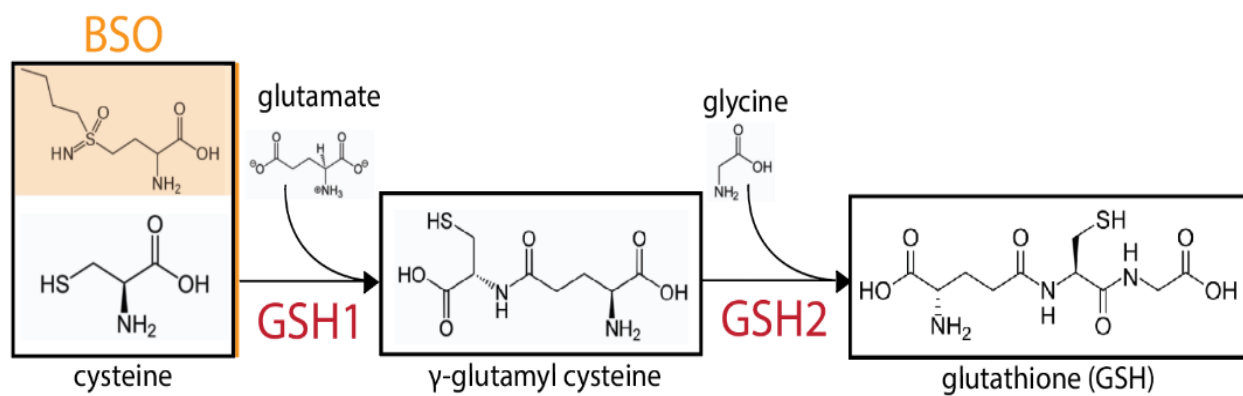


Figure 1.5 Inhibition of GSH1 synthesis. Buthionine sulfoximine (BSO) act as a permanent inhibitor of the enzyme, GSH1, that catalyzes the rate limiting step of glutathione synthesis.

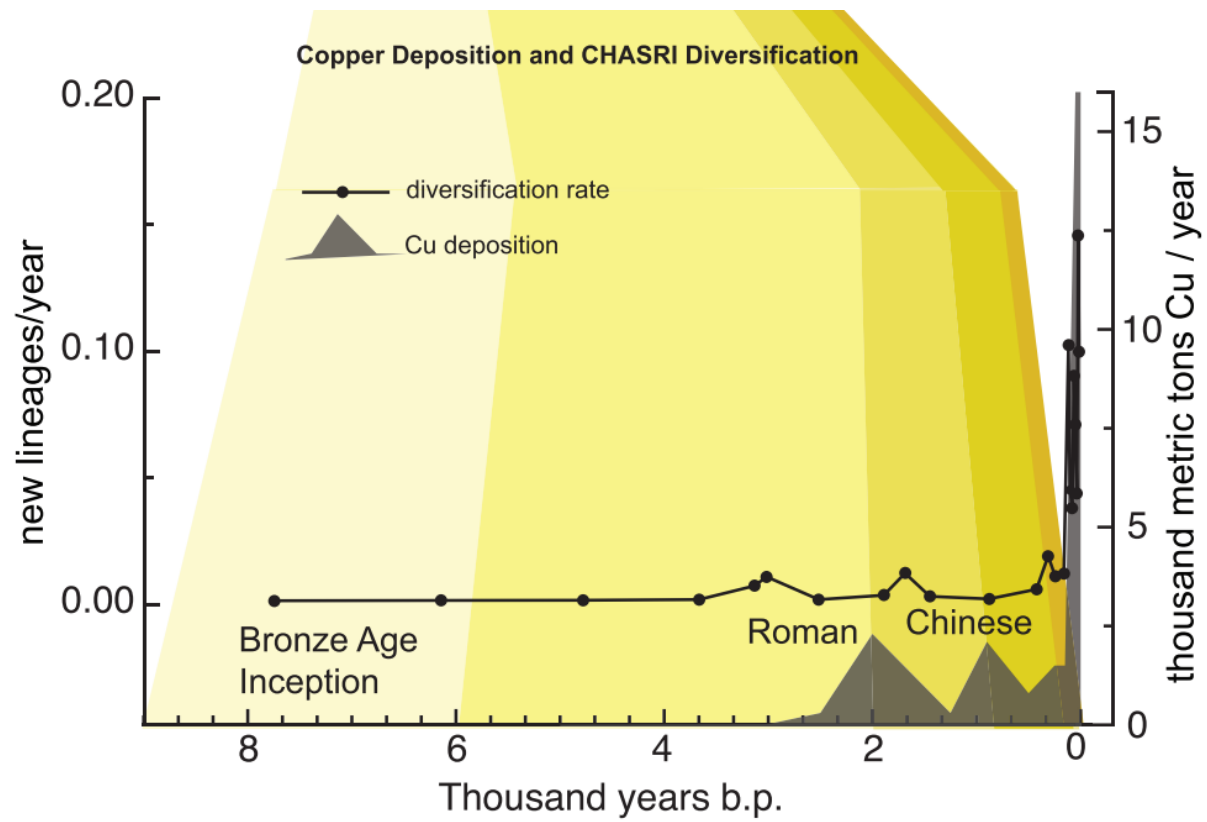


Fig 1.6 Association between increased anthropogenic Cu deposition and diversification rate of CHASRI in enteric bacteria. Genes clustered within CHASRI include *cus* and *pco* systems. (figure adapted from Staehlin et al. *Genome Biol Evol.* 2016)

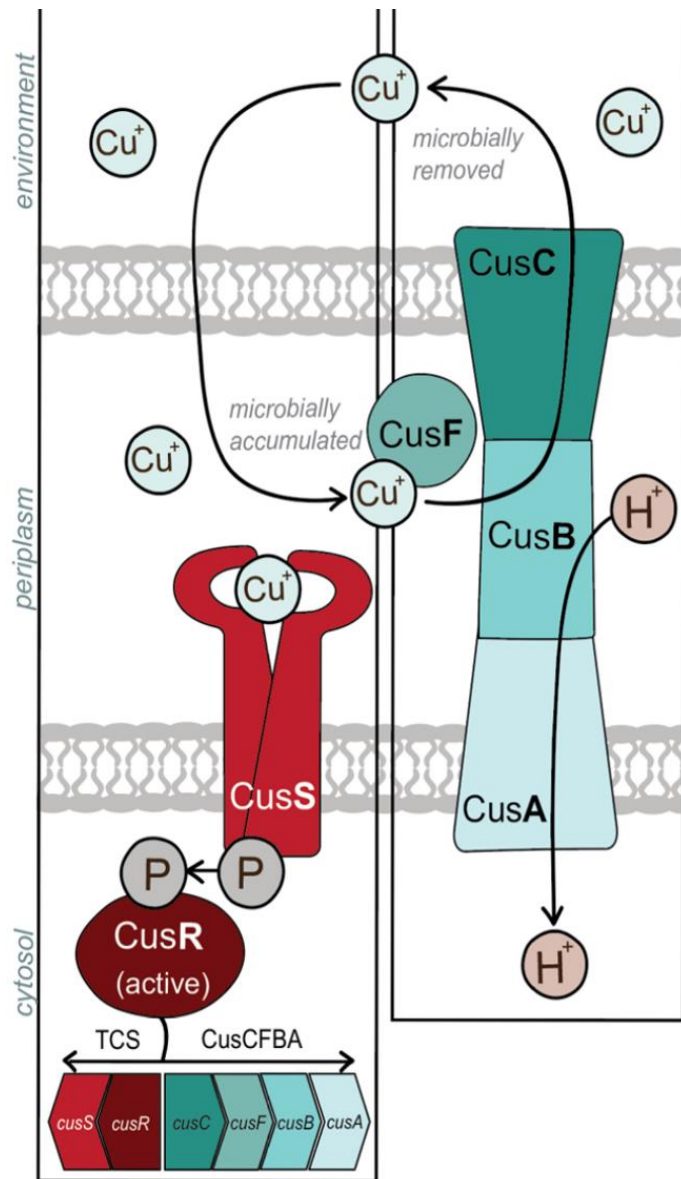


Fig. 1.7 CusRS and cusCFBA function. An example of a Cu homeostatic response in *E. coli* whereby activation of the cusRS two component system by periplasmic Cu(I) increases transcription of an antiporter pump, cusCFBA, driving the removal of excess Cu(I) from the cell.

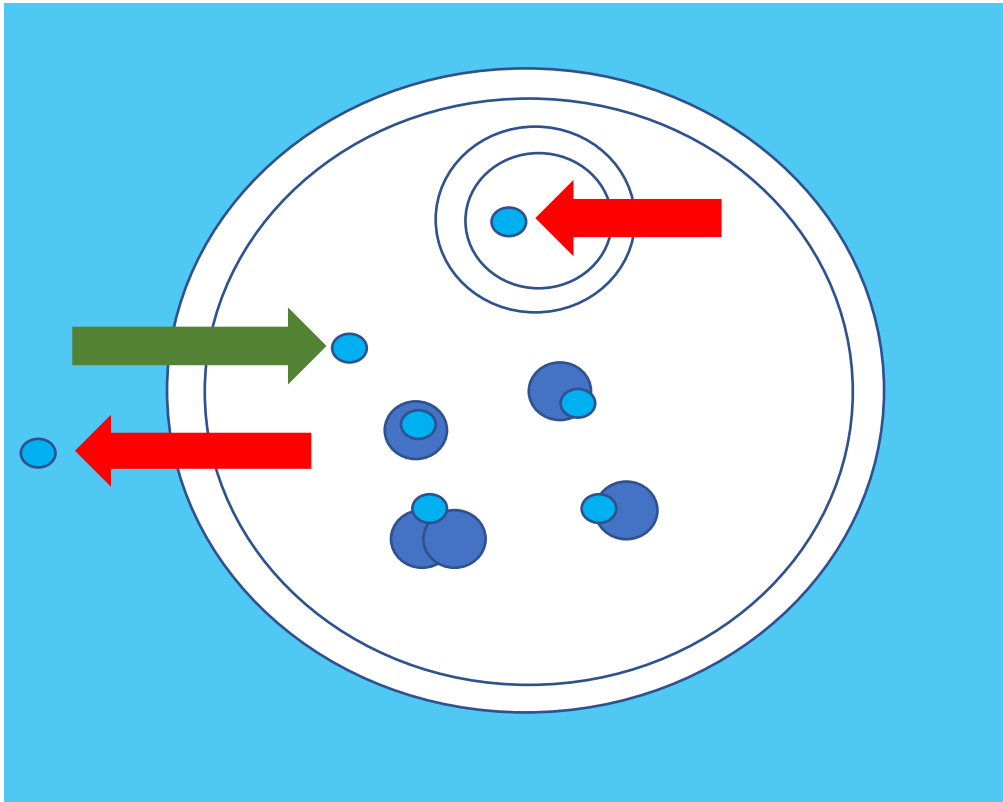


Fig. 1.8 Single-celled organism's homeostatic responses to environmental Cu. The green arrow indicates Cu (light blue circles) uptake into the cell. Red arrows depict either efflux or sequestration of Cu while dark blue circles describe methods of Cu distribution of subcellular locations. All of these homeostatic responses are coordinated in accordance with the concentration of Cu available in the environment.

1.9 References

1. Boal, A. K., and Rosenzweig, A. C. (2009) Structural biology of copper trafficking. *Chem Rev* **109**, 4760-4779
2. Waldron, K. J., Rutherford, J. C., Ford, D., and Robinson, N. J. (2009) Metalloproteins and metal sensing. *Nature* **460**, 823-830
3. Kropat, J., Gallaher Sean, D., Urzica Eugen, I., Nakamoto Stacie, S., Strenkert, D., Tottey, S., Mason Andrew, Z., and Merchant Sabeeha, S. (2015) Copper economy in *Chlamydomonas*: Prioritized allocation and reallocation of copper to respiration vs. photosynthesis. *Proceedings of the National Academy of Sciences* **112**, 2644-2651
4. Yuan, S., Sharma, A. K., Richart, A., Lee, J., and Kim, B. E. (2018) CHCA-1 is a copper-regulated CTR1 homolog required for normal development, copper accumulation, and copper-sensing behavior in *Caenorhabditis elegans*. *J Biol Chem* **293**, 10911-10925
5. Miller, K. A., Vicentini, F. A., Hirota, S. A., Sharkey, K. A., and Wieser, M. E. (2019) Antibiotic treatment affects the expression levels of copper transporters and the isotopic composition of copper in the colon of mice. *Proceedings of the National Academy of Sciences of the United States of America* **116**, 5955-5960
6. McArdle, H. J., and Erlich, R. (1991) Copper Uptake and Transfer to the Mouse Fetus during Pregnancy. *The Journal of Nutrition* **121**, 208-214
7. Jaiser, S. R., and Winston, G. P. (2010) Copper deficiency myelopathy. *J Neurol* **257**, 869-881

8. Berglund, M., Akesson, A., Nermell, B., and Vahter, M. (1994) Intestinal absorption of dietary cadmium in women depends on body iron stores and fiber intake. *Environmental health perspectives* **102**, 1058-1066
9. Dancis, A., Haile, D., Yuan, D. S., and Klausner, R. D. (1994) The *Saccharomyces cerevisiae* copper transport protein (Ctr1p). Biochemical characterization, regulation by copper, and physiologic role in copper uptake. *J Biol Chem* **269**, 25660-25667
10. Hill, K. L., and Merchant, S. (1992) In Vivo Competition between Plastocyanin and a Copper-Dependent Regulator of the *Chlamydomonas reinhardtii* Cytochrome c 6 Gene 1. *Plant Physiology* **100**, 319-326
11. Merchant, S. S., Schmollinger, S., Strenkert, D., Moseley, J. L., and Blaby-Haas, C. E. (2020) From economy to luxury: Copper homeostasis in *Chlamydomonas* and other algae. *Biochim Biophys Acta Mol Cell Res* **1867**, 118822
12. Takahashi, R., Ishimaru, Y., Senoura, T., Shimo, H., Ishikawa, S., Arao, T., Nakanishi, H., and Nishizawa, N. K. (2011) The OsNRAMP1 iron transporter is involved in Cd accumulation in rice. *Journal of Experimental Botany* **62**, 4843-4850
13. Bremner, I., and Campbell, J. K. (1978) Effect of Copper and Zinc Status on Susceptibility to Cadmium Intoxication. *Environmental Health Perspectives* **25**, 125-128
14. Duncan, A., Yacoubian, C., Watson, N., and Morrison, I. (2015) The risk of copper deficiency in patients prescribed zinc supplements. *J Clin Pathol* **68**, 723-725

15. Borkow, G., and Gabbay, J. (2004) Putting copper into action: copper-impregnated products with potent biocidal activities. *The FASEB Journal* **18**, 1728-1730
16. Au - Campbell, J. C., Au - Chin-Sang, I. D., and Au - Bendena, W. G. (2017) A *Caenorhabditis elegans* Nutritional-status Based Copper Aversion Assay. *JoVE*, e55939
17. Gudipaty, S. A., Larsen, A. S., Rensing, C., and McEvoy, M. M. (2012) Regulation of Cu(I)/Ag(I) efflux genes in *Escherichia coli* by the sensor kinase CusS. *FEMS Microbiol Lett* **330**, 30-37
18. Adamo, G. M., Brocca, S., Passolunghi, S., Salvato, B., and Lotti, M. (2012) Laboratory evolution of copper tolerant yeast strains. *Microbial Cell Factories* **11**, 1 - 1
19. Hausrath, A. C., Ramirez, N. A., Ly, A. T., and McEvoy, M. M. (2020) The bacterial copper resistance protein CopG contains a cysteine-bridged tetranuclear copper cluster. *J Biol Chem* **295**, 11364-11376
20. Giachino, A., and Waldron, K. J. (2020) Copper tolerance in bacteria requires the activation of multiple accessory pathways. *Molecular Microbiology* **114**, 377-390
21. Campos, O. A., Attar, N., Cheng, C., Vogelauer, M., Mallipeddi, N. V., Schmollinger, S., Matulionis, N., Christofk, H. R., Merchant, S. S., and Kurdistani, S. K. (2021) A pathogenic role for histone H3 copper reductase activity in a yeast model of Friedreich's ataxia. *Sci Adv* **7**, eabj9889
22. Fru, E. C., Rodríguez, N. P., Partin, C. A., Lalonde, S. V., Andersson, P., Weiss, D. J., Albani, A. E., Rodushkin, I., and Konhauser, K. O. (2016) Cu isotopes in

- marine black shales record the Great Oxidation Event. *Proceedings of the National Academy of Sciences* **113**, 4941-4946
23. Li, H., Webb, S. P., Ivanic, J., and Jensen, J. H. (2004) Determinants of the Relative Reduction Potentials of Type-1 Copper Sites in Proteins. *Journal of the American Chemical Society* **126**, 8010-8019
 24. Kroneck, P. M. H., Antholine, W. E., Kastrau, D. H. W., Buse, G., Steffens, G. C. M., and Zumft, W. G. (1990) Multifrequency EPR evidence for a bimetallic center at the CuA site in cytochrome c oxidase. *FEBS Letters* **268**, 274-276
 25. Mukhopadhyay, B. P. (2018) Recognition dynamics of trinuclear copper cluster and associated histidine residues through conserved or semi-conserved water molecules in human Ceruloplasmin: The involvement of aspartic and glutamic acid gates. *J Biomol Struct Dyn* **36**, 3829-3842
 26. Roeser, H. P., Lee, G. R., Nacht, S., and Cartwright, G. E. (1970) The role of ceruloplasmin in iron metabolism. *J Clin Invest* **49**, 2408-2417
 27. Kobayashi, K., Morita, S., Mizuguchi, T., Sawada, H., Yamada, K., Nagatsu, I., Fujita, K., and Nagatsu, T. (1994) Functional and high level expression of human dopamine beta-hydroxylase in transgenic mice. *J Biol Chem* **269**, 29725-29731
 28. Prohaska, J. R., Bailey, W. R., Gross, A. M., and Korte, J. J. (1990) Effect of dietary copper deficiency on the distribution of dopamine and norepinephrine in mice and rats. *J Nutr Biochem* **1**, 149-154
 29. Vendelboe Trine, V., Harris, P., Zhao, Y., Walter Thomas, S., Harlos, K., El Omari, K., and Christensen Hans, E. M. The crystal structure of human dopamine β -hydroxylase at 2.9 Å resolution. *Science Advances* **2**, e1500980

30. Höhner, R., Pribil, M., Herbstová, M., Lopez, L. S., Kunz, H.-H., Li, M., Wood, M., Svoboda, V., Puthiyaveetil, S., Leister, D., and Kirchhoff, H. (2020) Plastocyanin is the long-range electron carrier between photosystem II and photosystem I in plants. *Proceedings of the National Academy of Sciences* **117**, 15354-15362
31. Wood, P. M. (1978) Interchangeable copper and iron proteins in algal photosynthesis. Studies on plastocyanin and cytochrome c-552 in *Chlamydomonas*. *Eur J Biochem* **87**, 9-19
32. Ishigami, I., Lewis-Ballester, A., Echelmeier, A., Brehm, G., Zatspein, N. A., Grant, T. D., Coe, J. D., Lisova, S., Nelson, G., Zhang, S., Dobson, Z. F., Boutet, S., Sierra, R. G., Batyuk, A., Fromme, P., Fromme, R., Spence, J. C. H., Ros, A., Yeh, S.-R., and Rousseau, D. L. (2019) Snapshot of an oxygen intermediate in the catalytic reaction of cytochrome *c* oxidase. *Proceedings of the National Academy of Sciences* **116**, 3572-3577
33. Hitchler, M. J., and Domann, F. E. (2014) Regulation of CuZnSOD and its redox signaling potential: implications for amyotrophic lateral sclerosis. *Antioxid Redox Signal* **20**, 1590-1598
34. Ayala, A., Muñoz, M. F., and Argüelles, S. (2014) Lipid peroxidation: production, metabolism, and signaling mechanisms of malondialdehyde and 4-hydroxy-2-nonenal. *Oxid Med Cell Longev* **2014**, 360438
35. Popović-Bijelić, A., Mojović, M., Stamenković, S., Jovanović, M., Selaković, V., Andjus, P., and Bačić, G. (2016) Iron-sulfur cluster damage by the superoxide radical in neural tissues of the SOD1(G93A) ALS rat model. *Free Radic Biol Med* **96**, 313-322

36. Hosseini, M.-J., Shaki, F., Ghazi-Khansari, M., and Pourahmad, J. (2014) Toxicity of Copper on Isolated Liver Mitochondria: Impairment at Complexes I, II, and IV Leads to Increased ROS Production. *Cell Biochemistry and Biophysics* **70**, 367-381
37. Saenkham, P., Ritter, M., Donati, G. L., and Subashchandrabose, S. (2020) Copper primes adaptation of uropathogenic *Escherichia coli* to superoxide stress by activating superoxide dismutases. *PLOS Pathogens* **16**, e1008856
38. Dupont, C. L., Grass, G., and Rensing, C. (2011) Copper toxicity and the origin of bacterial resistance--new insights and applications. *Metallomics* **3**, 1109-1118
39. Djoko, K. Y., Phan, M.-D., Peters, K. M., Walker, M. J., Schembri, M. A., and McEwan, A. G. (2017) Interplay between tolerance mechanisms to copper and acid stress in *Escherichia coli*. *Proceedings of the National Academy of Sciences* **114**, 6818-6823
40. Halliwell, B., and Gutteridge, J. M. (1984) Oxygen toxicity, oxygen radicals, transition metals and disease. *The Biochemical journal* **219**, 1-14
41. Morgan, W. A., Kaler, B., and Bach, P. H. (1998) The role of reactive oxygen species in adriamycin and menadione-induced glomerular toxicity. *Toxicol Lett* **94**, 209-215
42. Li, Y., and Trush, M. A. (1993) DNA damage resulting from the oxidation of hydroquinone by copper: role for a Cu(II)/Cu(I) redox cycle and reactive oxygen generation. *Carcinogenesis* **14**, 1303-1311
43. Padilla-Benavides, T., George Thompson, A. M., McEvoy, M. M., and Argüello, J. M. (2014) Mechanism of ATPase-mediated Cu⁺ export and delivery to

- periplasmic chaperones: the interaction of Escherichia coli CopA and CusF. *J Biol Chem* **289**, 20492-20501
44. White, A. R., and Cappai, R. (2003) Neurotoxicity from glutathione depletion is dependent on extracellular trace copper. *Journal of Neuroscience Research* **71**, 889-897
 45. Peters, K., Pazos, M., Edo, Z., Hugonnet, J. E., Martorana, A. M., Polissi, A., VanNieuwenhze, M. S., Arthur, M., and Vollmer, W. (2018) Copper inhibits peptidoglycan LD-transpeptidases suppressing β -lactam resistance due to bypass of penicillin-binding proteins. *Proc Natl Acad Sci U S A* **115**, 10786-10791
 46. Irving, H., and Williams, R. J. P. (1953) 637. The stability of transition-metal complexes. *Journal of the Chemical Society (Resumed)*, 3192-3210
 47. Chillappagari, S., Seubert, A., Trip, H., Kuipers, O. P., Marahiel, M. A., and Miethke, M. (2010) Copper Stress Affects Iron Homeostasis by Destabilizing Iron-Sulfur Cluster Formation in *Bacillus subtilis*. *Journal of Bacteriology* **192**, 2512-2524
 48. Grattan, J. P., Adams, R. B., Friedman, H., Gilbertson, D. D., Haylock, K. I., Hunt, C. O., and Kent, M. (2016) The first polluted river? Repeated copper contamination of fluvial sediments associated with Late Neolithic human activity in southern Jordan. *Science of The Total Environment* **573**, 247-257
 49. Panagos, P., Ballabio, C., Lugato, E., Jones, A., Borrelli, P., Scarpa, S., Orgiazzi, A., and Montanarella, L. (2018) Potential Sources of Anthropogenic Copper Inputs to European Agricultural Soils. *Sustainability* **10**

50. Boyce, J. M. (2016) Modern technologies for improving cleaning and disinfection of environmental surfaces in hospitals. *Antimicrobial Resistance & Infection Control* **5**, 10
51. Staehlin, B. M., Gibbons, J. G., Rokas, A., O'Halloran, T. V., and Slot, J. C. (2016) Evolution of a Heavy Metal Homeostasis/Resistance Island Reflects Increasing Copper Stress in Enterobacteria. *Genome Biol Evol* **8**, 811-826
52. White, C., Lee, J., Kambe, T., Fritsche, K., and Petris, M. J. (2009) A role for the ATP7A copper-transporting ATPase in macrophage bactericidal activity. *J Biol Chem* **284**, 33949-33956
53. Grass, G., Wong, M. D., Rosen, B. P., Smith, R. L., and Rensing, C. (2002) ZupT Is a Zn(II) Uptake System in *Escherichia coli*. *Journal of Bacteriology* **184**, 864-866
54. Rensing, C., and Grass, G. (2003) *Escherichia coli* mechanisms of copper homeostasis in a changing environment. *FEMS Microbiol Rev* **27**, 197-213
55. Affandi, T., and McEvoy, M. M. (2019) Mechanism of metal ion-induced activation of a two-component sensor kinase. *Biochem J* **476**, 115-135
56. Affandi, T., Issaian, A. V., and McEvoy, M. M. (2016) The Structure of the Periplasmic Sensor Domain of the Histidine Kinase CusS Shows Unusual Metal Ion Coordination at the Dimeric Interface. *Biochemistry* **55**, 5296-5306
57. Mealman, T. D., Blackburn, N. J., and McEvoy, M. M. (2012) Metal export by CusCFBA, the periplasmic Cu(I)/Ag(I) transport system of *Escherichia coli*. *Curr Top Membr* **69**, 163-196

58. Conroy, O., Kim, E.-H., McEvoy, M. M., and Rensing, C. (2010) Differing ability to transport nonmetal substrates by two RND-type metal exporters. *FEMS Microbiol Lett* **308**, 115-122
59. Quinn, J. M., and Merchant, S. (1995) Two copper-responsive elements associated with the *Chlamydomonas* Cyc6 gene function as targets for transcriptional activators. *Plant Cell* **7**, 623-628
60. Page, M. D., Kropat, J., Hamel, P. P., and Merchant, S. S. (2009) Two *Chlamydomonas* CTR Copper Transporters with a Novel Cys-Met Motif Are Localized to the Plasma Membrane and Function in Copper Assimilation. *The Plant Cell* **21**, 928-943
61. Malasarn, D., Kropat, J., Hsieh, S. I., Finazzi, G., Casero, D., Loo, J. A., Pellegrini, M., Wollman, F. A., and Merchant, S. S. (2013) Zinc deficiency impacts CO₂ assimilation and disrupts copper homeostasis in *Chlamydomonas reinhardtii*. *J Biol Chem* **288**, 10672-10683
62. Kim, J.-H., Matsubara, T., Lee, J., Fenollar-Ferrer, C., Han, K., Kim, D., Jia, S., Chang, C. J., Yang, H., Nagano, T., Krausz, K. W., Yim, S.-H., and Gonzalez, F. J. (2021) Lysosomal SLC46A3 modulates hepatic cytosolic copper homeostasis. *Nature Communications* **12**, 290
63. Jamers, A., Blust, R., De Coen, W., Griffin, J. L., and Jones, O. A. H. (2013) Copper toxicity in the microalga *Chlamydomonas reinhardtii*: an integrated approach. *BioMetals* **26**, 731-740

64. Chun, H., Sharma, A. K., Lee, J., Chan, J., Jia, S., and Kim, B. E. (2017) The Intestinal Copper Exporter CUA-1 Is Required for Systemic Copper Homeostasis in *Caenorhabditis elegans*. *J Biol Chem* **292**, 1-14
65. Moyson, S., Town, R. M., Joosen, S., Husson, S. J., and Blust, R. (2019) The interplay between chemical speciation and physiology determines the bioaccumulation and toxicity of Cu(II) and Cd(II) to *Caenorhabditis elegans*. *J Appl Toxicol* **39**, 282-293
66. Gromadzka, G., Schmidt, H. H.-J., Genschel, J., Bochow, B., Rodo, M., Tarnacka, B., Litwin, T., Chabik, G., and Członkowska, A. (2005) Frameshift and nonsense mutations in the gene for ATPase7B are associated with severe impairment of copper metabolism and with an early clinical manifestation of Wilson's disease. *Clinical Genetics* **68**, 524-532
67. Liang, Z. D., Tsai, W.-B., Lee, M.-Y., Savaraj, N., and Kuo, M. T. (2012) Specificity Protein 1 (Sp1) Oscillation Is Involved in Copper Homeostasis Maintenance by Regulating Human High-Affinity Copper Transporter 1 Expression. *Molecular Pharmacology* **81**, 455-464
68. Geng, H., Shu, S., Dong, J., Li, H., Xu, C., Han, Y., Hu, J., Han, Y., Yang, R., and Cheng, N. (2018) Association study of gut flora in Wilson's disease through high-throughput sequencing. *Medicine (Baltimore)* **97**, e11743-e11743
69. Tvermoes, B. E., Boyd, W. A., and Freedman, J. H. (2010) Molecular characterization of numr-1 and numr-2: genes that increase both resistance to metal-induced stress and lifespan in *Caenorhabditis elegans*. *J Cell Sci* **123**, 2124-2134

70. Calafato, S., Swain, S., Hughes, S., Kille, P., and Stürzenbaum, S. R. (2008) Knock down of *Caenorhabditis elegans* cutc-1 Exacerbates the Sensitivity Toward High Levels of Copper. *Toxicological Sciences* **106**, 384-391
71. Mashock, M. J., Zanon, T., Kappell, A. D., Petrella, L. N., Andersen, E. C., and Hristova, K. R. (2016) Copper Oxide Nanoparticles Impact Several Toxicological Endpoints and Cause Neurodegeneration in *Caenorhabditis elegans*. *PLoS One* **11**, e0167613
72. Govindan, J. A., Jayamani, E., Zhang, X., Mylonakis, E., and Ruvkun, G. (2015) Dialogue between *E. coli* free radical pathways and the mitochondria of *C. elegans*. *Proc Natl Acad Sci U S A* **112**, 12456-12461
73. García-González, A. P., Ritter, A. D., Shrestha, S., Andersen, E. C., Yilmaz, L. S., and Walhout, A. J. M. (2017) Bacterial Metabolism Affects the *C. elegans* Response to Cancer Chemotherapeutics. *Cell* **169**, 431-441.e438
74. Backes, C., Martinez-Martinez, D., and Cabreiro, F. (2021) *C. elegans*: A biosensor for host–microbe interactions. *Lab Animal* **50**, 127-135

**CHAPTER 2: THE ROLE OF CTR UPREGULATION AND CYTOSOLIC
GLUTATHIONE DURING CRR1-DRIVEN CU UPTAKE AND TOLERANCE IN
*CHLAMYDOMONAS REINHARDTII***

2.1 Abstract

Cellular copper homeostasis is required of all living organisms today. In *Chlamydomonas reinhardtii*, a Cu-responsive transcription factor (CRR1) increases the expression of transcripts, including Cu-uptake transporters (CTRs), thought to promote passive Cu-uptake into the cell during Zn and Cu deficiency. However, it is not well understood how Cu is accumulated or how specific Cu toxicity is avoided. Accordingly, the research presented in this chapter describes the role of Cu uptake transporter (CTR) upregulation and cytosolic glutathione regulation during periods of CRR1 activation. Using a reverse genetic approach with artificial microRNAs (amiRNAs) and insertional mutants, CTR2 was found to be the major canonical CTR responsible for increased Cu accumulation during both Cu deficiency and Zn deficiency while CTR1 was responsible for high-affinity Cu-uptake when environmental Cu was exceedingly limited. The role of CTR3, the noncanonical CTR lacking a transmembrane domain, in Cu uptake and tolerance was not identified although it was found to be secreted to the periplasmic space during Cu deficiency. In identifying additional cytosolic factors that contribute to metal tolerance during periods of increased uptake, glutathione (GSH) was found to be a driver of passive Cu uptake during Zn deficiency as well as cytosolic metal tolerance during periods of increased CTR expression.

2.2 Introduction

2.2.1 *Chlamydomonas reinhardtii*

Chlamydomonas reinhardtii is a well-established model for metal metabolism that is ideal for this field of study for several reasons. First, it is readily grown as a homogenous cell type (1) in a well-defined growth medium that controls nutrients and other growth factors (e.g. aeration, light). Additionally, no amino acid or protein supplementation is required for growth (2). *Chlamydomonas* is also amenable to a variety of reverse genetic techniques (3) which is enabled by 3 fully sequenced genomes (nuclear, chloroplastic, mitochondrial).

2.2.2 Conditions for Cu uptake by *Chlamydomonas reinhardtii*

Passive transport of Cu into the cytosolic space is dependent on conserved CTRs that largely localize to the PM (4-5). Conservation of function across species was suggested when complementation studies demonstrated that human CTR1 (6) and *Chlamydomonas* CTRs are both capable of rescuing Cu-uptake in $\Delta ctr1$ yeast (defective in high-affinity Cu-uptake). Of the three genes that make up the CTR family in *Chlamydomonas*, the two canonical proteins (CTR1 and CTR2) were capable of complementation in *S. cerevisiae ctr1* mutants (4). In contrast, the non-canonical CTR3 lacks a transmembrane domain and is predicted to be a soluble protein (7). It is unknown what role CTR3 plays in Cu-assimilation in *Chlamydomonas*. In Cu-deficient situations, expression of all three members of the CTR family is upregulated in Cu deficiency (7) by a nutritional Cu sensor, Cu response regulator 1 (CRR1) to promote survival (Fig. 2.1). In addition to increasing the V_{max} of Cu(I) 20-fold with the expression of high-affinity Cu-uptake transporters (4), active CRR1 initiates Cu sparing programs to reduce the overall

Cu quota of the cell (8). Ubiquitously transcribed, active CRR1 binds Cu response elements (CuREs) to initiate these programs when Cu is bio-unavailable (9). However, it is unclear what controls this aspect of Cu-sensing.

Zn deficiency and excess is an environmental condition that paradoxically benefits the CRR1 transcription factor (Fig. 2.1), even though Cu hyper-accumulates during Zn deficiency (10). It is not known whether Zn itself directly interacts with CTRs to prevent Cu hyper-accumulation in replete conditions (a form of regulation that would be lost in Zn deficiency) or if another factor, regulated by CRR1, is contributing to a hyper-accumulating phenotype. Even with these inconsistencies, there is evidence that Zn-deficient cells require CRR1 activation for successful acclimation (11).

2.2.3 Copper complexation and distribution through the cytosol

Following uptake into the cytosol, free Cu would be toxic to the cell (mismetallation, redox cycling etc.) without the presence of cytosolic Cu-binding ligands. While the transfer of Cu from CTR to ATX1 via protein:protein interactions has been suggested in yeast (5), human models have instead supported a role for glutathione (GSH) as an intermediate between CTR and chaperone (12) because of its abundance in the cytosol and ability to form Cu(I)-GSH complexes (13) However, it was not known whether GSH was involved in Cu transfer between *Chlamydomonas* CTRs and ATX1. Regardless, after Cu is bound in the cytosol the metal is trafficked to chaperone-specific destinations within the cell. An interaction between these chaperones and P_{1B}-type ATPase Cu-transporters is thought to mediate the transport of Cu into multiple organelles (7).

Cu-ligand binding pools have the potential to contribute to Cu misregulation because of the inherent reliance of passive Cu-uptake on the maintenance of a

concentration gradient from the periplasmic space (high free Cu concentration) and into the cytosol (low free Cu concentration). As a result, non-toxic Cu hyper-accumulation could be one possible consequence of increasing the abundance of cytosolic Cu-binding ligands. For instance, *ATX1* and other predicted Cu binding ligands like *COX17*, *GSH1*(GSH synthesis) and *PCS1*(PC synthesis) are increasingly expressed in response to Cd exposures (where hyper-accumulated Cu is observed) (14). GSH redox pools are of particular interest regarding the maintenance of a Cu concentration gradient because of its high abundance and ability to bind Cu(I) in the sub-femtomolar range in cytosolic environments (15,16). It is unclear what role, if any, these cytosolic Cu-binding pool dynamics play in other Cu hyper-accumulating conditions like Zn deficiency where a xenobiotic stress (Cd) is not present.

2.2.4 Copper export out of the cytosol

Excretion of Cu from the cytosol can refer to two separate functions that are dependent upon the localization and orientation of P_{1B}-type ATPases (ATP7A and ATP7B in humans) in the membrane. When Cu-transporting ATPases localize to the TGN, ATP hydrolysis is coupled to Cu import, so that cuproproteins can be metallated. When the same P_{1B}-type ATPases are localized to vesicular compartments close to the PM, they transport Cu out of the cell (also against the concentration gradient). While the abundance of these active transporters do not vary greatly in response to Cu concentrations, localization is highly dependent on Cu concentration. Excess Cu initiates localization patterns that promote excretion out of the cell while replete or limited Cu promotes more localization to the TGN (17).

In *Chlamydomonas*, there are two putative Cu-transporting P_{1B}-type ATPases that are predicted to localize to the secretory pathway (CTP1 and CTP3) and two that are predicted to localize to the chloroplast membrane (CTP2 and CTP4) for metalation of plastocyanin in the photosynthetic apparatus (7). It is not known whether these putative transporters in *Chlamydomonas* change membrane localization in response to Cu concentration. However, selective organellar Cu-redistribution during Cu deficiency (18) implies the participation and coordination of the P_{1B}-type ATPases. An example of selective Cu-sparing mechanisms involves the maintenance of Cu-containing COXIIb in the mitochondria and simultaneous degradation of Cu-containing plastocyanin (monitored immunoblot of cultures in varying Cu concentrations). Plastocyanin abundance is decreased before COXIIb (8) because plastocyanin can be replaced with a functionally similar heme-containing cytochrome c6 (19). COXIIb, in comparison, has no such sparing mechanism. Furthermore, if these conserved P_{1B}-type ATPases respond to intracellular Cu-concentrations, it is unknown if they would localize in relation to Cu hyper-accumulation (excess Cu-condition) or downstream CRR1 signaling (functional deficiency condition) in response to Zn-deficient conditions.

2.2.5 Cu storage in the acidocalcisome

The acidocalcisome is a lysosome-related organelle (LRO) that is described as functioning in cation homeostasis. The LRO is similar to the platelet dense granules observed in human platelets (20). However, research characterizing these organelles is not well developed. In Zn-deficient *Chlamydomonas*, the Merchant group visualized the subcellular sequestration of hyper-accumulated Cu to an acidic, vacuolar compartments with rich deposits of Ca and polyphosphate which were hypothesized to be

acidocalcisomes (10). However, accumulation of a variety of metals to this acidic organelle has also been observed (21). Zn deficiency is an example of a condition where Cu foci, co-localized with Ca and polyP, have been observed. It has been suggested that Cu hyper-accumulation occurs as a way to prevent mismetallation of Zn-containing proteins with Cu (which is preferentially metallated ahead of Zn based on the Irving-Williams series) during limited Zn conditions (10). However, upon Zn resupply, hyper-accumulated Cu sequestered to the acidocalcisome becomes mobilized and the Cu quota returns to normal. Despite these observations, the formation, trafficking and mobilization of metals to the acidocalcisome remains poorly characterized.

2.3 Materials & Methods

2.3.1 Strains and culture conditions

Wildtype and insertional mutant strains were obtained from the Chlamydomonas Resource Center at the University of Minnesota. Artificial microRNA knockdowns were developed validated using RT-PCR. Cells were grown photomixotrophically in liquid Tris-acetate-phosphate (TAP) medium on a shaker at 22–25 °C for all experimental conditions and maintained by regularly inoculating fresh TAP medium with the appropriate culture. For longer term maintenance of cultures, agar-solidified TAP medium was also inoculated and stored under continuous light (50–100 $\mu\text{E m}^{-2} \text{s}^{-1}$, cool-white fluorescent lamps). Cell wall reduced strains CC425 and CC5390 were grown under the same light regime but with constant agitation of 140 rpm instead. TAP medium with or without Cu or Zn was used with revised trace elements (Special K) instead of Hunter's trace elements (25).

2.3.2 Growth rate determination

When measuring the growth rate during extended incubations, Chlamydomonas culture flasks were briefly removed from incubator conditions so that an aliquot of sample could be collected under a sterile hood. Once samples of all the cultures were collected, cell numbers and density of cultures were determined by counting 100x diluted samples using a hemocytometer.

2.3.3 Immunoblot Analysis

Immunoblot analysis required 15ml of cells at a density of 4-8 x 10⁶ cells/ml). Cultures were centrifuged at 1650xg before resuspension in 300 μ l buffer with 10mM Na-Phosphate buffer at a pH of 7.0. Membrane bound proteins were isolated with 3

freeze thaw cycles followed by centrifugation and resuspension in buffer containing 2% Triton. Following a snap freeze with LN₂, samples were store at -80°C until ready to be analyzed.

The Pierce BCA Protein Assay Kit with BSA standard was used to quantify protein concentrations. Then, 10µg of protein in each land was separated on SDS-containing polyacrylamide gels before transfer blotting onto nitrocellulose membranes. The nitrocellulose membranes were then blocked for 30 minutes with 3% dried non-fat milk in PBS with .1% (w/v) Tween 20 and incubated with primary antiserum. Antibodies directed against CF1 (1:40000), OEE1 (1:8000), Plastocyanin/Cyt c₆ (1:4000), CTR3 (1:1000) FEA1/2 (1:20000). The secondary antibody, used at 1:5000, was goat anti-rabbit conjugated to alkaline phosphatase, and processed according to the manufacturer's instructions.

2.3.4 Determination of metal concentrations

1x10⁸ cells were collected by centrifugation at the appropriate timepoints before the supernatant was either saved or discarded depending on experimental conditions. After removal of the supernatant, pellets were washed twice 1mM EDTA pH8.0 and once in Millipore grade water. After removal of the supernatant after the final wash, pellets were stored at -20C before further processing. Stored samples underwent batched ICP-MS/MS grade nitric acid digestion for 24h at room temperature or 2h at 65C before Millipore water was added for a final concentration of 2% nitric acid in samples. Prepared and digested samples were then analyzed on an Inductively coupled tandem mass spectrometer (ICP-MS/MS) for metal content. [32S] measurements were used to normalize concentrations across samples.

2.3.5 Establishment of Zn deficiency

To capture the development of zinc deficiency over time, cultures were initially maintained with media replete with zinc. When transitioning these cells to Zn-deficient media with 10 μ M Cu (added to visualize hyperaccumulation), Zn-replete cell cultures were first washed with 1mM EDTA pH of 8.0 to remove excess extracellular metals. Washed pellets were resuspended in Zn-deficient media to a concentration of 1x10⁶ cells/ml. For experiments testing the contribution of GSH in the rate of Cu uptake during the establishment of Zn deficiency, 10mM of L-Buthionine-sulfoximine (BSO) was added to the Zn-deficient media 24h after the initial transfer from Zn-replete media to inhibit the rate limiting step of GSH synthesis and reduce overall levels of cytosolic GSH as a result.

2.4 Results

2.4.1 CTR3 is secreted to the periplasm during Cu deficiency

CTR3, the noncanonical CTR3 that lacks a transmembrane domain and is upregulated during Cu deficiency to the same magnitude as the two canonical CTRs (CTR1 and CTR2)(17). To study its role in Cu deficiency, despite lacking a transmembrane domain, CTR3 was studied using western blot analysis (Fig 2.2). Unlike CoxIIb, the cytochrome oxidase subunit that is degraded as a copper sparing mechanism during Cu deficiency, changes in the CTR3 protein abundance in the intracellular space was not observed to change in response to environmental Cu concentrations. Conversely, in a cell-wall-reduced mutant, CTR3 was found to be a major component of the secretome in response to Cu deficiency, a response that mimics that Fe-concentrating soluble protein, FEA1/2.

2.4.2 *ctr3-1* does not produce CTR3 nor disrupt other CRR1-dependent activity

To better understand the function of the non-canonical CTR in *Chlamydomonas*, a validated KO line was required (Fig. 2.3). Once it was established that no CTR3 was detectable in *ctr3-1*(Fig 2.4), we sought to assess the extent to which the protein was required for the CRR1 response during Cu deficiency; specifically, the CRR1-dependent switch from the Cu-dependent plastocyanin to a functionally equivalent cytochrome c_6 which does not require Cu for its function. Though *ctr3* is upregulated during Cu deficiency, its absence does not impair the CRR1 functional switch from plastocyanin to Cytochrome c_6 or the maintenance of CoxIIb in the mitochondria (Fig 2.5). Therefore, any

Cu-deficient phenotypes observed in *ctr3-1* would be specific to the protein's absence and not a misregulation of other CRR1-dependent activity.

2.4.3 CTR3 is not required for Cu-uptake during Cu deficiency unlike CTR2

CTR3's upregulation in expression, in tandem with CTR2 and CTR3, and its accumulation in the periplasm during Cu deficiency suggests that it might contribute to or promote the increased uptake of Cu through the canonical CTRs by increasing the concentration gradient and rate of uptake. Therefore, Cu deficient cultures challenged with either 2uM and analyzed for Cu accumulation using ICP-MS/MS over a time course of one hour prior to challenge up to 3h after the addition of Cu to the deficient cultures (Fig. 2.6). However, *ctr3-1* was not found to impair the ability of the Cu-deficient cultures to accumulate copper within the timeframe tested when compared with CTR3. At Cu concentrations measured in mmol normalized to [32S], no significant changes were observed despite a small increase in the concentration of Cu observed 3h after the addition of metal to the deficient culture.

To understand which of the canonical CTR is responsible for driving copper uptake during periods of Cu deficiency in cell cultures, two insertional mutants for CTR2 (*ctr2-1* and *ctr2-2*) and one artificial microRNA knockdown for CTR1 (*ctr1*) were compared to cultures with fully functional CTR2 or CTR1 for their ability to drive Cu uptake during Cu deficiency (Fig. 2.6A-B). By challenging the cultures with the addition Cu to deficient, ICP-MS/MS analysis revealed that CTR2, but not CTR1, was required for Cu-uptake in low affinity condition when the availability of Cu in the media was greatly increased. During low-affinity Cu challenges in a deficient culture, CTR2 insertional mutants were less

effective at accumulating copper 30 minutes after the challenge when compared to CTR1 mutants.

2.4.4 CTR2 mediates Cu hyperaccumulation in transition to Zn deficiency

Upregulation of all canonical and noncanonical CTRs in *Chlamydomonas* is driven by CRR1 (Castruita, unpublished). While established Cu-deficiency requires CRR1 to maintain cell survival by promoting Cu-uptake and initiating Cu-sparing mechanisms, CRR1 is also required for cell survival during Zn deficiency where it promotes increased Cu uptake to prevent the competition of Cu with more limited Zn conditions. To determine whether CRR1-driven CTR2 expression plays a role in the establishment or maintenance of increased Cu uptake in this deficiency condition, a protocol (Fig. 2.7) was developed to transition Zn-replete cell cultures to Zn-deficient culture (Fig. 2.8) to monitor the rate of Cu accumulation (Fig 2.9) without disrupting the growth rate (Fig. 2.10) of the cultures which would impact the availability of the metals in the media. To this end, metal content analysis using ICP-MS/MS was undertaken for either the CTR2 insertional mutant, *ctr2-1*, and for CTR2 cell cultures at several timepoints while the culture was transitioning from a Zn-replete to a Zn-deficient media(Fig. 2.11). Within 24h of transfer to Zn deficient media, both CTR2 and *ctr2-1* cultures exhibited similar drops in the concentration of Zn observed in the cell pellets collected(Fig. 2.11). However, over the same period of time, Cu accumulation via the activation of CRR1 is significantly impaired in *ctr2-1* when compared to CTR2 where the insertional mutant for CTR2 exhibited less than half the Cu accumulation as the wildtype CTR2 cultures (Fig. 2.12). Therefore, the rapid uptake of Cu following a switch to Zn-deficient conditions is mediated, at least partially, by the upregulation of CTR2 by CRR1.

2.4.5 GSH drives CTR2-mediated Cu accumulation in transition to Zn deficiency

Driving passive Cu accumulation to the extremes observed during Zn toxicity likely requires the establishment and maintenance of a gradient by preventing the accumulation of free Cu beyond what is observed in the extracellular environment. To understand the cellular components maintaining this concentration for passive Cu uptake during Zn deficiency, we sought to analyze the role of the abundant tripeptide, glutathione which is independent of CRR1 regulation. The inhibition of gamma-glutamyl synthetase (the rate limiting enzyme for glutathione biosynthesis) using BSO 24h after the transfer of cultures to Zn deficiency allowed for the examination of glutathione's role in the establishment of Cu-hyperaccumulation during Zn deficiency (Fig. 2.13). Only 12h after the addition of BSO to the Zn-deficient media, the rate of hyperaccumulation is observed to slow via ICP-MS/MS quantification of cellular Cu concentrations. The trend of reduced Cu accumulation in BSO treated cells through 72h compared to cultures not exposed to BSO (Fig. 2.14), suggests that CRR1 independent factors also play a role in the establishment of Cu hyperaccumulation during Zn deficiency. Furthermore, the accumulation of Cu directly from the media was demonstrated by cumulative analysis of Cu concentrations if the combined pellet and supernatant measurements.

2.4.6 Loss of GSH sensitizes Chlamydomonas to non-essential metal toxicity

Increased CTR2 expression, as observed during Zn deficiency, in the absence of appropriate glutathione levels also has the potential to sensitize cultures to lower concentrations of non-essential metals that can hijack and compete with Cu (22). To test whether glutathione plays a role in preventing this consequence of Zn deficiency, knockdowns for *gsh1*, the rate limiting enzyme of glutathione synthesis were challenged

with excess Ag, which can compete with Cu for metal uptake likely through CTRs. Culture survival (Fig. 2.15) and cell growth of *gsh1* knockdown, when compared to control conditions (Fig. 2.16), was significantly more impaired by the addition of Ag to the media than empty vector controls (EVs)(Fig. 2.17), suggesting that the CRR1 response, during either Zn or Cu deficiency, could challenge the glutathione pool and sensitize cells to nonessential metal stress.

2.5 Paper in preparation

Functional redundancy and distinct features of CTR1 and CTR2 in copper assimilation in Chlamydomonas

^{1,2}Daniela Strenkert, ^{1,2}Stefan Schmollinger, ²Srinand Paruthiyil, ¹Bonnie C. Brown,

¹Kristen Holbrook, ¹Sydnee Green, ³Catherine Shafer, ²Jeffrey L. Moseley, ¹Patrice

Salomé, ¹Hosea Nelson, ⁴Crysten E. Blaby-Haas and ^{1,2,5}Sabeeha S. Merchant

¹Department of Chemistry and Biochemistry, University of California, Los Angeles, CA 90095

²California Institute for Quantitative Biosciences, University of California, Berkeley, CA, 94720

³Molecular Toxicology, University of California, Los Angeles, CA 90095

⁴Biology Department, Brookhaven National Laboratory, Upton, New York 11973

⁵Lawrence Berkeley National Laboratory, Berkeley, California 94720, USA

Short title: Copper transport and storage in Chlamydomonas

One sentence summary: Regulation of copper uptake and sequestration by members of the CTR family of proteins in Chlamydomonas

Corresponding author: Sabeeha S. Merchant (sabeeha@berkeley.edu).

ABSTRACT

Copper homeostasis is thoroughly regulated in most organisms in order to ensure its accurate and timely distribution to copper-requiring proteins while at the same time

avoiding toxicity of this highly reactive element. Successful acclimation to Cu deficiency and high affinity copper import are dependent on the CRR1 transcription factor, as *crr1* mutants fail to grow in Cu deficient growth media and are completely devoid of copper import. Among CRR1's target genes are a set of Cu transporters belonging to the Ctr/COPT gene family, that have important roles in the maintenance of high affinity Cu transport in various organisms. Based on sequence homology, localization and transcriptional profiling, we proposed that two putative Ctr/COPT-type Cu transporters, CrCTR1 and CrCTR2, both of which are CRR1 targets, are canonical copper importers in *Chlamydomonas*. Both CTR1 and CTR2 harbor a characteristic cysteine rich copper binding motif but also an unusually long extracellular N-terminal domain containing Met and/or His motifs. *ctr1* lines phenocopy the Cu dependent growth defect of *crr1*, which we attributed to their inability to acquire copper with high affinity. In contrast to that, copper import is impaired in *ctr2* mutants even at external copper concentrations in which *ctr1*'s copper import defect is rescued. It was shown previously that zinc deficiency disrupts the alga's copper quota, leading to a 20fold increase of intracellular copper which is stored in acidocalcisomes. Our data indicate that a combination of CTR1 and CTR2 dependent high affinity Cu import is the driving force in zinc deficiency dependent copper accumulation. Indeed, we showed that *crr1* mutants, which have been shown to be unable to hyper accumulate copper if grown in zinc deficiency can be forced to do so by nutritionally complementing the lack of function of CTR1 and CTR2 by an increase in external copper supply. Strikingly, we show that copper sequestration out of the acidocalcisome is also a *crr1* dependent process, specifically via CTR2, which we thus functionally localized to the acidocalcisome.

INTRODUCTION

Copper assimilation, trafficking and storage is tightly regulated in all kingdoms of life in order to ensure that demand meets supply in individual cellular compartments, but more so to avoid the inherent toxicity of this highly reactive element, either through its interactions with oxygen or indirectly through mis-metalation (23). The internalization of copper is highly conserved among eukaryotes and proceeds through a two-step reaction: extracellular reduction of Cu(II) to Cu (I) followed by cell entry via Cu(I) specific transporters (24-28, 4, 6). Non-specific divalent metal transporters belonging to the natural resistance-associated macrophage protein (NRAMP) metal ion transporters have a low affinity for copper and may function in copper acquisition under copper luxury conditions (29). High affinity copper transport is maintained by a number of different types of families of copper transporters, including copper uptake systems of the Ctr/COPT-type family and P-type heavy metal ATPases involved in copper export and sequestration.

CTR or COPT-type proteins (Copper TRansporter in prokaryotes and mammals, COPT for COPper TRansporter in land plants) contain conserved N- and C-terminal amino acid motifs and are highly selective for Cu(I) (7, 30). Ctr/COPT family members contain three putative transmembrane-spanning domains (TM1-3), an amino-terminal region that is rich in methionine residues, a cysteine rich, carboxy-terminal region and assemble to form trimeric pores (31-33). TM2 and TM3 contain two highly conserved signal motifs, MxxxM and GxxxG, respectively (34,35). It has been shown that the extracellular M-rich motif is essential for Cu transport activity by bringing Cu(I) to the entrance of the homotrimeric pore. The pore itself is composed of methionine triads

and serves to channel Cu across the lipid bilayer. After Cu sequestration through the pore, Cu(I) binds to Ctr's C-terminal Cysteine rich motifs, where it is delivered to soluble metallo- chaperones for intracellular distribution. The first characterization of members of the family of CTR-type copper transporters was done in *Saccharomyces cerevisiae*. The yeast genome encodes two canonical CTR-type copper transporters, Ctr1 and Ctr3, which are both localized to the plasma membrane. The two proteins have overlapping function (24, 36), disruption of both CTR1 and CTR3 is required to abolish high-affinity copper uptake in yeast. However, common yeast laboratory strains harbor a transposon mediated disruption of the CTR3 locus (24,37), allowing *yctr1* lines in this background to quickly become a valuable tool for evaluating CTR-type copper transporters from other organisms, based on their capability of rescuing *yctr1* phenotypes (38). A human homolog of yCtr1, hCTR1 (6) is localized to the plasma membrane and mediates high affinity copper uptake (39,40), while knockout of CTR1 in mice was lethal (41). *Drosophila melanogaster* expresses three Ctr1 genes, Ctr1A and Ctr1B both localize to the plasma membrane, are transcriptionally activated in response to copper limitation and are important in copper acquisition (42,43). In land plants, the CTR family of copper transporters seems to have undergone several duplication events. The *Arabidopsis thaliana* genome encodes six members belonging to the CTR-type family of copper transporters (*COPT1-COPT6*) (44). Of these, COPT1, COPT2 and COPT6 are plasma membrane localized, fully complementing the *yctr1* phenotype and are involved in Cu uptake into the cytosol (45-48). COPT5 has a similar function, but is a vacuolar copper exporter, required for copper re-allocation from intracellular storage organelles (49,50). Roles for COPT3/4 have yet to be defined. In rice, copper transport

and allocation is performed by *OsCOPT1* and *OsCOPT5*, which interact with each other (51). Each of *OsCOPT2*, *OsCOPT3*, and *OsCOPT4* interact with *OsCOPT6*, respectively, and mediate high affinity Cu import in the yeast *ctr1Δ ctr3Δ* double mutant (51).

To study plant-type Cu transporters in their native setting, we utilize the chlorophyte, unicellular green alga *Chlamydomonas reinhardtii* (*Chlamydomonas* here after) as a valuable reference system for trace metal homeostasis. Trace metal content of a defined culture media can be readily manipulated in *Chlamydomonas* to simulate different nutrient environments (25, 2), a high-quality reference genome is available for functional genomic studies (53) and, at the same time, the alga offers the utility of a fast-growing, facultative-phototrophic single-celled organisms with a wide range of metabolic capabilities. Copper is an essential nutrient in all eukaryotes, even at low intracellular concentrations, because it serves as a necessary cofactor in a number of essential enzymatic reactions involving redox chemistry. The major copper proteins in *Chlamydomonas* are well defined: (i) chloroplast localized plastocyanin, which serves as the favored soluble electron carrier from the cytochrome *b6f* complex to photosystem 1, (ii) mitochondrial cytochrome *c* oxidase subunit COXIIb which is essential for oxidative phosphorylation and (iii) the plasma membrane spanning ferroxidase FOX1, which is predominantly present in iron- limiting conditions and involved in high-affinity iron assimilation (54-56). Together these three proteins harbor the bulk of the cellular, protein-associated copper (8). Copper uptake in *Chlamydomonas* follows a saturation curve, which is indicative of a high affinity, carrier-mediated process (57-59, 27). Acclimation to limiting Cu environments is regulated on the transcriptional level by

Copper response regulator 1 (Crr1). Crr1 belongs to the family of SPL7 like transcription factors. Copper deficient *crr1* shows reduced growth as compared to the complemented line and was shown to regulate expression of 64 target genes in response to copper deficiency, the so-called Crr1 regulon (60,61). Based on sequence homology, biochemical localization and transcriptional profiling, two putative Cu transporters, CrCTR1 and CrCTR2 have been proposed to be canonical high affinity copper transporters in *Chlamydomonas* (4). Similar to other organisms' CTR proteins, their ability to transport Cu was confirmed by functionally complementing the growth defects of the yeast mutant *yctr1* (4). A Ctr-like protein, CrCTR3 appears to have arisen by a recent duplication event of CTR2, but it lacks the characteristic transmembrane domain and was shown to be a soluble protein (62). It was hypothesized that CTR3 might play a role in high affinity copper uptake in recruiting Cu in the periplasm to the site of reduction, similar to the proposed function of the soluble FEA proteins in iron assimilation (63).

Here, we report our findings on the regulation and functional characterization of both CTR-type Cu transporters: CrCTR1, CrCTR2 and the CTR-like protein CrCTR3. We localized CTR3 to the periplasmic space but concluded that only CTR1 and CTR2 are mediating copper import in *Chlamydomonas*, albeit with distinct affinities. Null mutants in *CTR1* show a copper deficiency dependent growth defect that can be explained by *ctr1*'s inability to acquire copper with high affinity. Interestingly, this phenotype can be rescued by as little as 12 percent residual CTR1. Notably, in addition to a defect in copper import, *ctr2* lines are unable to mobilize copper out of internal copper storage sites.

RESULTS

Impairment of copper uptake in a mutant defective in CRR1, the key transcription factor of copper homeostasis

Two members of the CTR family, CTR1, CTR2 and the CTR-like protein depicted CTR3, are among CRR1-regulated genes, as copper dependent expression of all of them is abolished in the *crr1* mutant, but is rescued to wild-type levels in a *CRR1* complemented line (Figure 2.18A). In order to assess the consequences of a reduced *CTR* transcript pool in *crr1* mutants on its ability to import copper, we grew the *crr1* mutant in parallel to a complemented line in growth medium that was not supplemented with copper. Once cells reached early stages of Cu-deficiency, copper was added back to the cultures (shown in Figure 2.18B). Copper import of *crr1* was estimated by measuring intracellular copper content before, during and after copper add-back using Inductively coupled plasma mass spectrometry (ICP-MS/MS). Interestingly, 3 hours after copper add back, copper content in *crr1* accounted for less than 10 percent of the amount that was observed in complemented lines (*CRR1*) (Figure 2.18C). We conclude that the observed impairment of copper import in *crr1* mutants is attributable to the loss of function in either CTR1, CTR2 or CTR3 or a combination thereof.

Features of CTR-type proteins in Chlamydomonas – a phylogenetic approach

In an effort to better understand the origins of Chlamydomonas CTR-type copper transporters and to allow functional prediction, we analyzed a total of 4676 CTR-type protein sequences from a wide variety of eukaryotic organisms via a phylogenetic approach (Figure 2.19). CTR1 and CTR2 share a number of common features characteristic for the CTR-type family of copper transporters

(Figure 2.19). These include an extracellular N-terminal domain containing Met and/or His motifs, an intracellular C-terminal domain containing Cys and/or His motifs, and three transmembrane domains (TM) constituting a pore for copper transport that is characteristic for this family of copper transporters. Most importantly, both, CTR1 and CTR2, harbor the MxxxM-x12-GxxxG motif across TM2 and TM3, which is considered the signature motif of CTR-type copper transporters. Notably, *Chlamydomonas* CTRs seem to be more closely related to fungi CTRs than to members of the CTR family found in land plants. Given the transmembrane domains, the presence of these conserved motifs and previous biochemical studies (4), we propose that CTR1 and CTR2 are canonical, periplasmic copper importers, while localization and functional prediction of CTR3 remained enigmatic. Based on protein similarity, most CTR-like proteins such as CTR3 are more similar to the CTR1 and CTR2 protein from each organism than to other CTR-like proteins, suggesting either multiple duplication and neo-functionalization events. We further propose that there is significant evolutionary pressure to maintain sequence identity between the soluble protein and the candidate transporter.

Localization of a CTR-like Cu transporters in *Chlamydomonas* revisited

While CTR1 and CTR2 both contain transmembrane domains and are localized to plasma membranes (4), subcellular localization of CTR3 still remained unclear. Since CTR3 lacks transmembrane domains and was determined to be a soluble protein (62), we hypothesize CTR3 to be either localized to the periplasmic space or to the cytosol. CTR3 might play a role in cellular copper import via concentrating copper within the periplasmic space or function as a Cu chaperone within the cytosol. In order to evaluate if CTR3

localizes to the periplasmic space, we took advantage of *Chlamydomonas* strains that are deficient in cell wall biosynthesis. If CTR3 is localized to the periplasma these strains should not be able to retain CTR3, instead we should be able to detect secreted CTR3 in the culture medium. To this end, we grew said strains in copper replete and copper deplete conditions. A comparison of TCA precipitated protein of spent culture medium with total cell lysate using immuno-detections with an antibody raised against CTR3, revealed the presence of the protein in the secreted proteome of copper deficiency grown cultures (Figure 2.20). Detection of copper conditional expressed FEA1 and FEA2 proteins, which have been shown to be secreted to the culture medium before served as experimental control, while copper dependent accumulation of one of the subunits of cytochrome *c* oxidase, CoxIIb, served as biological control (Figure 2.20). The observed secretion of CTR3 from the copper deficient wall-less mutant into the medium demonstrates that CTR3 is located to the periplasmic space, i.e. between the plasma membrane and the cell wall in wild-type cells (Figure 2.20). While both, the protein structure as well as subcellular localization excluded CTR3 to be a canonical, transmembrane spanning copper importer, we propose that CTR3 might help to increase the local copper concentration within the periplasmic space and therefor to enhance copper access to the CTR pore from the extracellular side.

A reverse genetics approach to *Chlamydomonas*' CTRs

To validate the function of CTR1, CTR2 and CTR3 in *Chlamydomonas* we used a combination of artificial microRNA (amiRNA) mediated gene targeting (64,65), CPF1/CRISPR based gene editing (66,67) and available insertion mutants from a *Chlamydomonas* mutant collection (*Chlamydomonas* Library Project, CLiP),(68). To

validate the function of CTR1, we generated *ctr1* knock-out lines using CRISPR/CPF1 gene editing adapted from previous protocols using homology-directed DNA replacement and the enzyme LbCPF1 as described in (66) in combination with a selection marker as described in (65). *CTR1* harbors a PAM (Protospacer Adjacent Motif) target sequence for LbCPF1 recruitment within its first exon (Figure 2.21A, orange line) and we used single stranded oligodeoxynucleotides (ssODNs) as a repair template to introduce two in-frame stop codons within the first exon of the *CTR1* gene (Figure 2.21A, grey filled arrow). From a total of 178 screened transformants, this approach resulted in a total of five independent lines depicted *ctr1-1*, *ctr1-2*, *ctr1-3*, *ctr1-4* and *ctr1-5*. Sequencing of the PCR product spanning the gene editing site confirmed the presence of the two stop codons in all five *ctr1* lines, with *ctr1-2* harboring an additional insertion of three in frame codons presumably introduced due to an error during DNA double strand repair (Supplemental Figure 2.S1). The insertion of the in two frame stop codons resulted in a lack of CTR1 transcripts (Figure 2.21B), which was also confirmed to result in the absence of the corresponding poly-peptide by immunodetection using CTR1 antiserum (Figure 2.21F). In addition, we generated artificial microRNA (amiRNA) lines targeting the 3 prime UTR of *CTR1* (64,65) (Figure 4, white arrow). Initial, positive assessment of amiRNA functionality was conducted using the reduction of *CTR1* mRNA abundance as readout. Three different, independent amiRNA lines, *ctr1-ami3*, *ctr1-ami8* and *ctr1-ami11* were chosen based on the level of residual *CTR1* mRNA abundance. *CTR1* mRNA abundance of *ctr1-ami3*, *ctr1-ami8* and *ctr1-ami11* was reduced to ~25, 20 and 12 percent as compared to control lines, respectively (Figure 2.21B). The reduction in mRNA abundance was reflected by a corresponding

reduction in CTR1 protein (Figure 2.21F). For phenotypic characterization of CTR2 and CTR3, we took advantage of the availability of insertional mutants from a mutant library (68). We identified two insertional *ctr2* mutants, depicted as *ctr2-1* and *ctr2-2* (Figure 2.21A, black arrows), and confirmed disruption of *CTR2* by PCR and Sanger sequencing. While *ctr2-1* harbors an insertion in the second exon of the gene and showed a complete loss of *CTR2* mRNA and the corresponding polypeptide (Figure 4C and G). In contrast to that, *ctr2-2* harbors an insertion within the second intron and expressed a low, but significant, amount of residual *CTR2* mRNA (Figure 2.21C, 3.2%), that was also confirmed by immuno-detection to result in residual amounts of translated protein (Figure 2.21G). The insertional mutant obtained with an insertion in *CTR3* was depicted *ctr3-1* and genotyping confirmed the predicted insertion of the cassette. Based on mRNA and protein abundance using qRT-PCR and immuno-detections, respectively, *ctr3-1* showed no residual CTR3 abundance (Figure 2.21D and H).

CTR1 and CTR2 are both mediating copper import in a copper replete environment

Copper content was measured by ICP-MS/MS. Interestingly, copper content was slightly but significantly reduced in *ctr1* knock-out lines, down to 77 percent of wildtype levels. In addition, *ctr2* mutants also showed a significant reduction in copper content that was correlated with the level of residual CTR2 protein in each respective mutant, with *ctr2-1* containing 23 percent and *ctr2-2* containing 34 percent less copper as compared to wildtype (Figure 2.22A). These data indicated that both CTR1 and CTR2 are involved in copper assimilation *in vivo*.

Copper conditional growth defect of a mutant in CTR1

As part of the initial characterization of all mutants, their growth on copper replete as well as copper deplete growth medium was assessed (Figure 2.22BC). Doubling times for all copper replete reference strains and mutants was between eight to ten hours, which is the expected generation time of photoheterotrophically grown *Chlamydomonas* cells (Figure 2.22B). We noted a subtle but significant growth defect of copper deficient *ctr2* lines, which were lagging behind the reference strain by approximately 2 hours in their doubling times (Figure 2.22B). Even more strikingly, *ctr1* lines were completely unable to grow if copper was omitted in the growth media and doubling times could not be determined (Figure 5C). The latter phenotype is strikingly similar to *crr1*'s inability to grow on copper deficient growth media (Figure 2.22C) and is causally connecting *crr1*'s growth phenotype to a lack of *CTR1* expression. Note that this is the case despite *ctr1*'s ability to substitute plastocyanin with Cyt c6, which is blocked in *crr1* mutants (Supplemental Figure 2.S2). In addition, growth of *ami-ctr1* lines was not affected at all if copper was omitted in the culture media (Figure 2.22B). The latter result is intriguing, since it indicates that as little as 12 percent of residual *CTR1* is sufficient to functionally rescue the copper conditional growth defect observed in *ctr1* mutants.

A major role for CTR1 in high affinity copper import?

Is the lack of growth of copper deficient *ctr1* lines resulting from the inability to acquire Cu with high affinity? If one, or all, of the candidate copper uptake proteins mediate copper assimilation, we should see a reduction in the copper content after Cu resupply in the respective mutant lines. For this purpose, intracellular copper content of mutant and wild-type strains was analyzed, with cells initially grown in copper deficient

media to induce Cu uptake systems until they reached early stages of Cu deficiency. Then either i) 2 μ M Cu (to probe low affinity Cu import) or ii) 100 nM Cu (to probe high affinity Cu import) was re-supplied to the growth medium and intracellular copper content was determined before and after Cu addition (Figure 2.23). When we probed for low affinity copper import, copper content looked similar in *ctr1* and *ctr3* mutants, as compared to their respective reference strains (Figure 2.23A and C), but was significantly lower in both *ctr2* knock-out strains (Figure 2.23B). We estimate that copper content in *ctr2-1* and *ctr2-2* lines was reduced to 14 and 20 percent of wild-type levels after 3 hours, respectively. Probing the cells for high affinity Cu import by adding 100 nM Cu validated our expectations based on our growth assays: after 3 hours, *ctr1* mutants show 10fold reduced copper content compared to reference lines, while *ctr2* mutants harbor 2-4fold less copper. Based on these results, we propose that CTR2 is the major copper assimilating importer in Chlamydomonas, while CTR1 has a specialized role to assimilate copper with high affinity.

More importantly, CTR1 and CTR2 are not functionally redundant, because i) *ctr2-2* lines show an impairment of copper import that parallels the one observed in *crr1* mutants despite wildtype expression of *CTR1* (Supplemental Figure 2.S3) and ii) *ctr1* mutants are unable to grow in copper deficiency despite a striking 30fold increase in *CTR2* mRNA abundance in this situation, indicative of a compensatory mechanism for a lack of CTR1 function (Supplemental Figure 2.S3).

Is copper hyper-accumulation in Zn deficient Chlamydomonas a CTR dependent pathway?

Zn deficient grown Chlamydomonas cells retain unusually high levels of

intracellular copper (10), The increase in intracellular Cu in a Zn deficient *Chlamydomonas* cell is concomitant with an increase in *CTR* expression (Figure 2.25). This increase in transcript abundance of *CTR1*, *CTR2* and *CTR3* in response to Zn deficiency is subtler than the one observed in copper deficient grown cells, but it is significant. Zinc is an essential trace element for all living cells as it is a co-factor of enzymes involved in DNA replication, transcription and carbon fixation. Accordingly, *Chlamydomonas* cells will cease growth if zinc is not supplemented in the growth medium. Notably, zinc deficient *crr1* mutants cease growth significantly earlier as compared to *CRR1* complemented lines, an observation that is not matched by any of the *ctr* mutants studied in this work (Supplemental Figure 2.S4). In order to investigate if copper uptake in zinc deficient cells is a CTR dependent pathway, we determined whether any of the *ctr* mutants showed reduced copper accumulation when grown in zinc deficiency. While all zinc deficient reference lines as well as *ctr3* lines were hyper-accumulating copper if 2 μM external copper was supplied, copper hyper-accumulation was significantly reduced in both, *ctr1* and *ctr2* mutant lines (Figure 2.25BC). Interestingly, the addition of excess exogenous copper to the growth medium (either 10 or 20 μM Cu, which corresponds to 5 and 10fold increase in copper) rescued this CTR-dependent, molecular phenotype. We noticed that the reduction of copper in zinc deficient *ctr1* mutants was more pronounced if we lowered the external copper supply (down to 200 nM Cu, Figure 2.25B). These data further underscore the role of CTR1 as a high affinity Cu importer.

Zn deficient *crr1* can be forced to accumulate copper by nutritionally complementing the loss of function of both CTRs

It has been shown previously that zinc deficient *crr1* mutants cease growth immediately and are unable to accumulate copper. But we showed in this work that zinc deficiency dependent copper accumulation is a CTR dependent pathway. We also showed, that the CTR-dependent copper import pathway can be by-passed by increasing the external amount of copper in the growth media. Accordingly, we wondered whether we can induce copper accumulation in zinc deficient *crr1*, if we increase the external supply of copper several fold. As *crr1* mutants completely cease to grow much earlier than wildtype cells, we established a time course experiment, in which we would start with a reasonable amount of cells, so that *crr1*'s zinc deficiency dependent growth defect would not impair our experiment. To this end, we grew *crr1* and *CRR1* lines in replete media and then washed exactly 2×10^8 cells with 1 mM EDTA to remove trace metals from the cell surface before transferring them to fresh medium with no Zn supplementation to a final concentration of 2×10^6 cells/ml (Figure 2.26). In addition, and to by-pass the block in copper import, we transitioned *crr1* lines to zinc deplete growth medium with 40 μ M external copper, which reflects an 20fold increase in copper as compared to the amount supplemented in the standard growth media. The accumulation of intracellular copper content was monitored by ICP-MS/MS. By the time cells had grown for 24 hours after the shift to Zn deplete medium, *crr1* mutants reached growth arrest. Strikingly, copper accumulation in *crr1* was 5 times more than its normal copper quota and corresponded to the amount that zinc deficient *CRR1* accumulates if grown in media supplemented with 1.2 μ M copper (Figure 9C).

Copper is sequestered into, but not out of the acidocalcisome in nutritionally complemented *crr1* mutants

It was shown previously that accumulated copper in zinc deficient grown *Chlamydomonas* is stored within lysosome related acidic organelles, so-called acidocalcisomes. Importantly, while accumulated copper is bio-unavailable to the cell, cells can utilize these copper storage sites if zinc is supplemented back to the growth media. We aimed to visualize spatial localization of accumulated copper in zinc deficient *crr1* using confocal microscopy with a previously validated Cu(I) sensitive dye, copper sensor-3 (CS3) (10). Using CS3, we can clearly visualize copper as distinct foci after 48 hours of growth in zinc deplete growth media in *CRR1*, and most importantly, copper accumulation was also observed in zinc deficient *crr1* mutants - if supplemented with excess (40 μ M) external copper (Figure 2.26D). The latter indicates that copper sequestration into the acidocalcisome is a *Crr1* independent process, but by increasing the external amount of copper 20fold, we were able to nutritionally complement *crr1* for CTR function. Notably, other candidate *CRR1* targets, like potential, organelle copper exporters, will still be genetically compromised. It was shown previously, that copper can be mobilized by the cell and transported out of the acidocalcisome after the addition of zinc to the growth medium. Indeed, and consistent with previous data, if we add back zinc to zinc depleted *CRR1*, cells show a complete reduction in acidocalcisome abundance after 7 hours, while the copper storage site abundance is not diminished in *crr1*. Accordingly, the copper transporter mobilizing copper from the copper storage site is also a *CRR1* target.

CTR2 is mobilizing internal copper storage sites in *Chlamydomonas*

As copper sequestration out of the acidocalcisome turns out to be a *CRR1* dependent pathway, we probed all *ctr* mutants for their ability to mobilize copper out of

the acidocalcisome after zinc addback using confocal microscopy and the copper(I) sensitive dye CS3. To this end, we grew *ctr* mutant and reference strains in growth medium without zinc supplementation. Distinct copper foci could be visualized in all strains using CS3, which is consistent with the moderate accumulation of copper in this situation (Figure 2.27BCD). Importantly, only *ctr2* mutants retain copper within the acidocalcisome even 7 hours after zinc was supplemented back to the growth medium, functionally co-localizing CTR2 to the acidocalcisome membrane (Figure 2.27).

DISCUSSION

Two paralogous CTRs - functional redundancy or neo-functionalization?

Copper homeostasis is tightly regulated in all kingdoms of life to ensure that intracellular demand meets extracellular supply. One such regulatory mechanism is the expression of a conserved family of high affinity Cu transporters belonging to the CTR/COPT family of transporters (69, 30). Our phylogenetic approach of over 4000 CTR/COPT family members from different species highlights domains that are structurally conserved and thus most likely functionally important during the evolution of these proteins. For example, all COPT/Ctr proteins contain three putative transmembrane regions (30).

Transcriptional profiling revealed copper nutritional responsive gene expression of CTR1, CTR2 and CTR3 and biochemical fractionation localized CTR1 and CTR2 to the plasma membrane (4). Previous results further suggested that *Chlamydomonas* CTR1 and CTR2, which may function either alone or cooperatively, can complement the loss of function of *ScCtr1* and *ScCtr3* in *S. cerevisiae* (4), thus we assumed that each of them contributes to copper homeostasis.

We show that both, CTR1 and CTR2 are involved in copper import, but we propose that CrCTR1 is the functional homologue of hCTR1 as it serves as the main high affinity copper importer in *Chlamydomonas* cells. In addition, CTR2 protein is expressed as two isoforms and seems to be heavily glycosylated based on the appearance using immuno-detections. Our data further implies that CrCTR1 and CrCTR2 are not functionally redundant, since overexpressed *CTR1* does not rescue *ctr2* specific phenotypes and vice versa.

While most well characterized COPT/Ctr proteins in other organisms are plasma membrane proteins that transport copper from extracellular spaces into the cytosol, members of the COPT/Ctr family were also shown to deliver copper to the cytosol out of copper storage sites, which can be vacuoles or lysosome related organelles (70-72). While copper sequestration into the copper storage site, the so-called acidocalcisome, is a CRR1 dependent process that can be bypassed by nutritionally complementing the CTR dependent copper import pathway, copper re-mobilization turns out to be also CRR1 dependent. More specifically, our data implies that CrCTR2 is indeed secondary localized to the acidocalcisome, as *ctr2* mutants are unable to sequester copper out of the copper storage site.

A novel, soluble CTR-like protein in the periplasma: CTR3

Like CTR1 and CTR2, the CTR3 protein has six Cys-Met motifs, but it does not contain any membrane-spanning α -helices and is a soluble protein (62). Data reported here strongly suggests the CTR-like protein, CTR3, to be localized within the periplasmic space. While CTR3 is not a copper transporter in the conventional sense, copper conditional expression still suggests a function for CTR3 in copper homeostasis.

CTR3's function might be similar to the one proposed for the FEA1/2 proteins, which are abundant soluble proteins that are localized to the periplasm and contribute to iron uptake. CTR3 could, by analogy with FEA1, feed the trimeric CTRs pore with copper from the periplasmic space.

While we did not observe implications pointing to a role for CTR3 in copper homeostasis, we propose that CTR3 might have a function in environmental conditions that we did not probe in this work. For example, Schirmer and colleagues showed that treatment of the heavy metal silver, that shares similar ion properties with copper, leads to induced accumulation of CTR3. It could well be that silver and other toxic heavy metals might be detoxified by chelation via CTR3 trapping the inert metal CTR3 complex thus impairing cell import.

Methods

Generation of CTR1 amiRNA strains

A miRNA targeting *Chlamydomonas* Ctr1 was designed according to (64,65) using the WMD3 tool at <http://wmd3.weigelworld.org/>. The resulting oligonucleotides for ctr1amiFor

ctagtGCGATCGGTGCTACTGGGTTAatctcgctgatcggcaccatgggggtggtggtgatcagcgctaT
AACTTAGTAGCACCGATCGCg and ctr1amiRev

ctagcGCGATCGGTGCTACTAAGTTAtagcgtgatcaccaccaccccatggtgccgatcagcgaga
TAACCCAGTAGCACCGATCGCa (uppercase letters representing miRNA*/miRNA sequences) were annealed by boiling and slowly cooling-down samples with a thermocycler before ligation into *SpeI*-digested pMS539, yielding pDS6. pDS6 was linearized by digestion with *HinDIII* and transformed into *Chlamydomonas* strain

CC4351 by vortexing with glass beads (73).

Overexpression of recombinant LbCPF1

LbCPF1 (Addgene # 102566) was expressed in Rosetta2(DE3)pLysS cells which were grown at 37°C to an OD₆₀₀ of 0.6. At this point, the cells were cooled to 16°C and induced with 0.5 mM IPTG. After overnight growth at 16°C, cells were harvested by centrifugation and resuspended in 15 ml per L of Nickel Buffer A (20 mM Tris-HCl pH 8.0, 500 mM NaCl, 5% glycerol, 25 mM imidazole) + 1 μg/ml leupeptin, 1 μg/ml pepstatin, 0.5 mM PMSF, then frozen at -80°C until ready for use. Cells from 2 L growth were lysed by sonication, clarified by centrifugation, then loaded onto two 5 ml HisTrap FF Crude columns (GE Life Sciences) connected in series, which were equilibrated in Nickel Buffer A. After washing off unbound material, bound protein was eluted with Nickel Buffer B (as for A, but at 250 mM imidazole). The eluted protein was desalted into Heparin Buffer A (20 mM HEPES-KOH, 5% glycerol, 280 mM KCl), and the protein concentration determined by absorption at 280 nm using a theoretical extinction coefficient of 1.25 (mg/ml)⁻¹cm⁻¹. TEV protease was added to a mass ratio of 1:50 protease to substrate, and tag removal proceeded overnight at 4°C. The sample was then filtered and loaded onto a 5 ml Heparin HP column. Bound protein was eluted with a gradient over 15 to 100% Heparin Buffer B (as for A, but at 1 M KCl). Fractions containing Cpf1 were pooled and concentrated. The concentrated protein was loaded onto a Sephacryl S-300 16/60 column equilibrated in 25 mM HEPES pH 7.5, 500 mM NaCl, 10% glycerol, 1 mM DTT. Fractions containing Cpf1 were pooled and concentrated to about 40 μM (5.9 mg/ml, by UV using ε = 1.17) and frozen in 10 μl aliquots at -80°C.

Generation of *ctr1* KO strains using LbCPF1/CRISPR

CC425, a cell wall reduced arginine auxotrophic strain, was used for transformation with a RNP complex consisting of a gRNA targeting a PAM sequence in exon1 of *CTR1* and LbCpf1 as described in (66) and modifications outlined in the following: Cultures were grown to 2×10^6 cells per milliliter and counted by using a hemocytometer. For optional pretreatment, 2×10^7 cells were suspended and centrifuged (5 min, 1424 x g) in Maxx Efficiency Transformation Reagent (1 mL) twice, followed by suspension in 230 μ L of the same reagent supplemented with sucrose (40 mM). Cells were incubated at 40°C for 20 minutes. Purified LbCPF1 (80 μ M) was preincubated with gRNA (1 nmol, targeting TTTGGGATGCGGCGGCTCAGCGG) at 25 °C for 20 min to form RNP complexes. For transfection, 230 μ L cell culture (5×10^5 cells) was supplemented with sucrose (40 mM) and mixed with preincubated RNPs and HindIII digested pMS666 containing the ARG7 gene conferring the ability to grow without arginine. In order to achieve template DNA-mediated editing, ssODN (~5 nmol, sequence containing two stop codons after the PAM target site (GTAGCTACTGACGTGTGCAGCTCGTTCATTTGGTAAGCGTAGGCGCTCAGCGG CTACTGCACGACGACCGGCGCTCTGGCGTACCGGTTCG) was added. Final volume was 280 μ L. Cells were electroporated in a 4-mm gap cuvette (Biorad) at 600 V, 50 μ F, 200 Ω by using Gene Pulser Xcell (Bio-Rad). Immediately after electroporation, 800 μ L of TAP with 40 mM sucrose was added. Cells were recovered overnight in darkness and without shaking in 5 mL TAP with 40 mM sucrose and polyethylene glycol 8000 0.4% (w/v) and then plated after a 5 min centrifugation at RT and 1424 x g using the starch embedding method. We were using 60% starch as

described in the following: Corn starch was washed sequentially twice with distilled water and once with ethanol. The washed starch was stored in 75% ethanol to prevent bacterial contamination. Before each experiment, the ethanol was replaced with TAP-sucrose medium by repeated centrifugations and resuspensions (5 times). The starch was finally resuspended to 60% (w/v) in TAP-sucrose medium and polyethylene glycol 8000 0.4% (w/v); 0.5 ml of the starch suspension was spread with one electroporation reaction after over night recovery over the top of solid TAP medium in a petri dish plate. After 14 days, colonies were transferred to new plates. Since we did not expect a phenotype, we used colony PCR to screen for successful genome editing at the *CTR1* locus. Colony PCR of transformants was performed as follows: after one week of growth, half of each colony on TAP plates was resuspended in 50 μ L 10 mM Tris-HCl (pH 8) buffer in a 96 well plate. Cells were heated to 96 °C for 10 min. After vortexing, 96 well plates were spun down for 4 min at \sim 1000 x *g*. Supernatants containing the DNA were transferred to new 96 well plates. qPCR on a total of 178 clones was performed using oligos Ctr1screenfor CAGCTCGTTCATTTGGGATG (which will not result in annealing and unsuccessful PCR amplification if genome editing occurred) and Ctr1unirev GTGTGAGAGCTGGCTGATCC. The following program was used for all qPCR reactions: 95°C for 5 min followed by 40 cycles of 95°C for 15 s, and 65°C for 60 s. This resulted in 11 clones that showed failed qPCR amplification and that were screened using oligos Ctr1seqfor ACGTGTGCAGCTCGTTCATT and Ctr1unirev GTGTGAGAGCTGGCTGATCC. Sequencing of the PCR products using oligo Ctr1unirev revealed that we had ssODN mediated gene editing within the first exon of *CTR1* in 5 of the clones which all showed successful introduction of the two stop

codons. One of the clones that we depicted *ctr1-3* also showed random integration of three base pairs downstream of the gene editing target site in addition to the two stop codons in exon1 (Supplemental Figure 2.S1).

Culture conditions and Chlamydomonas strains

Insertional mutant lines from the Chlamydomonas Library Project (CliP) (Li et al., 2019) depicted *ctr2-1* (LMJ.RY0402.151308), *ctr2-2* (LMJ.RY0402.163662), *ctr3-1* (LMJ.RY0402.179604) and corresponding wildtype strain CC4533 were genotyped by PCR and amplicons were sequenced to confirm predicted integration of the insertion cassette. The *crr1* mutants (CC5068) and *crr1* lines complemented with *CRR1* genomic sequence depicted as CRR1 (CC5070) were characterized previously. Unless stated otherwise, cells were grown in Tris-acetate-phosphate (TAP) with constant agitation in an Innova incubator (160 rpm, New Brunswick Scientific, Edison, NJ) at 24°C in continuous light (90 $\mu\text{mol m}^{-2} \text{s}^{-1}$), provided by cool white fluorescent bulbs (4100K) and warm white fluorescent bulbs (3000 K) in the ratio of 2:1. Cell wall reduced strains CC425 and CC5390 were grown under the same light regime but with constant agitation of 140 rpm instead. TAP medium with or without Cu or Zn was used with revised trace elements (Special K) instead of Hunter's trace elements (2). *Ctr1*-amiRNA strains were either inoculated from a plate into standard TAP(NH₄) to repress the artificial micro-RNA or a modified TAP(NO₃) medium where KNO₃ substituted NH₄Cl in the Beijerinck solution as the sole nitrogen source to induce the artificial micro-RNA promoted by the *NIT1* promoter (65). If cells were grown on TAP(NO₃) medium, we also substituted ammonium molybdate by sodium molybdate (one of the 7 components of the revised trace element solutions).

Precipitation of secreted proteins

Cell wall less CC5390 cells were grown in three rounds of Cu deficient TAP. Cells were collected by centrifugation at 4°C for 10 minutes at 1424 x *g*. Following centrifugation, pellets were resuspended in a lysis (125 mM Tris-HCl pH 6.8, 20% Glycerol, 4% SDS, 10% β-Mercaptoethanol, 0.005% Bromphenolblue). After a second centrifugation (4°C, 10min., 4000rpm), the supernatant was filtered through a 0.4 micron filter before 10% of ice cold TCA (100% w/v) was added to the samples. Samples were mixed overhead and incubated overnight at 4°C. Following incubation, the samples were centrifuged at 4°C for 10 min at 1424 x *g* and resuspended in acetone that had been kept on ice. Another centrifugation (4°C, 10min, 1424 x *g*) was completed before final cell pellets were resuspended in 2 x sample buffer (125 mM Tris-HCl pH 6.8, 20% Glycerol, 4% SDS, 10% β-Mercaptoethanol, 0.005% Bromphenolblue) and incubated for 10 minutes at 65°C before storage in -80°C.

RNA extraction and Quantitative real-time PCR

3 x 10⁷ cells were collected by centrifugation for 5 min at 1424 x *g*, 4°C. RNA was extracted using Trizol reagent. For subsequent DnaseI treatment of all RNA samples, Turbo DNase (Ambion) was used before concentrating and cleaning with the Zymo Research RNA Clean & Concentrator™-5 Kit according to the manufacturer's instructions. Reverse transcription was primed with oligo dT(18) using 2.5 µg of total RNA and SuperScript III Reverse Transcriptase (Invitrogen) according to the manufacturer's instructions. The subsequent cDNA was diluted 10-fold before use. qRT-PCR reactions contained 5 µL of cDNA corresponding to 100 ng of total RNA, 6 pmol of each forward and reverse oligonucleotide, and 10 µL of ITAQ Mastermix in a

20 μ L volume. The following program was used for all qRT-PCR reactions: 95°C for 5 min followed by 40 cycles of 95°C for 15 s, and 65°C for 60 s. Fluorescence was measured at the end of each 65°C cycle. A melting curve analysis was performed at the conclusion of the cycles from 65 to 95°C with fluorescence reads every 0.5°C. Relative abundances were calculated using LinReg, the abundance (No) of Rack1 served as reference transcript.

Antibody production and protein analyses by immunodetection

Antibodies to CTR1 were produced by COVANCE by immunization using the subcutaneous implant procedure of rabbits on 118 day protocol with synthetic peptide Ac-CNAKARRGSGDALGANTADHKKGASS-amide. For analyses of total proteins, 15 ml of a culture with (cell density of $4-8 \times 10^6$ cells/ml) was centrifuged at $1650 \times g$. The resulting cell pellet was resuspended in 300 μ l of a buffer composed of 10mM Na-phosphate buffer (pH 7), an EDTA-free Protease inhibitor (Roche), 2% SDS, and 10% sucrose. For analyses of soluble and membrane fractions, 15 ml of a culture (cell density of $4-8 \times 10^6$ cells/ml) was centrifuged at $1650 \times g$. The cell pellet was resuspended in 300 μ l of buffer containing 10 mM Na-Phosphate buffer (pH 7). Soluble and membrane fractions were isolated by lysing cells with 3 freeze thaw cycles (-20°C to room temperature). After lysing, centrifugation at 4°C separated soluble proteins (supernatant) from the membrane bound proteins (pellet). Membrane-bound proteins were resuspended in 200 μ l Na-Phosphate buffer supplemented with 2% Triton before a fast freeze of both fractions in liquid N₂. Samples were stored at -80°C prior to analysis. Protein amounts were determined using a Pierce BCA Protein Assay Kit against BSA as a standard and diluted with 2 x sample buffer (125 mM Tris-HCl pH 6.8,

20% Glycerol, 4% SDS, 10% β -Mercaptoethanol, 0.005% Bromphenolblue). Proteins were separated on SDS-containing polyacrylamide gels using 10 μ g of protein for each lane. The separated proteins were then transferred by semi-dry electro-blotting to nitrocellulose membranes (Amersham Protran 0.1 NC). The membrane was blocked for 30 min with 3% dried non-fat milk in phosphate buffered saline (PBS) solution containing 0.1% (w/v) Tween 20 and then incubated in primary antiserum. The PBS solution was used as the diluent for both primary and secondary antibodies. The membranes were washed in PBS containing 0.1% (w/v) Tween 20. Antibodies directed against CF1 (1:40000), OEE1 (1:8000), Plastocyanin/Cyt c6 (1:4000), CTR3 (1:1000) CTR2 (1:1000), CTR1 (1:1000), FEA1/2 (1:20000). The secondary antibody, used at 1:5000, was goat anti-rabbit conjugated to alkaline phosphatase, and processed according to the manufacturer's instructions.

Quantitative metal, phosphorus and sulfur content analysis

1×10^8 cells (culture density of $3-5 \times 10^6$ cells/ml) were collected by centrifugation at $1424 \times g$ for 3 min in a 50 ml falcon tube. The cells were washed 2 times in 50mL of 1 mM Na₂-EDTA pH 8 (to remove cell surface-associated metals) and once in Milli-Q water. The cell pellet was stored at -20°C before being overlaid with 286 μ l 70 % nitric acid and digested at room temperature for 24 h and 65°C for about 2 h before being diluted to a final nitric acid concentration of 2 % (v/v) with Milli-Q water. Complementary aliquots of fresh or spent culture medium were treated with nitric acid and brought to a final concentration of 2 % nitric acid (v/v). Metal, sulfur and phosphorous contents were determined by inductively coupled plasma mass spectrometry on an Agilent 8800 Triple Quadropole ICP-MS instrument by comparison to an environmental calibration

standard (Agilent 5183-4688), a sulfur (Inorganic Ventures CGS1) and phosphorus (Inorganic Ventures CGP1) standard. ^{89}Y served as an internal standard (Inorganic Ventures MSY-100PPM). The levels of analytes were determined in MS/MS mode. ^{23}Na , ^{24}Mg , ^{31}P , ^{55}Mn , ^{63}Cu and ^{66}Zn analytes were measured directly using He in a collision reaction cell. ^{39}K , ^{40}Ca and ^{56}Fe were directly determined using H_2 as a cell gas. ^{32}S was determined via mass-shift from 32 to 48 utilizing O_2 as a cell gas. An average of 4 technical replicate measurements was used for each individual biological sample. The average variation between technical replicate measurements was 1.1 % for all analytes and never exceeded 5 % for an individual sample. Triplicate samples (from independent cultures) were also used to determine the variation between cultures. Averages and standard deviations between these replicates are depicted in figures.

Confocal microscopy using CS3 dye

CS3 dye was synthesized as described in Supplemental File 1. Cell walled Chlamydomonas cells were cultured to early stationary phase and $1\text{-}2 \times 10^7$ cells were collected by centrifugation at RT and ($3,500 \times g$, 2 min). The supernatant was discarded and the cell pellet was resuspended in 10 mM Na-Phosphate buffer (pH 7) supplemented with 10 μM CS3 dye. To avoid mechanical stress to cell wall reduced strains, cell wall reduced cells were not centrifuged, but 10 μM CS3 dye was added directly to an aliquot of the culture instead. Microscopy was performed on a Zeiss LSM880. The following excitations and emissions were used: CS3 ex/em 514/537, Chl 633/696. All aspects of image capture were controlled via Zeiss ZEN Black software, including fluorescent emission signals from probes and/or chlorophyll.

Statistical Analyses

Unless stated otherwise, a one-way ANOVA was used to test for differences between samples. Successful ANOVA was followed by a Holm-Sidak Post-hoc Test. Asterisks indicates a p-value of <0.05.

Acknowledgments

Confocal microscopy experiments were conducted using a Zeiss LSM 880 with OPO, at the CRL Molecular Imaging Center, supported by the Helen Wills Neuroscience Institute. We would like to thank Holly Aaron and Feather Ives for their microscopy training and assistance. We want to thank Chris Jeans and the QB3 Macrolab at UC Berkeley for purification of LbCpf1. SM funding GM42143.

Author Contributions

Designed experiments: DS, SRS, Designed CS3 synthesis HN, Performed experiments: DS, SRS, SP, BCB, SG, CS, Analyzed data: DS, SRS, SP Prepared figures: DS, SRS, SP, CBH, Designed project: DS, SSM. Secured funding: SSM, HN.

2.6 Discussion

2.6.1 Consequences of Cu accumulation in cellular environments

Cu is essential for life, fulfilling enzymatic functions that could not be performed without its unique chemical properties. However, from a biochemical perspective, Cu can also cause toxicity. Free Cu, in particular, is even actively used as a part of the immune responses to selectively kill invading pathogens (74). With these considerations, cellular Cu homeostasis is tightly regulated to minimize toxicity and maximize utility. Normally, cells are effective at maintaining such essential homeostatic controls in response. (8, 21, 61,75). However, a number of genetic and environmental conditions have shed light on the involvement of Cu misregulation in degradative feedback loops and inappropriate Cu accumulation observed in a number of diseases (e.g. Parkinsonism related to Mn exposure (18), nephropathy induced by Cd (76), Wilson's disease, Menkes disease (77). Despite Cu dyshomeostasis overlapping these degenerative disorders, a mechanistic understanding of altered Cu accumulation has remained elusive. Confounding factors that have plagued research in this field have been highly tissue-specific accumulation observed in complex organisms and the understudied impact of nutritional status on toxicity risk (78). A homogenous single-celled and well-characterized alga like *Chlamydomonas*, whose nutritional status is easily manipulated in an established medium of inorganic salts, avoids many of these confounding factors when investigating the mechanistic controls of Cu homeostasis.

2.6.2 CRR1: master Cu quota determinant to avoid deficiency and toxicity

What Cu and Zn deficiency have in common is that both conditions dramatically shift how Cu is utilized in the cell to avoiding the changing thresholds of deficiency and toxicity over time. Reflecting the increased activation of CRR1 and subsequent RNA abundance of all 3 CRR1-dependent CTR transcripts, CTR expression is more vital for conditions of Cu deficiency than Zn deficiency where single mutants of canonical CTRs was sufficient to restrict growth in Cu deficiency but not Zn deficiency. One hypothesis that has been proposed for this discrepancy relates to the specific type of hazard CRR1 is avoiding in each condition. In Cu deficiency, the challenge for CRR1 is to obtain as much Cu from the environment as possible (75), depending on high-affinity transporters like CTR1 when Cu concentrations become exceedingly low, while also redistributing available Cu within the cell to minimize the Cu quota required for survival by substituting Cu-containing plastocyanin for the Fe-containing substitute cytochrome c6 to further decrease the threshold for Cu deficiency.

In Zn deficiency, it seems that the major challenge for a subset of CRR1-activated genes is first to redistribute and tightly control intracellular Cu pools to avoid mismetallation of any Zn-containing proteins that are already in short supply, potentially through sequestration in the acidocalcisome. In this case, the increased accumulation of Cu via CTR1 and CTR2 appears to less necessary than their function in Cu deficiency because a decrease in Cu accumulation in either *ctr1* or *ctr2* does not result in reduced growth for *Chlamydomonas* unlike Cu deficiency. The mobilization of Cu stores, mediated by CRR1-dependent CTR2 out of acidocalcisomes following Zn supplementation suggests that the threshold for Cu toxicity becomes higher once a supply of Zn is once again made available to the cell because it no longer needs to exert as much energy in

controlling Cu availability to the cell. When looked through the lens of Cu toxicity, benefits *Chlamydomonas* to become functionally Cu deficient during Zn deficiency because it reduces the number of places that Cu must be trafficked to until supply once again exceeds demand, as is the case when increasing Cu concentrations in the media during Zn deficiency drives the restoration of plastocyanin in the chloroplast (11).

2.6.3 CTR3 and GSH: Coordinating periplasmic and cytosolic free metal pools

Unlike the membrane-bound CTR1 and CTR2, CTR3 and GSH are components of a cell's soluble fraction. While these soluble factors cannot directly transport Cu across a membrane, their cellular localization means that CTR3 can act on the periplasmic Cu pool while GSH could act on the cytosolic Cu pool as the most abundant thiol in cellular systems whose affinity for Cu(I) may compete with known Cu chaperone like ATOX1 (79), GSH's ability to remove Cu from the cytosolic pool by forming a complex (13) with the metal may contribute to the concentration gradient driving Cu-uptake through the canonical CTRs during Zn deficiency. Alternatively, CTR3 would act on Cu pools in the periplasmic space of *Chlamydomonas*. Its similarity to iron assimilatory protein with a comparable pattern of subcellular localization suggests that CTR3 could play a role in Cu assimilation (4) in the periplasm by increasing the selective availability of Cu for CTR2. Future investigations could examine whether CTR3 functions in the CRR1 response to buffer the rate of Cu uptake into cells when environmental and periplasmic concentrations change before the CRR1 response can readjust the internal Cu-handling environment.

Alternatively, another possible reason for CTR3 upregulation during Cu and Zn deficiency without a clear effect on Cu uptake, could involve preventing increased uptake of toxic nonessential metals, like Ag, that can hijack the same uptake pathways increased

in these conditions as has previously been suggested (22, 80). As a nonessential metal lacking any cellular metal quota within cells, established mutants deficient in the rate limiting step of glutathione synthesis, *gsh1-2* and *gsh1-8*, demonstrate the susceptibility of cells to Ag when cytosolic thiols are not present at levels high enough to detoxify the incoming metal similar to the effects observed with BSO use (81). In the case of Cu deficiency where uptake channels that Ag may use, like CTR1 or CTR2, are upregulated to increase the amount of Cu taken up by cells(4), CTR3 may act to limit the uptake of Ag by these means to retain them in the periplasm while keeping the concentration of free Ag in the periplasmic space as low as possible to reduce the potential toxicity of the metal.

2.6 Conclusions

In Cu deficient *Chlamydomonas*, three Cu transporters (CTRs) are upregulated by a Cu-responsive transcription factor (CRR1). However, it was not known which of the three transporters contributed most to the survival of *Chlamydomonas* during conditions where the CRR1 response was necessary: Cu deficiency and Zn deficiency. Using a reverse genetic approach with artificial microRNAs (amiRNAs) and insertional mutants, the role of individual CTRs was determined. One of the two canonical, plasma-membrane-localized CTRs, CTR2, is the major low-affinity uptake transporter in Cu deficiency while CTR3, lacking a transmembrane domain, was found to be secreted to the periplasm instead (Fig 2.28). Despite progress, we have yet to identify a role in Cu assimilation for CTR3

In Zn deficiency, another condition that paradoxically induces the CRR1 regulon, only *ctr2* exhibited a reduced capacity for Cu uptake during Zn deficiency (Fig. 8). These results lend support to the hypothesis that CTR2 is the major low-affinity Cu transporter. Furthermore, this reduced capacity for Cu uptake was also observed during the establishment of Zn-deficient Cu hyperaccumulation. Since CTRs are considered passive uptake transporters, cytosolic factors that may accommodate/promote Cu hyperaccumulation were investigated; these results suggest a potential role for GSH in the establishment of Cu hyper-accumulation during Zn deficiency (Fig. 2.28). When a permanent inhibitor (BSO) of GSH1 (the rate limiting enzyme in GSH formation) was added to cultures that had been transferred from replete to Zn-deficient media (inducing

Cu-hyperaccumulation), the amount of hyperaccumulation over time was significantly reduced. Genetic kds with reduced levels of the same enzyme (*ami-gsh1*) were tested in to further demonstrate how this thiol pool played an important role in avoiding cytosolically accumulated metal toxicity.

2.7 Figures

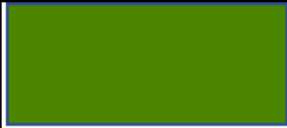







TAP Media Composition	Chlamydomonas Survival	
	<i>CRR1</i>	<i>crr1</i>
Control (replete)		
Cu deficient		
Zn deficient		
Zn excess		

Figure 2.1. Requirement for CRR1 in deficiency and excess essential transition metal conditions. Colors in table describe the growth of Chlamydomonas with a functional (*CRR1*) or nonfunction (*crr1*) copper response regulon. Darker and brighter green denote a higher rate of growth and survival in the photosynthetic organism than those culture colors that are paler and more yellow. Each culture color is the average color after the same amount of time in each nutritional condition (11 for Zn conditions)

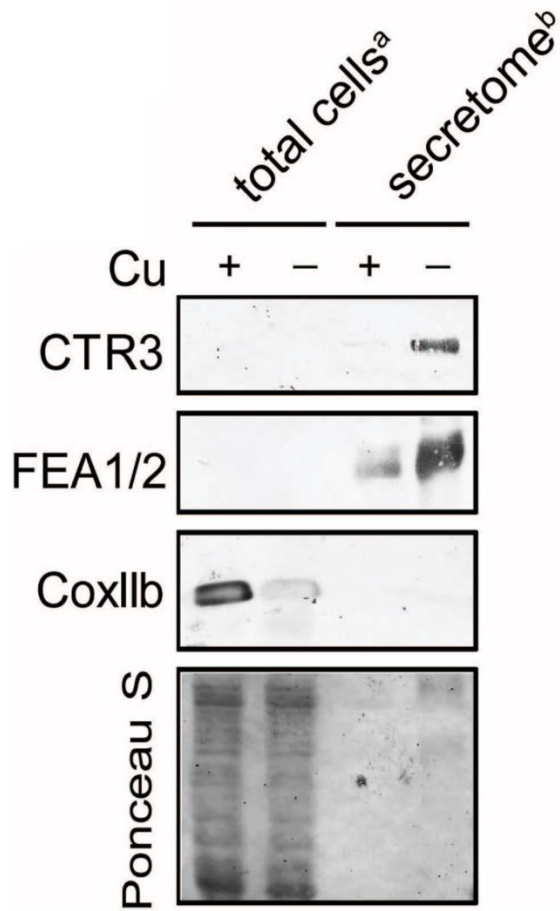
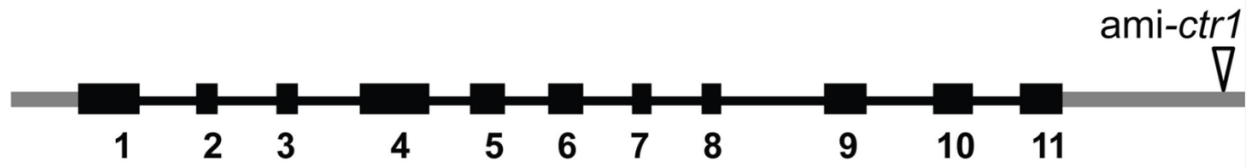


Figure 2.2. CTR3 is a secreted protein. Total cellular protein or proteins precipitated from spent medium of a cell wall-less mutant from Cu-deficient (–) and Cu-replete (+) media were separated by SDS-PAGE using protein derived from either ^a 2×10^6 cells or ^b 2×10^7 cells respectively. Membranes were exposed to antibodies against CTR3 (1:1000), FEA1/2 (1:20000) and COXIIb, Pon S= Ponceau stain. Shown is representative data from at least two independent experiments.

Cre13.g570600



Cre10.g434350



Cre10.g434650



Fig 2.3. Chlamydomonas strains. Artificial microRNA (open arrow) and insertional mutant (filled arrow) used in experiments. Black boxes indicate exons which are numbered while the connected black lines indicate introns.

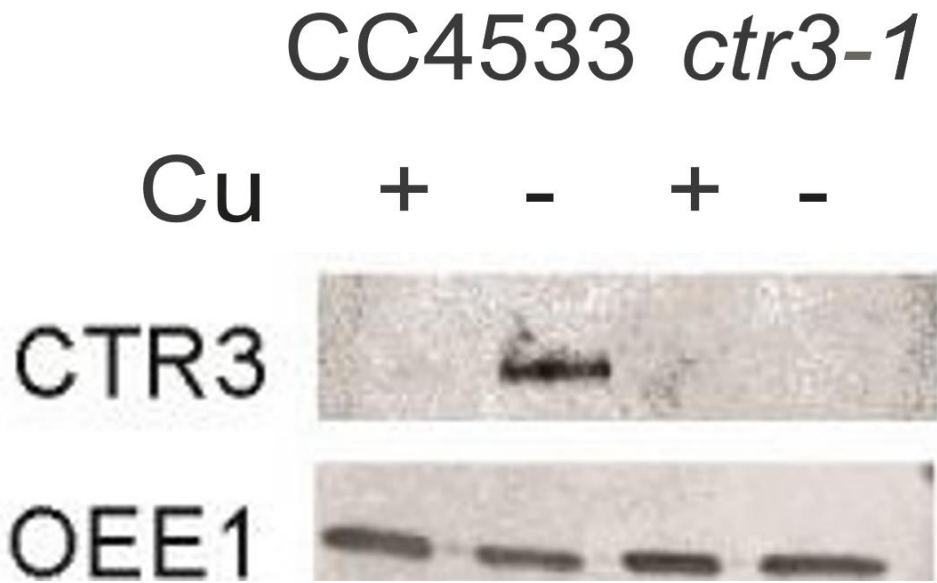


Figure 2.4. Validation of *ctr3-1*. Soluble protein fractions were separated by SDS-PAGE (10% monomer) followed by immunoblotting using antisera against CTR3 (1:1000). OEE1 (1:8000) serves as a loading control.

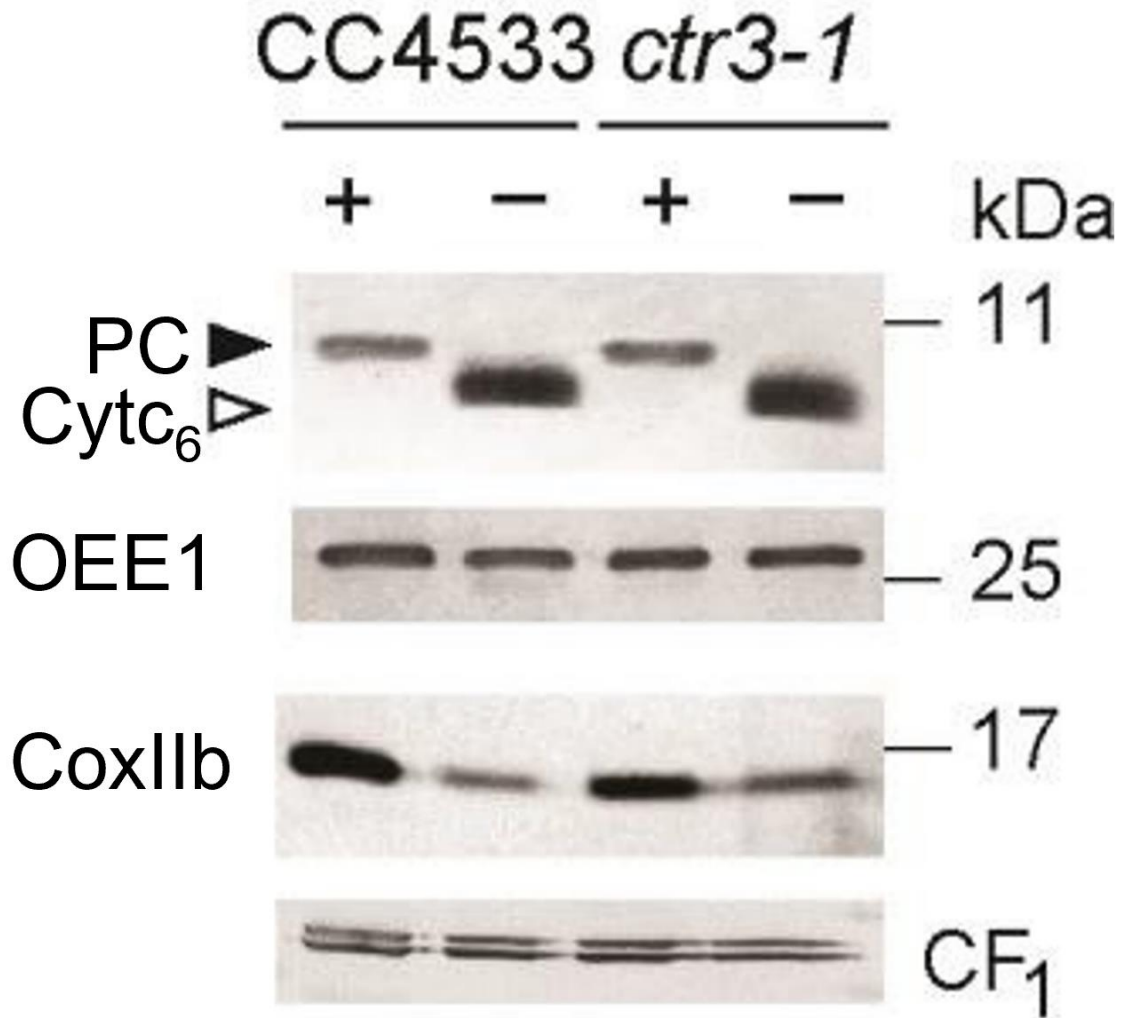


Figure 2.5. *ctr3-1* does not impair Cu-deficiency response. Protein fractions were separated by SDS-PAGE (10% monomer) Antibodies directed against CF1 (1:40000), OEE1 (1:8000), and Plastocyanin/Cyt c₆ (1:4000).

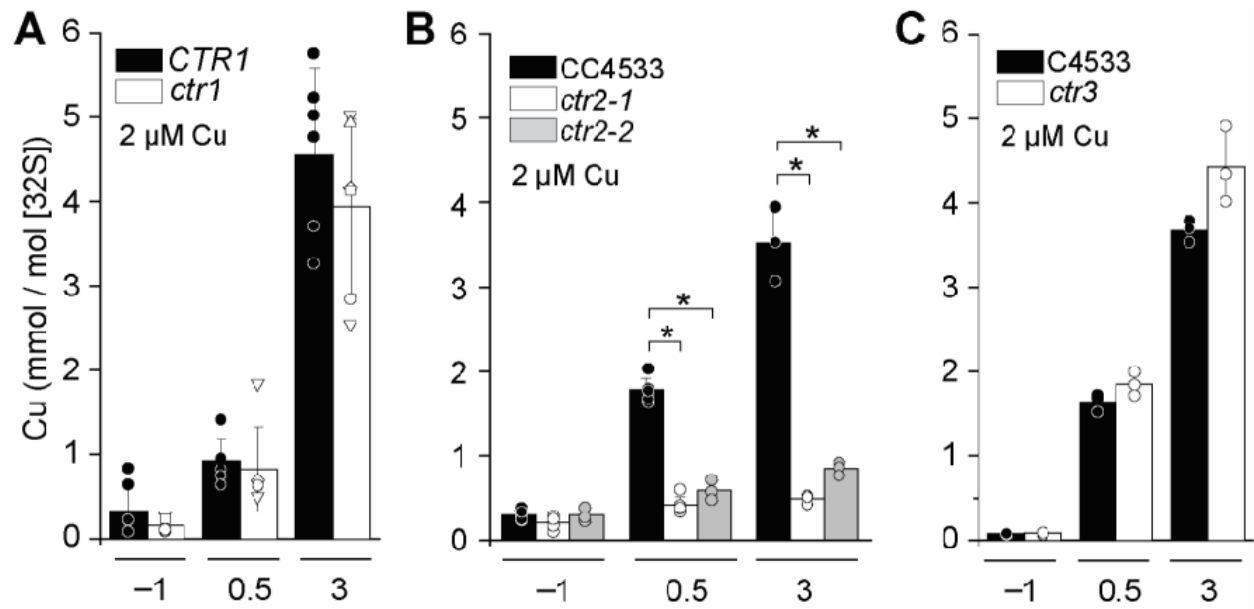


Figure 2.6. CTR1 and CTR2 are both functional copper importers *in vivo*, but CTR1 specifically mediates high affinity copper import. (A-C) Copper addback experiment was performed as described in Figure 1. ICP-MS was used to determine Cu content of **(A)** *CTR1* and independent *ctr1* CPf1/CRISPR mutants, *ctr1-1* (triangle up), *ctr1-2* (triangle down), *ctr1-3* (square), *ctr1-4* (circle), *ctr1-5* (diamond). **(B)** *CTR2* and *ctr2* cell lines and **(C)** *CTR3* and *ctr3* cell lines following the resupply of 2 μ M Cu as indicated to Cu-deficient cultures. Shown are data points, averages and StDEV of 3-6 independent experiments.

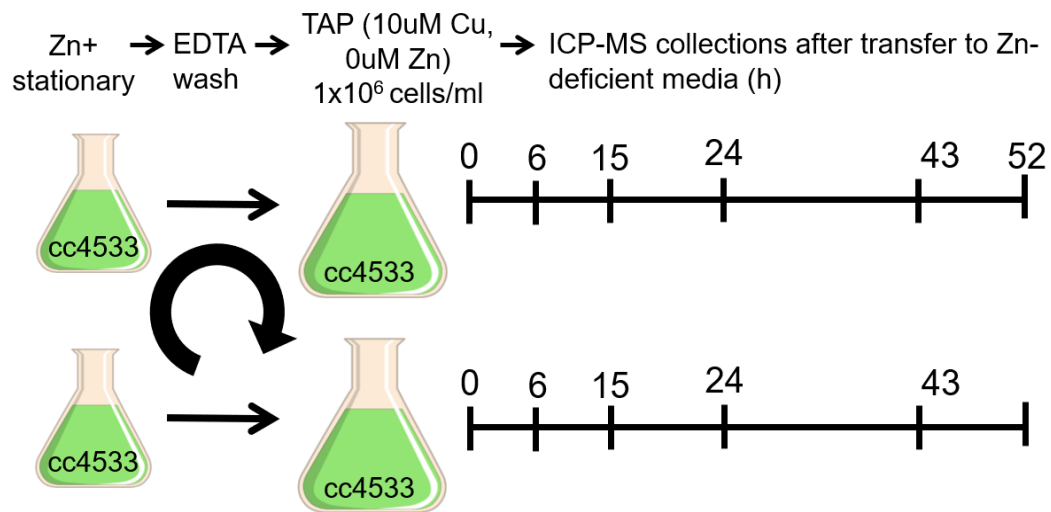


Fig.2.7. Experimental paradigm for capturing the transition of Zn-replete to Zn-deficient conditions for wild-type cc4533 Chlamydomonas. Stationary Zn-replete cultures were washed with EDTA to remove excess metal before transfer to Zn-deficient media. Following the transfer, samples were collected at various timepoint for metal content analysis using ICP-MS/MS.

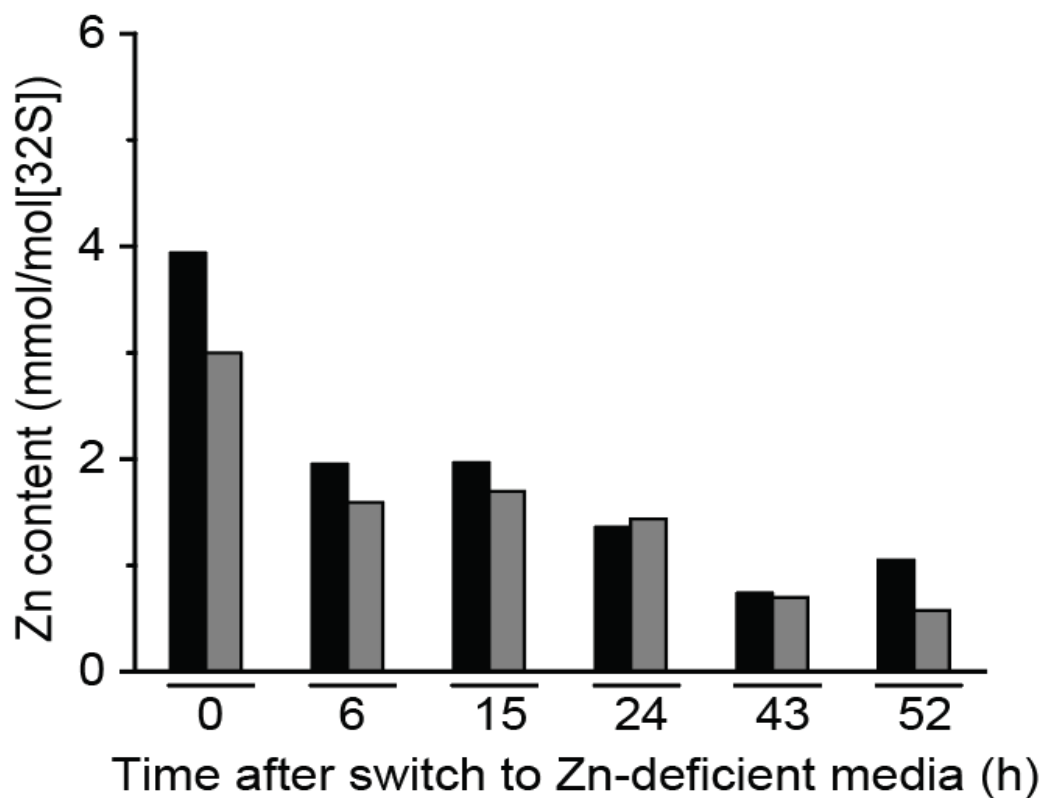


Fig.2.8. Zinc deficiency established after transfer to Zn-deficient media. ICP-MS/MS metal content analysis of various timepoints from a culture after transfer to deficient media. Black and grey bars represent 2 independent experimental replicates.

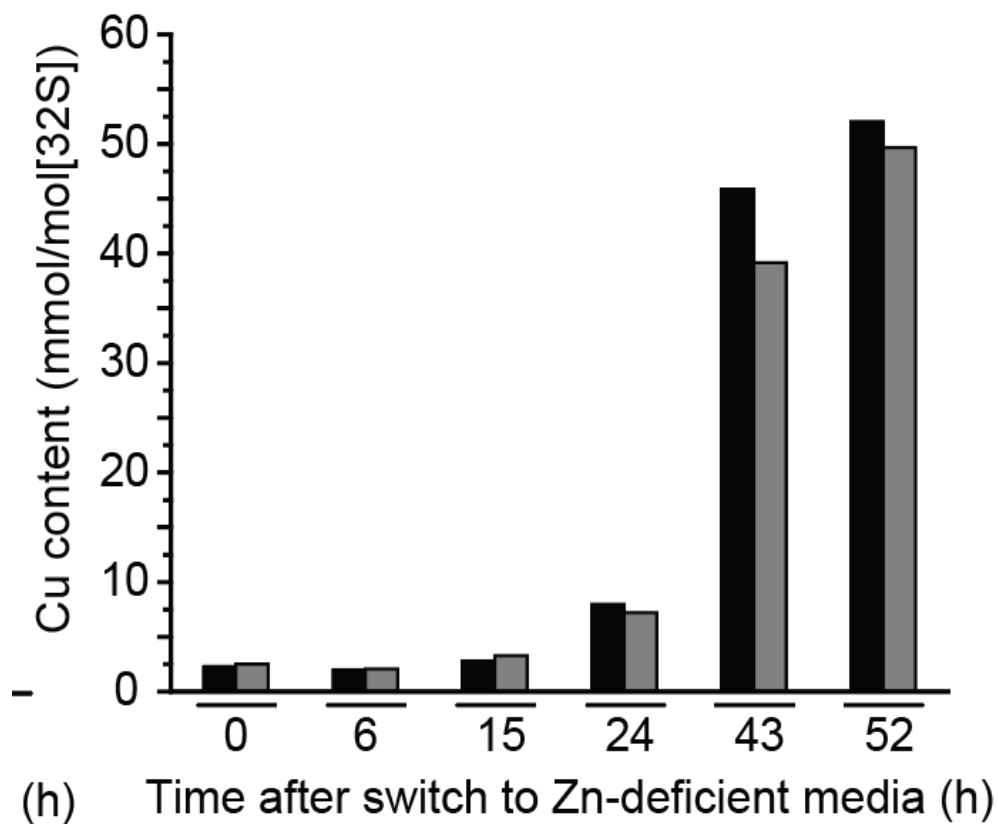


Fig.2.9. Cu hyperaccumulation established after transfer to Zn-deficient media.

ICP-MS/MS metal content analysis of various timepoints from a culture after transfer to deficient media. Black and grey bars represent 2 independent experimental replicates.

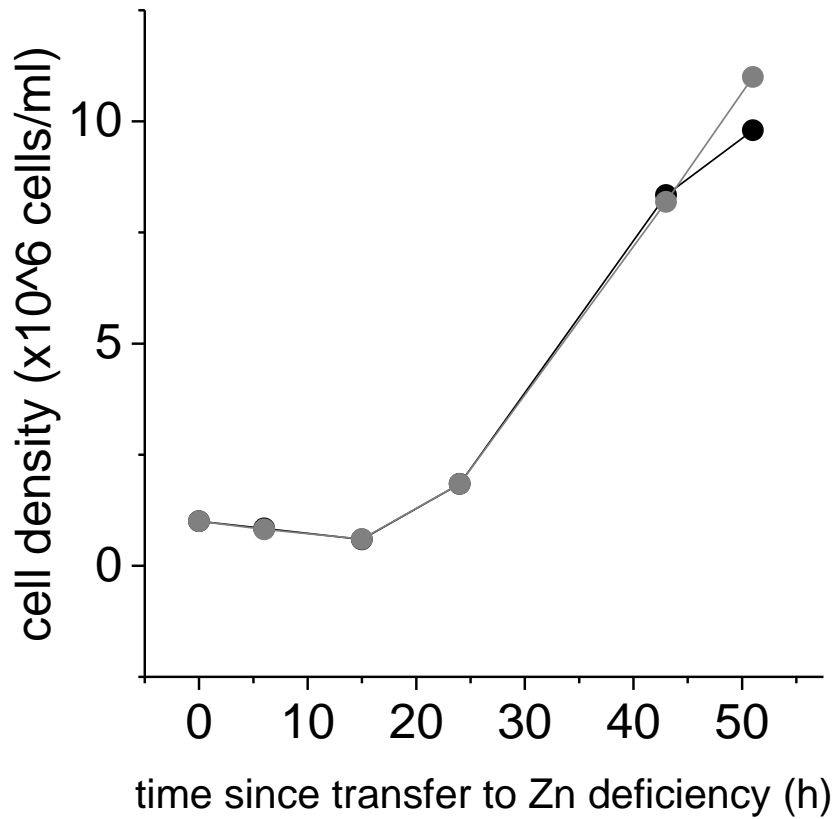


Fig.2.10 Growth rate of Chlamydomonas after transfer to Zn-deficient media.

Samples were collected various timepoints from a culture after transfer to deficient media to determine cell density over time. Black and grey bars represent 2 independent experimental replicates.

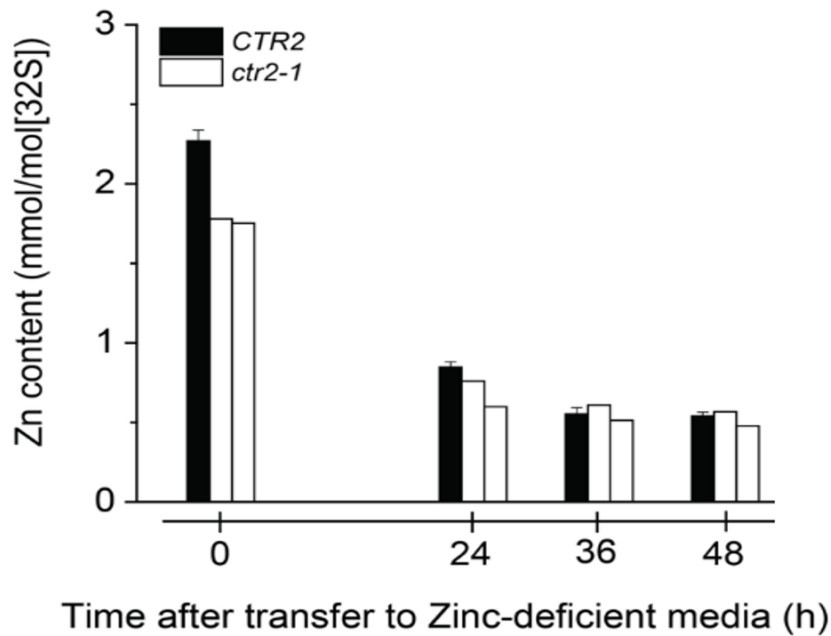


Fig.2.11 *ctr2-1* doesn't impair establishment of Zn deficiency. ICP-MS/MS metal content analysis of various timepoints from a culture after transfer to deficient media. Black bars represent the average of 3 experimental replicates of *CTR2* with error bars indicating standard deviation. White bars represent 2 independent experimental replicates of *ctr2-1* as indicates in the graph.

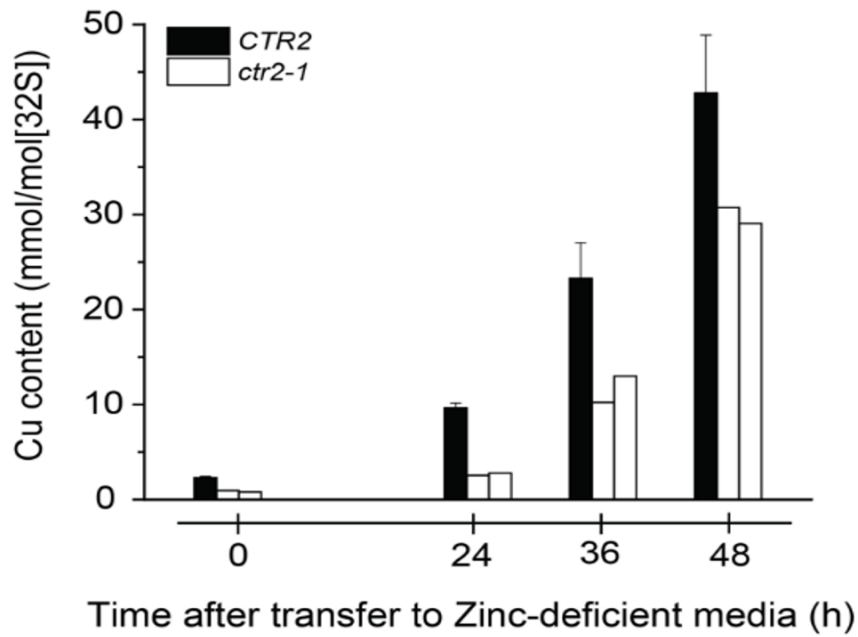


Fig.2.12 *ctr2-1* impairs establishment of Cu hyperaccumulation in response to Zn deficiency. ICP-MS/MS metal content analysis of various timepoints from a culture after transfer to deficient media. Black bars represent the average of 3 experimental replicates of *CTR2* with error bars indicating standard deviation. White bars represent 2 independent experimental replicates of *ctr2-1* as indicates in the graph.

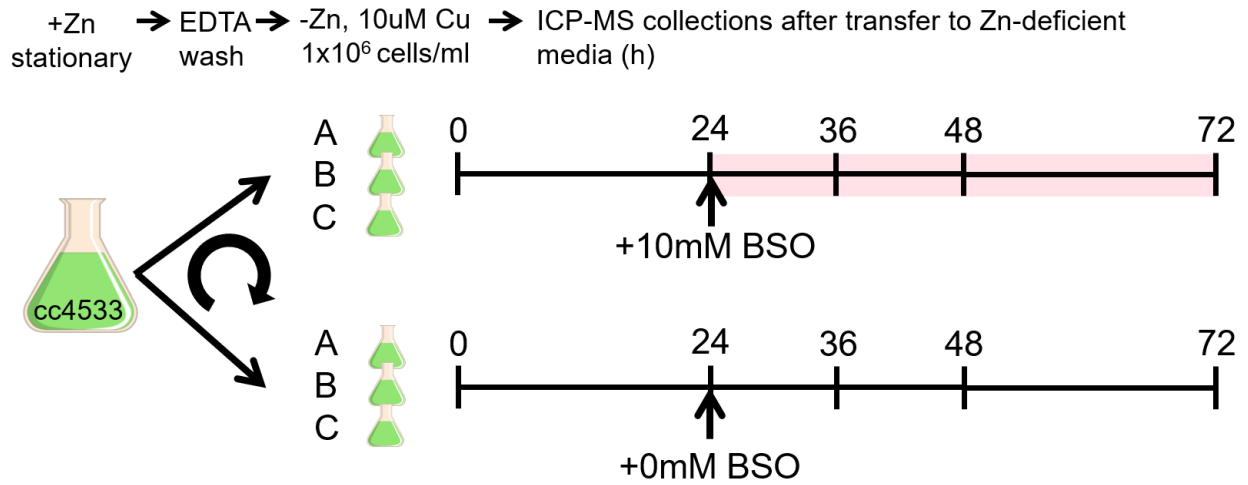


Fig.2.13 Experimental paradigm for capturing the role of GSH in transition of Zn-replete to Zn-deficient conditions for wild-type cc4533 Chlamydomonas.

Stationary Zn-replete cultures were washed with EDTA to remove excess metal before transfer to Zn-deficient media. 24h after transfer, 10mM BSO, an inhibitor of glutathione synthesis, was added to the media before samples were collected at various timepoint for metal content analysis using ICP-MS/MS.

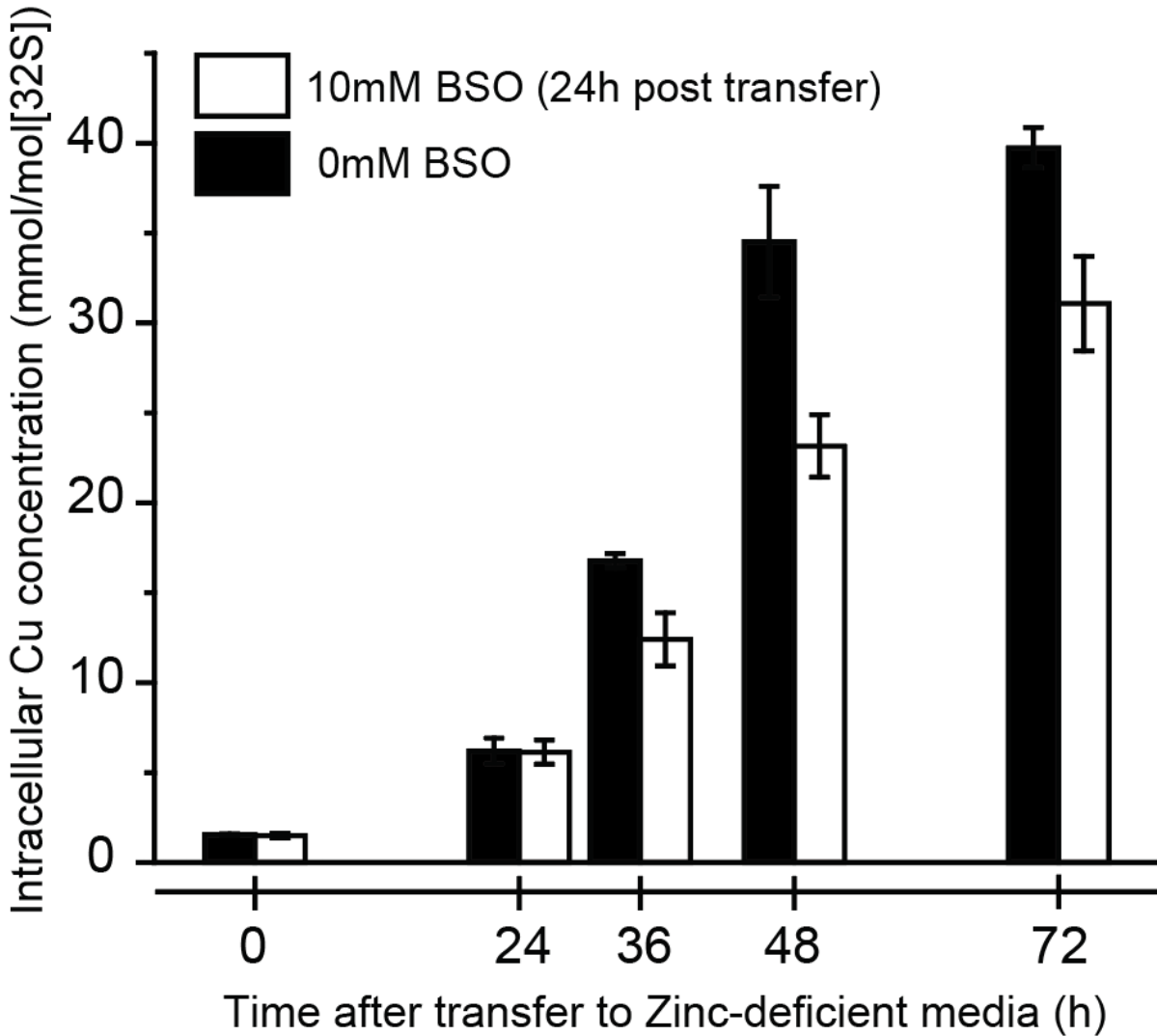


Fig. 2.14. GSH contributes to the establishment of Cu hyperaccumulation in response to Zn deficiency. ICP-MS/MS metal content analysis of various timepoints from a culture after transfer to deficient media. Black bars represent the average of 3 replicates without added BSO with error bars indicating standard deviation. White bars represent the average of 3 replicates with 10mM BSO where error bars indicate the standard deviation.

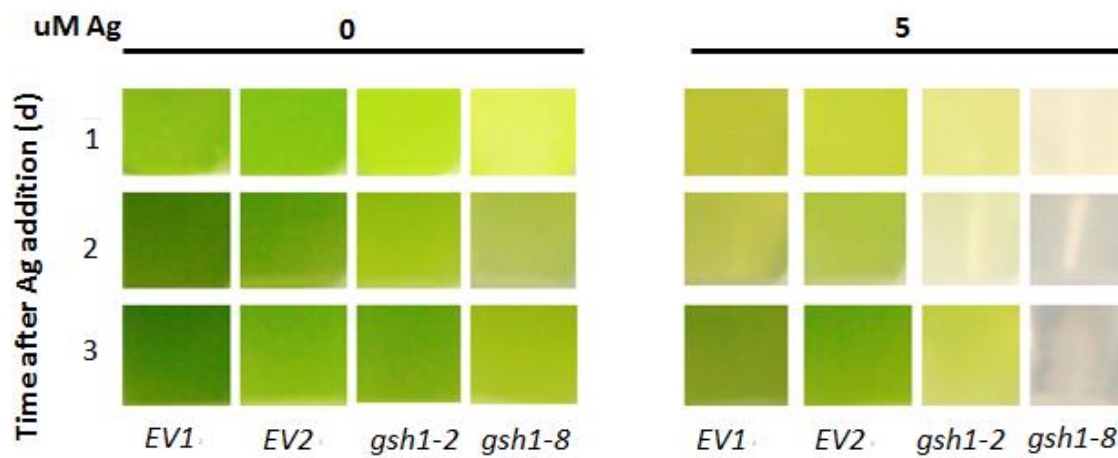


Fig.2.15. Ag toxicity via CTR uptake is minimized by GSH. Growth of established gamma-glutamyl synthetase mutants, *gsh1-2* and *gsh1-8*, after the addition of 0 μ M or 5 μ M Ag to the media. Representative pictures of culture color are presented for each timepoint.

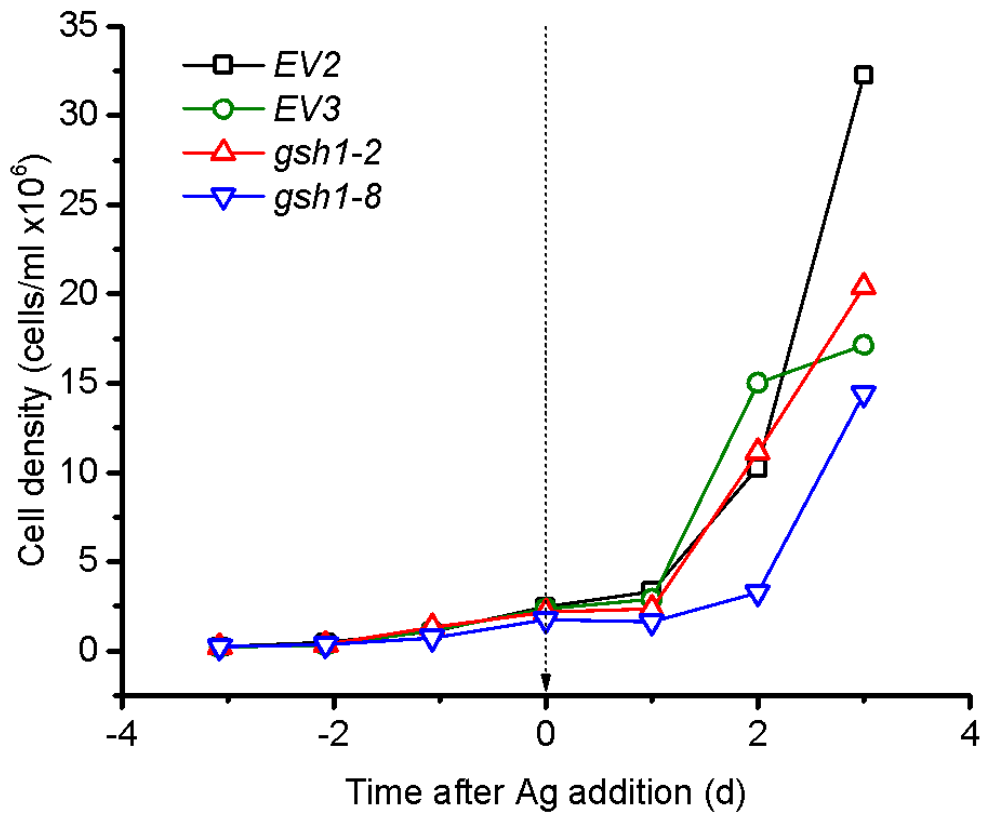


Fig.2.16 Growth rate of gamma-glutamyl synthetase mutants. Growth of established gamma-glutamyl synthetase mutants, *gsh1-2* and *gsh1-8*, after the addition of 0 μ M or 5 μ M Ag to the media. Samples were collected at indicated timepoints to measure the cell density of the culture and determine the growth rate.

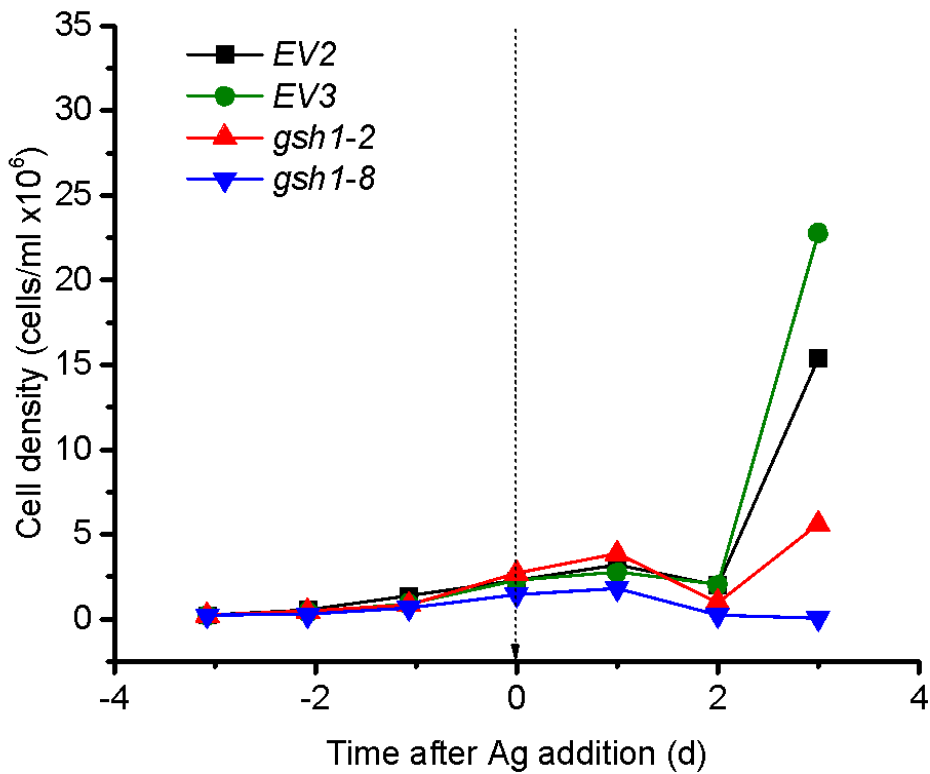


Fig.2.17 Ag-induced growth impairment in gamma-glutamyl synthetase mutants

Growth of established gamma-glutamyl synthetase mutants, *gsh1-2* and *gsh1-8*, after the addition of 0 μ M or 5 μ M Ag to the media. Samples were collected at indicated timepoints to measure the cell density of the culture and determine the growth rate.

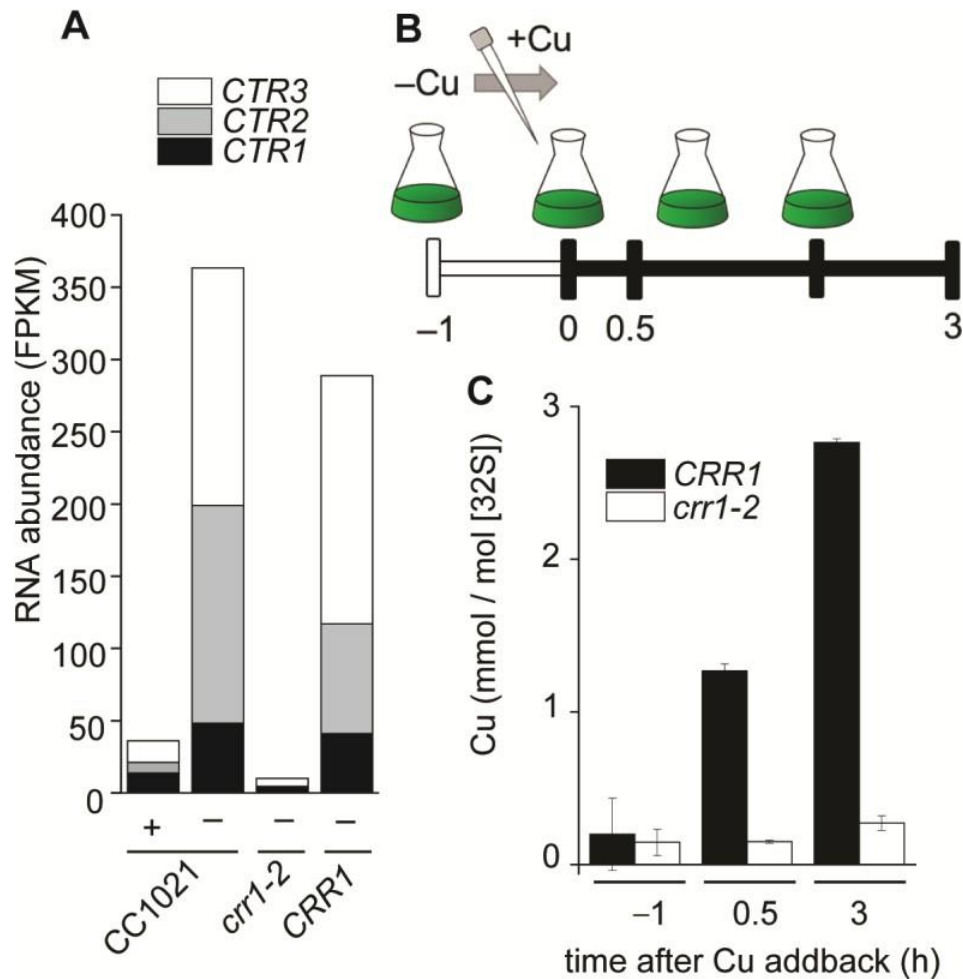


Figure 2.18. Cu uptake is impaired in *crr1*, consistent with Cu- and *crr1* dependent expression of *CTR1*, *CTR2* and *CTR3*. (A) *CTR1*, *CTR2* and *CTR3* mRNA abundances (in FPKMs) in CC1021, *crr1* and *CRR1* grown as indicated, according to (Castruita et al. 2011). (B) Experimental design for Cu resupply experiments. 2 μ M Cu was added back at timepoint 0. (C) ICP-MS/MS analysis at the indicated time points. Cu content was normalized to 32 S as a measure for biomass in *CRR1* and *crr1* strains before and after the addition of Cu. Shown are data points, averages and StDEV of three independent experiments.

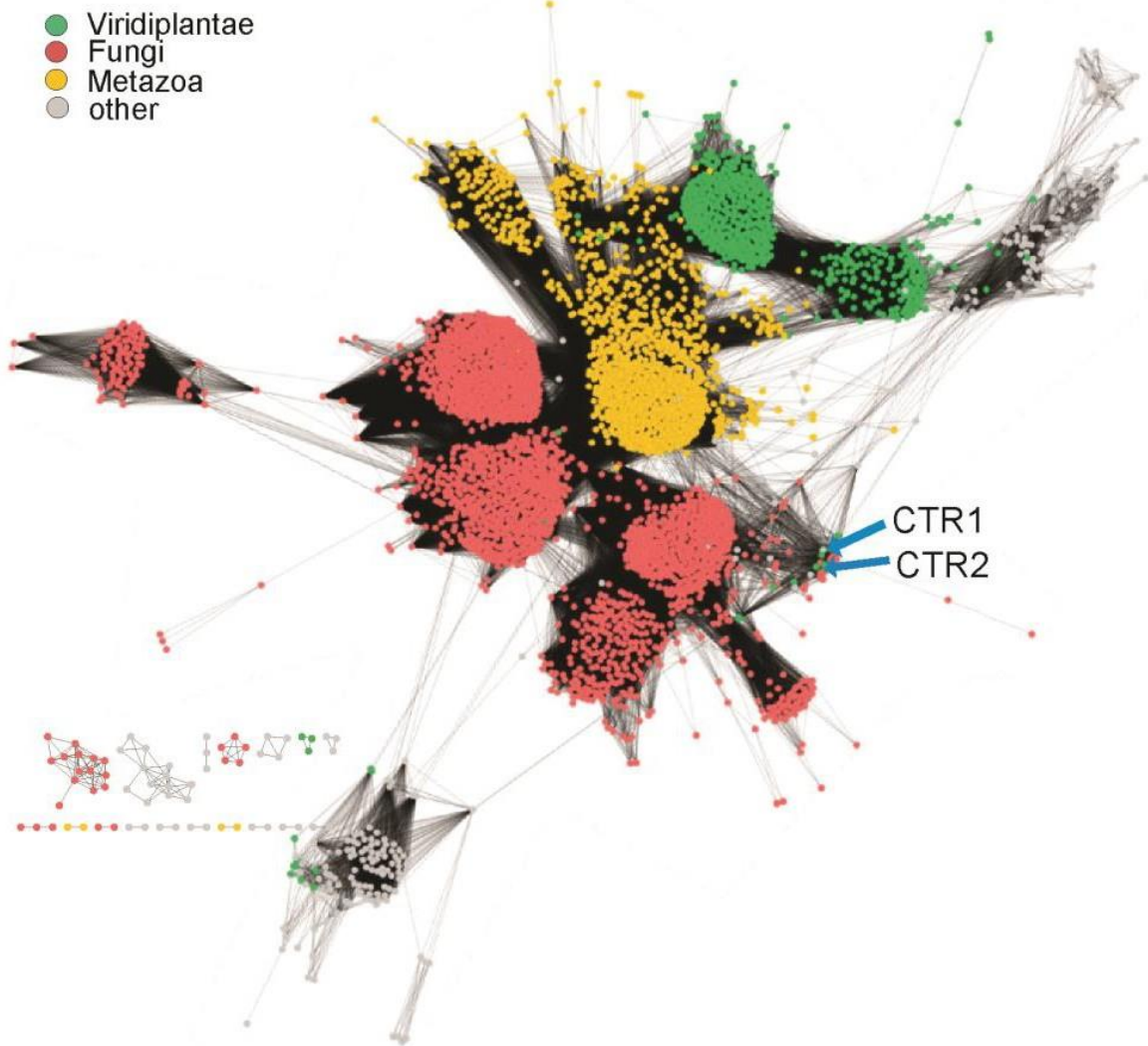


Figure 2.19. Protein similarity network of CTR type proteins. Protein similarity network of 4676 proteins proteins containing the PFam domain PF04145 (Ctr family). Locations of nodes representing the *C. reinhardtii* CTR proteins (CTR1, CTR2) are indicated with blue arrows. The major taxonomic groups Viridiplantae, Metazoa and Fungi are colored according to legend.

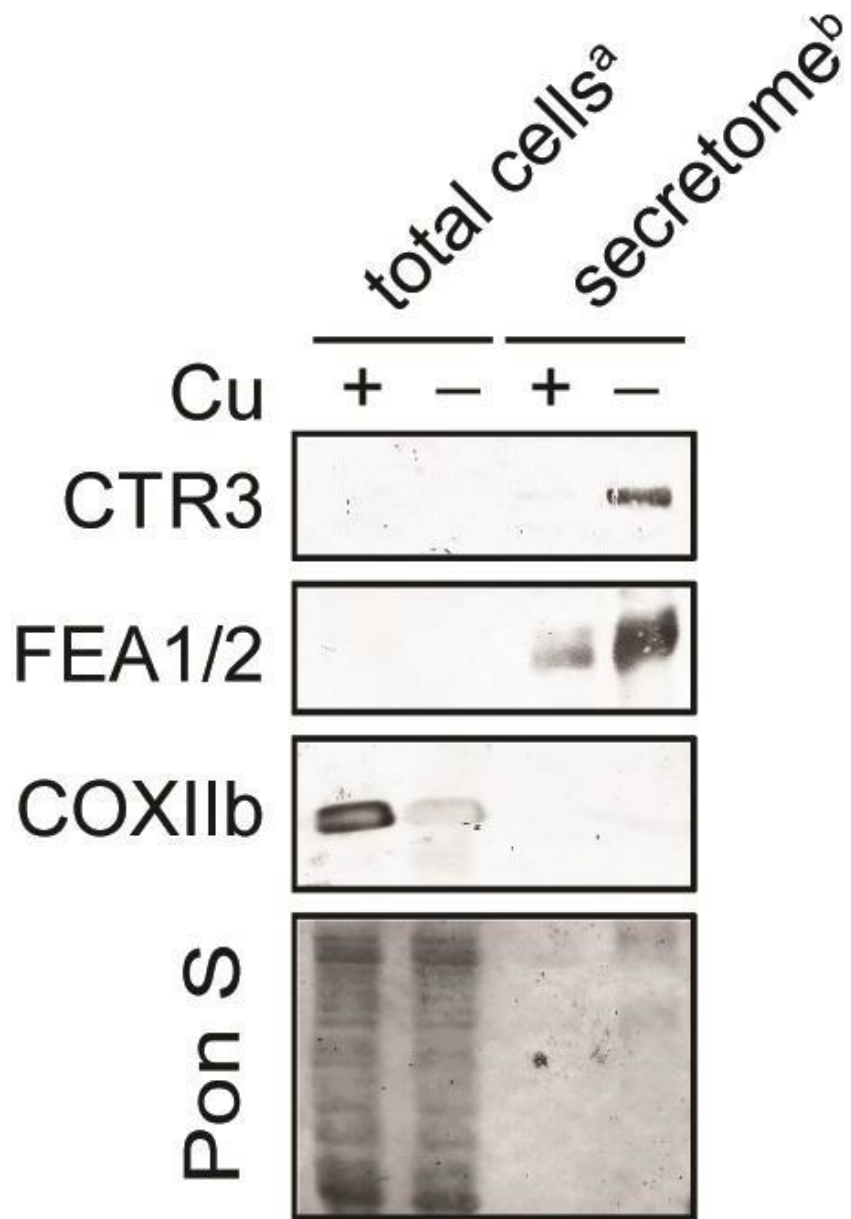


Figure 2.20. CTR3 is a secreted protein. Total cellular protein or proteins precipitated from spent medium of a cell wall-less mutant (secretome) from Cu-deficient (–) and Cu-replete (+) media were separated by SDS-PAGE using protein derived from either ^a2x10⁶ cells or ^b2x10⁷ cells as indicated. Membranes were decorated with antibodies against CTR3, FEAs and COXIIb, Pon S= Ponceau stain. Shown is representative data from at least two independent experiments.

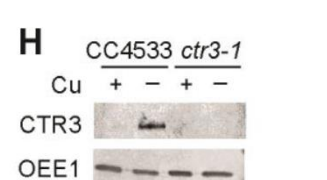
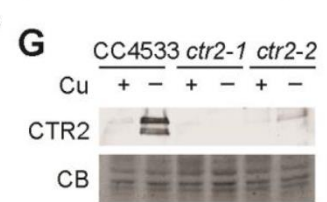
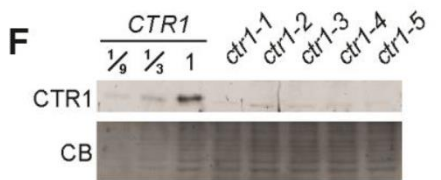
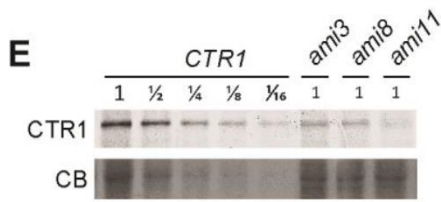
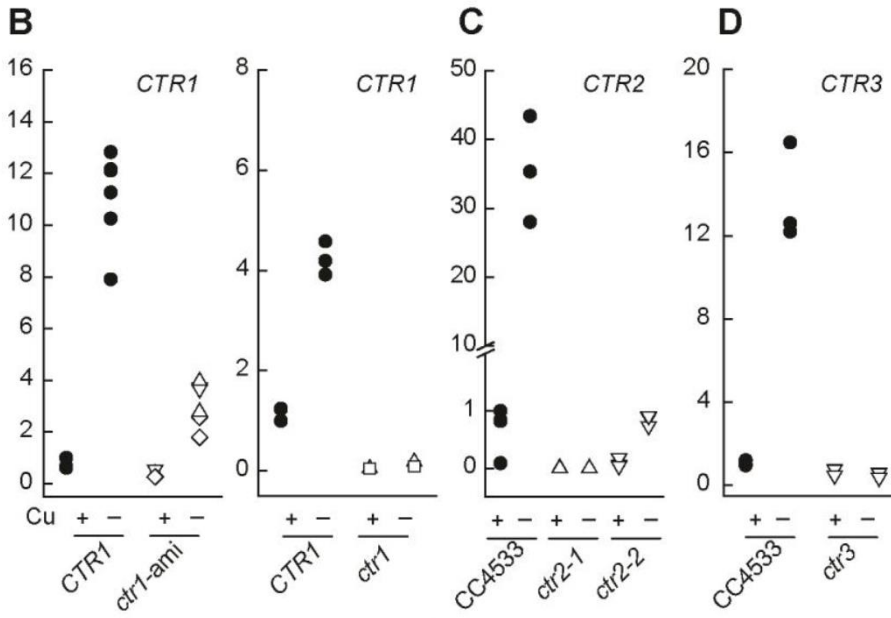
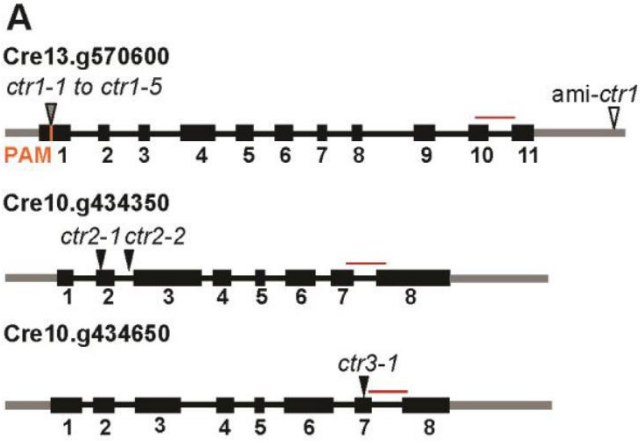


Figure 2.21. Molecular analysis of *ctr1* amiRNA lines, CPf1/CRISPR mediated *ctr1* mutants and *ctr2/ctr3* insertional mutants. (A) Location of inserts or target regions in all CTR gene models. The 3' and 5' untranslated regions are represented by a thin gray line, exons (black boxes) are numbered and thin black lines connecting exons are indicative of introns. The location of the amiRNA target site for *CTR1* (open arrowhead), the CPf1 target sequence (PAM, orange) and CPf1 mediated insertion site of two stop codons (grey arrowhead) and insertion sites for *CTR2* and *CTR3* (filled arrowheads) mutants are shown. Amplicons used for qRT-PCR in (B-D) are shown in dark red. (B-D) Relative transcript abundances of *CTR1*, *CTR2* and *CTR3* were determined using quantitative RT-PCR. Cells were grown in either Cu deficient (-) or replete (+) conditions as indicated. Each symbol represents an independent experiment. Samples collected from (B) *CTR1* (empty vector control lines) are represented by filled circles while open triangle up, down and diamond symbols indicate the *ctr1*-ami3, 8, and 11 lines, respectively. CPf1/CRISPR reference lines (*CTR1*) are represented by filled circles, while open triangle up symbols indicate *ctr1-1* lines and open square symbols indicate *ctr1-3* lines, (C) CC4533 (filled circles), *ctr2-1* (open, up triangles) and *ctr2-2* (open down triangles), (D) CC4533 (filled circles) and *ctr3-1* (open down triangle). Each symbol represents an independent experiment. (E-G) 20 µg of total cell lysates were separated by SDS-PAGE (10% monomer), followed by immunoblotting using antisera against *CTR1* or *CTR2*, respectively. Coomassie blue (CB) serves as a loading control. Samples shown in (E,F) were from cultures grown in copper deplete growth medium (H) Soluble protein fractions were separated by SDS-PAGE (10% monomer) followed by

immunoblotting using antisera against CTR3. OEE1 serves as a loading control. **(E-H)**

Shown is one example from at least two independent experiments.

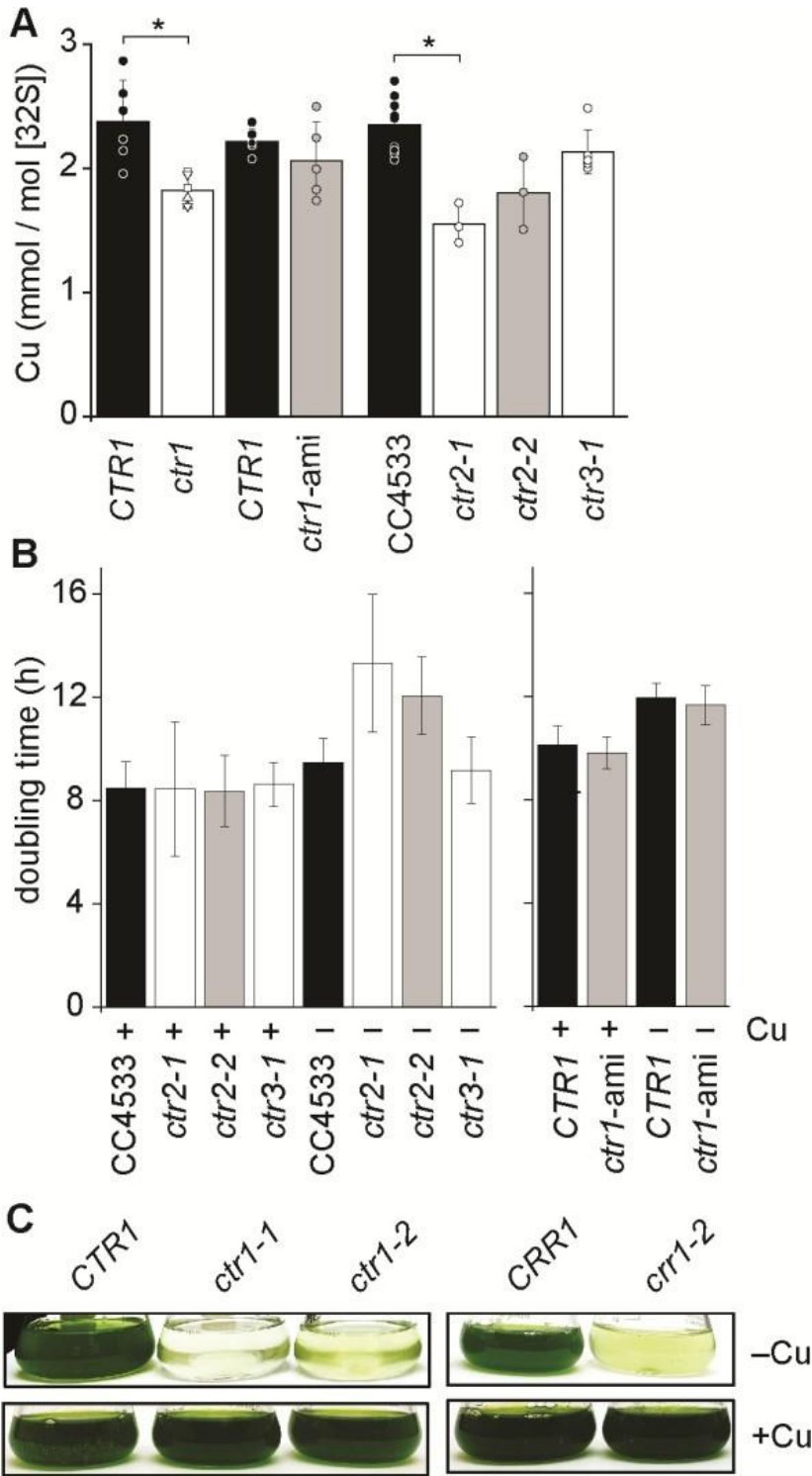


Figure 2.22. CTR1 and CTR2 are both implicated in copper import, while Cu conditional growth defect of *ctr1* CPf1/CRISPR mutants mimics *crr1* phenotype.

(B) Cu content was determined by ICP-MS/MS of copper replete grown: *CTR1* and independent *ctr1* CPf1/CRISPR mutants, *ctr1-1* (triangle up), *ctr1-2* (triangle down), *ctr1-3* (square), *ctr1-4* (circle), *ctr1-5* (diamond), *ctr1* amiRNA lines, *CTR2* and *ctr2* cell lines and *CTR3* and *ctr3* cell lines as indicated. Shown are data points, averages and StDEV of 3-9 independent experiments. (B) *CTR1* amiRNA lines, *ctr1-1*, *ctr2-1*, *ctr2-2*, *ctr3* and respective reference lines were grown photoheterotrophically under Cu-deficient (–) or Cu-replete (+) conditions. If growth occurred, cells were counted using a hemocytometer and doubling times estimated based on cell counts during the exponential growth phase. Shown are averages and StDEV of at least 3 independent experiments. (B) Pictures of flasks were taken six days post- inoculation. Shown is one example from at least two independent experiments.

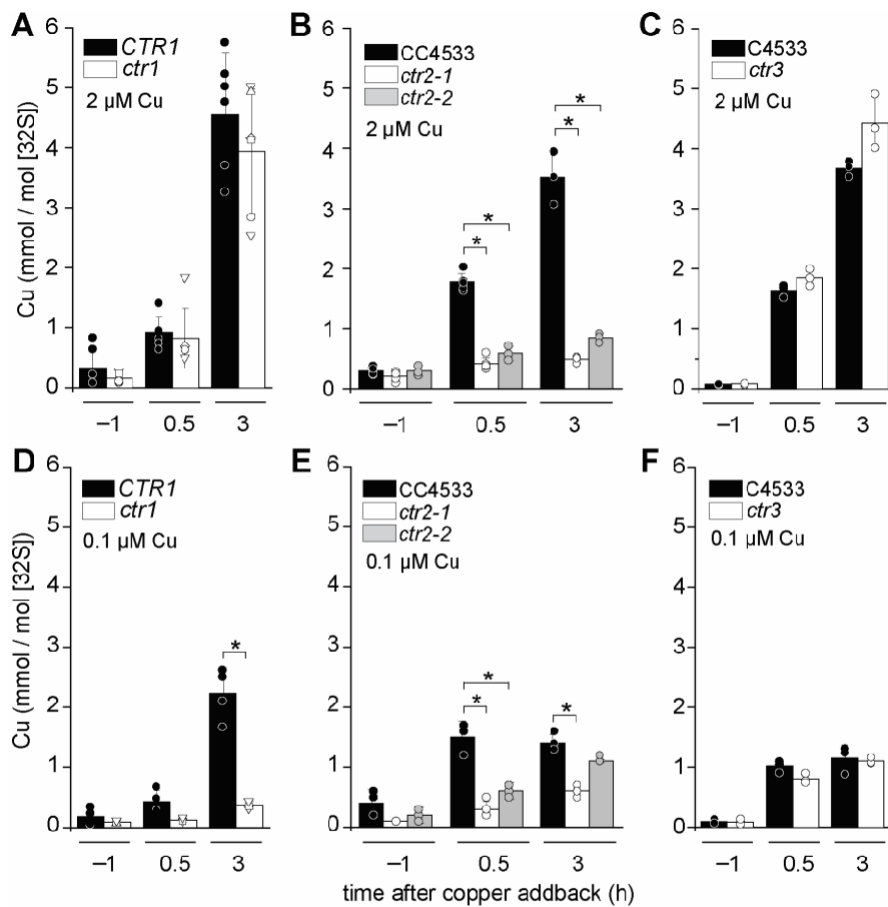


Figure 2.23. CTR1 and CTR2 are both functional copper importers *in vivo*, but CTR1 specifically mediates high affinity copper import. (A-F) Copper addback experiment was performed as described in Figure 1. ICP-MS was used to determine Cu content of (A,D) *CTR1* and independent *ctr1* Cpfl/CRISPR mutants, *ctr1-1* (triangle up), *ctr1-2* (triangle down), *ctr1-3* (square), *ctr1-4* (circle), *ctr1-5* (diamond). (B,D) *CTR2* and *ctr2* cell lines and (C,F) *CTR3* and *ctr3* cell lines following the resupply of either 2 μM or 100 nM Cu as indicated to Cu-deficient cultures. Shown are data points, averages and StDEV of 3-6 independent experiments.

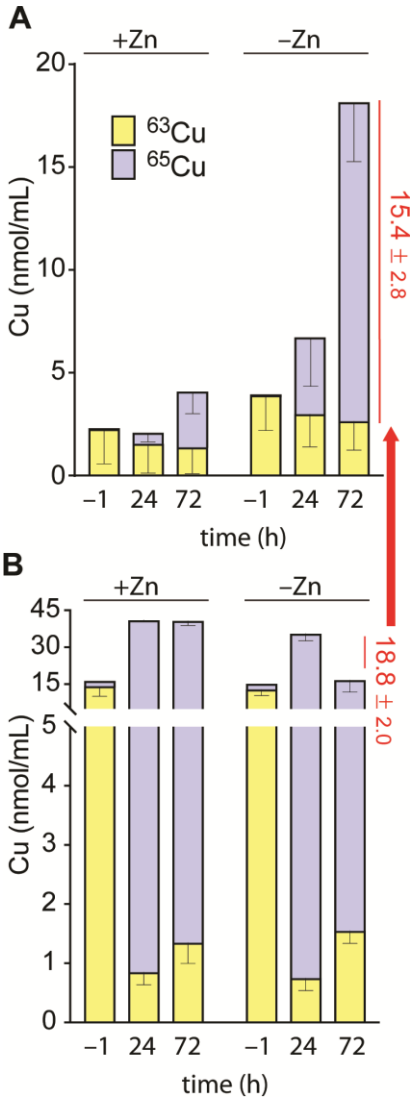


Figure 2.24. Zn-deficiency increases uptake but does not inhibit export. Cells were grown in growth medium without or with supplemented Zn as indicated, collected by centrifugation and transferred to medium that was supplemented with 0 and 2.5 μM Zn and in which ^{65}Cu was added. Cells (A) and spend media (B) were collected and isotope specific Cu content was measured by ICP-MS/MS. Shown are averages and STDEV of three independent experiments..

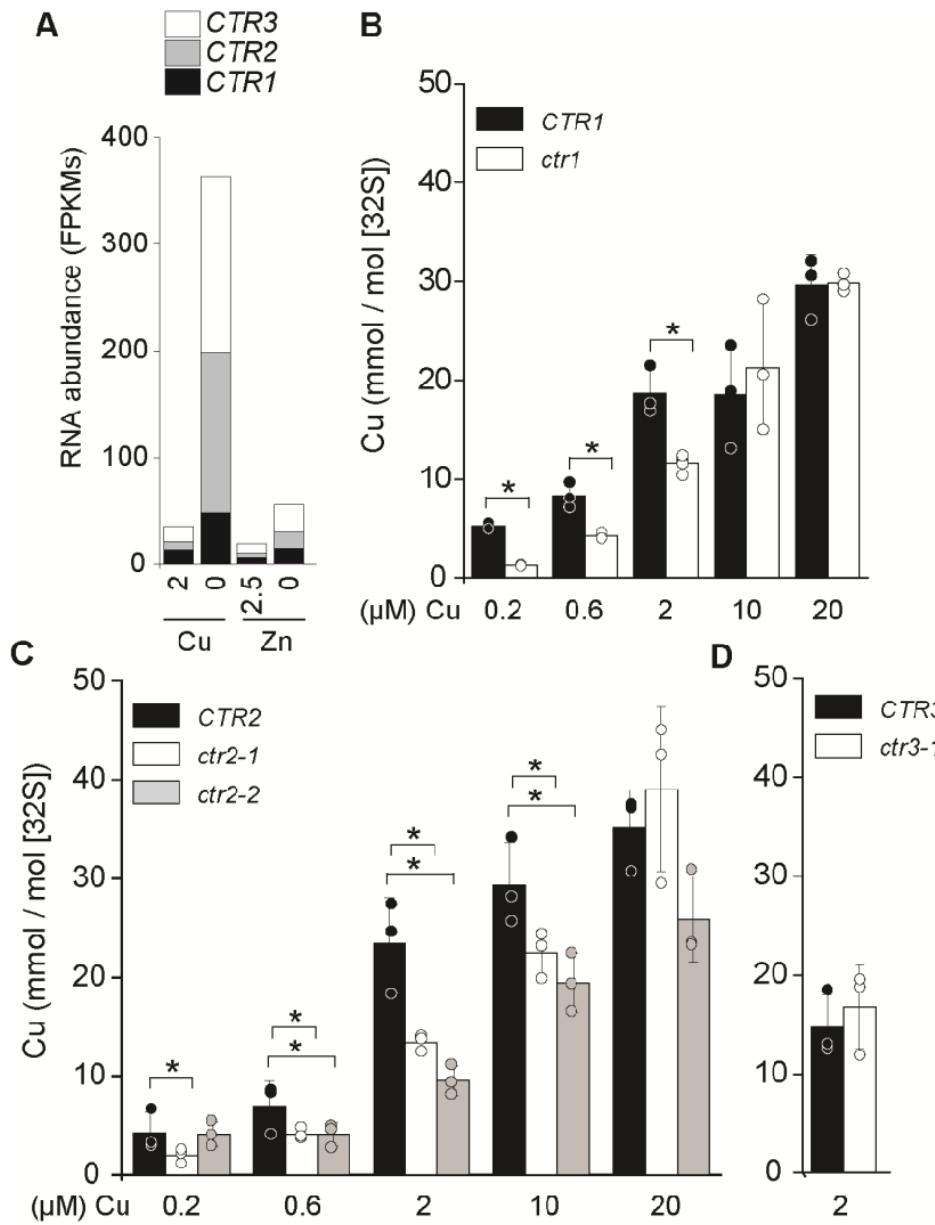


Figure 2.25. Copper accumulation is impaired in zinc deficient *ctr1* and *ctr2* mutants. (A) Expression of *CTR1*, *CTR2* and *CTR3* is up-regulated in zinc deficiency. (BCD) Cu content of *ctr1*, *ctr2* and *ctr3* mutants and corresponding reference strains grown in zinc deplete media that was supplemented with Cu as indicated was measured using ICP-MS/MS. Shown are data points, averages and StDEV of at least three independent experiments.

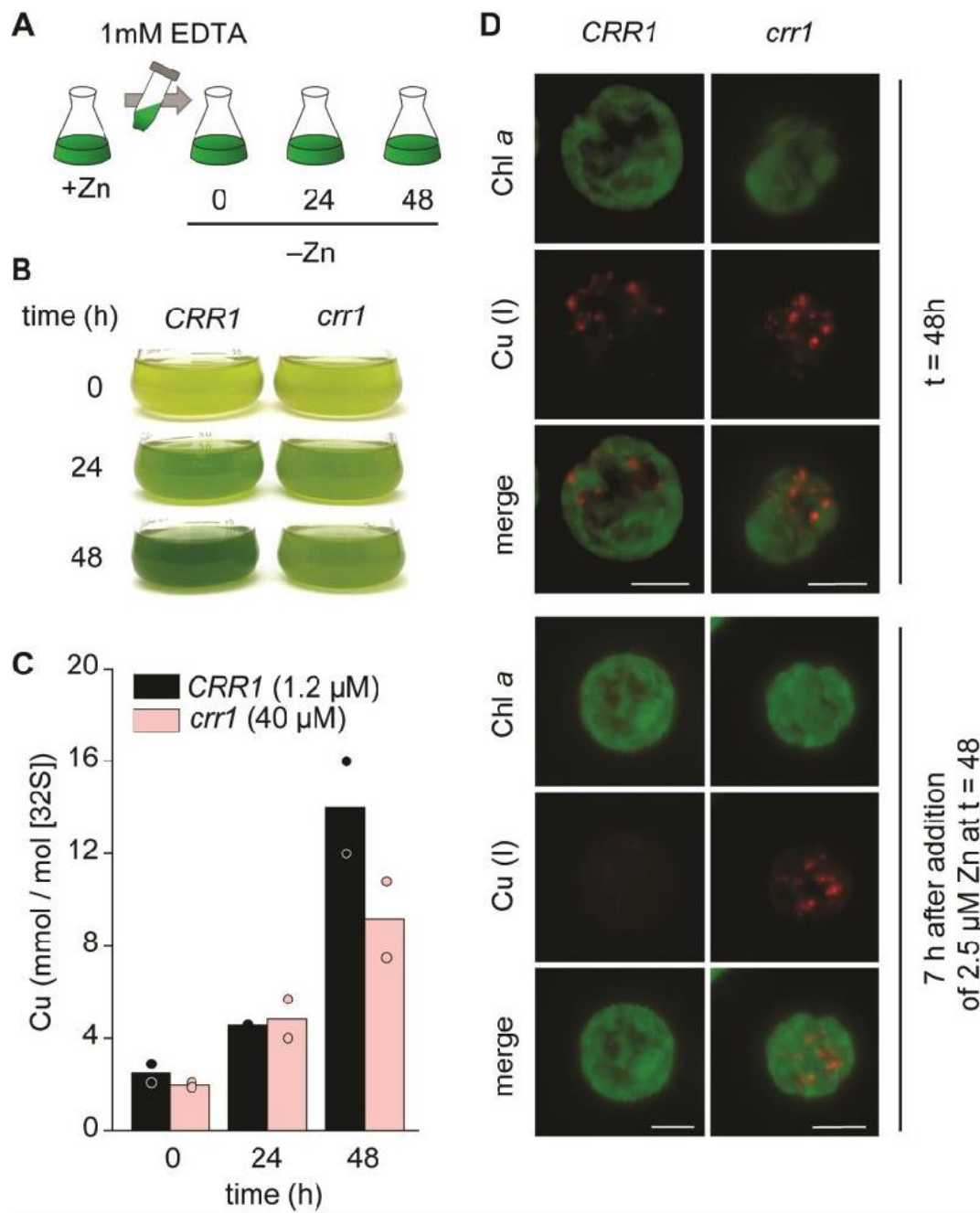


Figure 2.26. Copper accumulated in zinc deficient *crr1* is stored in acidocalcisomes, but cannot be mobilized after zinc add back. Cells were grown in copper replete media, washed with 1mM EDTA and resuspended in zinc deplete media as shown in (A). (B) Pictures of flasks were taken every 24 hours during the experiment. (C) Cu content of *CRR1* and *crr1* cell lines was measured using IC-MS/MS.

Growth medium was supplied with either 1.2 μ M (*CRR1*) or 40 μ M Cu (*crr1*) to Zn-deplete growth medium as indicated. Shown are averages and individual data points of two independent experiments. **(D)** After 48 hours in zinc deficiency, zinc was added back to the culture media. Samples for imaging were taken right before and 7 hours after zinc add back. Copper was visualized using the Cu(I) sensitive dye CS3 (red), cells were visualized using chlorophyll autofluorescence (green). Shown are max intensity projections of each channel. Scale bars represents 5 μ m. Experiment was performed at least twice with independent cultures. At least 6 cells were imaged and are shown in Supplemental Figure 2.S3.

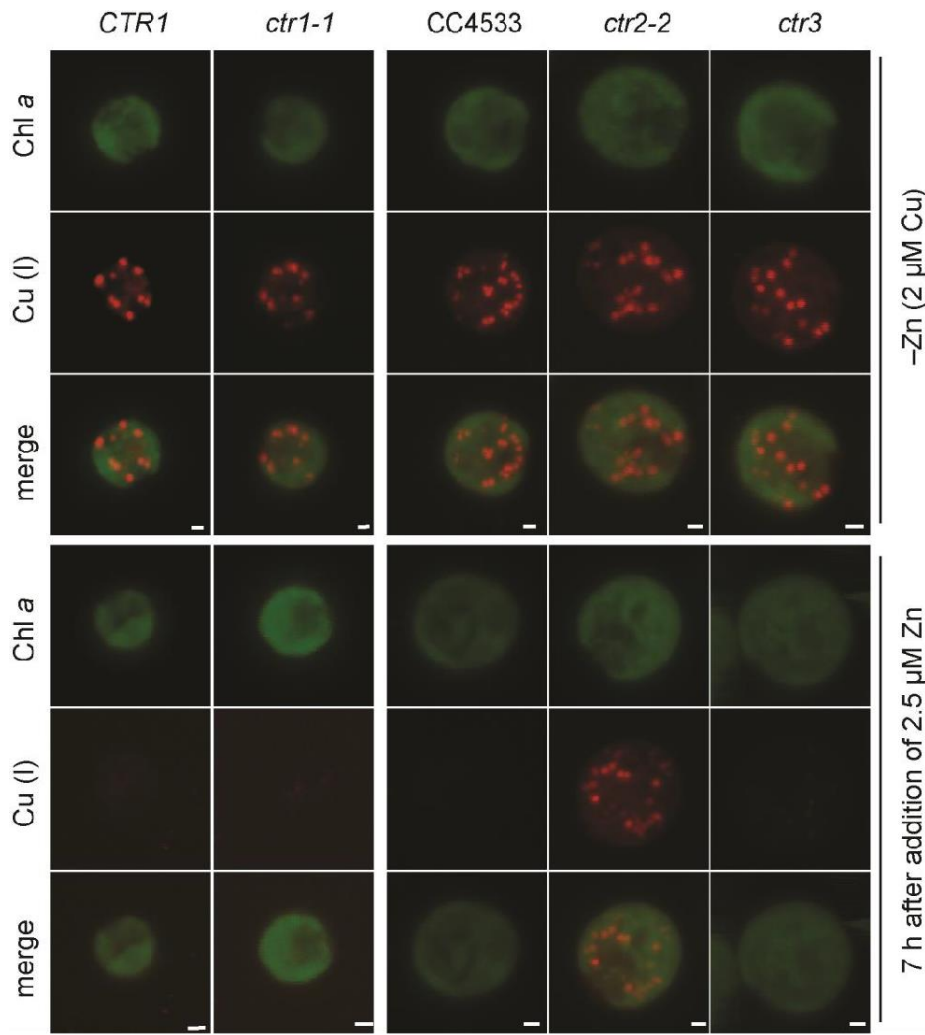
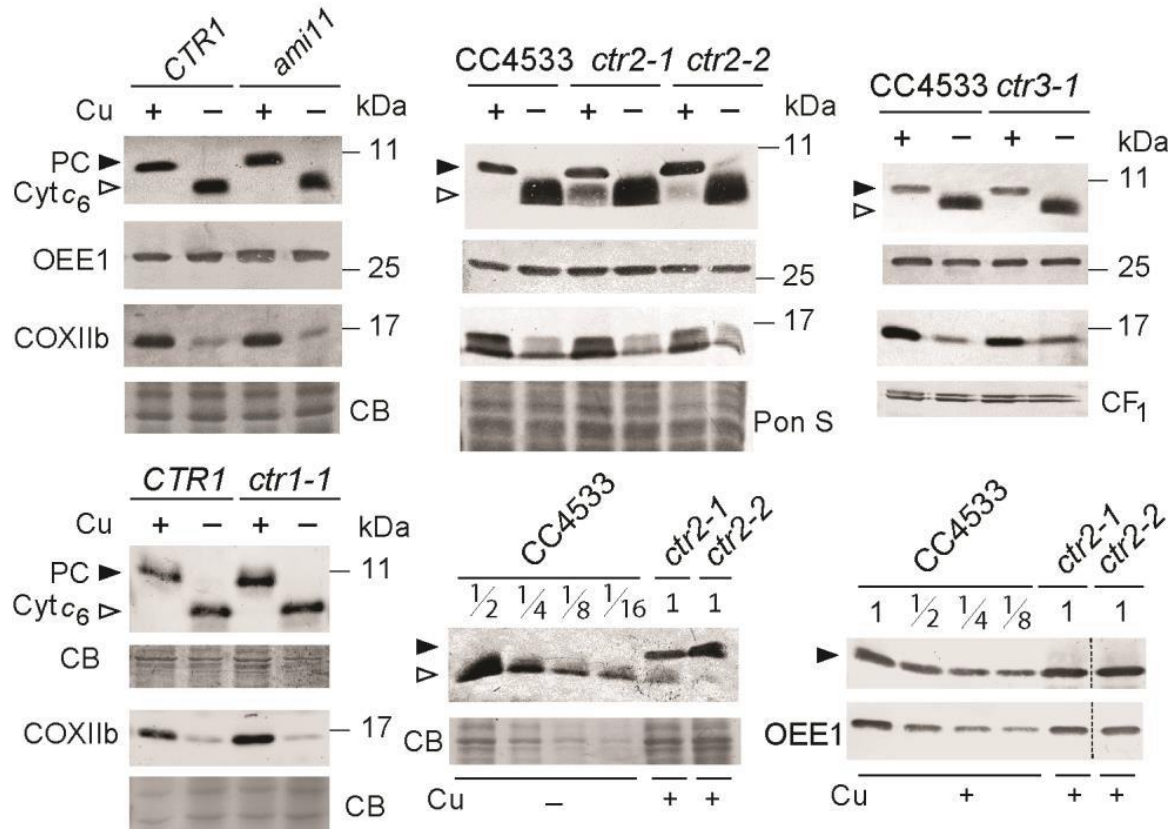


Figure 2.27: CTR2 is exporting copper out of the acidocalcisomes. Cells were grown in media without zinc supplementation. At a cell density between $2-4 \times 10^6$ cells/ml, zinc was added back to the culture media. Samples for imaging were taken right before and 7 hours after zinc add back. Copper was visualized using the Cu(I) sensitive dye CS3, cells were visualized using chlorophyll autofluorescence. Scale bars represents 5 μm. Experiment was performed at least twice with independent cultures. At least 5 cells of two independent mutants were imaged and are shown in Supplemental Figure 2.S4 and 2.S5

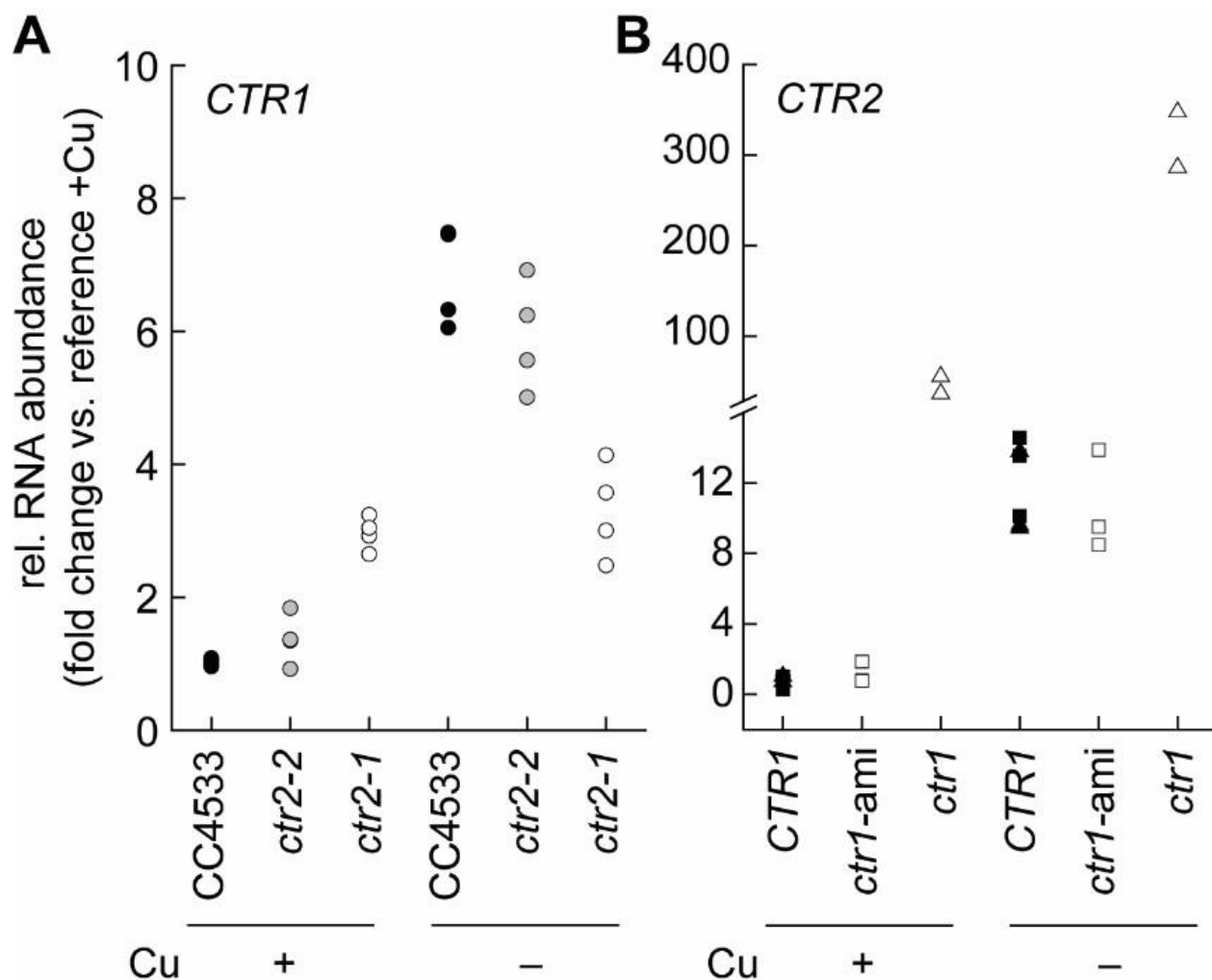
	PAM	Wild-type target	
CC-425	CAGCTCGTTCA	<u>TTTC</u> GGATGCGGCGGCGCTCAGCGCCTA	CTGCACGACGACCGGCGCTCTGGCGTACCGG
<i>ctr1-1</i>	CAGCTCGTTCA	<u>TTTC</u> <u>GTAAGCGTAG</u> GCGCTCAGCGCCTA	CTGCACGACGACCGGCGCTCTGGCGTACCGG
<i>ctr1-2</i>	CAGCTCGTTCA	<u>TTTC</u> <u>GTAAGCGTAG</u> GCGCTCAGCGCCTA	CTGCACGACGAC <u>GAC</u> CGGCGCTCTGGCGTACCGG
<i>ctr1-3</i>	CAGCTCGTTCA	<u>TTTC</u> <u>GTAAGCGTAG</u> GCGCTCAGCGCCTA	CTGCACGACGACCGGCGCTCTGGCGTACCGG
<i>ctr1-4</i>	CAGCTCGTTCA	<u>TTTC</u> <u>GTAAGCGTAG</u> GCGCTCAGCGCCTA	CTGCACGACGACCGGCGCTCTGGCGTACCGG
<i>ctr1-5</i>	CAGCTCGTTCA	<u>TTTC</u> <u>GTAAGCGTAG</u> GCGCTCAGCGCCTA	CTGCACGACGACCGGCGCTCTGGCGTACCGG

Knock-in fragment

Supplemental Figure 2.S1 ssODN mediated CRISPR/CPF1 gene editing introducing two in- frame stop codons in exon 1 of *CTR1*. Sequencing of cells edited at *CTR1* using LbCpf1 (Ribonucleoproteins) RNPs. *CTR1* was amplified from arginine- resistant colonies growing on solid TAP growth media. Green background indicates the PAM target site, blue background indicates the wildtype sequence, yellow background indicates the region after the cleavage site that contains nucleic acids that deviated in the ssODN from the wildtype sequence. Stop codons are underlined in red, other deviations from the wildtype sequence are highlighted in red.

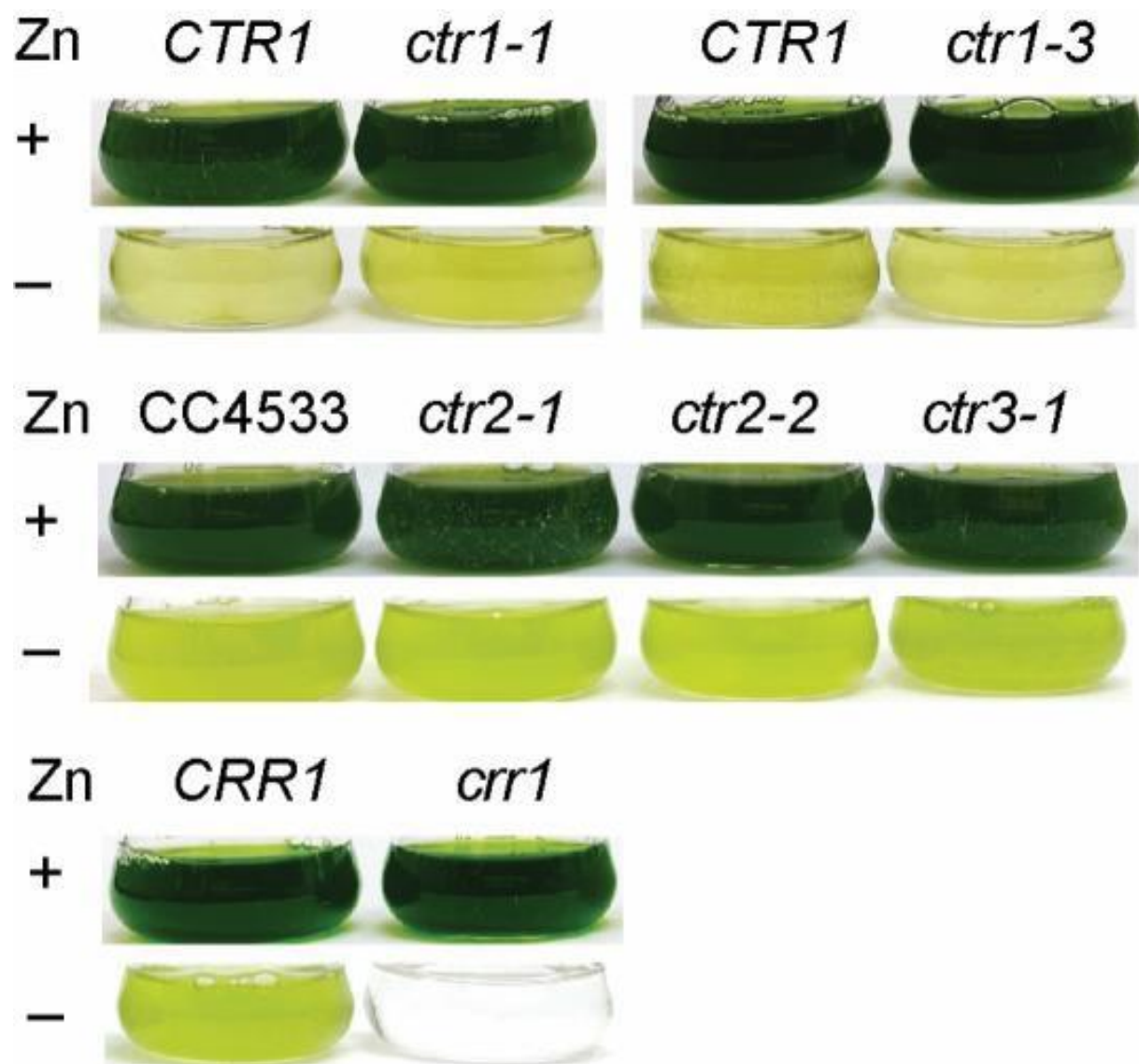


Supplemental Figure 2.S2 Cytochrome c_6 accumulation indicates internal copper deficiency in *ctr2*. *CTR1* amiRNA lines, *ctr1-1*, *ctr2-1*, *ctr2-2*, *ctr3* and respective reference lines were grown photoheterotrophically under Cu-deficient (–) or Cu-replete (+) conditions. Abundance of Plastocyanin and Cytochrome c_6 was determined by separating 10 μ g of total soluble cell lysate using SDS-PAGE (15% monomer), followed by immunoblotting using antisera cross-reactive to plastocyanin (PC, black arrow) and Cyt c_6 (white arrow). In order to check abundance of CoxIIb, total cell lysates were separated by SDS-PAGE (15% monomer) followed by immunoblotting for CoxIIb. Either OEE1, alpha and beta subunits of CF₁, Ponceau S stain (Pon S) or Coomassie blue (CB) were used as loading controls. Shown is one example from at least two independent experiments.

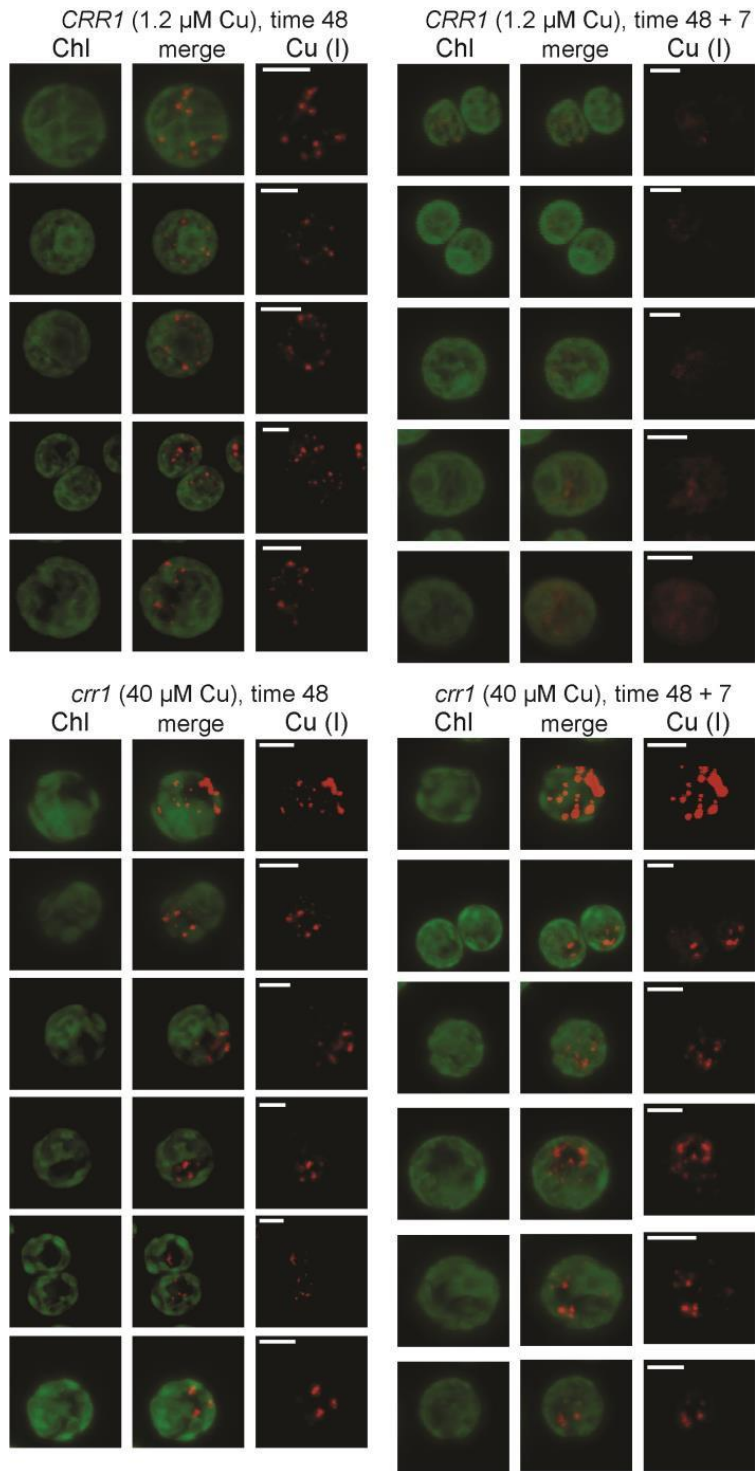


Supplemental Figure 2.S3 Co-regulation between *CTR1* and *CTR2* expression.

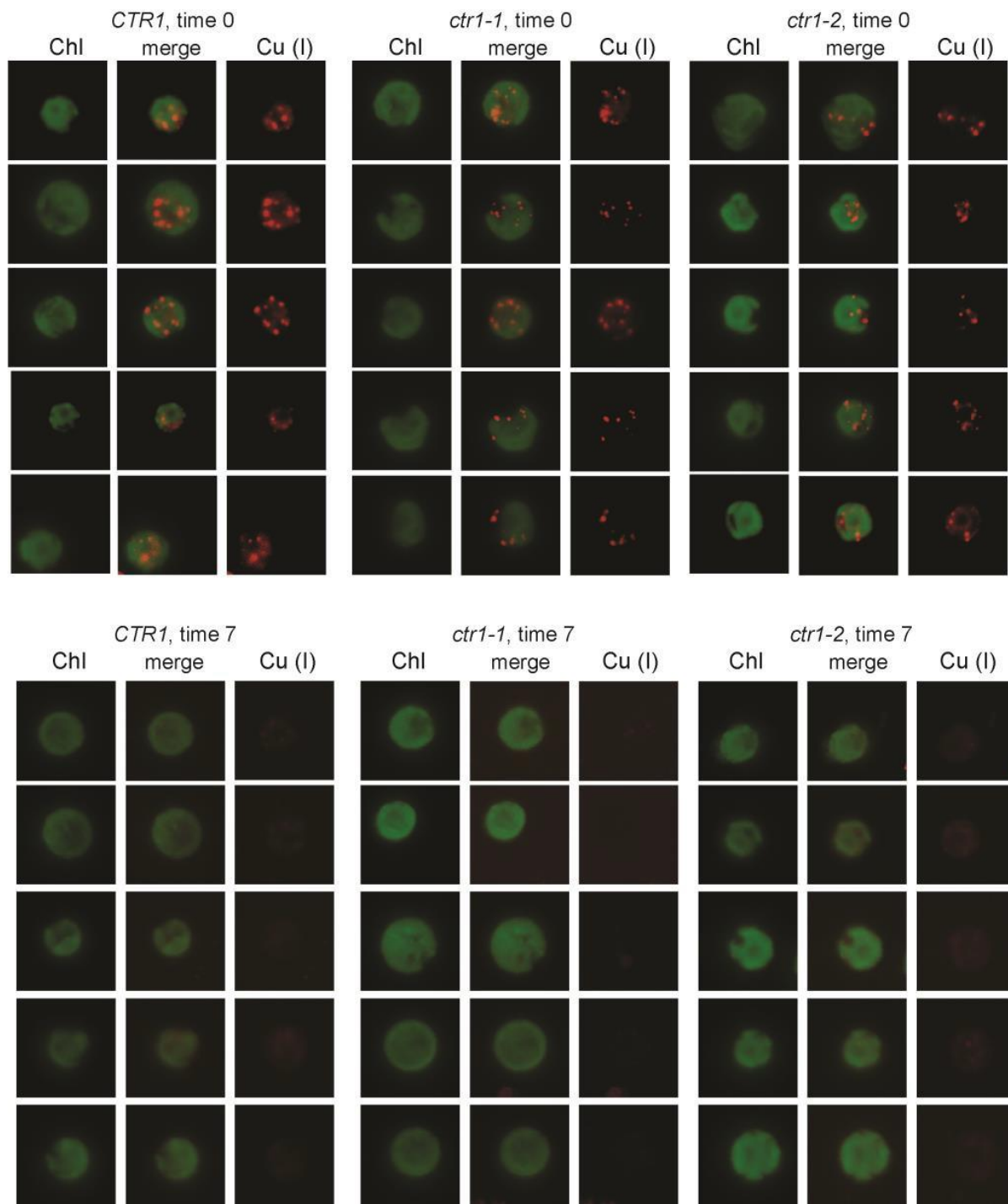
Relative transcript abundances of *CTR1* and *CTR2* were determined using quantitative RT-PCR. Cells were grown in either Cu deficient (–) or replete (+) conditions as indicated. Samples collected from (A) Reference strain CC4533 (filled circles), *ctr2-2* (open, gray circles) and *ctr2-1* (open white circles), (B) *CTR1* (empty vector control lines, black filled squares, and CPF1-mediated mutant background strain, black triangle up), *ctr1-ami* lines (open, white squares) and *ctr1* mutant lines (white triangle up). Each symbol represents an independent experiment.



Supplemental Figure 2.S4 Zinc deficient growth defect is not exacerbated in *ctr* mutants. Pictures of flasks of *ctr1*, *ctr2*, *ctr3* and *crr1* mutants and corresponding reference strains grown in zinc deplete media were taken eight days post-inoculation.

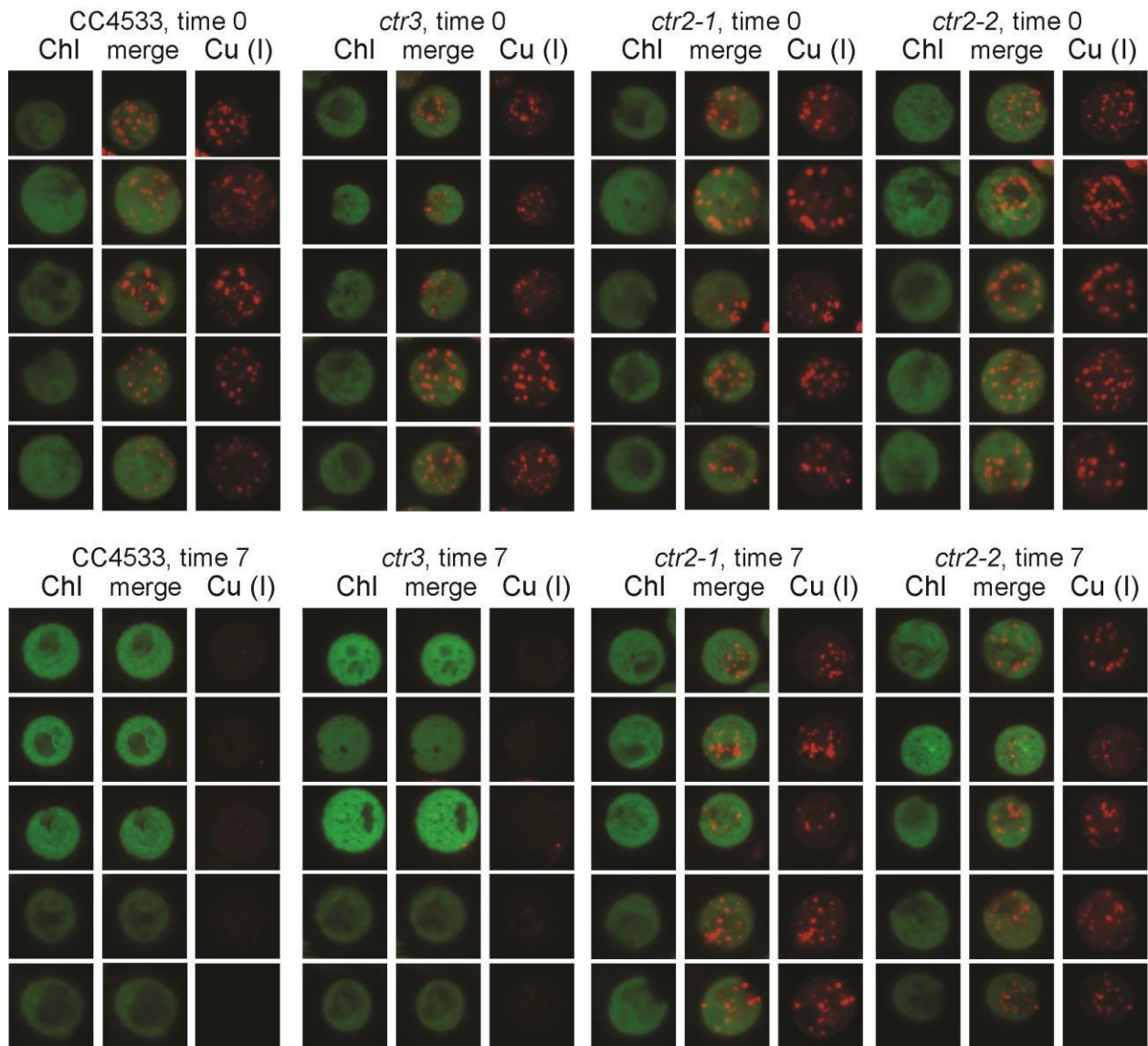


Supplemental Figure 2.S5 Copper accumulated in zinc deficient *crr1* is stored in distinct foci, but copper cannot be mobilized after zinc add back. Figure shows all cells that were imaged in experiments shown and described in Figure 10.



Supplemental Figure 2.S6 Copper accumulated in zinc deficient *ctr1* mutants.

Figure shows all cells that were imaged in experiments shown and described in Figure 11.



Supplemental Figure 2.S7 Copper accumulated in zinc deficient *ctr2* and *ctr3* mutants. Figure shows all cells that were imaged in experiments shown and described in Figure 11.

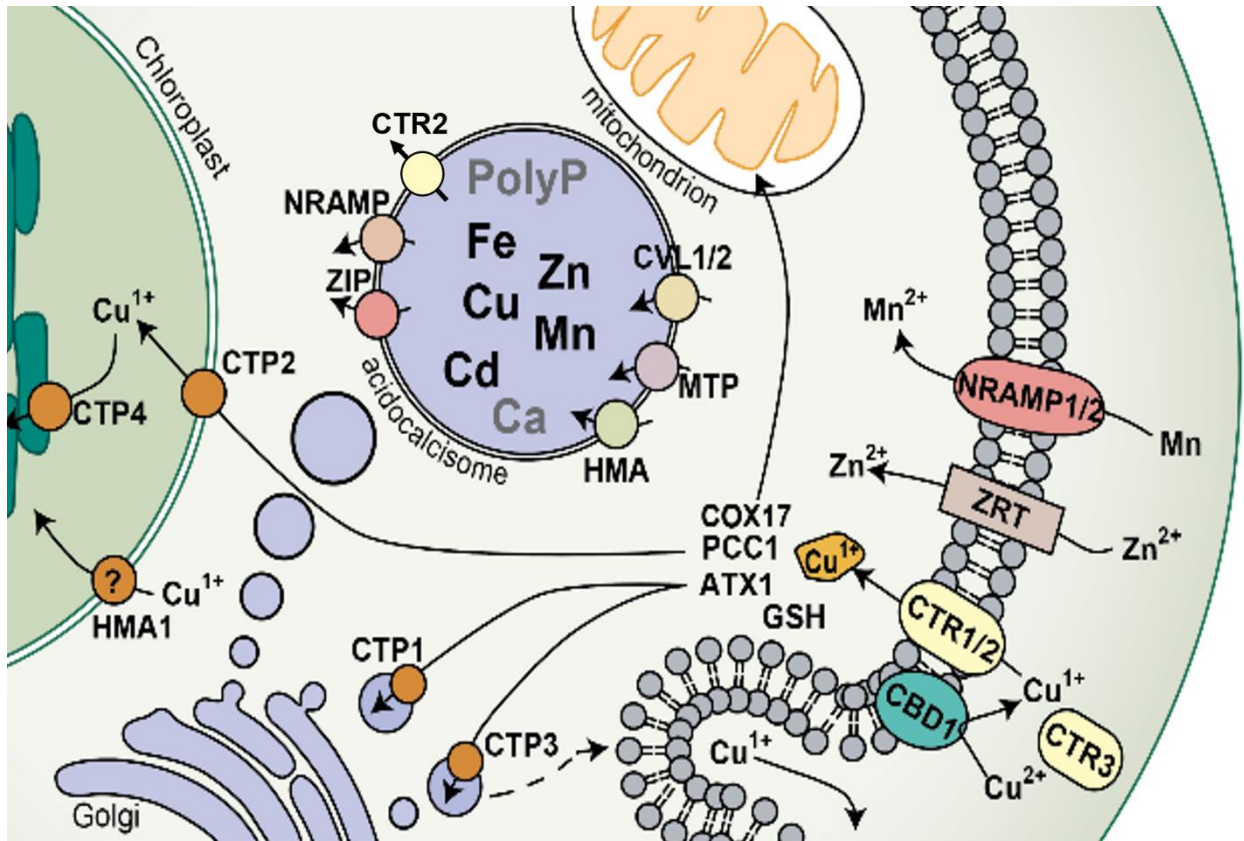


Fig. 2.28 Model of Cu homeostatic network in *Chlamydomonas reinhardtii* (modified from figure made by Stefan Schmollinger)

2.8 References

- 1) (34) Merchant SS, Allen MD, Kropat J, Moseley JL, Long JC, Tottey S, Terauchi AM (2006) Between a rock and a hard place: trace element nutrition in *Chlamydomonas*. *Biochim Biophys Acta* 1763: 578-594.
- 2) (25) Kropat J, Hong-Hermesdorf A, Casero D, Ent P, Castruita M, Pellegrini M, Merchant SS, and Malasarn D. (2011) A revised mineral nutrient supplement increases biomass and growth rate in *Chlamydomonas reinhardtii*. *Plant Journal* 66: 770-780.
- 3) (56) Jinkerson RE, Jonikas MC (2015) Molecular techniques to interrogate and edit the *Chlamydomonas* nuclear genome. *The Plant Journal* 82:393-412.
- 4) (17) Page DM, Kropat PP, Hamel PP, and Merchant SS. (2009). Two *Chlamydomonas* CTR Copper Transporters with a Novel Cys-Met Motif are localized to the plasma membrane and function in copper assimilation. *The Plant Cell*. 21: 928-943.
- 5) (22) Boal AK, and Rosenzweig AC. Structural Biology of Copper Trafficking. *American Chemical Review*. 109: 4760-4779.
- 6) (42) Zhou B, and Gitschier J. (1997) hCTR1: human gene for copper uptake identified by complementation in yeast. *PNAS* 94:7481-7486.
- 7) (15) Blaby-Haas CE, and Merchant SS. (2012) The ins and outs of algal metal transport. *Biochimica et Biophysica Acta*. 1823: 1531-1552.
- 8) (2) Kropat J, Gallaher SD, Urzica EI, Nakamoto SS, Strenkert D, Tottey S, Mason AZ, and Merchant SS. (2015) Copper economy in *Chlamydomonas*: Prioritized

allocation and reallocation of copper to respiration vs. photosynthesis. *Proceedings of the National Academy of the Sciences*. 112: 2644-2651.

- 9) (43) Sommer F, Kropat J, Malasarn D, Grosseohme NE, Chen X, Giedroc DP and Merchant SS (2010) The CRR1 Nutritional Copper Sensor in *Chlamydomonas* contain Two Distinct Metal-Responsive domains. *The Plant Cell* 22: 4098-4113.
- 10)(21) Hong-Hermesdorf A, Miethke M, Gallaher SD, Kropat J, Dodani SC, Chan J, Barupala D, Domaille DW, Shirasaki DI, Loo JA, Weber PK, Pett-Ridge J, Stemmler TL, Chang CJ and Merchant SS. (2014). Sub-cellular metal imaging identifies dynamic sites of Cu accumulation in *Chlamydomonas*. *Nature Chemical Biology*. 10: 1034-1042.
- 11)(7) Malasarn D, Kropat J, Hsieh SI, Finazzi G, Casero D, Loo JA, Pellegrini M, Wollman FA, and Merchant SS. (2013). Zinc Deficiency Impacts CO₂ Assimilation and Disrupts Copper Homeostasis in *Chlamydomonas reinhardtii*. *Journal of Biological Chemistry*. 288: 10672-10683.
- 12)(11) Maryon EB, Molloy SA, and Kaplan JH. (2013). Cellular glutathione plays a key role in copper uptake mediated by human copper transporter 1. *American Journal of Physiology*. 304:C768-C779.
- 13) Speisky H., Gomez M., Carrasco-Pozo, C., Pastene E., Lopez-Alarcon C., Olea-Azar, C. (2008). Cu(I)-glutathione complex: a potential source of superoxide radicals generation. *Bioorganic Medical Chemistry*. 13:6568-74.
- 14)(castruita, unpublished) Castruita, M., D. Casero, S.J. Karpowicz, J. Kropat, A. Vieler, S.I. Hsieh, W.H. Yan, S. Cokus, J.A. Loo, C. Benning, M. Pellegrini, and S.S. Merchant. 2011. Systems Biology Approach in *Chlamydomonas* Reveals

Connections between Copper Nutrition and Multiple Metabolic Steps. *The Plant cell*. 23:1273-1292.

- 15)(18) Morgan MT, Nguyen LAH, Hancock HL, and Fahrni CJ. (2017). Glutathione limits aquacopper(I) to sub-femtomolar concentration through cooperative assembly of a tetranuclear cluster. *Journal of Biological Chemistry*. 292: 21558-21567.
- 16)(39) Noctor G, Queval G, Mhamdi A, Chaouch S, and Foyer CH (2011) Glutathione. *The Arabidopsis Book*. 9: 1-32.
- 17)(12) La Fontaine S, and Mercer, JFB. 2007. Trafficking of the copper-ATPases, ATP7A and ATP7B: Role in copper homeostasis. *Archives of Biochemistry and Biophysics*. 463:149-167.
- 18)(10) Fu X, Zhang Y, Jiang W, Monnot AD, Bates CA, and Zheng W. (2014) Regulation of copper Transport Crossing Brain Barrier systems by Cu-ATPases: Effect of Manganese Exposure. *Toxicological Sciences*. 139: 432-451.
- 19)(60) Wood P (1978) Interchangeable Copper and Iron Proteins in Algal Photosynthesis. *European Journal of Biochemistry* 87: 9-19
- 20)(23) Ruiz FA, Lea CR, Oldfield E, and Docampo R. (2004) Human Platelet Dense Granules Contain Polyphosphate and Are Similar to Acidocalcisomes of Bacteria and Unicellular Eukaryotes. *The Journal of Biological Chemistry*. 279: 44250-44257.
- 21)(24) Blaby-Haas CE, and Merchant SS. (2014). Lysosome-related organelles as mediators of metal homeostasis. *The Journal of Biological Chemistry*. 289: 28129-28136.

- 22)(46) Howe G and Merchant S (1992) Heavy Metal-Activated Synthesis of Peptides in *Chlamydomonas reinhardtii*. *Plant Physiology* 98: 127-136.
- 23) Festa, R.A., and D.J. Thiele. 2011. Copper: An essential metal in biology. *Curr Biol.* 21:R877-R883.
- 24) Dancis, A., D. Haile, D.S. Yuan, and R.D. Klausner. 1994. The *Saccharomyces cerevisiae* Copper Transport Protein (Ctr1p) - Biochemical, Characterization, Regulation by Copper, and Physiological-Role in Copper Uptake. *Journal of Biological Chemistry.* 269:25660-25667.
- 25) Georgatsou, E., L.A. Mavrogiannis, G.S. Fragiadakis, and D. Alexandraki. 1997. The yeast Fre1p/Fre2p cupric reductases facilitate copper uptake and are regulated by the copper-modulated Mac1p activator. *The Journal of biological chemistry.* 272:13786-13792.
- 26) Hassett, R., and D.J. Kosman. 1995. Evidence for Cu(II) reduction as a component of copper uptake by *Saccharomyces cerevisiae*. *The Journal of biological chemistry.* 270:128-134.
- 27) Hill, K.L., R. Hassett, D. Kosman, and S. Merchant. 1996. Regulated copper uptake in *Chlamydomonas reinhardtii* in response to copper availability. *Plant physiology.* 112:697-704.
- 28) Kampfenkel, K., S. Kushnir, E. Babiychuk, D. Inze, and M. Van Montagu. 1995. Molecular characterization of a putative *Arabidopsis thaliana* copper transporter and its yeast homologue. *The Journal of biological chemistry.* 270:28479-28486.
- 29) Liu, X.F., F. Supek, N. Nelson, and V.C. Culotta. 1997. Negative control of

- heavy metal uptake by the *Saccharomyces cerevisiae* BSD2 gene. *The Journal of biological chemistry*. 272:11763-11769.
- 30) Puig, S., and D.J. Thiele. 2002. Molecular mechanisms of copper uptake and distribution. *Current opinion in chemical biology*. 6:171-180.
- 31) Aller, S.G., E.T. Eng, C.J. De Feo, and V.M. Unger. 2004. Eukaryotic CTR copper uptake transporters require two faces of the third transmembrane domain for helix packing, oligomerization, and function. *The Journal of biological chemistry*. 279:53435-53441.
- 32) Kim, B.E., T. Nevitt, and D.J. Thiele. 2008. Mechanisms for copper acquisition, distribution and regulation. *Nat Chem Biol*. 4:176-185.
- 33) Wang, H.L., H.M. Du, H.Y. Li, Y. Huang, J.Z. Ding, C. Liu, N. Wang, H. Lan, and S.Z. Zhang. 2018. Identification and functional characterization of the ZmCOPT copper transporter family in maize. *Plos One*. 13.
- 34) Peñarrubia, L., N. Andrés-Colás, J. Moreno, and S. Puig. 2010. Regulation of copper transport in *Arabidopsis thaliana*: a biochemical oscillator? *Journal of biological inorganic chemistry : JBIC : a publication of the Society of Biological Inorganic Chemistry*. 15:29-36.
- 35) Petris, M.J. 2004. The SLC31 (Ctr) copper transporter family. *Pflugers Archiv : European journal of physiology*. 447:752-755.
- 36) Peña, M.M.O., S. Puig, and D.J. Thiele. 2000. Characterization of the *Saccharomyces cerevisiae* high affinity copper transporter Ctr3. *Journal of Biological Chemistry*. 275:33244-33251.
- 37) Knight, S.A.B., S. Labbe, L.F. Kwon, D.J. Kosman, and D.J. Thiele. 1996. A

widespread transposable element masks expression of a yeast copper transport gene. *Gene Dev.* 10:1917-1929.

- 38) Puig, S., V. Sancenón, L. Peñarrubia, and D.J. Thiele. 2003. Utilization of *S. cerevisiae* mutants defective in high affinity copper uptake to characterize copper transporters from plants and mammals. *Yeast.* 20:S243-S243.
- 39) Eisses, J.F., and J.H. Kaplan. 2002. Molecular characterization of hCTR1, the human copper uptake protein. *Journal of Biological Chemistry.* 277:29162-29171.
- 40) Lee, J., M.M.O. Pena, Y. Nose, and D.J. Thiele. 2002. Biochemical characterization of the human copper transporter Ctr1. *Journal of Biological Chemistry.* 277:4380-4387.
- 41) Lee, L.W., J.R. Prohaska, and D.J. Thiele. 2001. Essential role for mammalian copper transporter Ctr1 in copper homeostasis and embryonic development. *P Natl Acad Sci USA.* 98:6842-6847.
- 42) Turski, M.L., and D.J. Thiele. 2007. *Drosophila* Ctr1A functions as a copper transporter essential for development. *Journal of Biological Chemistry.* 282:24017-24026.
- 43) Zhou, H., K.M. Cadigan, and D.J. Thiele. 2003. A copper-regulated transporter required for copper acquisition, pigmentation, and specific stages of development in *Drosophila melanogaster*. *The Journal of biological chemistry.* 278:48210-48218.

- 44) Sancenón, V., S. Puig, H. Mira, D.J. Thiele, and L. Peñarrubia. 2003. Identification of a copper transporter family in *Arabidopsis thaliana*. *Plant molecular biology*.51:577-587.
- 45) Andres-Colas, N., A. Perea-Garcia, S. Puig, and L. Penarrubia. 2010. Deregulated copper transport affects Arabidopsis development especially in the absence of environmental cycles. *Plant physiology*. 153:170-184.
- 46) Garcia-Molina, A., N. Andres-Colas, A. Perea-Garcia, U. Neumann, S.C. Dodani, P. Huijser, L. Penarrubia, and S. Puig. 2013. The Arabidopsis COPT6 Transport Protein Functions in Copper Distribution Under Copper-Deficient Conditions. *Plant and Cell Physiology*. 54:1378-1390.
- 47) Jung, H.I., S.R. Gayomba, M.A. Rutzke, E. Craft, L.V. Kochian, and O.K. Vatamaniuk. 2012. COPT6 is a plasma membrane transporter that functions in copper homeostasis in Arabidopsis and is a novel target of SQUAMOSA promoter-binding protein-like 7. *The Journal of biological chemistry*.287:33252-33267.
- 48) Sancenon, V., S. Puig, I. Mateu-Andres, E. Dorcey, D.J. Thiele, and L. Penarrubia. 2004. The Arabidopsis copper transporter COPT1 functions in root elongation and pollen development. *Journal of Biological Chemistry*. 279:15348-15355.
- 49) Garcia-Molina, A., N. Andres-Colas, A. Perea-Garcia, S. Del Valle-Tascon, L. Penarrubia, and S. Puig. 2011. The intracellular Arabidopsis COPT5 transport protein is required for photosynthetic electron transport under severe copper deficiency. *Plant J*. 65:848-860.

- 50)Klaumann, S., S.D. Nickolaus, S.H. Furst, S. Starck, S. Schneider, H.E. Neuhaus, and O. Trentmann. 2011. The tonoplast copper transporter COPT5 acts as an exporter and is required for interorgan allocation of copper in *Arabidopsis thaliana*. *New Phytol.* 192:393-404.
- 51)Yuan, M., Z. Chu, X. Li, C. Xu, and S. Wang. 2010. The bacterial pathogen *Xanthomonas oryzae* overcomes rice defenses by regulating host copper redistribution. *The Plant cell.* 22:3164-3176.
- 52)Yuan, M., X. Li, J. Xiao, and S. Wang. 2011. Molecular and functional analyses of COPT/Ctr-type copper transporter-like gene family in rice. *BMC plant biology.* 11:69.
- 53)Merchant, S.S., S.E. Prochnik, O. Vallon, E.H. Harris, S.J. Karpowicz, G.B. Witman, A. Terry, A. Salamov, L.K. Fritz-Laylin, L. Marechal-Drouard, W.F. Marshall, L.H. Qu, D.R. Nelson, A.A. Sanderfoot, M.H. Spalding, V.V. Kapitonov, Q. Ren, P. Ferris, E. Lindquist, H. Shapiro, S.M. Lucas, J. Grimwood, J. Schmutz, P. Cardol, H. Cerutti, G. Chanfreau, C.L. Chen, V. Cognat, M.T. Croft, R. Dent, S. Dutcher, E. Fernández, H. Fukuzawa, D. González-Ballester, D. González-Halphen, A. Hallmann, M. Hanikenne, M. Hippler, W. Inwood, K. Jabbari, M. Kalanon, R. Kuras, P.A. Lefebvre, S.D. Lemaire, A.V. Lobanov, M. Lohr, A. Manuell, I. Meier, L. Mets, M. Mittag, T. Mittelmeier, J.V. Moroney, J. Moseley, C. Napoli, A.M. Nedelcu, K. Niyogi, S.V. Novoselov, I.T. Paulsen, G. Pazour, S. Purton, J.P. Ral, D.M. Riaño-Pachón, W. Riekhof, L. Rymarquis, M. Schroda, D. Stern, J. Umen, R. Willows, N. Wilson, S.L. Zimmer, J. Allmer, J. Balk, K. Bisova, C.J. Chen, M. Elias, K. Gendler, C. Hauser, M.R. Lamb, H. Ledford, J.C. Long, J.

- Minagawa, M.D. Page, J. Pan, W. Pootakham, S. Roje, A. Rose, E. Stahlberg, A.M. Terauchi, P. Yang, S. Ball, C. Bowler, C.L Dieckmann, V.N. Gladyshev, P. Green, R. Jorgensen, S. Mayfield, B. Mueller- Roeber, S. Rajamani, R.T. Sayre, P. Brokstein, et al. 2007. The *Chlamydomonas* Genome Reveals the Evolution of Key Animal and Plant Functions. *Science (New York, N.Y.* 318:245-250.
- 54)Chen, J.C., S.I. Hsieh, J. Kropat, and S.S. Merchant. 2008. A ferroxidase encoded by FOX1 contributes to iron assimilation under conditions of poor iron nutrition in *Chlamydomonas*. *Eukaryotic cell.* 7:541-545.
- 55)La Fontaine, S., J.M. Quinn, S.S. Nakamoto, M.D. Page, V. Gohre, J.L. Moseley, J. Kropat, and S. Merchant. 2002. Copper-dependent iron assimilation pathway in the model photosynthetic eukaryote *Chlamydomonas reinhardtii*. *Eukaryotic cell.* 1:736-757.
- 56)Terzulli, A., and D.J. Kosman. 2010. Analysis of the high-affinity iron uptake system at the *Chlamydomonas reinhardtii* plasma membrane. *Eukaryotic cell.* 9:815- 826.
- 57)Adams, M.S., C.T. Dillon, S. Vogt, B. Lai, J. Stauber, and D.F. Jolley. 2016. Copper Uptake, Intracellular Localization, and Speciation in Marine Microalgae Measured by Synchrotron Radiation X-ray Fluorescence and Absorption Microspectroscopy. *Environ Sci Technol.* 50:8827-8839.
- 58)Croot, P.L., B. Karlson, J.T. van Elteren, and J.J. Kroon. 2003. Uptake and efflux of Cu-64 by the marine cyanobacterium *Synechococcus* (WH7803). *Limnol Oceanogr.* 48:179-188.

- 59) Knauer, K., R. Behra, and L. Sigg. 1997. Adsorption and uptake of copper by the green alga *Scenedesmus subspicatus* (Chlorophyta). *J Phycol.* 33:596-601.
- 60) Blaby-Haas, C.E., M. Castruita, S.T. Fitz-Gibbon, J. Kropat, and S.S. Merchant. 2016. Ni induces the CRR1-dependent regulon revealing overlap and distinction between hypoxia and Cu deficiency responses in *Chlamydomonas reinhardtii*. *Metallomics : integrated biometal science.* 8:679-691.
- 61) Castruita, M., D. Casero, S.J. Karpowicz, J. Kropat, A. Vieler, S.I. Hsieh, W.H. Yan, S. Cokus, J.A. Loo, C. Benning, M. Pellegrini, and S.S. Merchant. 2011. Systems Biology Approach in *Chlamydomonas* Reveals Connections between Copper Nutrition and Multiple Metabolic Steps. *The Plant cell.* 23:1273-1292.
- 62) Hsieh, S.I., M. Castruita, D. Malasarn, E. Urzica, J. Erde, M.D. Page, H. Yamasaki, D. Casero, M. Pellegrini, S.S. Merchant, and J.A. Loo. 2013. The proteome of copper, iron, zinc, and manganese micronutrient deficiency in *Chlamydomonas reinhardtii*. *Mol Cell Proteomics.* 12:65-86.
- 63) Allen, M.D., J.A. del Campo, J. Kropat, and S.S. Merchant. 2007. FEA1, FEA2, and FRE1, encoding two homologous secreted proteins and a candidate ferrireductase, are expressed coordinately with FOX1 and FTR1 in iron- deficient *Chlamydomonas reinhardtii*. *Eukaryotic cell.* 6:1841-1852.
- 64) Molnár, A., A. Bassett, E. Thuenemann, F. Schwach, S. Karkare, S. Ossowski, D. Weigel, and D. Baulcombe. 2009. Highly specific gene silencing by artificial microRNAs in the unicellular alga *Chlamydomonas reinhardtii*. *Plant J.* 58:165-174.

- 65) Schmollinger, S., D. Strenkert, and M. Schroda. 2010. An inducible artificial microRNA system for *Chlamydomonas reinhardtii* confirms a key role for heat shock factor 1 in regulating thermotolerance. *Current genetics*. 56:383-389.
- 66) Ferenczi, A., D.E. Pyott, A. Xipnitou, and A. Molnar. 2017. Efficient targeted DNA editing and replacement in *Chlamydomonas reinhardtii* using Cpf1 ribonucleoproteins and single-stranded DNA. *Proc Natl Acad Sci U S A*. 114:13567-13572.
- 67) Greiner, A., S. Kelterborn, H. Evers, G. Kreimer, I. Sizova, and P. Hegemann. 2017. Targeting of Photoreceptor Genes in *Chlamydomonas reinhardtii* via Zinc-Finger Nucleases and CRISPR/Cas9. *The Plant cell*. 29:2498-2518.
- 68) Li, X.B., W. Patena, F. Fauser, R.E. Jinkerson, S. Saroussi, M.T. Meyer, N. Ivanova, J.M. Robertson, R. Yue, R. Zhang, J. Vilarrasa-Blasi, T.M. Wittkopp, S. Ramundo, S.R. Blum, A. Goh, M. Laudon, T. Srikumar, P.A. Lefebvre, A.R. Grossman, and M.C. Jonikas. 2019. A genome-wide algal mutant library and functional screen identifies genes required for eukaryotic photosynthesis. *Nat Genet*. 51:627-+.
- 69) Kim, B.E., T. Nevitt, and D.J. Thiele. 2008. Mechanisms for copper acquisition, distribution and regulation. *Nat Chem Biol*. 4:176-185.
- 70) Bellemare, D.R., L. Shaner, K.A. Morano, J. Beaudoin, R. Langlois, and S. Labbe. 2002. Ctr6, a vacuolar membrane copper transporter in *Schizosaccharomyces pombe*. *The Journal of biological chemistry*. 277:46676-46686.
- 71) Rees, E.M., J. Lee, and D.J. Thiele. 2004. Mobilization of intracellular copper

stores by the *ctr2* vacuolar copper transporter. *The Journal of biological chemistry*. 279:54221-54229.

72) van den Berghe, P.V., D.E. Folmer, H.E. Malingre, E. van Beurden, A.E.

Klomp, B. van de Sluis, M. Merks, R. Berger, and L.W. Klomp. 2007. Human copper transporter 2 is localized in late endosomes and lysosomes and facilitates cellular copper uptake. *The Biochemical journal*. 407:49-59.

73) Kindle, K.L., R.A. Schnell, E. Fernandez, and P.A. Lefebvre. 1989. Stable

Nuclear Transformation of *Chlamydomonas* Using the *Chlamydomonas* Gene for Nitrate Reductase. *J Cell Biol*. 109:2589-2601.

74) White C, Lee J, Kambe T, Fritsche K, Petris MJ (2009) A role for the ATP7A

copper-transporting ATPase in macrophage bactericidal activity. *Journal of Biological Chemistry* 284: 33949-33956.

75) Strenkert D, Limso CA, Fatihi A, Schmollinger S, Basset GJ, and Merchant SS.

(2016). Genetically Programmed Changes in Photosynthetic Cofactor Metabolism in Copper-deficient *Chlamydomonas*. *Journal of Biological Chemistry*. 291: 19118-19131.

76) Waalkes MP, Kovatch R, and Rehm S. (1991). Effect of Chronic Dietary Zinc

Deficiency on Damium Toxicity and Carcinogenesis in the mammal Wistar [Hsd: (WI)BR] Rat. *Toxicology and applied Pharmacology* 108: 448-456.

77) Singleton C, and Le Brun NE (2007) Atx1-like chaperones and their cognate P-

type ATPases: copper-binding and transfer. *Biometals* 20: 275-289.

- 78) Jarup L, Berglund M, Elinder CG, Nordberg G, and Vahter M (1998) Health effects of cadmium exposure – a review of the literature and a risk estimate. *Scandinavian journal of Work and Environmental Health*. 24:1-52.
- 79) Banci L, Bertini I, Ciofi-Baffoni S, Kozyreva T, Kairit Z, Palumaa P. (2010) Affinity gradients drive copper to cellular destinations. *Nature*. 7298: 645-8.
- 80) Wang S, Lv J, Zhang S. (2019) Discovery of CRR1-targeted copper deficiency response in *Chlamydomonas reinhardtii* exposed to silver nanoparticles. *Nanotoxicology*. Epub 2019.
- 81) Drew, R., Miners, J.O. (1984) The effects of buthionine sulfoximine (BSO) on glutathione depletion and xenobiotic biotransformation. *Biochemical Pharmacology*. 19:2989-94.

CHAPTER 3: STRENGTH OF CU-EFFLUX RESPONSE IN *E. COLI* COORDINATES METAL RESISTANCE IN *C. ELEGANS* AND CONTRIBUTES TO THE SEVERITY OF ENVIRONMENTAL TOXICITY

3.1 Abstract

Without effective homeostatic systems in place, excess Cu is universally toxic to organisms. While increased utilization of anthropogenic Cu in the environment has driven the diversification of Cu-resistance systems within enterobacteria, little research has focused on how this change in bacterial architecture impacts host organisms that need to maintain their own Cu homeostasis. Therefore, we utilized a simplified host-microbe system to determine whether the efficiency of one bacterial Cu-resistance system, increasing Cu-efflux capacity via the ubiquitous CusRS two-component system, contributes to the availability and subsequent toxicity of Cu in host *C. elegans* nematode. We found that a fully functional Cu-efflux system in bacteria increased the severity of Cu toxicity in host nematodes without increasing the *C. elegans* Cu-body burden. Instead, increased Cu toxicity in the host was associated with reduced expression of the protective metal stress-response gene, *numr-1*, in the posterior pharynx where pharyngeal grinding breaks apart ingested bacteria to release their contents before passing into the digestive tract. The spatial localization of *numr-1* transgene activation and loss of bacterially-dependent Cu-resistance in nematodes without an effective *numr-1* response supports the hypothesis that *numr-1* is responsive to the Cu-efflux capacity of bacteria. We propose that the bacterial Cu-efflux capacity acts as a robust spatial determinant for a host's response to chronic Cu stress.

3.2 Introduction

Bacteria define an organism's relationship with the environment. Their presence in a host at all three major routes of environmental exposure absorption (dermal, respiratory, digestive) broadly impacts drug metabolism and efficacy (1-3), pathogenicity (4), nutrient biosynthesis (5) and disease progression (6-9). However, the contributions of bacterial activity to a host's response during toxicant exposure are only beginning to be examined (10). One such toxicant whose environmental excess elicits conserved homeostatic responses in prokaryotes (11-13) and eukaryotes (14) alike is Copper (Cu), an essential transition metal recognized by the Agency of Toxic Substances and Disease Registry (ATSDR) for its ability to catalyze Fenton-like reactions, displace metal cofactors lower on the Irving-Williams series and oxidize lipids (15-17). In high Cu conditions, without effective appropriate homeostatic responses, toxicity can develop rapidly and coincide with the development of disease pathology (18,19). However, little is known about how these challenged prokaryotic and eukaryotic systems interact. Outside of treatments that limit overall bacterial density (20), how specific bacterial activity contributes to homeostatic responses in the host has yet to be examined. Diversification rates in enterobacteria suggest that Cu-efflux systems are under considerable selective pressure from increasing anthropogenic Cu deposition in the environment (21,22). Furthermore, research from the human microbiome project has found that bacterial activity involved in metal detoxification, such as increasing Cu-efflux capacity, is indeed a ubiquitous component of the digestive microbiome today (23). The pervasiveness and necessity of bacterial Cu-efflux systems at major sites of Cu-uptake, like the digestive tract, compels

a more thorough investigation into how specific bacterial responses contribute to the development of Cu toxicity in host organisms.

Previous work in our lab (24-26) developed strains of *E. coli* with variable Cu-efflux capacities as measured by quantifying their Cu accumulation. Targeted deletions in genes for a Cu-handling system, CusRS, within a Cu oxidase (*cueO*) deletion background maximized the Cu(I) interaction with Cu(I)-specific CusRS and produced mutants with approximately 50 and 25% Cu-efflux capacity compared to *E. coli* with $\Delta cueO$ alone (100% WT) (26). CusRS is a conserved two component system (TCS) composed of a Cu(I) histidine kinase sensor (CusS) and response regulator (CusR) (24). The combined action of this sensor and response regulator drives the expression of a Cu-efflux pump, CusCFBA, with a narrow substrate range that selectively removes excess periplasmic Cu(I) (27) (Fig. 3.1). We hypothesized that alterations in bacterial Cu removal would modify the availability and subsequent toxicity of Cu in a simplified host-microbe system. *Caenorhabditis elegans* (*C. elegans*), a soil-dwelling nematode which thrives on single-culture *E. coli* lawns in laboratory conditions, is a well-established model for studying conserved host-microbe interactions involved in Cu homeostasis and detoxification (4,28-30). Evidence for conserved Cu-homeostatic elements are found in orthologs for a passive Cu-uptake transporter (31) and the active Cu exporter ATP7A/B (32) which are both expressed along the nematode's digestive tract, mirror the expression patterns and physiology of higher organisms (14,20). Under Cu stress, nematodes also present dose-dependent Cu toxicity responses that encompass developmental, behavioral, reproductive, and aging trajectories which may be influenced by bacterial activity (33-40). Furthermore, these responses to metal stress are often consistent and conserved across

species, allowing for a detailed investigation of host stress responses mediated by bacterial activity. For instance, activation of heat-shock factor 1 following metal toxicity is observed in both humans and nematodes (41,42) and is signaled in *C. elegans* with the activation of a nuclear-localized metal-responsive gene (*numr-1*) which is proposed to influence RNA splicing in response to impaired RNA-processing machinery during metal stress (42).

Using this *C. elegans/E.coli* host-microbe system, we show that an increase in bacterial Cu-efflux, through the activity of CusRS, alters the magnitude and spatial distribution of *numr-1* activation and sensitizes the host to environmental Cu over time. Despite increasing sensitivity to equimolar Cu exposures, the overall Cu-body burden of the host did not account for the increasing toxicity in the host. Taken together, these findings reveal how a ubiquitous bacterial response, selected for through persistent anthropogenic Cu release over generations, establishes the spatial distribution and efficiency of Cu detoxification in a host model.

3.3 Materials & Methods

3.3.1 *C. elegans* genetics and strains

All *C. elegans* strains were obtained from the Caenorhabditis Genetic Center (CGC) in Minneapolis, MN, USA. Only non-starved cultures maintained on *OP50* at 20°C on nematode growth media (NGM: 3g NaCl, 17g agar, 2.5g peptone, 1mL 1M CaCl₂, 1mL 5 mg/mL cholesterol in ethanol, 1mL 1M MgSO₄, 25mL 1M KPO₄ per liter) were used for all downstream experiments. The *C. elegans* strains used were

- *N2*: wild-type for all general toxicity endpoints
- *JF85*: mtEx60 [numr-1p::GFP + rol-6(su1006)] for visualization of a metal-stress specific transgene
- *RB1749*: *numr-1(ok2239)* III for matricidal-hatching experiments.

3.3.2 *E. coli* genetics and strains

E. coli strains were either ordered from the CGC or previously isolated and characterized (1,2) in which established methods were used to disrupt targeted chromosomal genes. The *E. coli* strains used were:

- *OP50* -*E. coli* B uracil auxotroph
- *WT* -BW25113/ Δ *cueO*::catR/pET21b(+), control, 100% *WT* bacterial Cu-efflux capacity
- Δ *cusS* -BW25113/ Δ *cueO Δ *cusS*/pET21b(+), 50% *WT* bacterial Cu-efflux capacity*
- Δ *cusR* -BW25113/ Δ *cueO Δ *cusR*/pET21b(+) (1), 25% *WT* bacterial Cu-efflux capacity*
- *E. coli* BL21(*DE3*), pLIC-egfp inducible expression

All *E. coli* strains except *OP50* and *BL21(DE3)* were maintained at 4°C as single colony plates on Luria broth agar (10g bacto-tryptone, 10g NaCl, 5g yeast extract, 15g bacto-agar per liter) supplemented with 5µL 100ng/mL ampicillin. *OP50* and *BL21(DE3)* were maintained on Luria broth agar without ampicillin.

3.3.3 Bacterial culture conditions

Bacterial lawns were prepared by growing overnight cultures at 37°C from a single colony then normalizing to 1×10^8 cells/mL before pipetting 200µL of culture onto the appropriate NGM plates. Seeded plates were incubated at room temperature for 48h prior to storage at 4°C.

3.3.4 Bacterial growth rate and plate density

For each bacterial strain, a single colony was grown overnight at 37°C. From this overnight culture, a 1:100 dilution was made with fresh LB to reach a starting concentration of 0.05 OD₆₀₀. The OD₆₀₀ was measured every 30 minutes until 0.1 was reached. The culture was then diluted by 1:20 with LB containing the desired amount of CuSO₄. The OD₆₀₀ in this culture was measured every hour through exponential growth until the stationary phase was observed. Plate density was determined following a 48h incubation after plates were seeded. 2mL of media were used to wash plates of bacterial lawn and diluted 1:100 before OD₆₀₀ quantification.

3.3.5 Exposure conditions

Dosage was chosen based on previously described 1) dose-dependent toxicity endpoints and EC50 values in the host nematode 2) concentrations relevant to environmental exposures reported globally and 3) dosage studies reporting acute digestive distress upon oral administration in humans and 4) at a concentration that would not impact survival or growth of the *E. coli* strains (25,32,33,35,55-57). All Cu exposures were prepared by adding 0 μ M or 100 μ M CuSO₄ to Nematode growth media (NGM) agar immediately prior to pouring the media plates. Developmentally synchronous populations of *C. elegans* used for toxicity endpoint analysis were obtained from non-starved *OP50* maintenance plates through the use of hypochlorite bleach egg selection (58). In addition to synchronizing populations, hypochlorite bleaching allowed for direct and sterile transfer of eggs from maintenance plates to those that had been seeded with other *E. coli* strains instead. A second transfer 48h after bleach synchronization allowed for a population of nematodes to begin exposure to +/- CuSO₄ at the L4 developmental stage.

3.3.6 Length determination

Nematode length was measured 48h post L4 transfer to +/- Cu plates. For each of the independent experiments, approximately 12 adults from each condition were washed with M9 buffer (3g KH₂PO₄, 6g Na₂HPO₄, 5g NaCl, 1mL 1M MgSO₄ per liter) (59) and placed on bacteria-free NGM. The nematodes were recorded for 15s while roaming around the plate. Video analysis using WormLab tracking software was used to quantify average length for each worm from head to tail.

3.3.7 Body-burden measurements

48 hours after +/- Cu exposure starting at L4, 20 to 50 adult nematodes from each plate were collected for metal-content analysis as previously described (47). Briefly, *C. elegans* were moved to unseeded NGM plate before being transferred to a 1.5mL microfuge tube containing 200µL M9 buffer. Microfuge tubes were rotated by inversion continually for at least 30 minutes to remove excess bacteria. After the first incubation, worms were washed 3 times with 200µL M9 buffer and 3 times with ddH₂O to effectively remove all traces of residual bacteria. The supernatant was removed between each wash under a stereomicroscope to prevent sample loss. Following the last wash, samples were flash frozen in liquid nitrogen and desiccated using an SPD1010 SpeedVac vacuum concentrator. 20µL of 70% HNO₃ was added to desiccated samples before incubation at room temperature overnight followed by a 1 hour incubation at 60°C the next morning to fully digest the pellet. 380µL of 1% HNO₃ was added to samples for a final HNO₃ concentration of 4%. Prepared samples were analyzed for Cu content using graphite furnace atomic absorption spectroscopy (GFAAS) and run in triplicate before the average concentration was determined from an established calibration curve. Body burden is reported as pg/nematode or pg/µm after normalizing for nematode size

3.3.8 Lethality

All lethality experiments were conducted as previously described in *N2 C. elegans* transferred from bleach synchronized populations at L4 to exposure conditions after preconditioning of the bacterial condition following bleach synchronization in early development (60). With the exception of the 36h timepoint after transfer to the exposure condition, all nematodes were transferred every 48h to new plates to keep generations

distinguishable while the nematode was still egg laying and then to prevent starvation at later stages of the lethality experiments. Lethality was tested at least every 48h using a worm pick to look for a touch response. If no movement or response is detected, the nematodes were presumed dead and recorded as such. Nematode populations were simultaneously assessed to account for censorship via disappearance from the plate, MH, everted vulva or death resulting from worm pick or transfer. Kaplan-Meier curve analysis was conducted on collected data to determine significant differences between groups.

3.3.9 Cumulative population risk of matricidal hatching

Occurrence of matricidal hatching (MH) in a population was assessed every 48h for seven days after L4 transfer to +/- Cu plates under a dissecting microscope through the reproductive period of the nematode. Analysis of data used a cumulative incidence model to adjust for a smaller population over time caused by death or censored *C. elegans* not attributable to a bagging phenotype. For every 48h period, the cumulative incidence was divided by the number of subjects at risk in the population at the beginning of the period. Multiplying for the duration of each population's active reproductive period where the majority of bagging occurs (about 7.5 days) gives total cumulative risk among replicate populations. 5 to 8 independent experiments of 25-30 nematodes were conducted for each conditional exposure. A modified Kaplan-Meier risk assessment was used to measure this parameter to minimize the effect of variable survival in the populations (60); for instance, a smaller population as a result of increased death in one condition could artificially reduce incidence of MH observed if the actual population at risk is not accounted for at each timepoint.

3.3.10 Brood-size measurement

Viable brood size was assessed on an individual basis: 1 nematode was placed in +/- Cu plates with the preconditioned bacteria at the L4 stage. 36 hours after initial transfer each nematode was transferred to a new plate. Transfers to new plates were performed every 24 hours after the initial 36 hours transfer. After 30 minutes at 4°C to slow movement, each progeny plate was counted 2 days after the initial egg lay before the F1 began to produce progeny. Each bacterial/Cu condition was tested with 3 independent replicates composed of 5 individual nematode replicates.

3.3.11 Imaging

Before imaging, *C. elegans* exposure and control groups were derived from the same bleach-synchronized population for each bacterial condition and exposed in late development for 48h from L4 to early adulthood. Nematodes were then incubated in 100µM levamisole to inhibit movement while pharyngeal images were taken at 40x using a Nikon H600L fluorescence microscope with uniform exposure times and Z-stack width and processing. The GFP induction was quantified using ImageJ 1.52p for each pharyngeal region. Images taken with a different camera were normalized using the signal to background ratio calculated with an identical sample imaged on both camera set ups. Corrected mean intensity was calculated by subtracting normalized background signals from all samples before subtracting the corrected mean intensity of 0µM Cu controls from the matched 100µM mean intensity for each experimental replicate.

3.3.12 Statistical Analysis

Experimental designs are reported in figure legends such that N= independent experimental replicates and n=biological replicates in each experimental replicate. All statistical analysis was performed in GraphPad Prism (v8.2.0). For lifespan analyses, a Log-rank (Mantel-Cox) test was used to calculate significance. Significant interactions were analyzed for cumulative MH risk, Cu-body burden, brood size, and length. An ordinary one-way ANOVA with Tukey's multiple comparison test was used to analyze interactions between *numr-1p::GFP* transgene activation and bacterial Cu-efflux capacity. A two-way ANOVA with Tukey's multiple comparison's test was also used to confirm that sample size did not account for variation in Cu-body burden determination.

3.4 Results:

3.4.1 A simplified exposure paradigm to test the impact of bacterial Cu-efflux capacity on host Cu sensitivity

We first assessed common Cu-toxicity endpoints observed in *C. elegans* as hallmarks of Cu stress coping mechanisms to determine whether they could be influenced by the bacterial Cu-efflux capacity in the environment. To this aim, we used a simplified exposure paradigm for the *C. elegans/E. coli* host-microbe system that, first, used exogenous (0 μ M) or excess (100 μ M) Cu concentrations that did not strongly impair bacterial growth rate (Fig. 3.S1A) or plate density (Fig. 3.S1B) to ensure that the CusRS response could be active at the same molarity at which *C. elegans* Cu toxicity is observed (32). Second, Cu exposure to *C. elegans* was limited to developmentally synchronous populations that excluded the early developmental stress responses that can confound the severity of toxicity endpoints (32, 39). As described below, this experimental exposure paradigm allowed us to clearly distinguish the impact of varying bacterial Cu-efflux capacity on the *C. elegans* host Cu sensitivity.

C. elegans developmental stage can greatly impact the physiological response to environmental challenges (39). Therefore, multiple, specific dose-dependent chronic Cu-toxicity endpoints were originally selected to capture adverse outcomes on two central biological processes: aging and reproduction (Fig. 3.2A). Initially, all endpoints were assessed for their sensitivity to 100 μ M Cu in the presence of bacteria with 100% *WT* Cu-efflux capacity (control). Across their lifespan, nematode populations exposed to 100 μ M Cu on 100% *WT* control bacteria experienced a 41% reduction in median lifespan (Fig. 3.2B, thick blues lines, $p < 0.0001$, Long-rank Mantel-Cox test), from 14.5d to 8.5d, when

compared to those exposed to 0 μ M Cu in the media. The decreased survival of *C. elegans* exposed to 100 μ M Cu confirms the sensitivity of median lifespan analysis to Cu.

To test whether nematode Cu toxicity also impacted earlier life events in our simplified exposure paradigm, we monitored the reproductive period -where active egg laying takes place (Fig. 3.2A)- by assessing *C. elegans* neuromuscular inability to lay eggs over time, resulting in Matricidal Hatching (MH), and the total number of viable eggs laid (average viable brood size) over the same period. MH, when the offspring of hermaphroditic nematodes hatch inside the parent without being expelled from the vulva, is a response to environmental stress that increased by 25.4% (Fig. 3.2C, blue circles, $p > 0.0001$, two-way ANOVA with Tukey's multiple comparisons) on 100% *WT* control bacteria when 100 μ M Cu exposures are compared to 0 μ M Cu exposures. Furthermore, this trend became more pronounced in the later reproductive period (Fig. 3.2D, thick blue lines). In contrast, over the same reproductive period (Fig. 3.S2A), cumulative brood size was unaffected by the presence of 100 μ M Cu. Further analysis found that brood size was not significantly reduced by the addition of Cu in any bacterial condition tested (Fig. 3.S2B), indicating that any bacterial-dependent variation in brood size appears independent of Cu stress in our simplified exposure paradigm. Taken together, these results identify MH, but not brood size, as a responsive and sensitive endpoint reflective of Cu stress.

To better understand the discrepancy between MH and brood size, we investigated the impact of Cu exposure on the nematode germline. While DAPI-stained germlines early in the reproductive period showed some reduced proliferation of pachytene nuclei indicative of developmental delay (43) (average number of nuclei across in 0 μ M Cu is 10,

but only 8 in 100 μ M Cu) (Fig. 3.S2C-D), there were no strong indicators of acute germline toxicity such as nuclei gaps or aggregates which indicate embryonic lethality and precede reductions in the viable brood size (44) independent of MH. These results suggest that germline toxicity does not contribute to the Cu toxicity observed in *C. elegans* either because this endpoint is less sensitive to Cu stress, as has previously been observed (38), or is more dependent on early developmental exposures.

3.4.2 Role for Bacterial Cu-efflux capacity in host toxicity endpoints

Next, we used the two Cu sensitive endpoints, lifespan and MH, to test whether an impaired bacterial Cu-efflux capacity modifies *C. elegans* response to the addition of 100 μ M Cu in the media. Lifespan assays revealed that nematode populations on bacterial lawns with reduced Cu-efflux capacity (25% or 50% of normal Cu-efflux) exhibited increased median survival compared to those grown with 100%*WT* control bacteria, increasing 47% from 8.5d to 12.5d ($p < 0.0001$, Log-rank Mantel-Cox test) (Fig. 3.2B). MH is similarly improved by reduced bacterial Cu-efflux; 50%*WT* Cu-efflux capacity during Cu stress resulted in a reduced cumulative population risk of just 6.2% (+/-4.4%) compared to 26.7% (+/-4.8%) on 100%*WT* control bacteria ($p < 0.0001$, two-way ANOVA with Tukey's multiple comparisons) while 25%*WT* Cu-efflux capacity reduced cumulative risk of MH by over half of the risk compared to control bacterial lawns (11.7% +/-6.4 vs. 26.7% +/-4.8, respectively $p = 0.0025$, two-way ANOVA with Tukey's multiple comparisons) during exposure to 100 μ M Cu (Fig. 3.2C).

We further assessed whether *E. coli* with impaired bacterial Cu-efflux capacity could act on *C. elegans* Cu-toxicity endpoints independent of their variable Cu-handling induced by 100 μ M Cu, for example via bacterial nutritional status or pathogenicity instead

(45,46). In testing the Cu-independent effects of *E. coli* strains with 25% and 50% *WT* Cu-efflux capacity in 0 μ M Cu, we found that nematodes raised on bacterial lawns with reduced Cu-efflux capacity did not demonstrate any significant difference from those raised on 100% *WT* control bacteria. Without exogenous Cu, median survival ranged from 14.5 to 17.5 days (Fig. 2B, $p = 0.3615$, Log-rank Mantel-Cox test) and total cumulative MH ranged from 2.7 \pm 1.92 to 1.07 \pm 1.53% (Fig. 3.2C, $p = 0.9841$, two-way ANOVA with Tukey's multiple comparisons) with increasing bacterial Cu-efflux capacity. Thus, any variation observed in these Cu-toxicity endpoints during exposures to 100 μ M Cu could be directly attributed to the variable bacterial Cu-efflux capacity. Taken together, these experiments indicate that a decrease in bacterial Cu-efflux capacity is correlated with a reduction in two chronic Cu-toxicity endpoints in *C. elegans*.

3.4.3 Temporal dependence of MH on bacterial Cu-efflux capacity

We further examined MH risk and monitored how MH risk changes over time to better distinguish the effects of Cu-dependent and Cu-independent adverse outcomes. In the absence of 100 μ M Cu, an early uptick in MH risk is observed in 25% *WT* Cu-efflux capacity; between 48 and 72h after L4 transfer to the 0 μ M exposure condition (Fig. 3.2D). However, this early increase is not observed in the 50 or 100% *WT* Cu-efflux capacity conditions. After 72h, no further increase in MH risk is observed in any bacterial genetic background without 100 μ M Cu in the media (Fig 3.2D). Part of this Cu-independent discrepancy may lie in the *cusR* deletion unique to 25% *WT* Cu-efflux capacity *E. coli* which impairs a bacterial H₂O₂ stress response that is activated by CusR independent of Cu stress (45). No such crosstalk exists with the *cusS* deletion responsible for the 50% *WT*

Cu-efflux capacity *E. coli*. These results suggest that Cu-independent roles in the 25% *WT* Cu-efflux capacity *E. coli* are responsible for an early increase in MH risk.

Conversely, the majority of nematode MH risk associated with bacterial Cu-excess occurs later during the nematode's life span, i.e. at timepoints after 72h of exposures in 100% *WT* control bacteria (Fig. 2D). However, this late MH risk is greatly reduced when the bacterial Cu-efflux capacity is limited to either 50% or 25% *WT*. In fact, no significant variation in MH risk is observed in 50% *WT* Cu-efflux capacity bacterial lawns between 0 μ M and 100 μ M Cu exposures by the end of the reproductive period (Fig. 3.2C). While starvation or nutrient deprivation can be a contributing factor in the appearance of nematode MH in late development (46) this effect was minimized by 1) transferring nematodes to new bacterial lawns every two days and 2) utilizing Cu concentrations that had no impact on bacterial growth rates or survival (Fig. 3.S1). These results therefore suggest that late MH risk is mostly dependent on the bacterial response to Cu stress. The timing of MH risk also suggests that bacterial Cu-efflux capacity acts directly on the neuromuscular function of the vulva where age-related degeneration can result in late MH during periods of Cu excess (46).

3.4.4 Early Cu toxicity does not coincide with Cu-body burden in *C. elegans*

Early developmental exposures to Cu strongly impact the growth of *C. elegans*, manifesting as reduced length and larval arrest at the L3 larval stage (32). The potential for our simplified exposure paradigm to initiate growth delays before lifespan and MH risk becomes significant is suggested by the slight reduction in germline proliferation observed after 24h of Cu exposure (Fig. 3.S2C-D). Therefore, we assessed whether reduced bacterial Cu-efflux capacity could alter the nematode's growth after a 48h exposure to 0

or 100 μ M Cu starting at the L4 stage (Fig. 3.3A). While we observed a Cu-dependent decrease in *C. elegans* length on 100%*WT* control bacteria (Fig. 3.3B), the effect on growth was less severe when nematodes were raised on bacterial lawns with 25% or 50%*WT* Cu-efflux capacity: from 886.2 \pm 82.54 μ m on 100%*WT* control to 954.2 \pm 123.5 (p = 0.001, two-way ANOVA with Tukey's multiple comparisons) and 953.9 \pm 96.73 μ m (p < 0.001, two-way ANOVA with Tukey's multiple comparisons) respectively. Thus, these results indicate that the impact of Cu on L4 to young adult's growth and the ameliorating effect of reduced bacterial Cu-efflux capacity, followed the same trends as later life endpoints (MH and lifespan).

Next, we tested whether reduced bacterial Cu-efflux capacity improved the aforementioned *C. elegans* Cu-toxicity endpoints by reducing the overall quantity, or internal dose, of Cu in *C. elegans* since increases in measured Cu-body burden are consistent indicators of excess metal concentration in the environment and predictive of dose-dependent toxicity (40). To quantify the *C. elegans* Cu-body burden, nematodes were collected after the same limited 48h exposure (Fig. 3.3A) and washed to ensure that graphite furnace atomic absorption spectroscopy (GFAAS) analysis would capture the nematode Cu-body burden with minimal contamination from bacterially-accumulated Cu (Fig. 3.S3). Contrary to expectations, we found there was no significant reduction in Cu-body burden in nematodes exposed to 100 μ M Cu when the bacterial Cu-efflux capacity was reduced (Fig. 3.3C). On the contrary, the Cu-body burden showed a null or inverse trend, depending on the extent of bacterial Cu-efflux capacity reduction. During 100 μ M Cu exposures, reducing bacterial Cu-efflux capacity to 25%*WT* increased the overall body burden of the metal to 445 pg/nematode from 303.5 pg/nematode for worms raised on

bacterial lawns with 100% *WT* Cu-efflux capacity ($p = 0.0150$, two-way ANOVA with Tukey's multiple comparisons) while raising nematodes on 50% *WT* Cu-efflux capacity bacteria did not significantly increase the Cu-body burden compared to 100% *WT* control bacteria. These results indicate that bacterially-dependent improvements in nematode Cu-toxicity endpoints are not the result of a broad bacterial sequestration of excess Cu and subsequent reduction in the nematode Cu-body burden.

We also asked whether nematode mass could contribute to the observed variation in Cu-body burden. Among Cu exposed groups, the longer length of *C. elegans* raised on some bacterial strains could artificially increase the Cu-body burden calculated relative to smaller nematodes when reported as pg/nematode. Nevertheless, using the average length collected at the same timepoint, populations normalized to pg/ μm did not fully account for this variation in Cu-body burden (Fig. 3.3D); pg/ μm of Cu-body burden increased by nearly 27% ($p = 0.0150$, two-way ANOVA with Tukey's multiple comparisons), from $0.342 \pm 0.05 \text{ pg}/\mu\text{m}$ on 100% *WT* to $0.466 \pm 0.09 \text{ pg}/\mu\text{m}$ when the bacterial lawn retained only 25% *WT* bacterial Cu-efflux capacity. Together, these experiments show that nematode Cu-body burden is not significantly reduced by impairing the bacterial Cu-efflux capacity despite the marked improvement in other toxicity measures in *C. elegans*.

3.4.5 Spatial activation of *numr-1* is dependent on bacterial Cu-efflux capacity

Since the nematode Cu-body burden did not explain the bacterially-dependent Cu resistance in *C. elegans*, we sought to test whether the robustness of the nematode metal-stress response could account for the variation. To this end, we monitored the expression of the protective metal stress response gene, *numr-1*, which has been

associated with improved survival during metal stress as well as MH risk related to neuromuscular function in the vulva (42,43). We focused on pharyngeal activation of a transgene reporter for *numr-1*, *mtEx60 [numr-1p::GFP + rol-6(su1006)]* (JF85) within a 48h exposure window (Fig. 3.4A) since activation of this transgene in the pharynx is unique to Cu and not responsive to other environmental challenges such as pathogenic infection, endoplasmic reticulum stress, starvation, or oxidative stress responses (48). Furthermore, pharyngeal filter feeding is responsible for concentrating and breaking down bacteria in *C. elegans*; after expelling extra fluid from the anterior pharynx, the nematode pushes a concentrated bacterial pellet via neuromuscular contractions back to the posterior pharynx where pharyngeal grinding disrupts most of the bacteria before passage into the intestine (Fig. 3.4B) (50). Therefore, the intensity and location of *numr-1p::GFP* activation within the nematode pharynx was used to characterize the impact of bacterial Cu-handling dynamics on this conserved metal-stress marker.

Under control conditions (0 μ M Cu), negligible corrected mean intensities of *numr-1p::GFP* expression were reported in all regions (Fig. 3.S4) and minimal constitutive expression was noted in the head neurons surrounding the pharynx for all bacterial conditions (Fig. 3.4C). As anticipated, following Cu exposure over a 48h window starting at the L4 stage (Fig 3.4A), a strong activation of the *numr-1p::GFP* transgene is observed when nematodes are raised in 100%*WT* bacteria (Fig. 3.4C). However, while under Cu stress, transgene activation in the pharynx was variably impacted by reducing the bacterial Cu-efflux capacity; 50%*WT* bacteria resulted in a higher corrected mean intensity than the 100%*WT* control bacteria ($p = 0.0127$, one-way ANOVA with Tukey's multiple comparisons) while 25%*WT* bacteria had a comparable mean intensity to the

100% *WT* control ($p = 0.0455$, one-way ANOVA with Tukey's multiple comparisons) (Fig. 3.4D).

The difference in cumulative mean intensity between bacterial conditions also coincided with highly variable transgene activation within the four regions of the pharynx in response to Cu (Fig. 3.4C), suggesting that pharyngeal *numr-1* may be spatially influenced by the bacterial Cu-efflux capacity. Thus, we further analyzed and quantified the spatial regulation of *numr-1p::GFP* expression in the pharynx. Within the anterior pharynx, where diluted bacteria and media are collected from the environment prior to filtration, the nematodes on 25% *WT* bacteria exhibited a significant reduction in the most anterior procorpus compared to either 50 or 100% *WT* bacterial Cu-efflux groups ($p = 0.0006$ and 0.0256 respectively, one-way ANOVA with Tukey's multiple comparisons). All other corrected mean intensities reported in the regions of the anterior pharynx are unaffected by the bacterial Cu-efflux. In contrast, both regions of the posterior pharynx, encompassing the isthmus and posterior bulb which respectively concentrates and grinds the bacterial pellet, exhibited significant increases in the corrected mean intensity for 50% *WT* bacteria compared to 100% *WT* control (isthmus $p = 0.0120$, posterior bulb $p = 0.0067$, one-way ANOVA with Tukey's multiple comparisons). Similarly, the levels of posterior transgene activation observed in nematodes on 25% *WT* bacteria compensates for their depressed activation in the procorpus enough to retain similar cumulative mean intensity to 100% *WT* controls (Fig. 3.4E). Visualized in a heat map of the average reported intensities (Fig. 3.4F), these observations suggest that reduced Cu-efflux capacity shifts the *numr-1* response posteriorly. These results suggest that *numr-1* activation in the anterior pharynx is dependent on the environmental concentration of Cu

in the media while *numr-1* activation in the posterior pharynx is dependent on the concentration and release of bacterially-accumulated Cu which is present at higher levels in bacteria with reduced Cu-efflux capacity.

3.4.6 *numr-1* mediates toxicity responses to bacterially-accumulated Cu

Since spatial activation of *numr-1p::GFP* positively correlated with reduced toxicity, we tested whether the *numr-1* mediated metal stress response is required for bacterially-dependent Cu resistance (Fig. 3.5A). To this end, we chose to specifically monitor MH risk since this endpoint shows the most sensitive (i.e. magnitude difference) response between different bacterial Cu-efflux capacities (Fig. 3.2F) and because endogenous expression of *numr-1* is also observed in the vulval muscles where maintained function is necessary for egg laying (47). Without Cu, we did not observe a difference in MH risk between WT and *numr-1* loss of function mutants (*numr-1*) (Fig. 3.5B,D) despite previous reports of metal-independent increases in MH risk in *numr-1* loss of function mutants (48). However, when Cu was added to the media, a different pattern of MH risk emerged between the *N2* control populations and mutants. While *N2* nematodes raised on bacterial lawns with reduced Cu-efflux capacity still exhibited a significantly reduced MH risk relative to those raised on bacteria with 100% WT Cu-efflux capacity during Cu stress (Fig. 3.5C, $p = 0.0283$, two-way ANOVA with Tukey's multiple comparisons), *numr-1* mutants did not exhibit the same reduction in MH risk in the presence of reduced bacterial Cu-efflux capacity (Fig. 3.5C, $p = 0.9839$, two-way ANOVA with Tukey's multiple comparisons). Though there is slightly higher Cu-independent MH observed across all bacterial and nematode strain combinations in these matched experimental replicates when compared to earlier experiments, the loss of bacterially-

dependent protection against MH at later timepoints in *numr-1* (Fig. 3.5E) is consistent with our imaging results and suggests that *numr-1* plays a role in Cu-dependent MH risk associated with bacterial Cu handling. Taken together, these results indicate that the expression of *numr-1* in *C. elegans* plays a role in the decreased Cu-toxicity response observed when the bacterial Cu-efflux capacity is reduced.

3.5 Discussion

Cu excess is a condition that organisms have evolved to counteract for millions of years. Without the prospect of degradation, homeostatic responses and methods of detoxification through chelation are deeply conserved across phyla. Though it is understood that single-celled and multicellular organisms respond to environmental challenges like Cu excess (13,49,50), the coordination between organisms exposed to the same environmental challenge has not been thoroughly explored. In this work, we used a simplified host-microbe system to isolate the contribution of a ubiquitous bacterial response to Cu stress (Fig. 3.1). We found that increasing bacterial Cu-efflux capacity drives increased sensitivity to Cu stress in the host nematode (Fig. 3.2). Without the addition of 100 μ M Cu in the media, the contribution of bacterial Cu-efflux capacity is negligible to nematode lifespan (Fig. 3.2B), MH risk (Fig. 3.2C), length (Fig. 3.3B) and Cu-body burden (Fig. 3.3C-D). However, when 100 μ M Cu is present in the media, the contribution of bacterial Cu-efflux becomes a major determinant of lifespan (Fig. 3.2B) and MH risk (Fig. 3.2D) over time. Rather than an increase in Cu-body burden (Fig. 3.3C-D) driving sensitization in the nematode, worsened outcomes during Cu stress coincide with reduced activation of a protective metal-responsive gene in the posterior pharynx (Fig. 3.4E). Reduced activation of this gene localized to the procorpus and increased activation localized to the isthmus and posterior bulb (Fig. 3.4F) of the pharynx identify bacterial Cu-efflux capacity as a spatial determinant of the host nematode's early metal-stress response system. Without this effective early metal-stress response system, bacterially-dependent Cu resistance observed in MH risk was no longer present during 100 μ M Cu exposures (Fig. 3.5). These results support a model whereby an environment's

bacterial Cu-efflux capacity determines the activation of the host nematode *numr-1* metal-stress response and the development of subsequent Cu-toxicity endpoints (Fig. 3.6).

3.5.1 Disconnecting dose-dependent toxicity in the host

We assessed the impact of bacterial Cu resistance on the Cu-homeostatic system in *C. elegans*. The removal or silencing of Cu-homeostatic elements reduces Cu-body burden in nematodes while increasing the severity of Cu-toxicity endpoints at higher concentration of environmental Cu (31,32). Without genetic silencing of Cu homeostatic elements in nematodes, the free water-borne fraction of Cu in the environment was shown to be the most significant contributor to the Cu-body burden and subsequent toxicity in conditions of Cu excess (33,40). While the potential role for bacterially-associated Cu is recognized, the impact was considered minimally additive to the body-burden and toxicity of free water-borne exposures (35,38). Our work assesses the significance of bacterially-accumulated Cu in a host-microbe system. The protective quality of a reduced bacterial Cu-efflux capacity in the *C. elegans/E. coli* system challenges the previous assumption that bacterially-accumulated and waterborne Cu have similar additive effects on nematode toxicity. We determined whether altered Cu bioavailability or the nematode's homeostatic response contributed to the variable toxicity observed between bacterial strains during Cu stress; rather than bacterially-accumulated Cu being less bioavailable, reducing the Cu-body burden concurrently with Cu toxicity *in vivo*, the observed dissociation of Cu-body burden from other Cu-toxicity endpoints suggests that the nematode's own homeostatic response to Cu is responsive to bacterial Cu-handling.

However, excess Cu elicits a range of transcriptomic and behavioral responses that may contribute to organismal Cu toxicity related to longevity, MH risk and development. For instance, the late MH risk associated with Cu toxicity (Fig. 2D) can also be seen after periods of starvation beginning at L4 (51). *C. elegans* MH has been proposed as a model for myometrial degeneration (52), a disorder which manifests in conditions of Cu excess and misregulation, as reported here, and associates with spontaneous miscarriage for women afflicted with Wilson's disease, a disorder of impaired Cu homeostasis that results in widespread Cu toxicity (53). Other factors that can cause an increased MH risk include high salt, pathogen infection and developmental defects (51). However, these factors typically associate with earlier MH than what is reported here (Fig. 2D). Therefore, future work with altered bacterial Cu-efflux capacities will serve to 1) identify the variety of transcriptomic responses in the nematode impacted before and after Cu stress and 2) determine the extent to which the bacterial Cu-efflux capacity alters perceived food quality which may contribute to the development of starvation. For example, reductions in pharyngeal pumping in response to increasing Cu concentrations in the media or changes to food quality and quantity could contribute to starvation-associated MH (35,38,48). Similarly, behavioral aversion to media Cu concentrations do not appear significant in the literature until around 200 μ M, which suggests altered bioavailability of the metal due to differing bacterial efflux rates would not greatly increase the nematodes aversion response to feeding in our model (31). Perceived and functional food deprivation studies through these means can determine whether starvation or aversion responses contribute to the Cu-toxicity endpoints that are modified by the bacterial Cu-efflux capacity.

3.5.2 Pharyngeal signal for protective Cu-stress response

Researchers previously identified the intestinal tract as the major contributor to Cu homeostasis in *C. elegans*, in line with what is known of other organisms like mice and humans (20,32). This conclusion was supported by the ability of intestine specific expression of an ATP7A/B homolog to rescue mutant nematodes during Cu deficiency. However, expression of the same homolog within the pharyngeal region implied that this organ may play a role in Cu homeostasis (32). The Cu-specific pharyngeal activation of *numr-1p::GFP*, dependent on the bacterial Cu-efflux capacity, reported here further supports the pharynx as an organ involved in Cu homeostasis.. Furthermore, *numr-1* expression was previously reported to be protective against metal-specific toxicity induced by RNA-processing errors (42,48). Our work also expands upon this research by reporting on the unexpected impact of bacterial Cu-efflux on the spatial distribution of this metal-specific response; bacterially accumulated Cu has greater impact on *numr-1* posterior pharyngeal expression while the media concentration appears to have a stronger influence on the anterior pharynx (Fig. 4). Our results demonstrate the significance of regional variation in microbial composition and function throughout the digestive tract of higher organisms (20). Despite the ubiquitous expression of microbial Cu-resistance genes across the digestive tract (23), the developmental timing and early localization of this activity may serve to inform the subsequent host responses to excess metal.

3.6 Conclusion

Bacterial Cu-resistance has evolved in response to increasing widespread anthropogenic release of Cu into the environment (22). Gene clusters conferring this resistance often persist and undergo horizontal gene transfer among Enterobacteriaceae that require stronger resistance to survive changing environments (21). However, the consequences of this shift in a host-microbe system have not been documented. Using a simplified host-microbe system, we found that increasing one aspect of bacterial Cu resistance, conferred by the Cus system, sensitized the host to Cu toxicity independent of an increased Cu-body burden (Fig. 3.2-3) and disrupts the efficacy of a host metal-specific stress response *in vivo* (Fig. 3.4-5). Nevertheless, while the Cus system is particularly important for conferring Cu resistance in anaerobic environments through Cu removal, it does not act in isolation. For instance, the plasmid-borne Cu-resistance system (*pco*), homologous to the Cu-resistance operon (*cop*) in *Pseudomonas*, serves to detoxify intracellular Cu rather than remove it from the cell (21,54). Earlier experiments in host-microbe interactions using *C. elegans* found that bacterial mutations that induce free radical detoxification in bacteria activated mitochondrial stress responses in nematodes (28). Our own experiments suggest that variations in baseline and early MH, independent of Cu stress, may result from the unique disruption of the H₂O₂ response pathway in *E. coli* (Fig. 3.2D). Together, these experiments highlight the unexpected consequences of increasingly Cu-resistant microbial populations in the environment and describes how one aspect of bacterial Cu resistance, Cu-efflux capacity, spatially modulates host metal-stress responses.

3.7 Figures

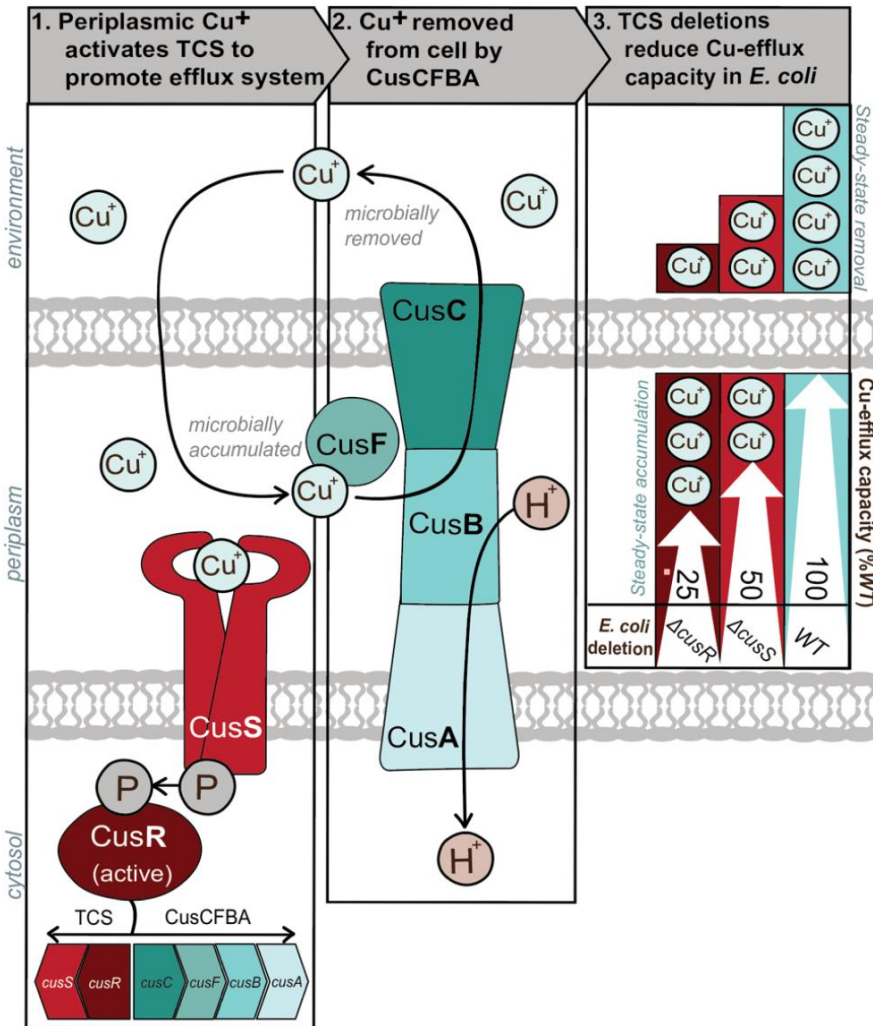


Figure 3.1. CusRS regulates Cu-efflux capacity in an *E. coli* model system Cross section of *E. coli* showing a response system that deals with Cu^+ excess in the environment. Removal of excess Cu^+ by bacteria is dependent upon (1) activation of a TCS that responds to Cu^+ in the periplasm. Signal transduction from the periplasmic domain of CusS, a histidine kinase, to the cytosol leads to temporary phosphorylation and activation of CusR which promotes expression of the *cus* operon. (2) Expression of the *cus* operon drives increased efficiency in the removal of periplasmic Cu^+ via the CusCFBA antiporter. (3) Targeted deletions of the genes for the CusS-CusR TCS within a periplasmic copper oxidase ($\Delta cueO$) background increases the ratio of accumulated Cu^+ to removed Cu^+ by varying degrees.

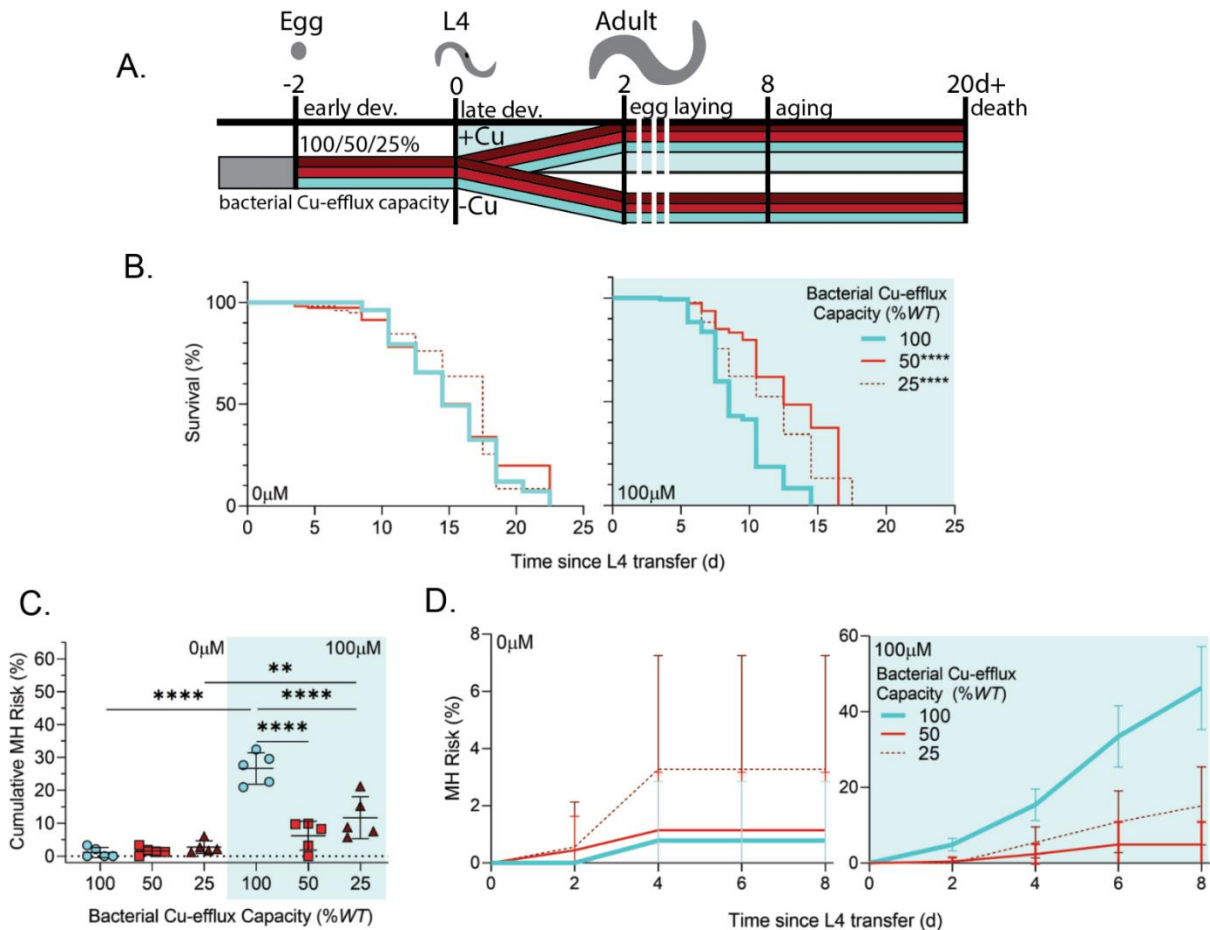


Figure 3.2. Host sensitivity to chronic Cu excess is dependent on bacterial Cu-efflux capacity

(A) Experimental design. For chronic exposures, adults were transferred to new plates at least every 48h after initial L4 transfer. (B) Kaplan-Meier lifespan analysis with 0µM or 100µM Cu. Significance between lifespan data was calculated using a Mantel-Cox log-rank test ($N = 3-4$, $n > 50$) where **** $p < 0.0001$. (C) Cumulative incidence MH risk through reproductive lifespan in *N2* nematodes ($N = 5$, $n = 62-121$) Each symbol on a graph denotes the average of one experimental replicate composed of at least 60 nematodes. (D) MH incidence risk analysis was performed on nematodes exposed to 0µM or 100µM Cu over time. Shaded regions on graphs highlight conditions of excess Cu. Significance was determined using a two-way ANOVA with Tukey's multiple comparison's test where ** $p \leq 0.01$, **** $p < 0.0001$, and error bars mark the upper and lower SD from calculated mean.

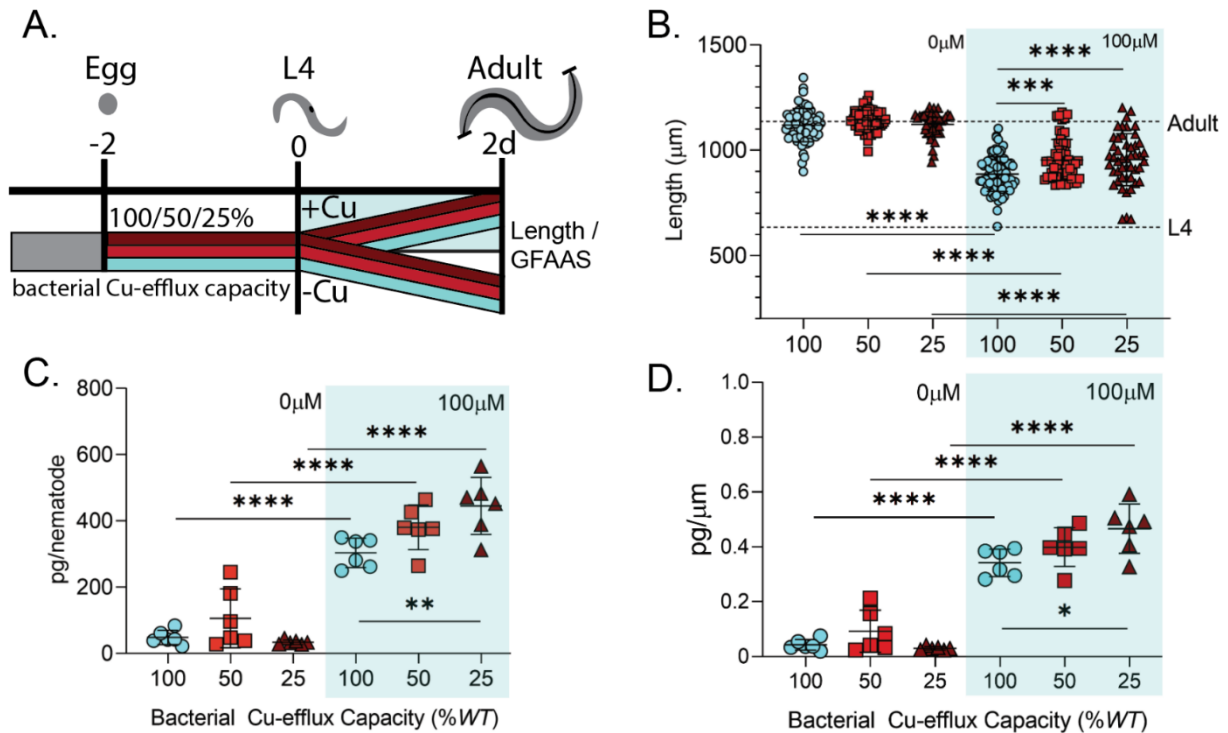


Figure 3.3. Association between bacterially-dependent Cu-sensitivity and *C. elegans* Cu-body burden

(A) Experimental design. All measurements were taken in developmentally synchronous 2d adult populations after 48h exposure to 0 or 100 μ M Cu. (B) Length of developmentally synchronous *N2* nematodes (N = 3-6, n = 7-24). Dotted lines represent the average length of nematodes relative to their developmental stage as reported by WormAtlas. (C) Nematode Cu-body burden normalized to pg/nematode (N = 6, n = 20 or 50) (C) or (D) nematode body burden normalized to average length of nematode population. Shaded regions on graphs highlight conditions of excess Cu. Significance was determined by a two-way ANOVA with Tukey's multiple comparisons test. Error bars denote SD and mean. * $p \leq 0.05$. ** $p \leq 0.01$. *** $p \leq 0.001$. **** $p < 0.0001$.

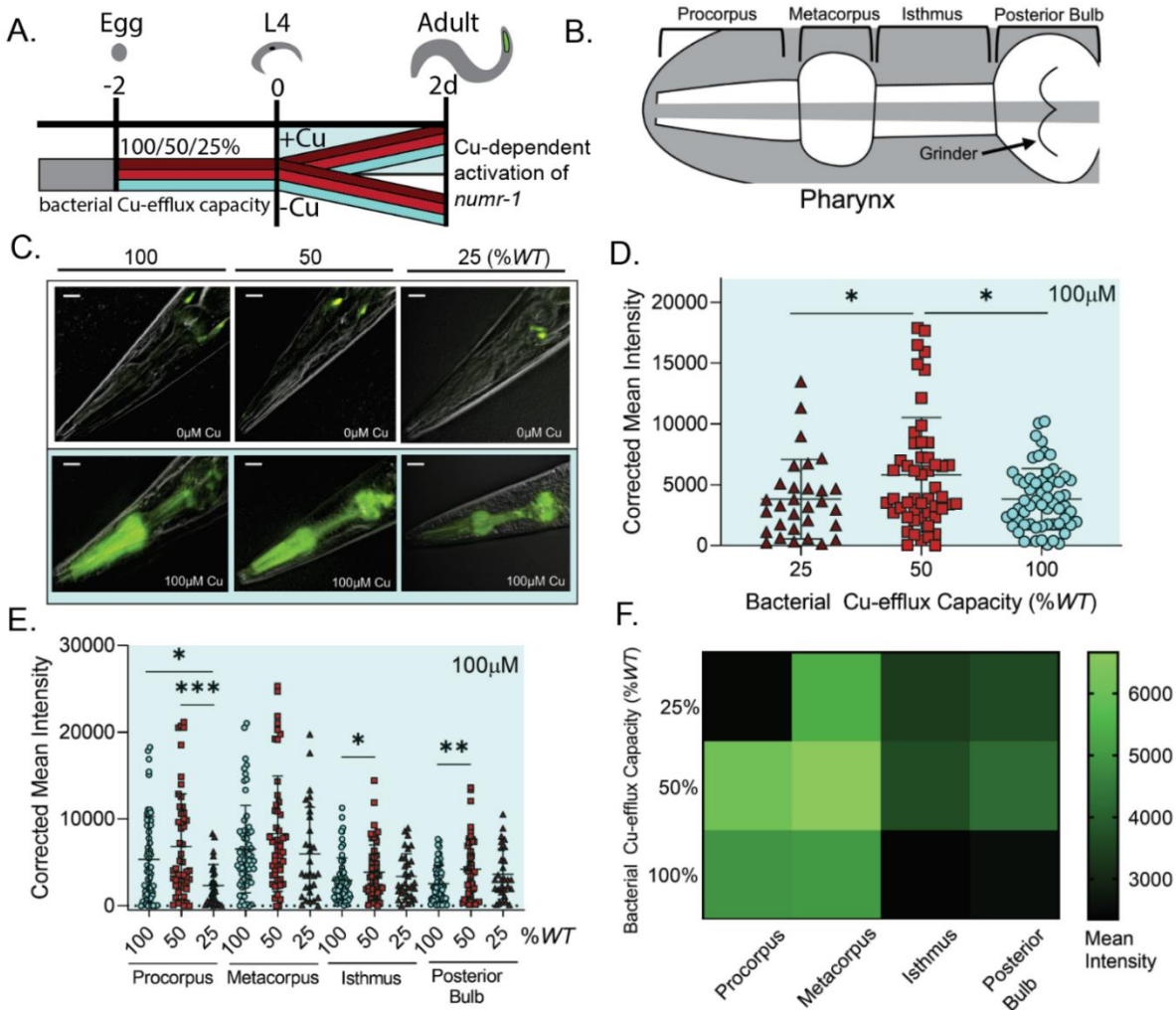


Figure 3.4. Bacterial Cu-efflux capacity effects Cu-dependent pharyngeal *numr-1* activation (A) Exposure design prior to GFP transgene imaging. (B) Diagram of nematode pharynx divided into four anatomical regions encompassing the anterior (procorpus and metacarpus) and posterior (isthmus and posterior bulb) pharynx. (C) Representative fluorescence microscopy images of *numr-1p::GFP* responding to 0µM or 100µM Cu. Scale bar in upper right corner is 20µm long. (D) Quantification of corrected mean intensity of GFP signal present in the pharynx or (E) the separate anatomical regions (N = 4-6, n = 5-12). Shaded regions on graphs highlight conditions of excess Cu. A one-way ANOVA with Tukey's multiple comparison analysis was used to determine significance while error bars denote mean and SD. * $p \leq 0.05$. ** $p \leq 0.01$. *** $p \leq 0.001$. (F) Summary heat map of regional mean intensity of GFP signal present in the pharynx when exposed to 100µM Cu.

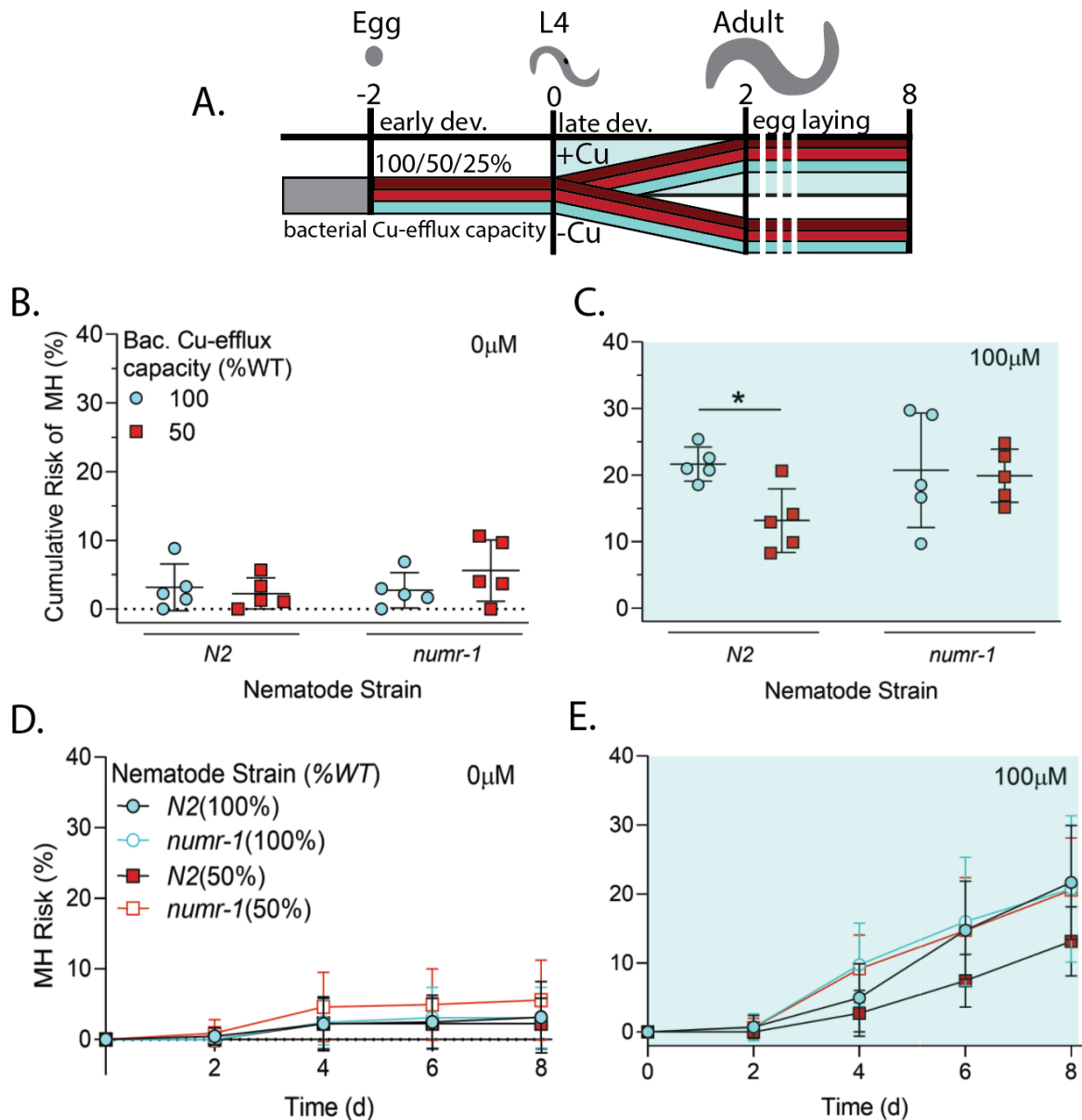


Figure 3.5. *numr-1* involvement in bacterially-dependent Cu resistance

(A) Experimental design. Cumulative MH risk of experimentally matched *N2* nematodes and *numr-1* nematodes with an impaired *numr-1* response in (B) 0 μM or (C) 100 μM Cu (N = 5, n = 62-134). Shaded regions on graphs highlight conditions of excess Cu. A two-way ANOVA with Tukey's multiple comparison analysis was used to determine significance while error bars denote mean and SD and *p ≤ 0.05.

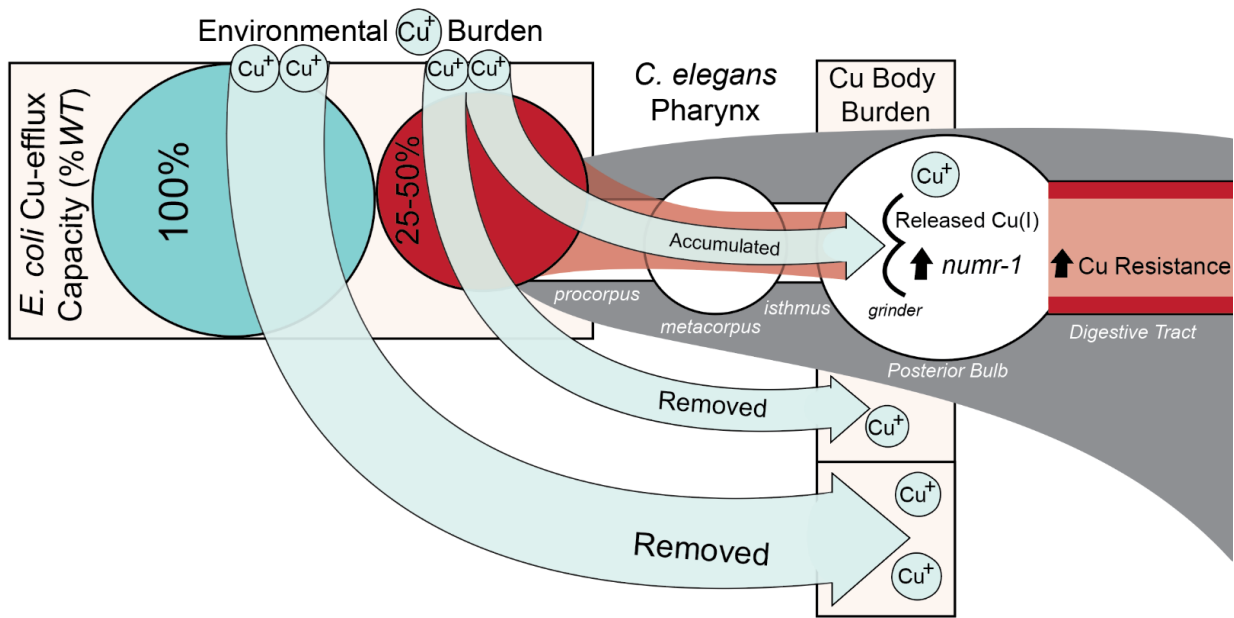
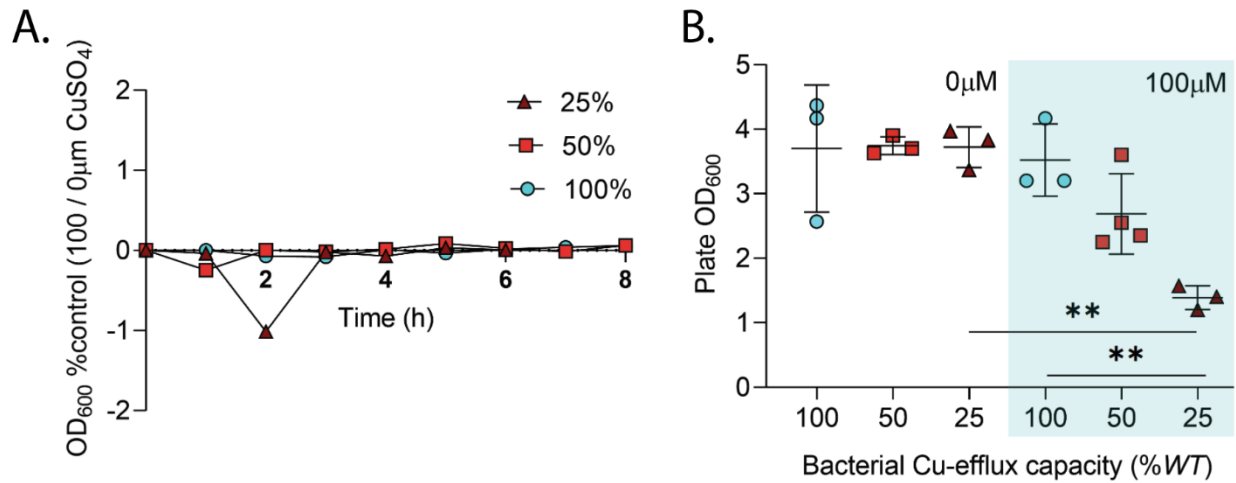


Figure 3.6. Bacterial Cu-efflux capacity acts spatially on host response to environmental metal-stress

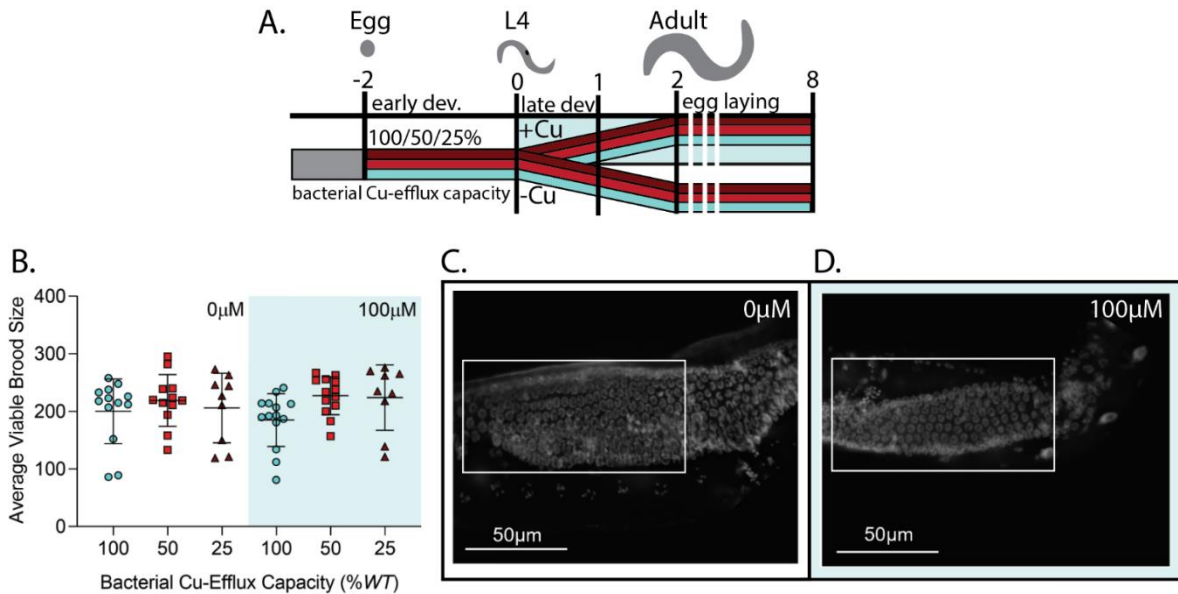
The efficiency of bacterial Cu efflux, during conditions of metal excess, alters the spatial distribution of metal stress in host organisms. Specifically, increasing bacterial Cu-efflux capacity reduces the protective upregulation of the host's metal-responsive *numr-1* by reducing the fraction of bacterially accumulated Cu in the posterior bulb. When bacterial Cu-efflux capacity is reduced, subsequently increased activation of metal-responsive *numr-1* contributes to improved Cu-toxicity endpoints in the host without reducing the host's overall Cu-body burden.

SUPPORTING INFORMATION:

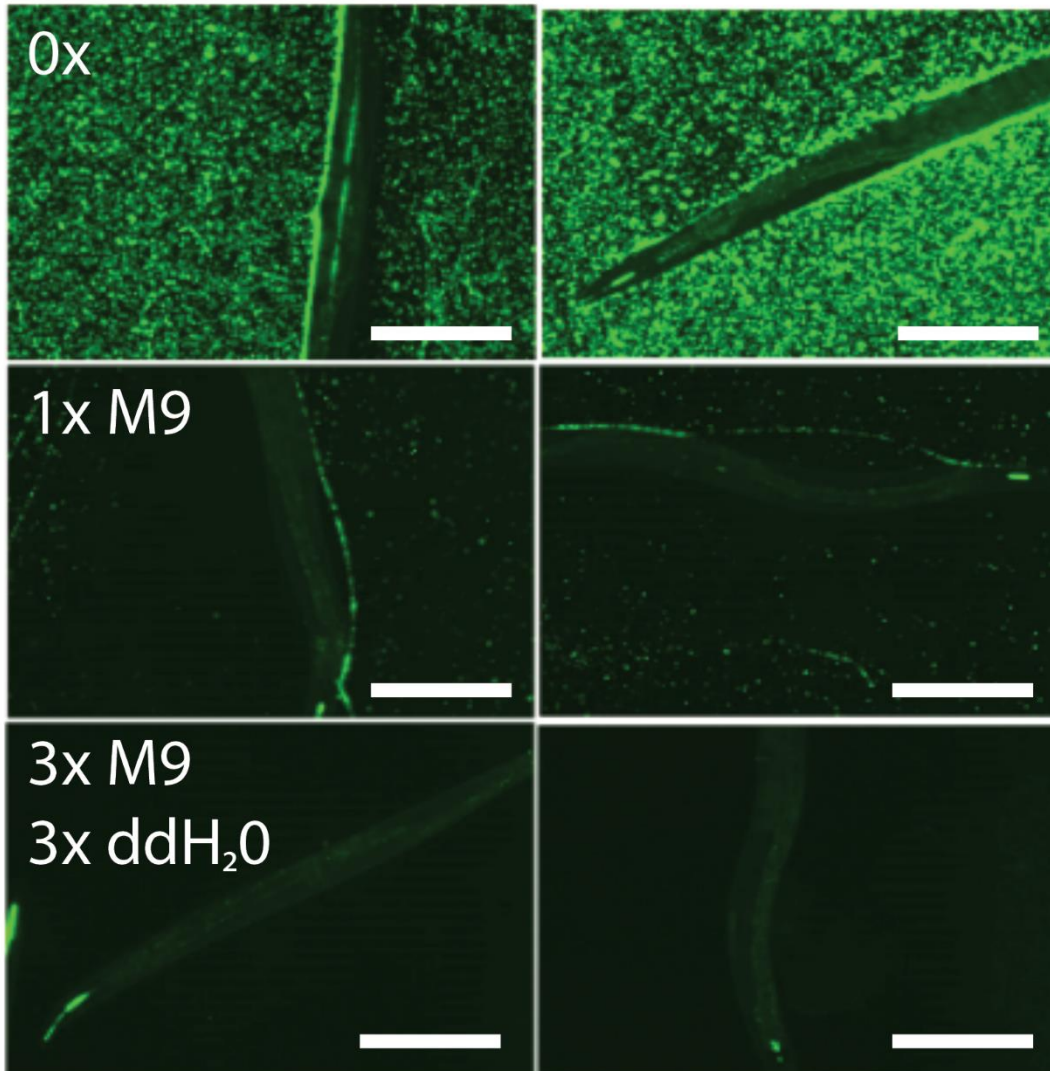


Supporting Figure 3.S1. Bacterial growth and density in response to Cu-stress

(A) Calculated % change in growth rate of bacterial strains with variable Cu-efflux capacities with the addition of 100 μM Cu to LB media over time (N = 3). (B) Bacterial NGM plate OD₆₀₀ after 48h room-temperature incubation prior to storage in 4°C (N = 3). Shaded regions on graphs highlight excess Cu conditions. Significance was calculated using a two-way ANOVA with multiple comparisons where **p ≤ 0.01.

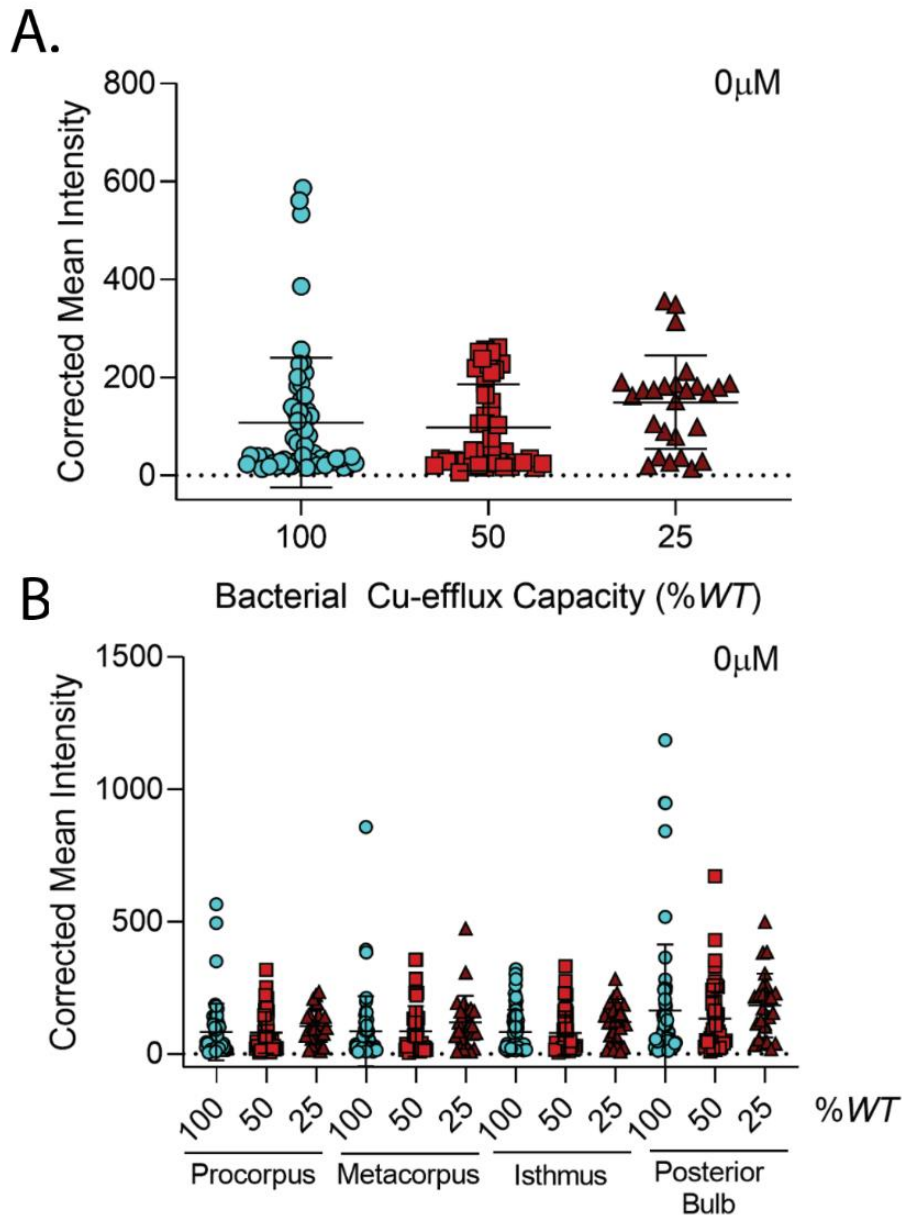


Supporting Figure 3.S2. Reproductive impact of Cu-stress exposure in *C. elegans*
 (A) Experimental design. (B) Average viable brood size over the reproductive lifespan of *C. elegans* in different exposure conditions (N = 3, n = 5). Significance was determined using a two-way ANOVA with Tukey's multiple comparisons for each Cu concentration where *p ≤ 0.05. (C-D) representative DAPI-stained nuclei in germline following 24h exposure to 0 or 100 μM Cu starting in late development on control 100% WT bacterial lawns. White boxes denote altered expansion of pachytene nuclei specifically.



Supporting Figure 3.S3. Validation of wash steps prior to GFAAS Cu-content analysis

Representative images of *N2* nematodes raised on *E. coli* containing plasmid for inducible expression of pLIC-egfp in *BL21(DE3)* after collection but before washes (0), after 1x wash with M9 buffer (1x M9) and finally after 3 washes with M9 and 3 with ddH₂O (3x M9, 3x ddH₂O). White scale bars are 250µm.



Supporting Figure 3.S4. Pharyngeal *numr-1* activation without addition of excess Cu

(A) Quantification of corrected mean intensity of GFP signal present in the pharynx (N = 4-6, n = 4-10). (B) Regional quantification of corrected mean intensity of GFP signal intensity present in the 4 regions of the pharynx (N = 4-6, n = 4-10). Shaded regions on graphs highlight conditions of excess Cu. A one-way ANOVA with Tukey's multiple comparison analysis was used to determine significance while error bars denote mean and SD.

3.8 References

1. Pryor, R., Norvaisas, P., Marinos, G., Best, L., Thingholm, L. B., Quintaneiro, L. M., De Haes, W., Esser, D., Waschina, S., Lujan, C., Smith, R. L., Scott, T. A., Martinez-Martinez, D., Woodward, O., Bryson, K., *et al.* (2019) Host-microbe-drug-nutrient screen identifies bacterial effectors of metformin therapy. *Cell* 178, 1299–1312.e1229
2. Scott, T. A., Quintaneiro, L. M., Norvaisas, P., Lui, P. P., Wilson, M. P., Leung, K. Y., Herrera-Dominguez, L., Sudiwala, S., Pessia, A., Clayton, P. T., Bryson, K., Velagapudi, V., Mills, P. B., Typas, A., Greene, N. D. E., *et al.* (2017) Host-microbe co-metabolism dictates cancer drug efficacy in *C. elegans*. *Cell* 169, 442–456.e418
3. Javdan, B., Lopez, J. G., Chankhamjon, P., Lee, Y. J., Hull, R., Wu, Q., Wang, X., Chatterjee, S., and Donia, M. S. (2020) Personalized mapping of drug metabolism by the human gut microbiome. *Cell* 181, 1661–1679.e1622
4. Tan, M. W., and Shapira, M. (2011) Genetic and molecular analysis of nematode-microbe interactions. *Cell. Microbiol.* 13, 497–507
5. Watson, E., MacNeil, L. T., Ritter, A. D., Yilmaz, L. S., Rosebrock, A. P., Caudy, A. A., and Walhout, A. J. (2014) Interspecies systems biology uncovers metabolites affecting *C. elegans* gene expression and life history traits. *Cell* 156, 759–770
6. Dutta, S. K., Verma, S., Jain, V., Surapaneni, B. K., Vinayek, R., Phillips, L., and Nair, P. P. (2019) Parkinson's disease: The emerging role of gut dysbiosis, antibiotics, probiotics, and fecal microbiota transplantation. *J. Neurogastroenterol. Motil.* 25, 363–376

7. Hill-Burns, E. M., Debelius, J. W., Morton, J. T., Wissemann, W. T., Lewis, M. R., Wallen, Z. D., Peddada, S. D., Factor, S. A., Molho, E., Zabetian, C. P., Knight, R., and Payami, H. (2017) Parkinson's disease and Parkinson's disease medications have distinct signatures of the gut microbiome. *Mov. Disord.* 32, 739–749
8. Brown, E., Tanner, C., and Goldman, S. (2018) The microbiome in neurodegenerative disease. *Curr. Geriatr. Rep.* 7, 81–91
9. Geng, H., Shu, S., Dong, J., Li, H., Xu, C., Han, Y., Hu, J., Han, Y. Yang, R., and Cheng, N. (2018) Association study of gut flora in Wilson's disease through high-throughput sequencing. *Medicine (Baltimore)* 97, e11743.
10. Le Pennec, G., and Ar Gall, E. (2019) The microbiome of *Codium tomentosum*: Original state and in the presence of copper. *World J. Microbiol. Biotechnol.* 35, 167.
11. Bondarczuk, K., and Piotrowska-Seget, Z. (2013) Molecular basis of active copper resistance mechanisms in Gram-negative bacteria. *Cell Biol. Toxicol.* 29, 397–405
12. Yamamoto, K., and Ishihama, A. (2005) Transcriptional response of *Escherichia coli* to external copper. *Mol. Microbiol.* 56, 215–227
13. Boal, A. K., and Rosenzweig, A. C. (2009) Structural biology of copper trafficking. *Chem. Rev.* 109, 4760–4779
14. Petris, M. J., Smith, K., Lee, J., and Thiele, D. J. (2003) Copper-stimulated endocytosis and degradation of the human copper transporter, hCtr1. *J. Biol. Chem.* 278, 9639–9646
15. Dupont, C. L., Grass, G., and Rensing, C. (2011) Copper toxicity and the origin of bacterial resistance—new insights and applications. *Metallomics* 3, 1109–1118
16. Ala, A., Walker, A. P., Ashkan, K., Dooley, J. S., and Schilsky, M. L. (2007) Wilson's

disease. *Lancet* 369, 397–408

17. Vallières, C., Holland, S. L., and Avery, S. V. (2017) Mitochondrial ferredoxin determines vulnerability of cells to copper excess. *Cell Chem. Biol.* 24, 1228–1237.e1223
18. Gupte, A., and Mumper, R. J. (2009) Elevated copper and oxidative stress in cancer cells as a target for cancer treatment. *Cancer Treat. Rev.* 35, 32–46
19. Bourassa, M. W., Leskovjan, A. C., Tappero, R. V., Farquhar, E. R., Colton, C. A., Van Nostrand, W. E., and Miller, L. M. (2013) Elevated copper in the amyloid plaques and iron in the cortex are observed in mouse models of Alzheimer's disease that exhibit neurodegeneration. *Biomed. Spectrosc. Imaging* 2, 129–139
20. Miller, K. A., Vicentini, F. A., Hirota, S. A., Sharkey, K. A., and Wieser, M. E. (2019) Antibiotic treatment affects the expression levels of copper transporters and the isotopic composition of copper in the colon of mice. *Proc. Natl. Acad. Sci. U. S. A.* 116, 5955–5960
21. Staehlin, B. M., Gibbons, J. G., Rokas, A., O'Halloran, T. V., and Slot, J. C. (2016) Evolution of a heavy metal homeostasis/resistance island reflects increasing copper stress in enterobacteria. *Genome Biol. Evol.* 8, 811–826
22. Xing, C., Chen, J., Zheng, X., Chen, L., Chen, M., Wang, L., and Li, X. (2020) Functional metagenomic exploration identifies novel prokaryotic copper resistance genes from the soil microbiome. *Metallomics* 12, 387–395
23. Segata, N., Haake, S. K., Mannon, P., Lemon, K. P., Waldron, L., Gevers, D., Huttenhower, C., and Izard, J. (2012) Composition of the adult digestive tract bacterial microbiome based on seven mouth surfaces, tonsils, throat and stool

- samples. *Genome Biol.* 13, R42
24. Gudipaty, S. A., Larsen, A. S., Rensing, C., and McEvoy, M. M. (2012) Regulation of Cu(I)/Ag(I) efflux genes in *Escherichia coli* by the sensor kinase CusS. *FEMS Microbiol. Lett.* 330, 30–37
 25. Affandi, T., Issaian, A. V., and McEvoy, M. M. (2016) The structure of the periplasmic sensor domain of the histidine kinase CusS shows unusual metal ion coordination at the dimeric interface. *Biochemistry* 55, 5296– 5306
 26. Affandi, T., and McEvoy, M. M. (2019) Mechanism of metal ion-induced activation of a two-component sensor kinase. *Biochem. J.* 476, 115–135
 27. Conroy, O., Kim, E.-H., McEvoy, M. M., and Rensing, C. (2010) Differing ability to transport nonmetal substrates by two RND-type metal exporters. *FEMS Microbiol. Lett.* 308, 115–122
 28. Govindan, J. A., Jayamani, E., Zhang, X., Mylonakis, E., and Ruvkun, G. (2015) Dialogue between *E. coli* free radical pathways and the mitochondria of *C. elegans*. *Proc. Natl. Acad. Sci. U. S. A.* 112, 12456–12461
 29. Kishimoto, S., Uno, M., Okabe, E., Nono, M., and Nishida, E. (2017) Environmental stresses induce transgenerationally inheritable survival advantages via germline-to-soma communication in *Caenorhabditis elegans*. *Nat. Commun.* 8, 14031
 30. Martinez-Finley, E. J., and Aschner, M. (2011) Revelations from the nematode *Caenorhabditis elegans* on the complex interplay of metal toxicological mechanisms. *J. Toxicol.* 2011, 895236
 31. Yuan, S., Sharma, A. K., Richart, A., Lee, J., and Kim, B. E. (2018) CHCA-1 is a

- copper-regulated CTR1 homolog required for normal development, copper accumulation, and copper-sensing behavior in *Caenorhabditis elegans*. *J. Biol. Chem.* 293, 10911–10925
32. Chun, H., Sharma, A. K., Lee, J., Chan, J., Jia, S., and Kim, B. E. (2017) The intestinal copper exporter CUA-1 is required for systemic copper homeostasis in *Caenorhabditis elegans*. *J. Biol. Chem.* 292, 1–14
33. Calafato, S., Swain, S., Hughes, S., Kille, P., and Stürzenbaum, S. R. (2008) Knock down of *Caenorhabditis elegans* cutc-1 exacerbates the sensitivity toward high levels of copper. *Toxicol. Sci.* 106, 384–391
34. Anderson, G. L., Boyd, W. A., and Williams, P. L. (2001) Assessment of sublethal endpoints for toxicity testing with the nematode *Caenorhabditis elegans*. *Environ. Toxicol. Chem.* 20, 833–838
35. Boyd, W. A., Cole, R. D., Anderson, G. L., and Williams, P. L. (2003) The effects of metals and food availability on the behavior of *Caenorhabditis elegans*. *Environ. Toxicol. Chem.* 22, 3049–3055
36. Boyd, W. A., and Williams, P. L. (2003) Comparison of the sensitivity of three nematode species to copper and their utility in aquatic and soil toxicity tests. *Environ. Toxicol. Chem.* 22, 2768–2774
37. Harrington, J. M., Boyd, W. A., Smith, M. V., Rice, J. R., Freedman, J. H., and Crumbliss, A. L. (2012) Amelioration of metal-induced toxicity in *Caenorhabditis elegans*: Utility of chelating agents in the bioremediation of metals. *Toxicol. Sci.* 129, 49–56
38. Mashock, M. J., Zanon, T., Kappell, A. D., Petrella, L. N., Andersen, E. C., and

- Hristova, K. R. (2016) Copper oxide nanoparticles impact several toxicological endpoints and cause neurodegeneration in *Caenorhabditis elegans*. *PLoS One* 11, e0167613
39. Twumasi-Boateng, K., Wang, T. W., Tsai, L., Lee, K. H., Salehpour, A., Bhat, S., Tan, M. W., and Shapira, M. (2012) An age-dependent reversal in the protective capacities of JNK signaling shortens *Caenorhabditis elegans* lifespan. *Aging Cell* 11, 659–667
40. Moyson, S., Town, R. M., Joosen, S., Husson, S. J., and Blust, R. (2019) The interplay between chemical speciation and physiology determines the bioaccumulation and toxicity of Cu(II) and Cd(II) to *Caenorhabditis elegans*. *J. Appl. Toxicol.* 39, 282–293
41. Richards, A. L., Watza, D., Findley, A., Alazizi, A., Wen, X., Pai, A. A., Pique-Regi, R., and Luca, F. (2017) Environmental perturbations lead to extensive directional shifts in RNA processing. *PLoS Genet.* 13, e1006995
42. Wu, C. W., Wimberly, K., Pietras, A., Dodd, W., Atlas, M. B., and Choe, K. P. (2019) RNA processing errors triggered by cadmium and integrator complex disruption are signals for environmental stress. *BMC Biol.* 17, 56
43. Kimble, J. E., and White, J. G. (1981) On the control of germ cell development in *Caenorhabditis elegans*. *Dev. Biol.* 81, 208–219
44. Shin, N., Cuenca, L., Karthikraj, R., Kannan, K., and Colaiácovo, M. P. (2019) Assessing effects of germline exposure to environmental toxicants by high-throughput screening in *C. elegans*. *PLoS Genet.* 15, e1007975
45. Urano, H., Umezawa, Y., Yamamoto, K., Ishihama, A., and Ogasawara, H. (2015)

- Cooperative regulation of the common target genes between H₂ O₂-sensing YedVW and Cu₂(+)-sensing CusSR in *Escherichia coli*. *Microbiology (Reading)* 161, 729–738
46. Angelo, G., and Van Gilst, M. R. (2009) Starvation protects germline stem cells and extends reproductive longevity in *C. elegans*. *Science* 326, 954
 47. Tvermoes, B. E., Boyd, W. A., and Freedman, J. H. (2010) Molecular characterization of numr-1 and numr-2: Genes that increase both resistance to metal-induced stress and lifespan in *Caenorhabditis elegans*. *J. Cell Sci.* 123, 2124–2134
 48. Chen, J., and Caswell-Chen, E. P. (2004) Facultative vivipary is a life-history trait in *Caenorhabditis elegans*. *J. Nematol.* 36, 107–113
 49. Djaman, O., Outten, F. W., and Imlay, J. A. (2004) Repair of oxidized iron-sulfur clusters in *Escherichia coli*. *J. Biol. Chem.* 279, 44590–44599
 50. Milne, L., Nicotera, P., Orrenius, S., and Burkitt, M. J. (1993) Effects of glutathione and chelating agents on copper-mediated DNA oxidation: Pro-oxidant and antioxidant properties of glutathione. *Arch. Biochem. Biophys.* 304, 102–109
 51. Pickett, C. L., and Kornfeld, K. (2013) Age-related degeneration of the egg-laying system promotes matricidal hatching in *Caenorhabditis elegans*. *Aging Cell* 12, 544–553
 52. Malik, A., Khawaja, A., and Sheikh, L. (2013) Wilson's disease in pregnancy: Case series and review of literature. *BMC Res. Notes* 6, 421
 53. Brown, N. L., Barrett, S. R., Camakaris, J., Lee, B. T., and Rouch, D. A. (1995) Molecular genetics and transport analysis of the copper-resistance determinant

- (pco) from *Escherichia coli* plasmid pRJ1004. *Mol. Microbiol.* 17, 1153–1166
54. Ahmad, J. U., and Goni, M. A. (2010) Heavy metal contamination in water, soil, and vegetables of the industrial areas in Dhaka, Bangladesh. *Environ. Monit. Assess.* 166, 347–357
 55. Knobeloch, L., Ziarnik, M., Howard, J., Theis, B., Farmer, D., Anderson, H., and Proctor, M. (1994) Gastrointestinal upsets associated with ingestion of copper-contaminated water. *Environ. Health Perspect.* 102, 958–961
 56. Stenhammar, L. (1999) Diarrhoea following contamination of drinking water with copper. *Eur. J. Med. Res.* 4, 217–218
 57. Rehman Khan, F., and McFadden, B. A. (1980) A rapid method of synchronizing developmental stages of *Caenorhabditis elegans*. *Nematologica* 26, 280–282
 58. Brenner, S. (1974) The genetics of *Caenorhabditis elegans*. *Genetics* 77, 71–94
 59. Ganio, K., James, S. A., Hare, D. J., Roberts, B. R., and McColl, G. (2016) Accurate biometal quantification per individual *Caenorhabditis elegans*. *Analyst* 141, 1434–1439
 60. Amrit, F. R., Ratnappan, R., Keith, S. A., and Ghazi, A. (2014) The *C. elegans* lifespan assay toolkit. *Methods* 68, 465–475

CHAPTER 4: BACTERIALLY-DEPENDENT TRANSCRIPTIONAL REGULATION IN *CAENHORHADITIS ELEGANS* EXPOSED TO CHRONIC ENVIRONMENTAL CU EXCESS

4.1 Abstract

While the transcriptional response to Cu has been described in previous *C. elegans* research, little is known about how bacterial Cu-handling contributes to quality and intensity of *C. elegans* Cu-stress. As mentioned in Chapter 2, a reduction in the bacterial Cu-efflux capacity resulted in a significant improvement in toxicity outcomes in the host *C. elegans*. Therefore, we sought to define the differentially expressed genes that may contribute to this variable host response to bacterial Cu-efflux capacity in *C. elegans*. Cu concentrations, regardless of bacterial Cu-efflux capacity, demonstrated the largest and most consistent variation in differentially expressed genes while enrichment analysis recapitulated the observed bacterially-dependent Cu resistance and predicted increased metal-stress sensitivity in neuronal tissue that was supported experimentally. However, bacterially-dependent differentially expressed genes (DEGs) were limited in the excess-Cu conditions tested and did not predict phenotypic outcomes tested. While the DEGs of nematodes raised on 100% *WT* bacterial Cu-efflux capacity during Cu stress clustered tightly together, those raised on 50% *WT* bacterial Cu-efflux capacity were more variable and exhibited more similar expression to the 0 μ M Cu control conditions. Future experiments, the variability observed within conditions could be reduced by better restricting the developmental stage where RNA collection or analysis takes place and by not using whole worm preparations.

4.2 Introduction

Unlike cell culture, whole worm RNAseq analysis can simultaneously capture tissue interactions and directly connect these interactions to organismal phenotypes during toxicity studies. This breadth of information has been used to better understand metal toxicity in organismal systems. Previous RNAseq analysis in *C. elegans* took advantage of this unique system to identify several genes whose expression responds to metal stress and may confer increased resistance to *C. elegans*. These metal-responsive genes include *numr-1*, *mtl-2*, *vit-1*, *kreg-1*.(1-3).

Nuclear metal responsive gene (*numr-1*) and metallothionein (*mtl-2*) are metal responsive genes that exemplify both the overlap and specificity of nematode genes exposed to different metals. For *numr-1*, most metals have been reported to increase its expression, most notably cadmium, where it localizes with heat shock factors (HSF-1) in nuclear stress granules to restore snRNA processing and subsequent RNA processing that is disrupted by metal stress to improve toxicity outcomes in the worm (4). By contrast, *mtl-2* is a conserved metal-responsive gene that is only upregulated by cadmium to promote its binding and detoxification. Unlike *numr-1*, *mtl-2* is not upregulated by metals like Cu which not strongly impacted by its until later generations(5). These two metal responsive genes reflect how organisms distinguish and respond to different metals in the environment.

The vitellogenin structural gene, *vit-1*, and the KGB-1 regulated gene, *kreg-1*, highlight the developmental sensitivity of metal-responsive networks. Increased expression of *vit-1* is specific to nematodes exposed to Cu early in development prior to the L4 stage(3). Similarly, KGB-1's nuclear-localized mitogen-activated protein kinase

phosphorylation activity drives the metal-stress response through increased *kreg-1* transcription (6) as well as the developmentally dependent activity of a FOXO transcription factor ortholog, DAF-16 (7). In fact, while KGB-1-mediated phosphorylation of DAF-16 confers metal-stress resistance when nematodes are exposed as adults, the same phosphorylation mark sensitizes nematodes exposed to metal early in development prior to the L4 stage (7)

Intracellular communication between different tissues has also been identified as a component of an organism's metal-stress response as well as the transmission of increased stress resistance to subsequent generations. For instance, it is the stress-induced DAF-16 activity in intestinal and neuronal tissue that was identified as a key driver of the generational inheritance of stress resistance by promoting epigenetic changes in the germinal cells of parental nematodes exposed to metal stress (8). Other environmental factors that contribute to this form of communication, like bacterial metabolism, have not yet been investigated.

Furthermore, both the *numr-1* response and DAF-16's role in transgenerational inheritance are mediated by the heat-shock-responsive HSF-1 (8), highlighting the overlap in environmental stress responses compared to those more specific to metal stress. For instance, while *numr-1* only reacts to metal-specific damage in the cellular environment (2), the transmission of increased stress resistance from the soma to the germline via DAF-16 activity responds to a wide range of environmental stresses including osmotic stress and starvation (7,8). In the broadly overlapping damage that can result from diverse environmental stresses, KGB-1 activity that promotes upregulation of metal-specific *kreg-1* is also a required component of the nematodes innate immune system where its

necessary for *C. elegans* to defend against the pore-forming toxin produced by *Pseudomonas aeruginosa* (9).

Outside the magnitude of gene upregulation, different metals also elicit different spatial expression patterns of *numr-1* in the nematode; cadmium promotes much more intestinal expression where Cu exposures are typified by increased expression isolated to the pharyngeal region (2). Another tissue particularly sensitive to Cu stress is the nervous system where excess Cu reduces clearance of amyloid-beta plaques of Alzheimer's patients (10) and promotes the aggregation of alpha synuclein in Parkinson's patients (11,12). Cu exposures have elicited similar neurodegeneration in *C. elegans* models of neurodegenerative diseases (13). However, the extent to which Cu-impaired neurotransmitter signaling in the host can be modified through bacterial pathways has not been explored.

In the cases highlighted above, whole transcriptome analysis can illuminate whether a given bacterial system, like those induced to increase bacterial Cu efflux when Cu excess is present in the environment, impact the metal response to the environmental stress in *C. elegans* or whether they alter other system responses like the immune response to foreign pathogens. The latter is of particular interest in studies of Cu toxicity because immune responses in eukaryotic organisms often rely on overwhelming a pathogen's Cu-stress resistance pathways by flooding their environment with excess Cu (14). Therefore, any alterations to the bacterial conditions responding to Cu stress could alter the pathogenic responses in host organisms. However, with the appropriate RNAseq analysis and toxicity endpoints, specific to neurodegeneration of the generational inheritance of stress resistance, a better understanding the interaction between metal-

handling responses (*numr-1* and *kreg-1*) and more general environmental stress responses (*kgb-1*, *daf-16*) can be achieved.

4.3 Materials & methods

4.3.1 *C. elegans* sample preparation

Populations of *OP50* nematodes were bleach-synchronized and exposed to CuSO_4 as previously described for 48h prior to collection for total RNA. Sample populations were enriched for adults using two M9 gradients and washed with ddH₂O twice. Immediately following ddH₂O washes, samples were disrupted under liquid nitrogen using a mortar and pestle and homogenized with needle and syringe. Lysates were stored at -80°C in RLT buffer containing β -ME prior to RNA isolation.

4.3.2 Total RNA isolation

Previously prepared and homogenized *C. elegans* samples stored at -80°C were thawed to 37°C prior to total RNA isolation using Qiagen's RNeasy mini kit with additional RNase-free DNase digestion step. RNA purity and concentration for samples eluted in RNase-free water were estimated using a nanodrop. The three experimental replicates with the highest average RNA concentration were selected for RNA sequencing.

4.3.3 RNA sequencing and analysis

Total RNA samples were sequenced by the TCGB at UCLA using the Hiseq3000 with a depth of coverage of 20 million reads/sample and a read length of 1X50. Reads were mapped by STAR v2.7.8 (15) and read counts per gene were quantified using the *C. elegans* WS200 reference genome (<https://wiki.wormbase.org/index.php/WS200>). In Partek Flow, read counts were normalized by $\text{CPM}+1e^{-4}$. All results of differential gene expression analysis utilized the statistical analysis tool, DESeq2 (16). For differentially

expressed gene list, p-values, FDR, and fold change (FC) filters were applied. The filter was $p < 0.01$, $FDR < 0.01$, and $FC > 2$ -fold for all differential gene expression results.

4.3.4 Generational H₂O₂ stress resistance determination

The determination of generational stress resistance was assessed as described by Kishimoto et al 2017. Briefly, P0 *C. elegans* were exposed to bacterial and Cu-stress conditions prior to a timed egg lay. Following generations were raised without any exposure to excess Cu. When offspring were 2day adults, nematodes were transferred in groups into drops of M9 containing 1.7mM hydrogen peroxide. Nematodes were checked every hour to determine the survival rate of the offspring over time.

4.3.5 Dopamine-dependent slowing in response to food signal

Quantifying the dopamine-dependent slowing in response to food signals were assessed based on protocols previously described in Sawin et al. 2000. Offspring raised in the absence of environmental stressors were raised to the L4 stage. For assessment of movement in response to food, 10-15 *C. elegans* from each parental condition were washed in M9 buffer twice before transfer to plates either with or without a food source. Five minutes after the transfer, the number of body bends in 20s was recorded using WormLab. Analysis of the WormLab recordings was further completed using ImageJ to calculate the final body bends per second (BBPS).

4.4 Results

4.4.1 In *C. elegans*, Cu conditions predict transcriptomic landscape more than bacterial Cu-efflux conditions

Principal component analysis was undertaken once read counts were normalized to gauge the extent of variation between biological replicates to determine the reliability of conclusions drawn from the experimental analysis. Overall, the analysis explains 52.13% of the total variation between exposure conditions; accordingly, PC1, 2 and 3 respectively accounted for 24.57, 15.44 and 12.11% (Fig. 4.1). Taken together, biological replicates in the absence (W and S) and presence (WC and SC) were generally distinguishable from each other. Therefore, a greater number of DEGs dependent on Cu stress could be reliably identified. However, the extensive variation within biological replicates indicated extensive overlap particularly between bacterial conditions in the same Cu conditions, suggesting that the bacterial Cu-efflux capacity does not greatly alter the transcriptomic response to Cu stress (Fig. 4.1). Therefore, the overall variation within biological replicates strongly limits the reliability of any conclusions drawn from this analysis.

4.4.2 Known Cu-responsive genes identified as DEGs

Several genes, in the Cu-dependent DEG analysis are already known to be responsive to Cu stress and serve to validate the genes pulled from the transcriptomic analysis. For instance, in both bacterial conditions, the nuclear localized metal responsive (*numr-1* and *numr-2*) genes were shown to increase in expression from their respective 0 μ M Cu controls. (Fig. 4.2-4.3) These results suggest that any bacterially-dependent Cu-

toxicity observed in nematodes would not be the result of increased transcription of *numr-1* expression as the Cu-responsive gene exhibited the same response regardless of the bacterially Cu-efflux condition. These results are consistent with the imaging analysis presented in Chapter 2 use a genetic reporter for *numr-1*.

Alternatively, the increased expression of a Cu-responsive gene, *kreg-1* (kgb-regulated), in 100% (Fig. 4.2) but not 50% (Fig. 4.3) bacterial Cu-efflux conditions during Cu stress indicates increased activity of a mitogen-activated protein kinase (MAPK) signal transduction pathway using c-Jun N-terminal kinases (JNK) in response to the bacterially Cu-efflux condition (6). The absence of this DEG in 50% bacterially Cu-efflux conditions exposed to the same concentrations of Cu suggests that 100% bacterially Cu-efflux conditions may influence the activation of this stress response pathway in nematodes. Furthermore, *kreg-1* requires increasing activation by KGB-1, an ortholog of human MAPK10, which has targets in the germline cells that could impact offspring beyond survival recorded by brood size Cu-toxicity measures. Although *kreg-1* was not explicitly identified as a DEG between the two excess copper conditions distinguished by their bacterial condition, *rrn-2.1* is differentially expressed between these conditions and is enriched in the germline like KGB-1 (Fig. 4.5). Additionally, *rrn-2.1* is similarly responsive to chemical exposures as well as *daf-16* and *skn-1* which are vital for the generational inheritance of parental stress responses (8). These results suggested that nematodes could be generationally impacted by variations in bacterially Cu-efflux during Cu stress.

While many metal-stress responsive pathways overlap, the specificity of the identified DEGs for copper stress in adults is further reflected in the downregulation of *mtl-2* and *vit-1* (Fig. 4.2, 4.3). For instance, increased *mtl-2* expression regardless of bacterially Cu-

efflux condition is specific to cadmium stress and instead known to be responsive to copper until offspring demonstrate a decrease in its expression after P0 exposures (5). Therefore, the DEG pattern resulting from the RNAseq analysis is specific to Cu stress and not other metals.

Further specificity can be gleaned from the developmental window of exposure looking at the expression of *vit-1*. Upregulation of *vit-1* was previously observed during Cu exposures between L1 and adulthood (3). However, many Cu-responsive genes are known to have age-dependent variation where early exposure prior to reproductive maturity exhibit the alternate pattern in adulthood (7). The downregulation of *vit-1* in both our adult exposures after L4 suggests that *vit-1* could follow the same developmental pattern of other metal-responsive genes. Also significant is the fact that none of the DEGs known to be responsive to environmental Cu stress were variably upregulated or downregulated in the absence of Cu excess (Fig. 4.4). Therefore, we can conclude that our exposure paradigm captured some of the unique adult nematode response to Cu stress instead of the earlier developmental exposures.

4.4.3 Bacterially-dependent Cu resistance is independent of increased *numr-1* gene expression

Toxicity endpoints indicative of Cu-stress demonstrated variable phenotypic enrichment following DEG analysis, supporting the role for bacterially-dependent Cu resistance in nematodes independent of altered gene expression in known Cu-responsive pathways. First, matricidal hatching, a Cu-toxicity endpoint previously shown to be greatly reduced in response to reduced bacterially Cu-efflux conditions, reflected in the phenotypic enrichment analysis as bag-of-worms. This bag-of-worms phenotype was

enriched in 100% bacterial Cu-efflux conditions (Table 4.1) but not 50% conditions (Table 4.2), reflecting the reduced rates of matricidal hatching observed when nematodes raised on 50% bacterial Cu efflux are exposed to excess copper. The second bacterially-dependent Cu-toxicity endpoint recapitulated by enrichment analysis was for nematode survival; only 50% bacterial Cu-efflux conditions demonstrate phenotypic enrichment for extended lifespan (Table 4.2), reflecting the increased survival rate observed in this group when exposed to excess copper. These results suggest that Cu-resistance demonstrated by nematodes raised in reduced bacterial Cu-efflux capacities did not arise from altered gene expression in known Cu-resistance pathways.

4.4.4 Bacterially-dependent DEGs during Cu-stress do not strongly predict neuronal or generational Cu-resistance

Of the bacterially-dependent DEGs identified during Cu stress, several are predicted to have tissue-specific expression in *C. elegans* in tissues known to be sensitive to Cu-stress. For instance, one DEG was specific to dopaminergic neurons, a tissue that is known to be damaged by excess copper in many organisms (17). To better understand the nature of the DEGs responsive to metal-stress in different bacterial conditions, enrichment analysis within the bacterial conditions was undertaken in Wormbase. Tissue enrichment unique to the 100% bacterial Cu-efflux condition exposed to excess copper includes PVD and the outer labial sensillum, both of which are neuronal in nature (Table 1). PVD neurons are sensory neurons that are glutamatergic while the outer labial sensillum is a sensory system that contains dopaminergic neurons. In comparison, the lack of neuronal tissue enrichment in the 50% bacterial Cu-efflux conditions exposed to

excess copper suggests neuronal involvement to Cu-stress may be unique to exposure conditions with increased bacterial Cu-efflux (Table 2).

Since neuronal deterioration is a known Cu-toxicity endpoint in nematodes, particularly for dopaminergic neurons (17), behavior dependent on an intact dopaminergic neural circuit, the basal slowing response to food (18), was tested within our exposure paradigm. Indeed, this slowing response, recorded in body bends per second using WormLab, was reduced in conditions with 100% (Fig. 4.6) bacterial Cu-efflux capacity (WT) but not to the same extent in conditions with just 50% (Fig. 4.7) or 25% (Fig. 4.8) bacterial Cu-efflux ($\Delta cusS$ and $\Delta cusR$ respectively). However, the variability in control conditions (0 μ M) and the observation that the loss of the significance in the slowing response for Cu-exposed nematodes of 100% *WT* bacterial Cu-efflux conditions seemed to be the result of slowing in the testing condition lacking food and not an increase in the basal slowing rate in the testing condition with food (Fig. 4.6). This distinction is more indicative of an overall loss of muscle function in the Cu-exposed group than a behavior specific to dopaminergic signaling. Given that slowed movement has been observed at higher concentrations of Cu exposures (19) this muscle-degeneration explanation cannot be excluded without more specific testing given the wide variation of dopaminergic behavioral responses (19,20).

Factors responsible for soma-germline stress communication also appeared regularly in our analysis. Two more bacterially-dependent DEGs were found to be positively regulated by *daf-16*, a transcriptional regulator that contributes to the transmission of stress resistance across generations (Fig. 4.5). HSF-1, the factor required for *numr-1* metal resistance activity, also contributes to the soma-germline transmission

of increased stress resistance over time (8). Therefore, we tested the hypothesis that bacterial Cu-efflux influenced generational stress resistance by testing the survival rate of F1 *C. elegans* following parental exposure to 0 μ M or 100 μ M Cu. In these experiments, high variability in 0 μ M Cu controls between 100% (Fig. 4.9) or 50% (Fig. 4.10) *WT* bacterial Cu-efflux was observed and no significant difference in survival following parental exposure to Cu was identified. However, while other forms of stress associated with increased resistance like heat and mitochondrial stress() were not explored in the bacterial conditions, parental Cu stress did not contribute to survival in response to oxidative stress in offspring regardless of the bacterial conditions.

4.5 Discussion

4.5.1 RNAseq analysis limited by experimental design

While previous research demonstrating a strong link between the bacterial Cu-efflux capacity and a host organism's ability to appropriately respond to excess copper in the environment, the same exposure paradigm did not appear to reveal a clear role for transcriptional regulation in mediating this effect. While transcriptional regulation may indeed play a minor role in this environmental stress response in host organisms, several components of the presented experimental design could also be masking its true contribution. Specifically, the loss of small RNA molecules during RNA isolation, and developmentally non-specific nematode populations should all be addressed in future experiments to better define this stress response in nematodes.

With total RNA isolations, gaining a general picture of overall gene expression is useful for consistent exposure conditions like those demonstrated between nematodes

exposed to either 0 μ M or 100 μ M CuSO₄. However, this method proved largely ineffective at distinguishing bacterial conditions under the same metal stress. One reason for this discrepancy may be the loss of RNA molecules smaller than 200 nucleotides during the isolation process while using Qiagen's RNeasy mini kit because of the significant role *numr-1* expression plays in the bacterially-dependent Cu-stress response in nematodes. Researchers previously found *numr-1* to be strongly induced when basal RNA metabolism is disrupted, specifically those complexes responsible for snRNA processing. Without the appropriate snRNAs, splicing factors no longer function appropriately (4). Future analysis would benefit from a focus on alternative splicing events that varies between 1) different Cu conditions and 2) differing bacterial Cu-efflux conditions to see whether alternative splicing contributes to the bacterially-dependent Cu resistance observed in nematodes raised with reduced bacterial Cu-efflux capacity. Furthermore, future experiments should also utilize RNA isolation kits that do not result in the loss of small RNA molecules like snRNAs to gain a fuller picture of the bacterially-dependent stress response to Cu.

A broad developmental window for nematode populations prior to isolation also likely contributed to noise between experimental replicates and conditions independent of the dependent variables being tested. Previously experiments that tested for bacterially-dependent Cu-stress responses in nematodes were designed to screen for individual nematodes within a very narrow developmental window, L4, prior to any data collection to avoid confounding developmental effects associated with metal exposures (7). For RNAseq analysis, the large populations required to attain enough RNA did not allow for as strict of a screen for the L4 developmental window. Furthermore, since whole-

worm preparations were used for RNA isolation, nematode eggs representing an early developmental and generational exposure, could not be excluded from the RNA collection process without adding further confounding variables. Two methods could be used in future work to control for this much more mixed population of nematodes. First gene expression specific to developmental stages outside of 2 day adults could be filtered out using data sets like modENCODE (21) to focus the data analysis on DEGs for adult responses to metal stress. Second, alternative RNA isolation kits that can use smaller sample sizes, like the RNAqueous-Micro Kit by ThermoFisher, could allow for a much stricter screen of developmental stages in a given nematode population prior to RNA isolation.

4.5.2 Tissue and spatial specificity of bacterially-dependent Cu-stress response in nematodes

Toxicity responses using the exposure paradigm for Cu-efflux toxicity appears to be more responsive in some tissues than others. For instance, although DEGs identified in 100 μ M CuSO₄ exposures between 100% and 50% bacterial Cu-efflux conditions highlighted genes expressed in the pharynx, germline and neuronal cells, only neuronal toxicity was implicated in the slowing response to food in nematodes while the germline remained unaffected by the bacterial Cu-efflux capacity. These results are consistent with previous research that showed brood size, a marker for germline toxicity, having no change in response to different bacterial Cu-efflux conditions at lower concentrations of metal stress that elicit consistent neuronal toxicity (17) or without exposure of early developmental timepoints to the stress (7)

Pharyngeal DEGs between bacterial conditions are also consistent with previous research on *numr-1* expression and localization in the nematode pharynx during copper stress. For instance, copper stress was responsible for increased gene expression for *numr-1* regardless of the bacterial Cu-efflux condition while a reporter for the *numr-1* gene using GFP to track expression also had similar increases in GFP fluorescence regardless of bacterial Cu-efflux within the nematode pharynx (2). However, any bacterially dependent spatial organization, like that revealed using the *numr-1p::GFP* reporter, was lost in the RNAseq analysis. Therefore, future experiments would benefit from screening genes expressed in both bacterial conditions responding to Cu stress by using GFP reporters for the genes and their protein products regardless of whether they were differentially expressed in the RNA analysis.

4.6 Conclusions

Research presented in this chapter represents the first time RNAseq analysis has sought to describe a host-microbe system response to Cu stress. While the chronic exposure paradigm that was utilized to focus on gene expression in aging adults effectively identified genes necessary for the nematode response to Cu stress, the bacterially-dependent contribution was not consistently identified in our RNA analysis. Although *numr-1* was recognized as a significant DEG between 0 μ M and 100 μ M CuSO₄ exposure, the experimental design of the RNA analysis limited our ability to analyze *numr-1*'s role in small RNA populations (<200 nucleotides) where its effect on RNA metabolism was previously observed. Despite these limitations, phenotype enrichment analysis of RNA data recapitulated 1) the increased matricidal hatching risk of nematodes exposed to Cu when the bacterial Cu-efflux capacity is high, and 2) the increased survival of nematodes exposed to Cu when the bacterial Cu-efflux capacity is lowered. Additionally, tissue enrichment analysis describing the increased neuronal Cu-toxicity when the bacterial Cu-efflux capacity is high was supported by behavioral experiments. This study concludes that RNA analysis and studying the tissue and spatial specificity of the bacterially-dependent stress response would strengthen the observations made in this chapter and has the potential to contribute to our understanding of environmental risk factors for neurodegenerative disorders like Parkinson's disease.

4.7 Figures

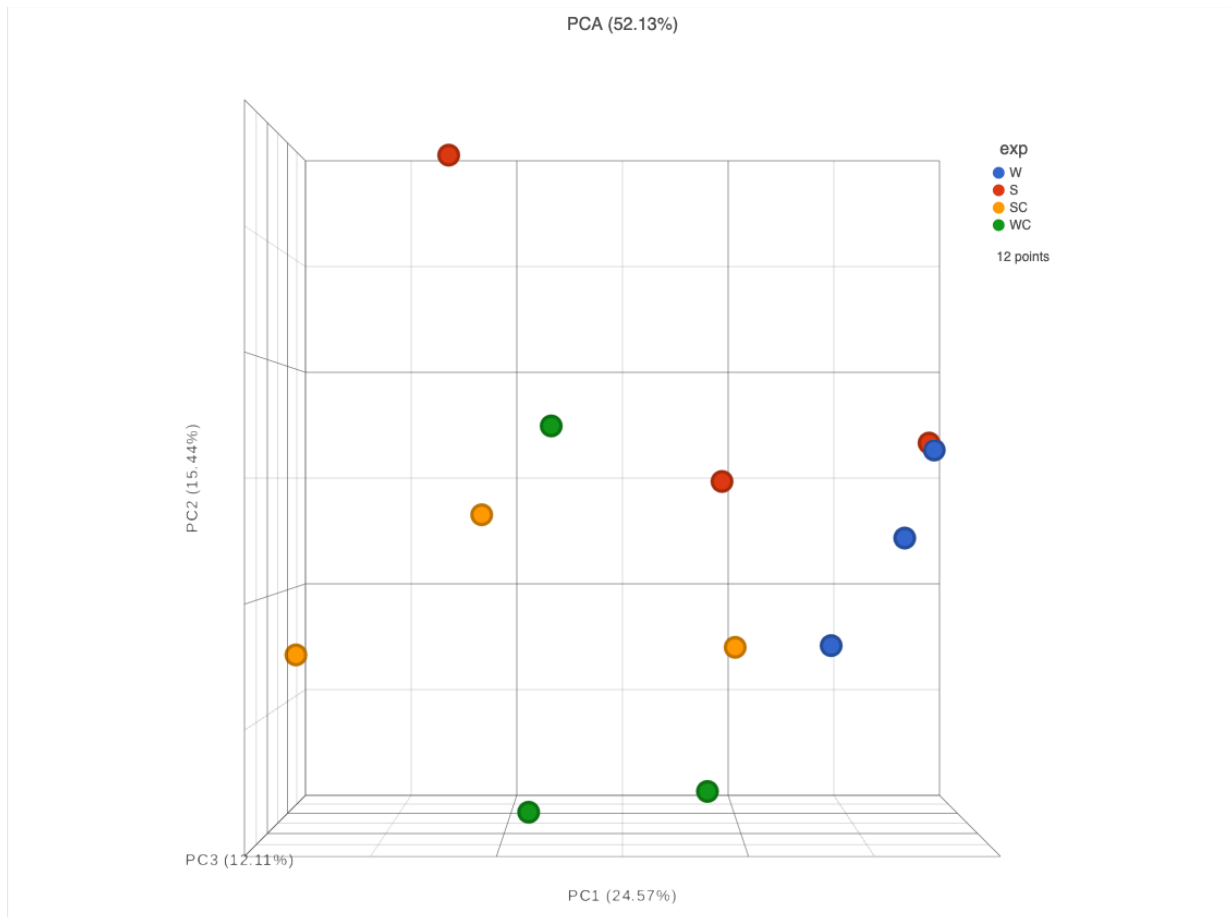


Fig. 4.1 Principal component analysis for normalized read counts of biological replicates. W (blue) or S (red) respectively indicates 100% or 50% bacterial Cu-efflux conditions in the absence of excess copper while WC (green) and SC (yellow) respectively indicate 100% or 50% bacterial Cu-efflux conditions in the presence of excess copper.

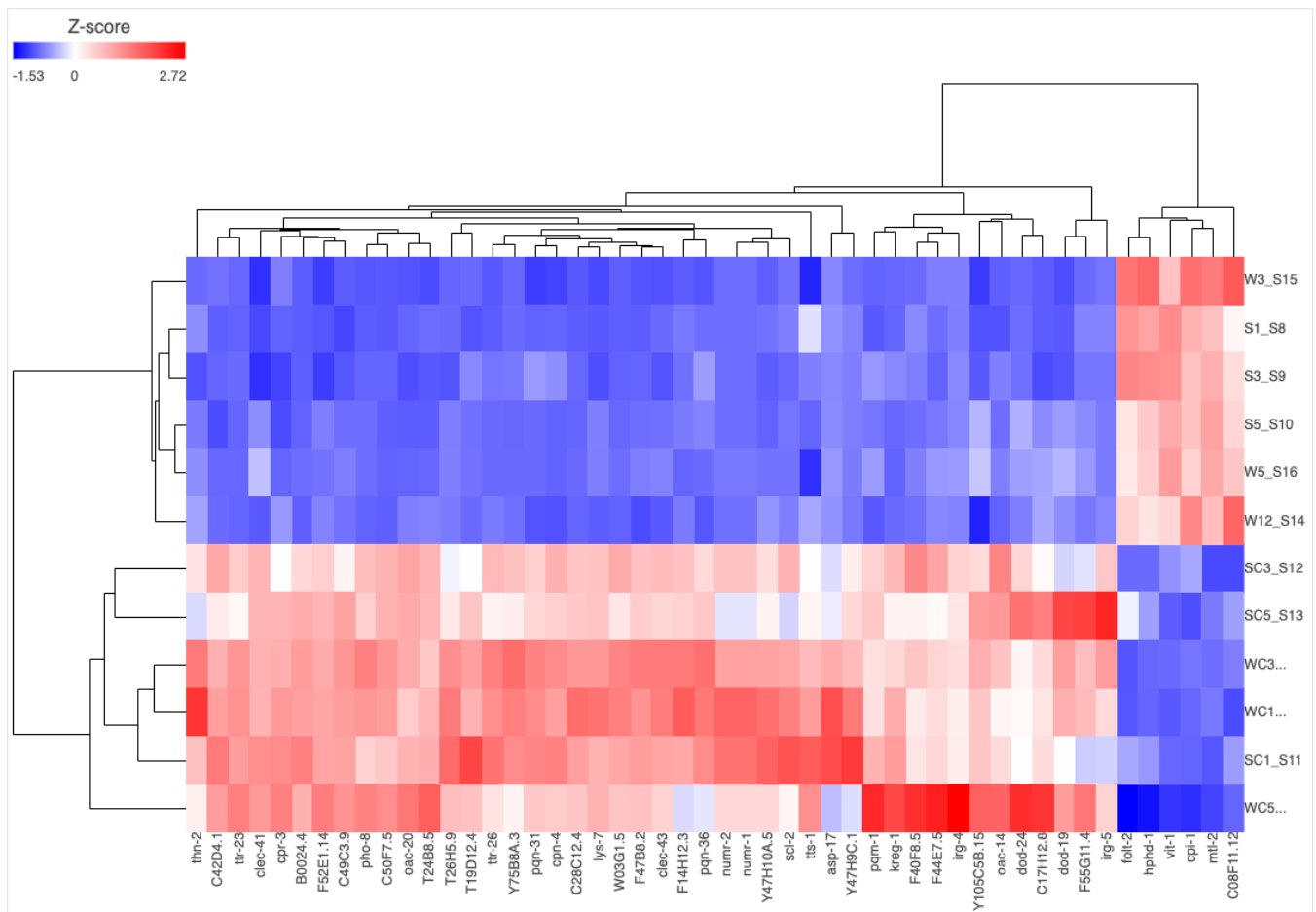


Fig. 4.2 DEGs dependent on copper concentration in 100% bacterial Cu-efflux conditions. The right-hand labels distinguish between biological replicates where the first letter indicates the bacterial Cu-efflux condition (W=100%, S=50%) and the second letter, if present, indicates excess copper. The remaining numbers indicate the experimental replicate. The top DEG hits are listed on the bottom of the graph for each of the biological replicates where increased expression is represented in red and decreased expression is represented by blue.

Tissue Enrichment Analysis Results

Term	Expected	Observed	Enrichment Fold Change	P value	Q value
intestine WBbt:0005772	17	39	2.3	8.3e-07	0.00026
cephalic sheath cell WBbt:0008406	1.8	8	4.4	0.00011	0.017
PVD WBbt:0006831	7.1	18	2.5	0.00013	0.017
head mesodermal cell WBbt:0004697	7.9	19	2.4	0.00016	0.017
outer labial sensillum WBbt:0005501	7.3	18	2.5	0.00017	0.017

Phenotype Enrichment Analysis Results

Term	Expected	Observed	Enrichment Fold Change	P value	Q value
cadmium hypersensitive WBPhenotype:0001655	0.086	4	46	3e-08	7.1e-06
nematode phenotype WBPhenotype:0000886	9.3	24	2.6	2.7e-06	0.00032
uptake by intestinal cell defective WBPhenotype:0001763	0.047	2	42	1.6e-05	0.0012
bag of worms WBPhenotype:0000007	0.059	1	17	0.0017	0.099

Gene Ontology Enrichment Analysis Results

Term	Expected	Observed	Enrichment Fold Change	P value	Q value
response to biotic stimulus GO:0009607	0.72	14	19	1.1e-15	3.4e-13
biological process involved in interspecies interaction between organisms GO:0044419	0.72	14	19	1.1e-15	3.4e-13
defense response GO:0006952	0.72	14	19	1.3e-15	3.4e-13
immune system process GO:0002376	0.73	14	19	1.4e-15	3.4e-13
extracellular region GO:0005576	1	9	8.9	9.3e-08	5.6e-06
membrane microdomain GO:0098857	0.086	3	35	1.8e-06	9.2e-05
defense response to Gram-positive bacterium GO:0050830	0.13	3	24	8.4e-06	0.00036
cell surface GO:0009986	0.18	2	11	0.00078	0.029
lytic vacuole GO:0000323	0.27	2	7.4	0.0026	0.087

Table 4.1. Enrichment analyses dependent on copper concentration in 100% bacterial Cu-efflux conditions performed in WormBase

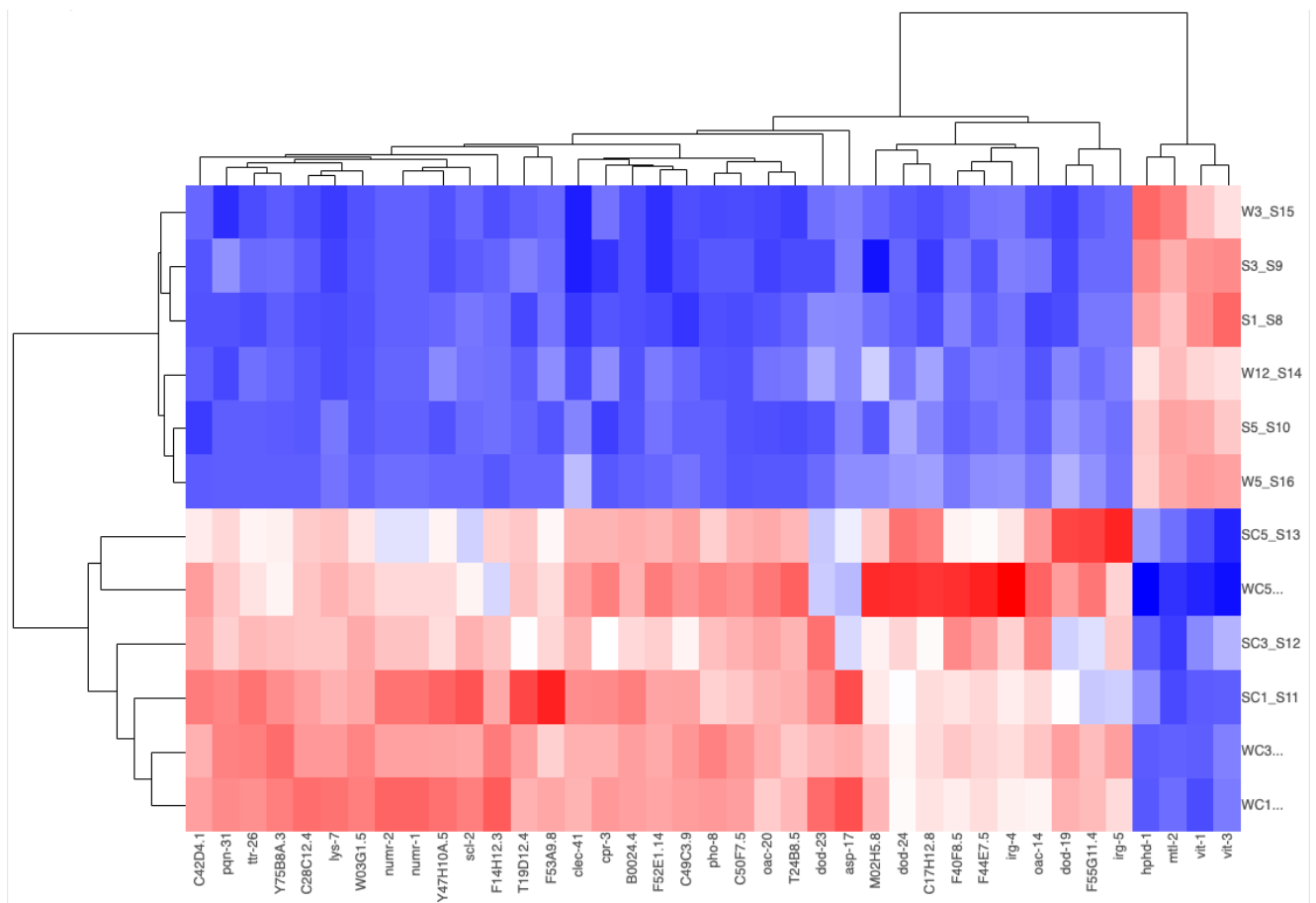


Fig. 4.3 DEGs dependent on copper concentration in 50% bacterial Cu-efflux conditions. The right-hand labels distinguish between biological replicates where the first letter indicates the bacterial Cu-efflux condition (W=100%, S=50%) and the second letter, if present, indicates excess copper. The remaining numbers indicate the experimental replicate. The top DEG hits are listed on the bottom of the graph for each of the biological replicates where increased expression is represented in red and decreased expression is represented by blue.

Tissue Enrichment Analysis Results

Term	Expected	Observed	Enrichment Fold Change	P value	Q value
intestine WBbt:0005772	14	32	2.3	3.6e-06	0.0011
cephalic sheath cell WBbt:0008406	1.5	8	5.5	1.9e-05	0.003
head mesodermal cell WBbt:0004697	6.3	16	2.5	0.00023	0.024

Phenotype Enrichment Analysis Results i

Term	Expected	Observed	Enrichment Fold Change	P value	Q value
cadmium hypersensitive WBPhenotype:0001655	0.1	4	40	6.4e-08	1.5e-05
uptake by intestinal cell defective WBPhenotype:0001763	0.055	2	36	2.4e-05	0.0029
nematode phenotype WBPhenotype:0000886	11	24	2.2	4.7e-05	0.0037
extended life span WBPhenotype:0000061	0.79	5	6.3	0.00015	0.0091

Gene Ontology Enrichment Analysis Results i

Term	Expected	Observed	Enrichment Fold Change	P value	Q value
biological process involved in interspecies interaction between organisms GO:0044419	0.54	13	24	4.5e-16	1.4e-13
response to biotic stimulus GO:0009607	0.54	13	24	4.5e-16	1.4e-13
defense response GO:0006952	0.54	13	24	5e-16	1.4e-13
immune system process GO:0002376	0.55	13	24	5.7e-16	1.4e-13
membrane microdomain GO:0098857	0.065	3	46	5.8e-07	3.5e-05
defense response to Gram-positive bacterium GO:0050830	0.094	3	32	2.7e-06	0.00013
extracellular region GO:0005576	0.76	6	7.9	1.3e-05	0.00054
lytic vacuole GO:0000323	0.2	2	9.8	0.0012	0.043

Table 4.2. Enrichment analyses dependent on copper concentration in 50% bacterial Cu-efflux conditions performed in WormBase

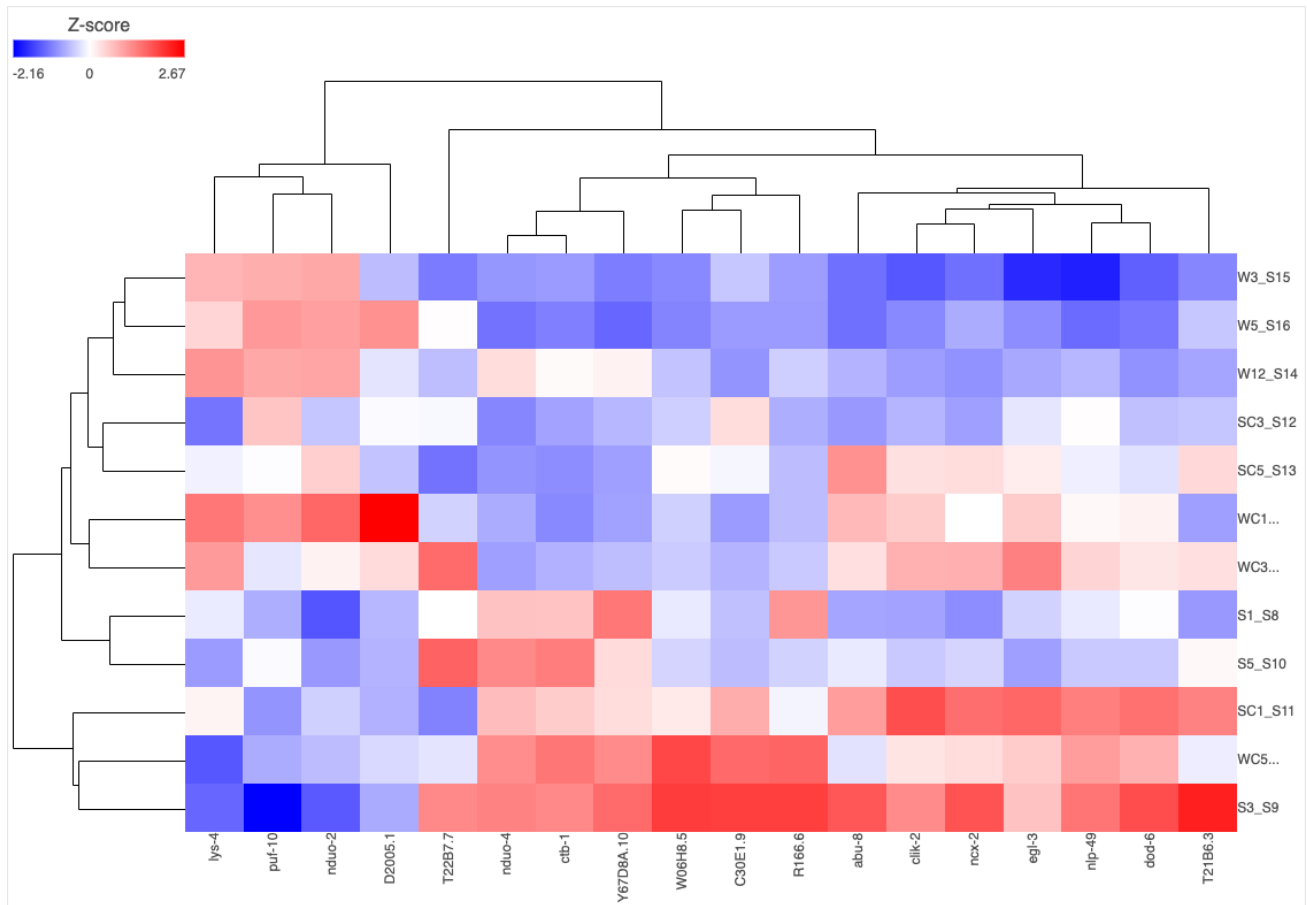


Fig. 4.4 DEGs dependent on bacterial Cu-efflux conditions in the absence of excess copper. The right-hand labels distinguish between biological replicates where the first letter indicates the bacterial Cu-efflux condition (W=100%, S=50%) and the second letter, if present, indicates excess copper. The remaining numbers indicate the experimental replicate. The top DEG hits are listed on the bottom of the graph for each of the biological replicates where increased expression is represented in red and decreased expression is represented by blue.

Tissue Enrichment Analysis Results

Term	Expected	Observed	Enrichment Fold Change	P value	Q value
AVK WBbt:0006823	1.4	7	5.1	7.7e-05	0.024
AVB WBbt:0005841	0.032	1	32	0.00047	0.074
SDQL WBbt:0004993	0.034	1	29	0.00055	0.074
uv1 WBbt:0006791	0.04	1	25	0.00075	0.074

Phenotype Enrichment Analysis Results

Term	Expected	Observed	Enrichment Fold Change	P value	Q value
bag of worms WBPhenotype:0000007	0.028	1	36	0.00036	0.086

Genotype Enrichment Analysis Results

Term	Expected	Observed	Enrichment Fold Change	P value	Q value
respirasome GO:0070469	0.074	3	41	1e-06	0.0003
NADH dehydrogenase complex GO:0030964	0.043	2	47	1.1e-05	0.0017
ATP synthesis coupled electron transport GO:0042773	0.057	2	35	2.7e-05	0.0027
transporter complex GO:1990351	0.15	2	13	0.00048	0.036
response to monoamine GO:0071867	0.036	1	27	0.00062	0.037
envelope GO:0031975	0.39	3	7.6	0.00069	0.037
locomotion involved in locomotory behavior GO:0031987	0.041	1	25	0.00078	0.037
thioester metabolic process GO:0035383	0.045	1	22	0.00095	0.037
response to organic cyclic compound GO:0014070	0.046	1	22	0.001	0.037
pharynx development GO:0060465	0.054	1	19	0.0013	0.04
calmodulin binding GO:0005516	0.055	1	18	0.0014	0.04
regulation of synapse structure or activity GO:0050803	0.056	1	18	0.0015	0.04
calcium ion transport GO:0006816	0.065	1	15	0.002	0.046
divalent inorganic cation homeostasis GO:0072507	0.068	1	15	0.0021	0.046
muscle system process GO:0003012	0.075	1	13	0.0026	0.052
defense response to Gram-positive bacterium GO:0050830	0.078	1	13	0.0028	0.053
digestive system development GO:0055123	0.098	1	10	0.0044	0.077
sodium ion transport GO:0006814	0.1	1	9.8	0.0048	0.079
serine-type endopeptidase activity GO:0004252	0.12	1	8.6	0.0061	0.096

Table 4.3. Enrichment analyses dependent on bacterial Cu-efflux conditions in the absence of excess copper performed in WormBase

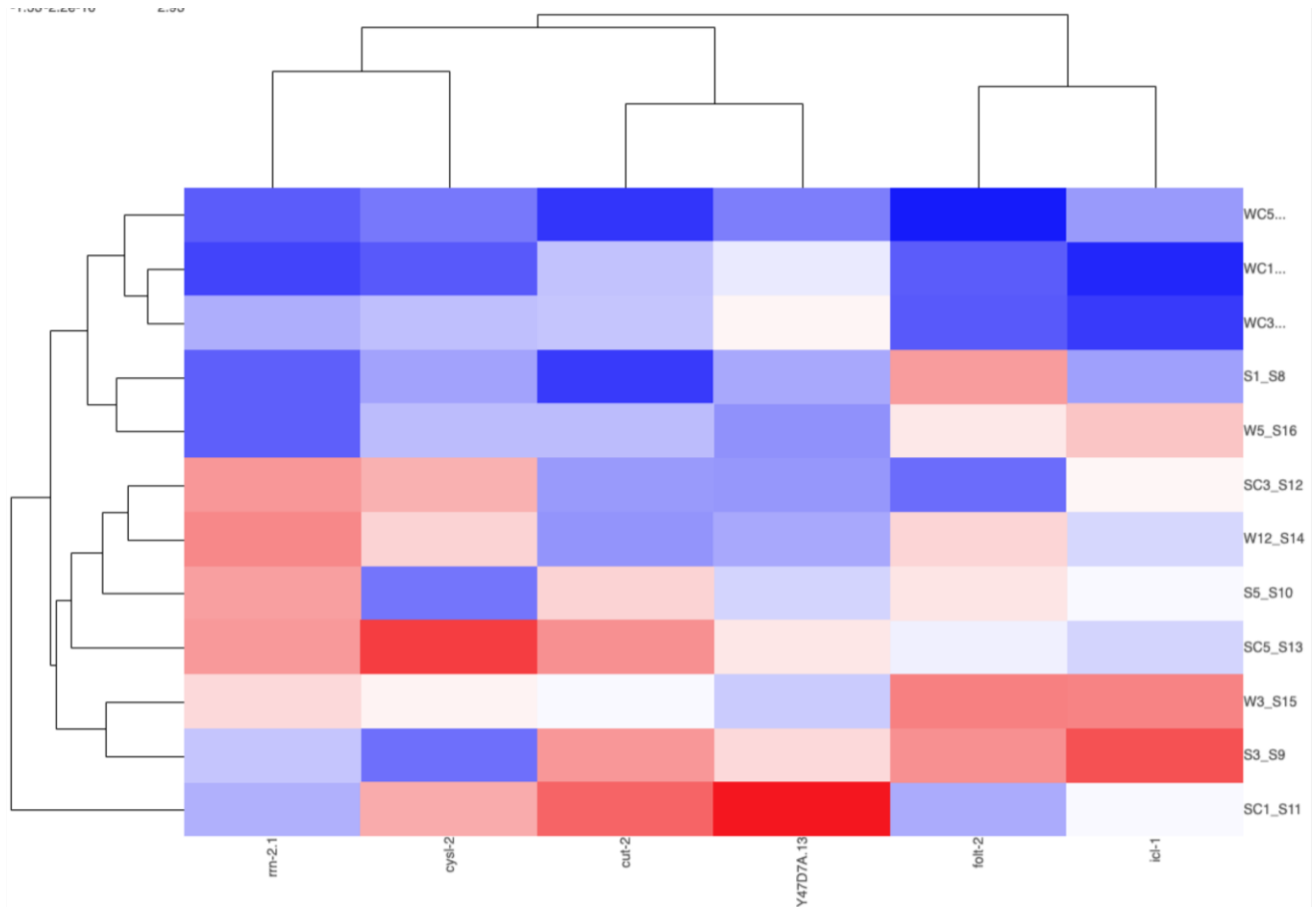


Fig. 4.5 DEGs dependent on bacterial Cu-efflux conditions in the presence of excess copper. The right-hand labels distinguish between biological replicates where the first letter indicates the bacterial Cu-efflux condition (W=100%, S=50%) and the second letter, if present, indicates excess copper. The remaining numbers indicate the experimental replicate. The top DEG hits are listed on the bottom of the graph for each of the biological replicates where increased expression is represented in red and decreased expression in represented by blue.

Gene Ontology Enrichment Analysis Results

Term	Expected	Observed	Enrichment Fold Change	P value	Q value
organic acid metabolic process GO:0006082	0.088	2	23	8.8e-05	0.026
external encapsulating structure GO:0030312	0.02	1	50	0.00018	0.027
structural constituent of cuticle GO:0042302	0.034	1	30	0.00053	0.053
aging GO:0007568	0.053	1	19	0.0013	0.096

Table 4.4. Enrichment analysis dependent on bacterial Cu-efflux conditions in the presence of excess copper

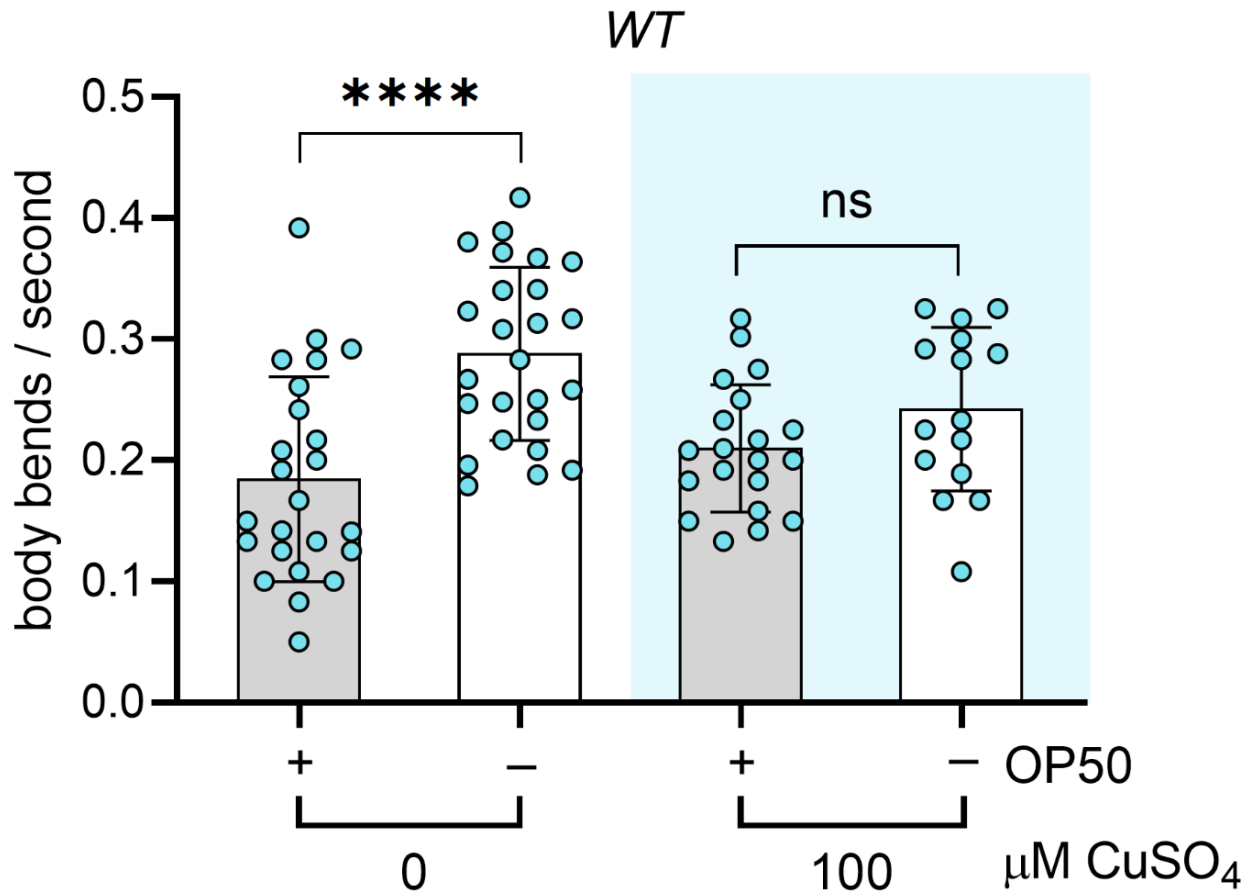


Fig. 4.6. Basal slowing response to food after Cu exposure on 100% WT Bacterial Cu efflux. Nematodes were exposed to 0μM or 100μM CuSO₄ starting at L4 on 100% WT bacterial Cu efflux lawns before determination of basal slowing rate w/ or w/out *OP50* present. N=3, n=6-10. Grey bars indicate testing conditions with food present while white bars indicate testing conditions without food present. Error bars represent standard deviation after a one-way ANOVA with tukey's multiple comparisons analysis.

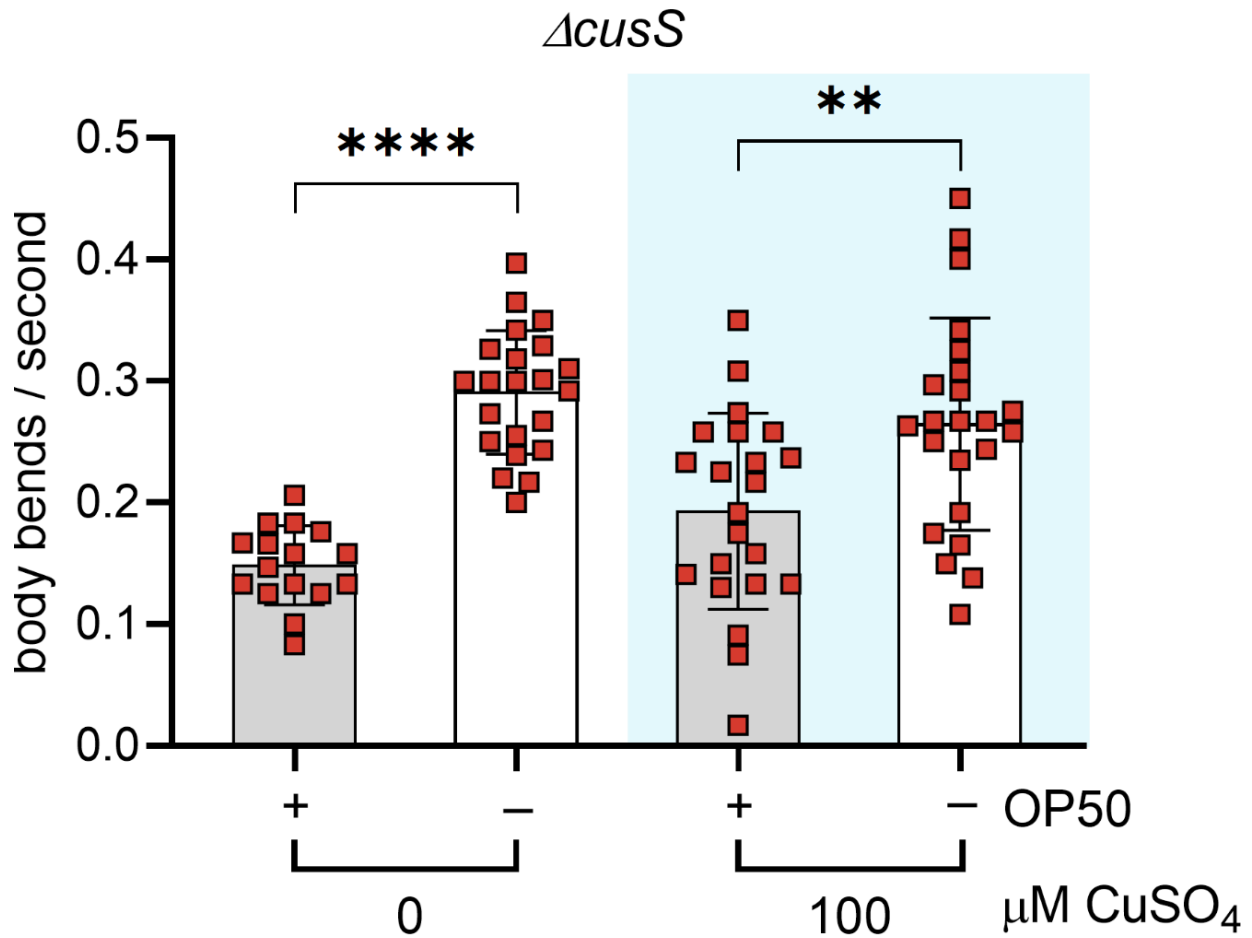


Fig. 4.7. Basal slowing response to food after Cu exposure on 50% *WT* Bacterial Cu efflux (*ΔcusS*). Nematodes were exposed to 0μM or 100μM CuSO₄ starting at L4 on 50% *WT* bacterial Cu efflux lawns before determination of basal slowing rate w/ or w/out *OP50* present. N=3, n=5-11. Grey bars indicate testing conditions with food present while white bars indicate testing conditions without food present. Error bars represent standard deviation after a one-way ANOVA with tukey's multiple comparisons analysis.

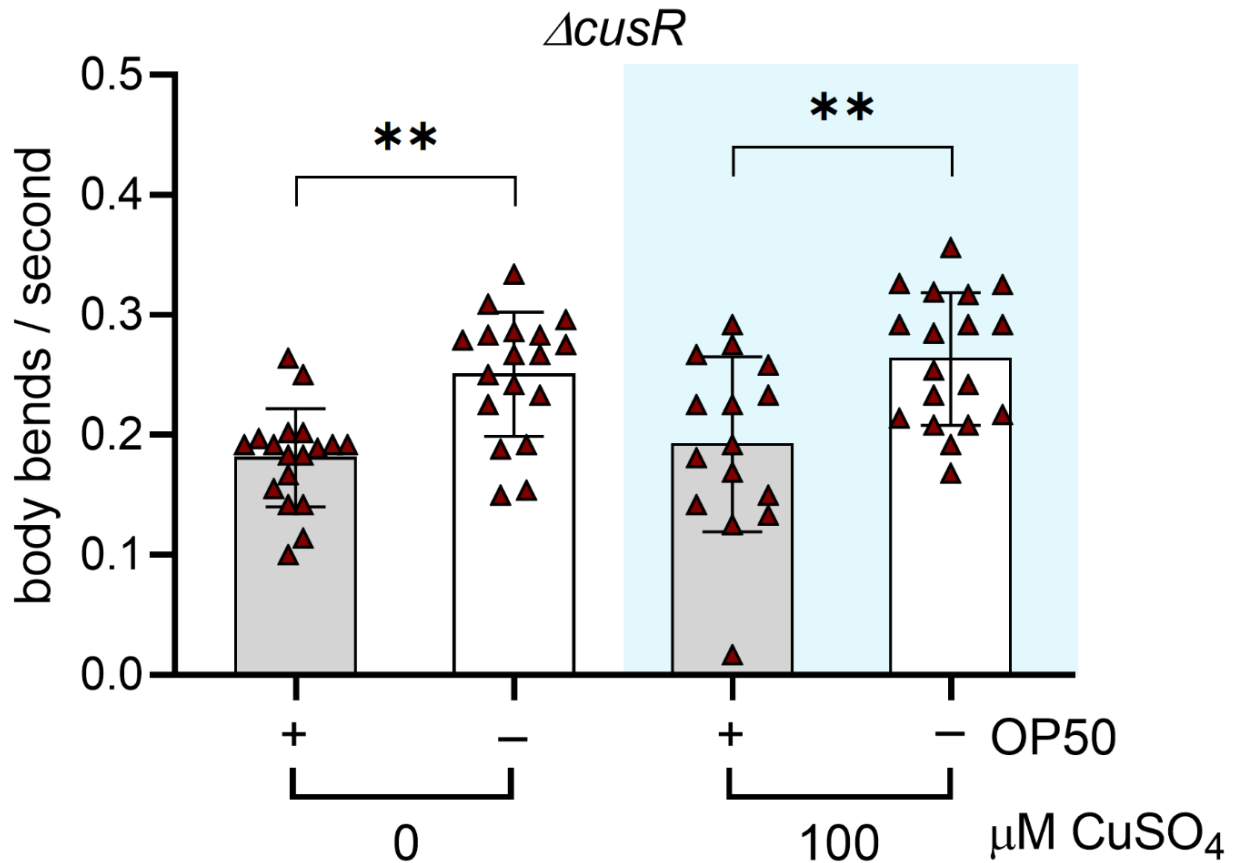


Fig. 4.8. Basal slowing response to food after Cu exposure on 25% WT Bacterial Cu efflux ($\Delta cusR$). Nematodes were exposed to 0 μ M or 100 μ M CuSO₄ starting at L4 on 25% WT bacterial Cu efflux lawns before determination of basal slowing rate w/ or w/out *OP50* present. N=3, n=6-12. Grey bars indicate testing conditions with food present while white bars indicate testing conditions without food present. Error bars represent standard deviation after a one-way ANOVA with tukey's multiple comparisons analysis.

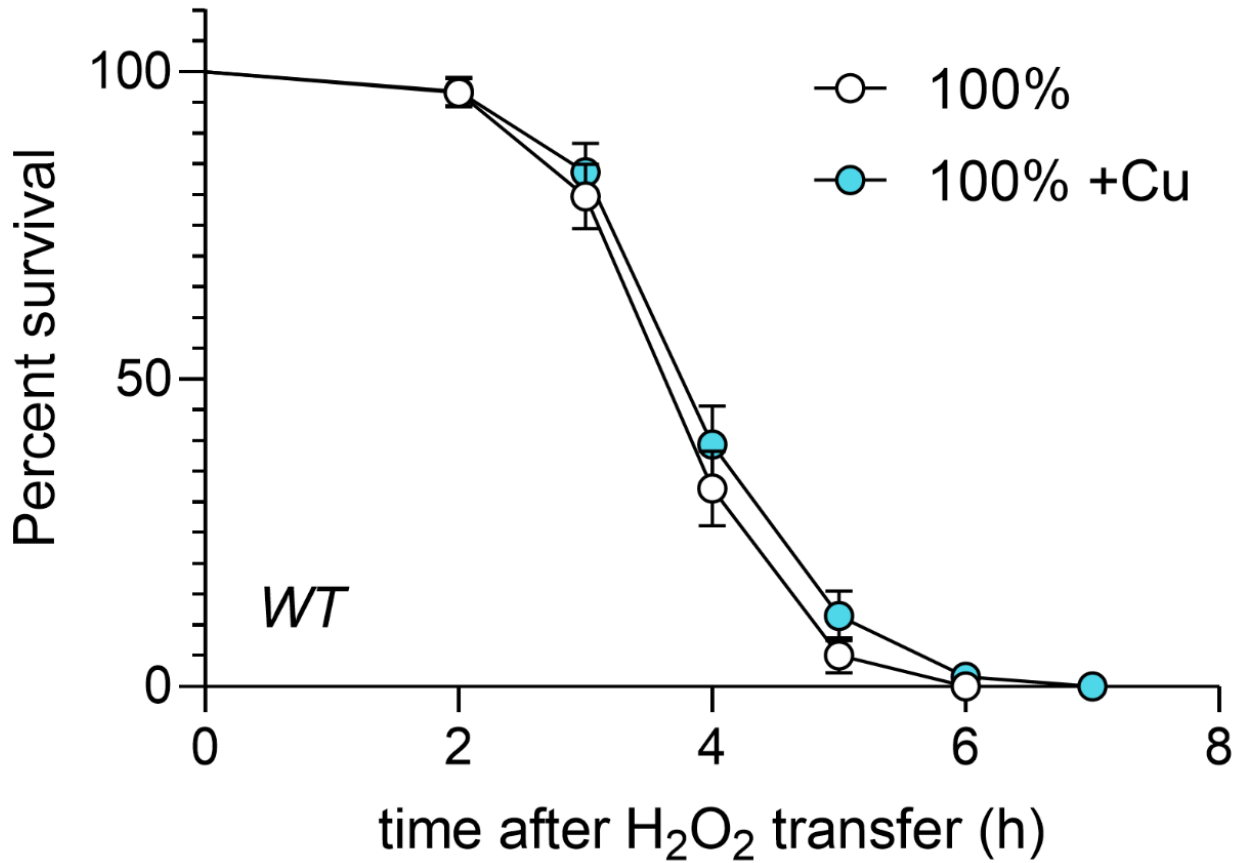


Fig. 4.9. 100% *WT* Bacterial Cu-efflux capacity does not generationaly increase oxidative stress resistance in F1 nematodes. F1 offspring of P0 exposed to either 0 μ M (white circles) or 100 μ M (blue circles) for 48h starting at the L4 developmental stage before an F1 egg lay without the environmental exposure. Error bars denote standard deviation. N=3 n=36-50. Significance was determined using Kaplan-Meier survival analysis.

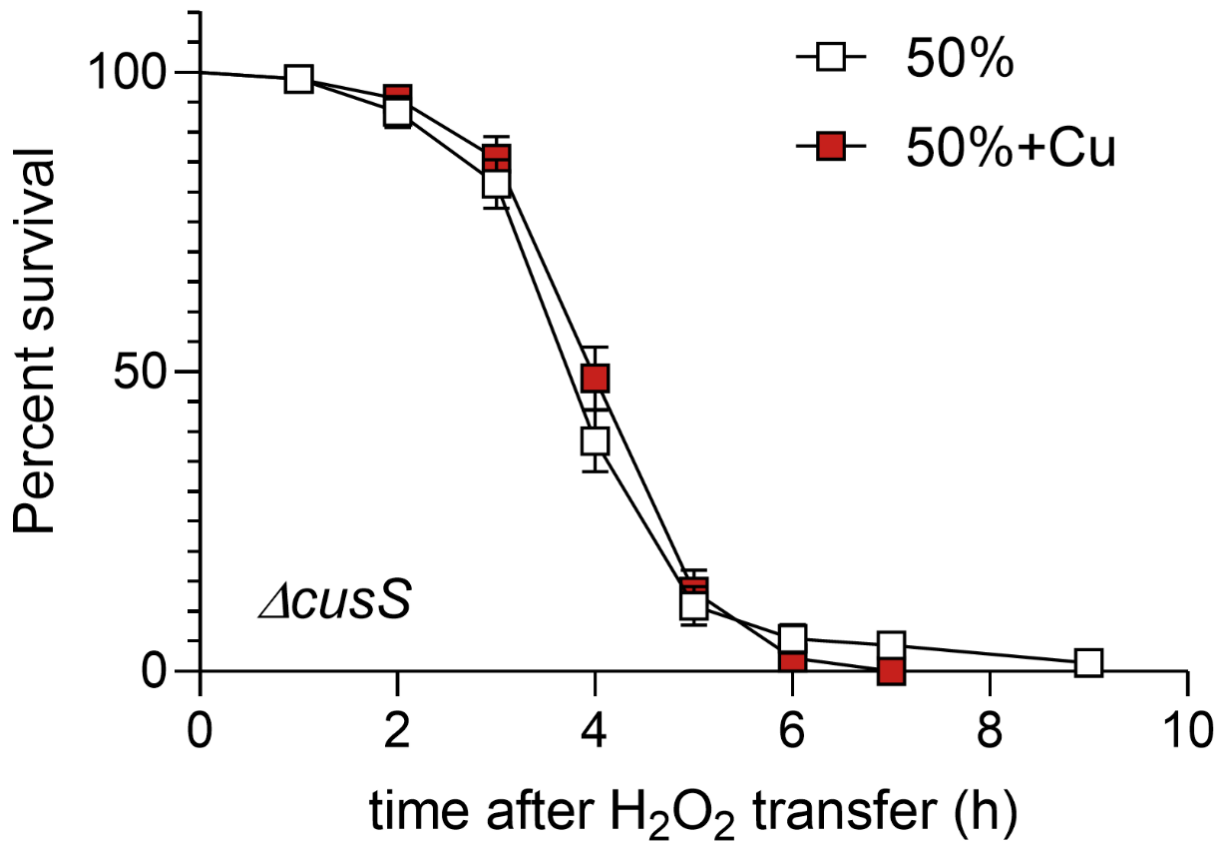


Fig. 4.10. 50% WT Bacterial Cu-efflux capacity does not generationally increase oxidative stress resistance in F1 nematodes. F1 offspring of P0 exposed to either 0 μ M (white squares) or 100 μ M (red squares) for 48h starting at the L4 developmental stage before an F1 egg lay without the environmental exposure. Error bars denote standard deviation. N=3 n=38-54. Significance was determined using Kaplan-Meier survival analysis.

4.9 References

1. Hattori, A., Mizuno, T., Akamatsu, M., Hisamoto, N., and Matsumoto, K. (2013) The *Caenorhabditis elegans* JNK signaling pathway activates expression of stress response genes by derepressing the Fos/HDAC repressor complex. *PLoS Genet* **9**, e1003315
2. Tvermoes, B. E., Boyd, W. A., and Freedman, J. H. (2010) Molecular characterization of numr-1 and numr-2: genes that increase both resistance to metal-induced stress and lifespan in *Caenorhabditis elegans*. *J Cell Sci* **123**, 2124-2134
3. Zhang, Y., Zhao, C., Zhang, H., Liu, R., Wang, S., Pu, Y., and Yin, L. (2021) Integrating transcriptomics and behavior tests reveals how the *C. elegans* responds to copper induced aging. *Ecotoxicology and Environmental Safety* **222**, 112494
4. Wu, C. W., Wimberly, K., Pietras, A., Dodd, W., Atlas, M. B., and Choe, K. P. (2019) RNA processing errors triggered by cadmium and integrator complex disruption are signals for environmental stress. *BMC Biol* **17**, 56
5. Zhang, Y., Zhao, C., Zhang, H., Lu, Q., Zhou, J., Liu, R., Wang, S., Pu, Y., and Yin, L. (2021) Trans-generational effects of copper on nerve damage in *Caenorhabditis elegans*. *Chemosphere* **284**, 131324
6. Hattori, A., Mizuno, T., Akamatsu, M., Hisamoto, N., and Matsumoto, K. (2013) The *Caenorhabditis elegans* JNK Signaling Pathway Activates Expression of Stress Response Genes by Derepressing the Fos/HDAC Repressor Complex. *PLOS Genetics* **9**, e1003315
7. Twumasi-Boateng, K., Wang, T. W., Tsai, L., Lee, K. H., Salehpour, A., Bhat, S., Tan, M. W., and Shapira, M. (2012) An age-dependent reversal in the protective

capacities of JNK signaling shortens *Caenorhabditis elegans* lifespan. *Aging Cell* **11**, 659-667

8. Kishimoto, S., Uno, M., Okabe, E., Nono, M., and Nishida, E. (2017) Environmental stresses induce transgenerationally inheritable survival advantages via germline-to-soma communication in *Caenorhabditis elegans*. *Nature Communications* **8**, 14031

9. Pukkila-Worley, R., and Ausubel, F. M. (2012) Immune defense mechanisms in the *Caenorhabditis elegans* intestinal epithelium. *Curr Opin Immunol* **24**, 3-9

10. Singh, I., Sagare, A. P., Coma, M., Perlmutter, D., Gelein, R., Bell, R. D., Deane, R. J., Zhong, E., Parisi, M., Ciszewski, J., Kasper, R. T., and Deane, R. (2013) Low levels of copper disrupt brain amyloid- β ; homeostasis by altering its production and clearance. *Proceedings of the National Academy of Sciences* **110**, 14771-14776

11. Ali, S. F., Binienda, Z. K., and Imam, S. Z. (2011) Molecular Aspects of Dopaminergic Neurodegeneration: Gene-Environment Interaction in Parkin Dysfunction. *International Journal of Environmental Research and Public Health* **8**, 4702-4713

12. Bisaglia, M., and Bubacco, L. (2020) Copper Ions and Parkinson's Disease: Why Is Homeostasis So Relevant? *Biomolecules* **10**

13. Metaxas, A. (2021) Imbalances in Copper or Zinc Concentrations Trigger Further Trace Metal Dyshomeostasis in Amyloid-Beta Producing *Caenorhabditis elegans*. *Frontiers in Neuroscience* **15**

14. White, C., Lee, J., Kambe, T., Fritsche, K., and Petris, M. J. (2009) A role for the ATP7A copper-transporting ATPase in macrophage bactericidal activity. *J Biol Chem* **284**, 33949-33956

15. Dobin, A., Davis, C. A., Schlesinger, F., Drenkow, J., Zaleski, C., Jha, S., Batut, P., Chaisson, M., and Gingeras, T. R. (2013) STAR: ultrafast universal RNA-seq aligner. *Bioinformatics* **29**, 15-21
16. Love, M. I., Huber, W., and Anders, S. (2014) Moderated estimation of fold change and dispersion for RNA-seq data with DESeq2. *Genome Biology* **15**, 550
17. Mashock, M. J., Zanon, T., Kappell, A. D., Petrella, L. N., Andersen, E. C., and Hristova, K. R. (2016) Copper Oxide Nanoparticles Impact Several Toxicological Endpoints and Cause Neurodegeneration in *Caenorhabditis elegans*. *PLoS One* **11**, e0167613
18. Sawin, E. R., Ranganathan, R., and Horvitz, H. R. (2000) *C. elegans* locomotory rate is modulated by the environment through a dopaminergic pathway and by experience through a serotonergic pathway. *Neuron* **26**, 619-631
19. Villanueva, A., Lozano, J., Morales, A., Lin, X., Deng, X., Hengartner, M. O., and Kolesnick, R. N. (2001) *jkk-1* and *mek-1* regulate body movement coordination and response to heavy metals through *jnk-1* in *Caenorhabditis elegans*. *The EMBO Journal* **20**, 5114-5128
20. Omura, D. T., Clark, D. A., Samuel, A. D., and Horvitz, H. R. (2012) Dopamine signaling is essential for precise rates of locomotion by *C. elegans*. *PLoS One* **7**, e38649
21. Li, J. J., Huang, H., Bickel, P. J., and Brenner, S. E. (2014) Comparison of *D. melanogaster* and *C. elegans* developmental stages, tissues, and cells by modENCODE RNA-seq data. *Genome Res* **24**, 1086-1101

CHAPTER 5: CONCLUSIONS AND FUTURE DIRECTIONS

This body of work focused on environmental conditions that modulate organismal Cu homeostasis, specifically the drivers of CRR1-mediated Cu uptake during Zn and Cu deficiency in *Chlamydomonas reinhardtii* and the contribution of reduced bacterial Cu-efflux capacity on *Caenorhabditis elegans* Cu tolerance. The role of CTRs and an abundant cytosolic thiol in uptake on Cu accumulation was identified in Cu-deficient and Zn-deficient environmental conditions. In *Caenorhabditis elegans*, Cu-toxicity dependent on the bacterial Cu-efflux capacity of the environment was identified. *C. elegans* gene expression analysis further determined the bacterially-dependent Cu-stress responses mediating this effect in the host nematode.

In chapter 2, environmental mediators of Cu uptake were investigated. As an essential transition metal, the acquisition of Cu from the environment is essential for all forms of life and is reflected in the ubiquity of CTR proteins and other homeostatic processes across prokaryotic, fungal, metazoan and photosynthetic organisms alike to avoid deficiency or toxicity of the metal (1-5). Previous studies found that failures of the Cu-homeostatic system in organisms associates with a number of pathologies coinciding with altered accumulation patterns of essential and nonessential transition metals alike. In particular, a consistent inverse relationship between Cu and Zn misregulation has been reported in several organisms and disease conditions without identifying robust causal relationship between the observations(6-9). Therefore, investigations in *Chlamydomonas* sought to determine how metal homeostatic factors function to maintain growth and survival during periods that elicit increases in Cu uptake like Zn and Cu deficiency.

The results in chapter 2 first identified the role of Cu uptake transporters for *Chlamydomonas reinhardtii* in two environmental conditions known to activate the Cu response regulon, CRR1(2). The two canonical Cu uptake transporters, CTR1 and CTR2, were found to be phylogenetically similar to each other than other CTRs and have similar CRR1-driven expression patterns in both Cu-deficient and Zn deficient conditions. To test the hypothesis that these proteins were functionally redundant, metal adback assays and metal quantification studies were performed in a range of concentrations. CTR1 was found to be responsible for high-affinity Cu uptake when concentrations of Cu are exceedingly low in the extracellular space. CTR2, in comparison, contributed to Cu uptake to a greater degree when Cu concentrations were at slightly higher. This variation of function extended to intracellular Cu distribution when CTR2, but not CTR1, was found to be responsible for Cu mobilization from the acidocalcisome after resupply of Zn following Zn-deficient conditions. The lack of redundancy observed between CTR1 and CTR2 held for both Cu-deficient and Zn-deficient conditions and was further supported when the increased expression of *ctr2* transcripts in *ctr1* mutants and vice versa failed to improve the respective mutant phenotypes.

Subsequent studies in *Chlamydomonas* focused on examining soluble factors that may modulate Cu-uptake: CTR3, the noncanonical CTR lacking a transmembrane region, and the abundant cytosolic thiol, GSH. Sublocalization studies using a mutant lacking a cell wall identified the subcellular localization of CTR3 to the periplasm. However, no clear role was found for CTR3 in promoting Cu-uptake during Cu deficiency or sustaining Cu hyperaccumulation in Zn deficiency unlike CTR1 or CTR2 despite a similar expression pattern in both conditions. However, the rate of Cu uptake was found to be modified by

the availability of cytosolic GSH which may compete and interact with known Cu chaperones in the cytosol, like ATOX1, for Cu(I) depending on the concentrations present (10-12). These investigations found that 1) multiple CTRs expressed by an organism can fine tune the rate of Cu uptake and cellular sequestration to the acidocalcisome to be responsive to different environmental concentrations, 2) CTR3 has a similar localization pattern to iron assimilatory proteins that are also soluble but doesn't yet have a known function during Cu or Zn deficiency, and 3) GSH contributes to the rate of Cu(I) uptake in Zn deficiency as soluble cytosolic factor.

The results presented in chapter 2 left several questions remaining that could be studied in the future. For instance, it is not known whether CTR3 plays a more subtle role on Cu-uptake, similar to that of GSH, where the rate of Cu uptake in the transition to Zn deficiency from Zn replete conditions is modulated by CTR3's effect on Cu availability in the periplasm. It has also been hypothesized that CTR3 may serve as a defense mechanism during period where CTR1 and CTR2 are upregulated, as increased uptake channels also increases the susceptibility of cells to Ag uptake and toxicity via these transporters (13,14). Examining CTR3's role in Ag uptake during Cu deficiency could determine whether CTR3 serves this defensive role similar to GSH when chemical inhibition of the rate limiting step of its synthesis or mutants for the same enzyme sensitize *Chlamydomonas* to Ag toxicity. Rescuing these phenotypes with mutants in CTR2 or CTR1 would further support the hypothesis that increased susceptibility to Ag is driven by uptake through these CTRs when the specific rate of uptake is further modulated by the soluble factors described.

Chapter 3 and 4 used a simplified host-microbe system to investigate the interactions between prokaryotic and eukaryotic Cu-homeostatic responses. Like *Chlamydomonas*, *C. elegans* are eukaryotes with defined CTRs and a P-type ATPase copper transporting protein where expression and localization are driven by environmental Cu conditions (3,15). Sensitization to Cu deficiency and toxicity had similarly been reported in *C. elegans* who had impaired Cu-homeostasis responses (3,15,16). However, the reliance of *C. elegans* on live bacterial food supplementation in lab conditions allowed investigations of host-microbe interactions during periods of where Cu homeostasis is challenged. While previous studies had sought to minimize this confounding factor by heat killing the bacterial supplement (17), others described the potential for active bacterial Cu handling as nematodes raised in the absence of bacteria were observed to be exposed to higher concentration of free Cu than nematodes raised with live bacterial cultures(18). While there is a great deal of bacterial activity that could contribute to these observations, we focused on genetically manipulating components of bacterial Cu homeostasis which were known to be active in conditions of Cu excess. One ubiquitous bacterial response to Cu stress is activation of a two component system, *cusRS*, that senses excess periplasmic Cu (I) to increase expression of an antiporter pump, *cusCFBA* to remove Cu(I)(5,19,20). Therefore, we sought to isolate the specific impact of this bacterial Cu response in the *C. elegans/E.coli* host microbe system.

Results in chapter 3 catalogue the bacterially-dependent moderation of established *C. elegans* Cu-toxicity endpoints. Nematodes were exposed to equimolar Cu concentrations after raising them on bacterial lawns with the same genetic background except for selective deletions that altered the overall Cu-efflux capacity before monitoring

the development of Cu toxicity over time. While excluding early developmental periods from Cu exposure in the nematode may have limited the reproductive toxicity previously observed in *C. elegans* exposed to excess Cu, all other toxicity endpoints tested improved when bacterial lawns were impaired in their ability to sense and respond to excess Cu. GFAAS analysis and quantification of metal-responsive genes in *C. elegans* were used to determine that bacterially-dependent resistance to Cu stress was not derived from reduced Cu-body burdens and instead the result of altered Cu-homeostatic responses in the nematode dependent on shifts in the distribution of Cu stress in the nematode.

However, bacterial species have demonstrated a tendency to increase their capacity for Cu-resistance over time with increasing environmental and antibiotic exposures from industrial and agricultural sources, particularly for enteric bacteria where Cu uptake in host organisms takes place (21,22). Therefore, future investigations could focus on whether increasing Cu resistance, either by increasing bacterial Cu efflux or with plasmid-borne genes known to be acquired in conditions of excess environmental Cu, sensitizes host organisms to lower concentrations of Cu stress. Other investigations into the metal responsive gene that confers much of the bacterially-dependent Cu resistance in nematodes would be noteworthy since the function is not well characterized beyond being a necessary for the maintenance of RNA processing machinery in the nucleus during metal stress (23).

Subsequent investigations in chapter 4 sought to identify any other transcriptomic responses contributed to the observed bacterially-dependent Cu resistance downstream in *C. elegans*. While previous studies had identified Cu-responsive genes in *C. elegans* during periods of environmental Cu excess (16,24,25), few studies had focused on adult

exposures independent are early developmental Cu stress. Therefore, an RNAseq experiment was designed to capture 1) the adult *C. elegans* response to Cu stress 2) the transcriptomic variation derived from bacterial strains independent of Cu stress and finally 3) the bacterially-dependent differentially expressed genes responding to excess Cu. While the RNAseq analyses employed did flag several known Cu-responsive genes, including *numr-1*, as DEGs in our Cu exposure paradigm, the experimental design limited the specificity of the developmental stage isolated in the RNA collection steps and therefore limited our confidence in assigning these DEGs to adult-specific Cu-stress. Additionally, Cu-responsive genes were not identified as DEGs between bacterial conditions in the absence of Cu stress, confirming that variations observed between the bacterial strains was conditional to Cu excess. Importantly, enrichment analysis of the identified DEGs also appeared to reflect some of the bacterially-dependent susceptibility to Cu toxicity observed in Chapter 3. However, there was also a negligible number of DEGs identified between bacterial conditions when Cu excess was present, suggesting that either the experimental design or RNA analysis was inappropriate or that the bacterially-dependent Cu response in *C. elegans* was not the result of changes to transcriptional activity.

The RNAseq protocol and analysis needs to be optimized before conclusions can be drawn. Future experiments would benefit from more tightly controlling the developmental stage studied through either controlling for the developmentally-specific gene expression in each sample during analysis or by more carefully selecting populations to be isolated for RNA collection prior to the analysis stage. One way to achieve this specificity is to reduce the amount of initial sample input required for RNA

isolation by selecting RNA isolation kits with lower material requirements. Additionally, many methods to isolate RNA lose RNAs smaller 200nt. However, further investigations into the bacterially-dependent effects on RNA processing components like snRNAs would require sample isolation that retains these small RNA molecules. More specific isolations focusing on for neuronal or nuclear expression run concurrently with imaging and quantification of neurotransmitter concentrations during the experimental conditions would further define the role *numr-1* plays in modulating Cu resistance to respond to changing environmental conditions.

This dissertation investigated the environmental factors that contribute to eukaryotic Cu homeostasis. Using a single-celled eukaryote, *Chlamydomonas reinhardtii*, this work expanded upon the knowledge of Cu uptake transporters by describing how their varying affinities for Cu determined their functionality during Cu deficient and Zn deficient conditions and identified a unique role for CTR2 in the mobilization of Cu from the understudied acidocalcisome. Soluble factors that contribute to the regulation and rate of metal transport across CTR1 and CTR2 was also described as balancing beneficial accumulation of Cu with the potentially detrimental accumulation of Ag. In subsequent studies, the use of *Caenorhabditis elegans* allowed for the study of bacterial Cu-resistance responses within a host-microbe system. These investigations identified increasing bacterial Cu-efflux as an environmental factor contributing to the sensitization of host *C. elegans* to Cu exposures by changing the localization of metal stress within the adult nematode. These investigations present health implications for the increasing Cu resistance observed in bacterial populations due to increased industry and metal

deposition and for the compounding risk of transition metal homeostasis in these increasingly manmade environments.

5.1 References

1. Boal, A. K., and Rosenzweig, A. C. (2009) Structural biology of copper trafficking. *Chem Rev* **109**, 4760-4779
2. Page, M. D., Kropat, J., Hamel, P. P., and Merchant, S. S. (2009) Two Chlamydomonas CTR Copper Transporters with a Novel Cys-Met Motif Are Localized to the Plasma Membrane and Function in Copper Assimilation. *The Plant Cell* **21**, 928-943
3. Yuan, S., Sharma, A. K., Richart, A., Lee, J., and Kim, B. E. (2018) CHCA-1 is a copper-regulated CTR1 homolog required for normal development, copper accumulation, and copper-sensing behavior in *Caenorhabditis elegans*. *J Biol Chem* **293**, 10911-10925
4. Dancis, A., Haile, D., Yuan, D. S., and Klausner, R. D. (1994) The *Saccharomyces cerevisiae* copper transport protein (Ctr1p). Biochemical characterization, regulation by copper, and physiologic role in copper uptake. *J Biol Chem* **269**, 25660-25667
5. Gudipaty, S. A., Larsen, A. S., Rensing, C., and McEvoy, M. M. (2012) Regulation of Cu(I)/Ag(I) efflux genes in *Escherichia coli* by the sensor kinase CusS. *FEMS Microbiol Lett* **330**, 30-37
6. Malasarn, D., Kropat, J., Hsieh, S. I., Finazzi, G., Casero, D., Loo, J. A., Pellegrini, M., Wollman, F. A., and Merchant, S. S. (2013) Zinc deficiency impacts CO₂ assimilation and disrupts copper homeostasis in *Chlamydomonas reinhardtii*. *J Biol Chem* **288**, 10672-10683
7. Duncan, A., Yacoubian, C., Watson, N., and Morrison, I. (2015) The risk of copper deficiency in patients prescribed zinc supplements. *J Clin Pathol* **68**, 723-725

8. Metaxas, A. (2021) Imbalances in Copper or Zinc Concentrations Trigger Further Trace Metal Dyshomeostasis in Amyloid-Beta Producing *Caenorhabditis elegans*. *Frontiers in Neuroscience* **15**
9. Bisaglia, M., and Bubacco, L. (2020) Copper Ions and Parkinson's Disease: Why Is Homeostasis So Relevant? *Biomolecules* **10**
10. Speisky, H., Gómez, M., Carrasco-Pozo, C., Pastene, E., Lopez-Alarcón, C., and Oleazar, C. (2008) Cu(I)-glutathione complex: a potential source of superoxide radicals generation. *Bioorg Med Chem* **16**, 6568-6574
11. Banci, L., Bertini, I., Ciofi-Baffoni, S., Kozyreva, T., Zovo, K., and Palumaa, P. (2010) Affinity gradients drive copper to cellular destinations. *Nature* **465**, 645-648
12. Maryon, E. B., Molloy, S. A., and Kaplan, J. H. (2013) Cellular glutathione plays a key role in copper uptake mediated by human copper transporter 1. *Am J Physiol Cell Physiol* **304**, C768-779
13. Wang, S., Lv, J., and Zhang, S. (2019) Discovery of CRR1-targeted copper deficiency response in *Chlamydomonas reinhardtii* exposed to silver nanoparticles. *Nanotoxicology* **13**, 447-454
14. Howe, G., and Merchant, S. (1992) Heavy Metal-Activated Synthesis of Peptides in *Chlamydomonas reinhardtii*. *Plant Physiol* **98**, 127-136
15. Chun, H., Sharma, A. K., Lee, J., Chan, J., Jia, S., and Kim, B. E. (2017) The Intestinal Copper Exporter CUA-1 Is Required for Systemic Copper Homeostasis in *Caenorhabditis elegans*. *J Biol Chem* **292**, 1-14

16. Tvermoes, B. E., Boyd, W. A., and Freedman, J. H. (2010) Molecular characterization of numr-1 and numr-2: genes that increase both resistance to metal-induced stress and lifespan in *Caenorhabditis elegans*. *J Cell Sci* **123**, 2124-2134
17. Mashock, M. J., Zanon, T., Kappell, A. D., Petrella, L. N., Andersen, E. C., and Hristova, K. R. (2016) Copper Oxide Nanoparticles Impact Several Toxicological Endpoints and Cause Neurodegeneration in *Caenorhabditis elegans*. *PLoS One* **11**, e0167613
18. Moyson, S., Town, R. M., Joosen, S., Husson, S. J., and Blust, R. (2019) The interplay between chemical speciation and physiology determines the bioaccumulation and toxicity of Cu(II) and Cd(II) to *Caenorhabditis elegans*. *J Appl Toxicol* **39**, 282-293
19. Affandi, T., and McEvoy, M. M. (2019) Mechanism of metal ion-induced activation of a two-component sensor kinase. *Biochem J* **476**, 115-135
20. Mealman, T. D., Blackburn, N. J., and McEvoy, M. M. (2012) Metal export by CusCFBA, the periplasmic Cu(I)/Ag(I) transport system of *Escherichia coli*. *Curr Top Membr* **69**, 163-196
21. Staehlin, B. M., Gibbons, J. G., Rokas, A., O'Halloran, T. V., and Slot, J. C. (2016) Evolution of a Heavy Metal Homeostasis/Resistance Island Reflects Increasing Copper Stress in Enterobacteria. *Genome Biol Evol* **8**, 811-826
22. Baker-Austin, C., Wright, M. S., Stepanauskas, R., and McArthur, J. V. (2006) Co-selection of antibiotic and metal resistance. *Trends in Microbiology* **14**, 176-182
23. Wu, C. W., Wimberly, K., Pietras, A., Dodd, W., Atlas, M. B., and Choe, K. P. (2019) RNA processing errors triggered by cadmium and integrator complex disruption are signals for environmental stress. *BMC Biol* **17**, 56

24. Hattori, A., Mizuno, T., Akamatsu, M., Hisamoto, N., and Matsumoto, K. (2013) The *Caenorhabditis elegans* JNK Signaling Pathway Activates Expression of Stress Response Genes by Derepressing the Fos/HDAC Repressor Complex. *PLOS Genetics* **9**, e1003315
25. Zhang, Y., Zhao, C., Zhang, H., Liu, R., Wang, S., Pu, Y., and Yin, L. (2021) Integrating transcriptomics and behavior tests reveals how the *C. elegans* responds to copper induced aging. *Ecotoxicology and Environmental Safety* **222**, 112494